Imperial College London

London Institute of Medical Sciences

The role of mTOR signalling in primordial germ cell development

Theresa Schoenherr

October 2018

This dissertation is submitted for the degree of Doctor of Philosophy

Declaration of Originality

The research presented in this thesis is the result of my own work, unless stated otherwise and specifically referenced in the text. The work was completed under the supervision of Prof Petra Hajkova and Prof Dominic Withers.

Theresa Schoenherr

Copyright

Acknowledgements

The past four years have been an exciting, enjoyable and at times challenging journey. The work presented in this thesis would not have been possible without the support from countless people. I would like to take this opportunity to say thank you.

First and foremost, I would like to acknowledge my supervisors Petra Hajkova and Dominic Withers. Thank you both for taking me on as a student and giving me the opportunity to complete my PhD in your laboratories. In particular, thank you Petra for your excellent supervision, scientific guidance and support over the years. Thank you Dominic for your critical feedback and helpful suggestions. Further, thank you to my academic mentors Veronique Azuara and Jesus Gil for their discussions and critical assessments of the project along the way.

I would also like to thank all the current and past members of the Reprogramming and Chromatin Group. Special thanks to Peter who taught me many techniques at the start of my PhD, which I have been using since, and who was always willing to discuss ideas. Also thanks to Kirsten for technical support, advice and guidance, particularly at the beginning of my PhD. Further, I'd like to thank Harry for critical and useful feedback during lab meetings. Also special thanks to Ina for taking the time to proof read my thesis. Tien-Chi, thank you for your technical advice and all our (philosophical) discussions about science and life over the years. Thank you Cristina, Gosia, Eric and Yuki for your support and advice. Karl and Eren, best of luck for the rest of your PhD. Last but not least, thanks to all of you for making work such an enjoyable place!

Further, I would also like to thank all the current and past members of the Metabolic Signalling Group. Special thanks to Elaine, Silvia and Darran for their patience, technical support and assistance regarding mouse colony management. Also, thanks to Munim for technical support.

Additionally, I would like to extend my thanks to Dirk and Chad from the Microscopy Facility for their training, technical advice and support. In no particular order, I would also like to thank: George, Zach, Carla, Piotr, Amy and Ola for their technical advice and assistance taking care of my mouse colonies when I couldn't.

Outside of work, special thanks to my flatmates, Marta and Raquel, for sharing the joyful and stressful moments with me. Also, thanks to Lisa and Jan for their amazing support.

Finally, I'd like to say a big thank you to my family. Mum and Dad, thanks for your constant support and always believing in me no matter what. To my great sisters, Carolin and Laura, thanks for your advice and always being at the end of the phone.

Abstract

Primordial germ cells (PGCs) are the embryonic precursors of mature egg and sperm cells. In the mouse, following specification at embryonic day (E) 7.25, PGCs proliferate and migrate through the embryonic hindgut towards the genital ridges (future gonads). At E10.5, upon genital ridge entry, developing PGCs undergo epigenetic reprogramming followed by sex differentiation, committing to either oogenesis or spermatogenesis. Signalling cross-talk between PGCs and soma is a key feature of germ cell development. However, to what extent extrinsic signals emanating from the gonadal environment influence key germ cell processes is still not well understood. Here, I describe for the first time a crucial role of a key nutrient and hormone sensing pathway (mTOR) during PGC development. mTOR signals via two distinct multi-protein complexes, mTORC1 and mTORC2. Most of the presented work focuses on mTORC1 and its downstream translational regulators 4E-binding proteins (4E-BPs) and S6 kinases (S6Ks), respectively. Using an immunofluorescence-based approach, I show that in mouse PGCs, mTORC1 signals mainly via 4E-BP1, rather than the S6K1-S6 signalling axis. Interestingly, the observed activation of mTORC1-4E-BP1 signalling in PGCs shortly follows their entry into the genital ridge, suggesting a possible role at this developmental transition. However, global deletion of either 4E-BPs or S6Ks revealed only a minor phenotype in PGCs. Further, my results also point towards activation of AKT, a potential upstream mTORC1 activator in PGCs. This indicates a possible link to mTORC2 signalling. In view of that, I carried out a germline specific conditional deletion of *Mtor* (using a newly generated Blimp1-iCre mouse line), that leads to the loss of mTORC1 and mTORC2. Preliminary observations show a strong phenotype of very few germ cells surviving at E13.5. In summary, my results suggest a critical role for mTOR signalling during PGC development.

Table of Contents

List of Figures

List of Tables

Abbreviations

4E-BP1	4E binding protein 1
4E-BP2	4E binding protein 2
4E-BP3	4E binding protein 3
4-OHT	4-hydroxytamoxifen
Akt	Akt serine/threonine kinase 1
Akt1s1	see PRAS40
AP	alkaline phosphatase
BAC	bacterial artificial chromosome
BLIMP1	B-lymphocyte-induced maturation protein 1, also known as PRDM1
BMP	bone morphogenetic protein
bp	base pairs
BSA	bovine serum albumin
CKO	conditional knockout
ctrl	control
DAPI	4′,6-diamidino-2-phenylindole
DAZL	deleted in azoospermia-like
DEPTOR	DEP-containing mTOR interacting protein
DNMT1	DNA (cytosine-5)-methyltransferase 1
E	embryonic day
EGCs	embryonic germ cells
EGFP	enhanced green fluorescent protein
eIF4E	eucaryotic initiation factor 4E
Eif4ebp1	eucaryotic initiation factor 4E binding protein 1 (gene name) - 4E-BP1 (protein)
Eif4ebp2	eucaryotic initiation factor 4E binding protein 2 (gene name) - 4E-BP2 (protein)
Eif4ebp3	eucaryotic initiation factor 4E binding protein 3 (gene name) - 4E-BP3 (protein)
EpiLCs	epiblast-like cells
ExE	extraembryonic endoderm
F	female
FPKM	fragments per kilobase of transcript per million mapped read
GDNF	glial cell-derived neurotrophic factor
GSK3β	glycogen synthase kinase 3 beta
iCre	improved Cre recombinase
IF	immunofluorescence
IGF	insulin-like growth factor
IRS	insulin-like receptor substrate
KIT ligand	also known as stem cell factor (SCF) or steel factor
LB	luria-bertani broth
M	male
Mapkap1	see mSIN1
MEFs	mouse embryonic fibroblasts
MIS	meiosis inducing signal
mLST8	mammalian lethal with Sec13 protein 8

MPS	meiosis preventing signal
mSIN1 (*Mapkap1*)	mammalian stress-activated protein kinase interacting protein 1 (gene name)
mTOR	mammalian target of rapamycin
mTORC1	mTOR complex 1
mTORC2	mTOR complex 2
MVH	mouse vasa homolog, also known as DDX4
OCT4	octamer-binding transcription factor 4
p.	page
pAKT	phosphorylated AKT
PBS	phosphate-buffered saline
PCR	polymerase chain reaction
PDK1	phosphoinositide dependent kinase 1
PFA	paraformaldehyde
PFGE	pulse-field gel electrophoresis
PGC	primordial germ cell
PGCLCs	primordial germ cell-like cells
PI3K	phosphoinositide-3-kinase
PLZF	promyelocytic leukemia zinc finger
PRAS40 (*Akt1s1*)	proline-rich Akt substrate 40kDa (gene name)
PRDM1	PR domain containing protein 1, also known as BLIMP1
PRDM14	PR/SET domain 14
PROTOR1/2 (*Prr5*)	protein observed with Rictor-1 (gene name)
Prr5	see PROTOR1/2
PTEN	phosphatase and tensin homologue
RA	retinoic acid
RAPTOR (*Rptor*)	regulatory associated protein of mTOR (gene name)
RHEB	small Ras protein enriched in the brain
RICTOR	rapamycin insensitive companion of mTOR
rpS6	ribosomal protein S6
Rps6k1	ribosomal protein S6 kinase 1 (gene name) - S6K1 (protein)
Rps6k2	ribosomal protein S6 kinase 2 (gene name) - S6K2 (protein)
S	serine
S6K1	S6 kinase 1
S6K2	S6 kinase 2
SCC	spermatogonial stem cells
SEM	standard error of the mean
Ser	serine
SOX2	SRY (sex determining region Y)-box 2
SpA-TGCs	spiral artery-associated trophoblast giant cells
SPC	spermatogonial progenitor cell
SSEA1	stage specific antigen 1
STRA8	stimulated by retinoic acid gene 8
SYCP3	synaptonemal complex protein 3
T	threonine
TFAP2C	Transcription Factor AP-2 Gamma, also known as AP2γ
THR	threonine
TNAP	tissue non-specific alkaline phosphatase
TSC	tuberous sclerosis complex
VE	visceral endoderm

1. Introduction

1.1. Germ cell development and life cycle in the mouse

In a sexually reproducing organism, germ cells provide a link between generations. Upon fertilization, mature haploid gametes (oocyte and sperm) combine and form a totipotent zygote. The zygote is capable of developing into a whole new organism with a unique combination of parental genetic material. In the developing embryo, some pluripotent cells divert from the somatic fate to establish the germline again, enabling the next generation to reproduce and pass on their genetic information.

In the next sections, I will give an overview of murine germ cell development starting from the induction of germ cell fate in the embryo all the way to sex differentiation. Some of the remarkable and unique abilities of germ cells will be highlighted, with a particular focus on the importance of signalling events (Figure 1.1).

1.1.1. Induction of germ cell fate

Formation of the germ cell lineage can be governed by two different mechanisms - preformation or epigenesis. Preformation is based on the localized maternal inheritance of key factors, also called germplasm, which leads to the formation of germ cells shortly after fertilization (Extavour and Akam 2003). Species such as *D. melanogaster*, *C. elegans* and *D. rerio* rely on asymmetric segregation of cytoplasmic determinates, including RNA binding proteins, to prospective PGCs (Extavour and Akam 2003; Strome and Updike 2015).

Alternatively, in epigenesis, germ cell formation is induced in pluripotent embryonic cells via signals from surrounding tissues slightly later in development (Extavour and Akam 2003). In most mammals, including mice, formation of the germline occurs via epigenesis (Extavour and Akam 2003).

In the mouse, PGCs can first be identified as a cluster of approximately 40 alkaline phosphatase (AP) positive cells at the posterior end of the primitive streak at E7.25, constituting the founder population of the germline (Chiquoine 1954; Ginsburg, Snow, and McLaren 1990; Lawson and Hage 1994).

Clonal analysis in the gastrulating mouse embryo revealed that proximal epiblast cells, located close to the extraembryonic ectoderm, give rise to PGCs (Lawson and Hage 1994). Interestingly, following lineage tracer injection into single epiblast cells at E6.0 and E6.5, some resulting clones also consisted of somatic cells from the extraembryonic mesoderm

(Lawson and Hage 1994). Based on these observation, the authors concluded at the time that at E6.5, epiblast cells are not germ cell lineage restricted yet (Lawson and Hage 1994). Of note, genetic lineage tracing experiments carried out almost a decade later identified about six epiblast cells at E6.25, which expressed the transcription factor *Blimp1* and were indeed lineage restricted PGC precursors (Ohinata et al. 2005). It is likely that in the clonal analysis experiments, some marked cells were initially negative for *Blimp1*.

The inductive nature of germline specification was first observed through transplantation experiments of Tam and Zhou. When distal epiblast cells, which normally give rise to neurectoderm, were transplanted to the proximal region of the epiblast, they differentiated into PGCs (Patrick P.L. Tam and Zhou 1996). These observations demonstrated that murine PGC fate depends on extrinsic signals from surrounding tissues, rather than cell-autonomous inherited determinants as observed during transplantation experiments in *D. melanogaster* (Illmensee and Mahowald 1974) and *X. laevis* (Tada et al. 2012).

One of the most crucial signals for germ cell induction in proximal epiblast cells are bone morphogenetic proteins BMP4, BMP8b and BMP2 originating from extraembryonic ectoderm (ExE) and visceral endoderm (VE). Mice lacking bone morphogenetic proteins (BMP4, BMP2, BMP8b), or BMP receptors (ALK2) or BMP signal transducing proteins (SMAD1, SMAD4, SMAD5) all show reduced number or complete loss of PGCs (Lawson et al. 1999; Ying and Zhao 2001; Ying et al. 2000; de Sousa Lopes et al. 2004; Tremblay, Dunn, and Robertson 2001; Chu et al. 2004; H. Chang and Matzuk 2001). *In vitro* culture experiments of early embryo fragments show that ExE (production of BMP4 and BMP8b) can induce *Blimp1* expression in epiblast cells in the absence of VE (production of BMP2). Further, addition of BMP4 potentiates *Blimp1* induction (Ohinata et al. 2009). However, in the reciprocal experiment, VE can only induce *Blimp1* expression in epiblast cells if BMP4 and BMP8b are added, addition of BMP4 alone is not sufficient. These and subsequent *in vitro* differentiation experiments demonstrate that BMP4/BMP2 are inductive signals, whereas BMP8b confines inhibitory signals from the anterior VE to allow successful PGC induction (Ohinata et al. 2009).

In addition to BMPs, WNT signalling has been implicated in PGC induction. Loss of WNT3A (secreted glycoprotein) or its main cytoplasmic effector β-catenin leads to impaired gene induction of *Blimp1* and *Prdm14* (see next section) (Figure 1.1) (Ohinata et al. 2009; Aramaki et al. 2013).

How BMP and WNT3A signalling is integrated in epiblast cells to induce primordial germ cell specification at a molecular level is still not entirely clear. One possibility is that WNT3A signalling from the surrounding VE and in proximal epiblast cells allows a few proximal epiblast cells to respond to BMP4 signalling (Ohinata et al. 2009).

1.1.2. Specification of murine primordial germ cells

At the molecular level, proximal epiblast cells induce expression of *Fragilis*, an interferon inducible transmembrane protein, upon inductive signalling (Figure 1.1) (Saitou, Barton, and Surani 2002). *Fragilis* positive cells have acquired competence to become primordial germ cells (PGCs), however only a small subset will do so. Of these *Fragilis* positive cells, around 6 cells in the posterior region of the proximal epiblast will upregulate the transcription factor *Blimp1* (B-lymphocyte-induced maturation protein 1; also known as Prdm1 – PR domain-containing protein 1) at E6.25 (Ohinata et al. 2005). Lineage tracing experiments showed that all early *Blimp1* expressing cells are lineage restricted and the direct precursor cells of PGCs (Ohinata et al. 2005). Of note, it has been suggested that new proximal epiblast cells can be recruited to the Blimp1 positive PGC precursor population between E6.5 and E7.25, based on estimated cell cycle rates and the size of the PGC founder pool (~40 cells) at E7.25 (Ohinata et al. 2005).

Early *Blimp1*-expressing cells already express mesodermal genes such as *Hoxa1* and *Hoxb1* and are destined for a somatic cell fate (Saitou, Barton, and Surani 2002; Kurimoto et al. 2008).

A network of transcription factors, consisting of BLIMP1, PRDM14 (PR/SET domain 14) and TFAP2C (also known as AP2γ), induce a distinct transcriptional program driving PGC specification. Together, these transcription factors repress the somatic program (e.g. mesodermal genes) and induce expression of germ cell specific genes and pluripotency genes (Figure 1.1) (Magnúsdóttir et al. 2013).

Blimp1 is the earliest expressed transcription factor in PGC precursors (at E6.25). Global loss of *Blimp1* leads to a small number of PGC-like cells being formed, as identified by alkaline phosphatase (AP) staining and expression of germ cell specific marker STELLA (Ohinata et al. 2005). These cells, however, fail to proliferate and migrate out of the cluster and have aberrant gene expression profiles, including inefficient repression of *Hox* genes. Thus, BLIMP1 plays an important role in repressing the somatic transcriptional program during PGC specification (Ohinata et al. 2005; Kurimoto et al. 2008).

Prdm14 and *Tfap2c* start to be expressed slightly after *Blimp1* is induced, at E6.5 and E7.25, respectively (Yamaji et al. 2008; Weber et al. 2010). *Tfap2c* is a putative target of BLIMP1 and represses the somatic program, whereas PRDM14 is important to induce the expression of pluripotency genes such as *Sox2* (Weber et al. 2010; Yamaji et al. 2008).

Overall, the transcriptional changes lead to the re-acquisition of the pluripotency network which is crucial for the specification and survival of germ cells (Okamura et al. 2008; Kehler et al. 2004; Chambers et al. 2007; Yamaguchi et al. 2009; Campolo et al. 2013). Primordial germ cells continuously express *Oct4*, in addition to regaining expression of *Nanog* and *Sox2* (Figure 1.1) (Saitou and Yamaji 2012).

Another key pluripotency factor is the RNA binding protein LIN28 (Shyh-Chang and Daley 2013). An *in vitro* RNAi screen showed that Lin28A is important for primordial germ cell specification from embryonic stem cells. Lin28A represses *Let-7* micro RNA maturation and hence promotes translation of the *Let-7* target *Blimp1* (West et al. 2009). In line with that, *in vivo* knockout of *Lin28a* or overexpression of *Let-7* leads to decreased PGC numbers and reduced fertility (Shinoda et al. 2013).

During specification, early BLIMP1 expressing cells increase in number to form a cluster of ~ 20 cells by E6.75 and subsequently give rise to a founder population of about ~40 PGCs by E7.25. These cells can be identified at the posterior end of the primitive streak (Ginsburg, Snow, and McLaren 1990; Lawson and Hage 1994), are AP positive and express germ cell specific markers BLIMP1 and STELLA (also known as DPPA3/PGC7) (Chiquoine 1954; Sato et al. 2002; Saitou, Barton, and Surani 2002).

1.1.3. Proliferation and migration

From the posterior end of the primitive streak, PGCs start to migrate directly into adjacent tissue - the developing allantois, extraembryonic and embryonic endoderm. In the embryonic endoderm, PGCs migrate along the developing hindgut towards the mesoderm. Egression from the hind-gut is followed by bilateral invasion of the dorsal body wall, and eventual colonization of the genital ridges (developing gonads) at E10.5 (Molyneaux et al. 2001). Only PGCs which have directly migrated to the embryonic endoderm will eventually colonize the genital ridges (R. Anderson et al. 2000). Notably, about 5% of PGCs will not have reached the genital ridges by E11.5 and most ectopic PGCs are eliminated by apoptosis (Laird et al. 2011; Runyan et al. 2006).

Once initiated, migration is governed via intrinsic and extrinsic signals. KIT ligand (also known as steel factor or stem cell factor) and its receptor C-KIT are important for PGC survival, proliferation and migration (Richardson and Lehmann 2010). In KIT ligand null embryos, PGCs migrate in the right direction, however at a greatly reduced rate. Hence, KIT ligand – C-KIT signalling regulates PGC motility rather than directionality during migration (Figure 1.1) (Gu et al. 2009; Runyan et al. 2006).

In addition, the chemoattractant SDF1 (or CXCL12), expressed by somatic cells of the genital ridge and surrounding mesenchyme, and its receptor CXCR4 (expressed by PGCs) play an important role in later stages of migration (after egression from the hindgut). In knockout embryos of either protein, genital ridge colonization is impaired (Figure 1.1) (Ara et al. 2003; Molyneaux et al. 2003).

Of note, during migration PGCs actively proliferate and the population of initially 40 founder cells at E7.5 expands to about 25,000 cells at E13.5 (P. P. L. Tam and Snow 1981). Interestingly, between E7.75-8.75, the majority of PGCs enter G2 cell cycle arrest until around E9.5, when proliferation resumes (Seki et al. 2007). In addition to migration and proliferation, PGCs undergo a first wave of epigenetic reprogramming, which will be discussed in a separate section (see 1.2.1, p. 41).

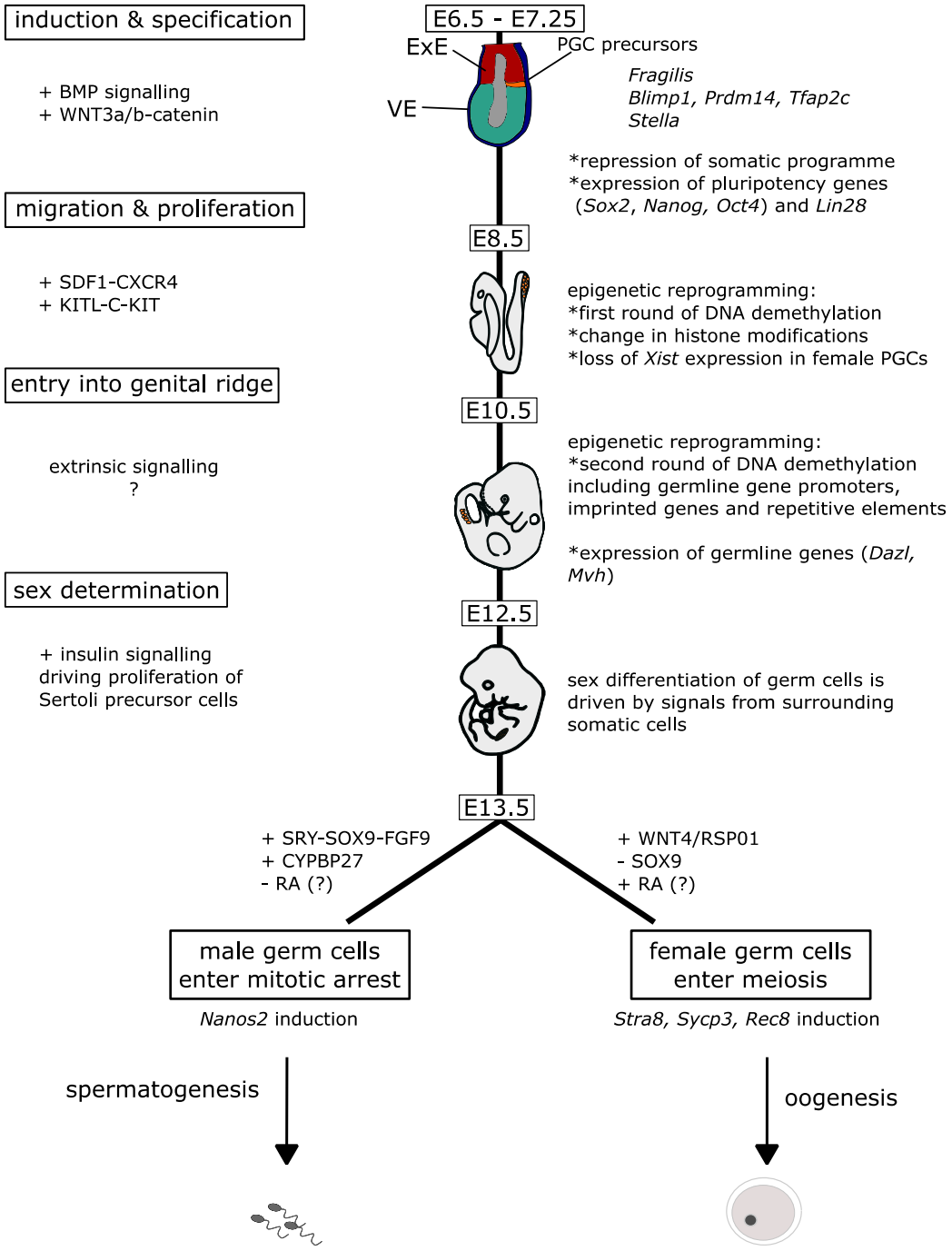

Figure 1.1 Key stages of early mouse germ cell development.

On the left, extrinsic signalling events are depicted, on the right key processes during each developmental stage are described. Primordial germ cells specify from epiblast cells upon inductive signalling from the extraembryonic ectoderm (ExE) and visceral endoderm (VE). Migration through the hindgut allows colonization of the genital ridges. Gonadal germ cells then undergo a series of events and eventually differentiate and embark on sex specific developmental routes (oogenesis and spermatogenesis) to give rise to haploid mature germ cells.

1.1.4. Gonadal germ cells

Once primordial germ cells have reached the genital ridge at E10.5, they initially divide mitotically for a few rounds with incomplete cytokinesis, forming germ cell cysts (Pepling and Spradling 2001; Lei and Spradling 2013). At the same time, they undergo a second wave of epigenetic reprogramming (see 1.2.2, p. 42), start to express genes specific of gonadal germ cells and eventually will enter sexual differentiation and meiosis (females) or mitotic arrest (males) (Figure 1.1) (Kocer et al. 2009).

1.1.4.1. Expression of germ cell specific genes

Upon the genital ridge entry, germ cells start to express genes involved in gametogenesis and meiosis. Many of these genes have been suggested to be methylation sensitive (Borgel et al. 2010; Guibert, Forné, and Weber 2012). As gonadal germ cells undergo global DNA demethylation (see 1.2.2, p. 42), expression of these genes follows the loss of methylation at their promoter regions.

I would like to particularly point out two key germ cell specific genes: the deleted in azoospermia-like (*Dazl*) gene and the mouse vasa homolog (*Mvh,* also known as *Ddx4)* gene. Expression of both genes is dependent on their promoter methylation levels, as demonstrated using *Dnmt1* mutant embryos with reduced methylation levels (Maatouk et al. 2006).

Mvh is expressed specifically in germ cells from E10.5 onwards until the post-meiotic stages in both males and females (Toyooka et al. 2000). The protein is an ATP-dependent RNA helicase belonging to the DEAD box family of genes and essential for male gametogenesis. Males lacking *Mvh* cannot produce mature sperm - pre-meiotic germ cells are unable to progress past the zygotene stage and undergo apoptosis (Fujiwara et al. 1994; Tanaka et al. 2000). MVH has been shown to bind over 800 mRNA species in adult testis including but not limited to many mRNAs involved in spermatogenesis (Nagamori, Cruickshank, and Sassone-Corsi 2011).

Dazl is expressed from E11.5 onwards in male and female germ cells (Cooke et al. 1996; Seligman and Page 1998). DAZL is a RNA binding protein and knockout studies have demonstrated that it is absolutely essential for gametogenesis. Both adult male and female *Dazl* knockout mice are sterile due to the lack of mature and functional gametes (egg or sperm) (Ruggiu et al. 1997; Saunders et al. 2003; Y. Lin and Page 2005; Y. Lin et al. 2008). The

underlying phenotype depends on the genetic background of the knockout mouse model. On a mixed genetic background, a loss in germ cell numbers is first observed at E17.5 in females and at E19.5 in males (Ruggiu et al. 1997; Saunders et al. 2003). More importantly, *Dazl* knockout germ cells are able to initiate meiosis, however, fail to progress through meiosis. Female germ cells are lost before completion of meiosis, while the majority of male germ cells appear to be blocked at the leptotene to zygotene transition (Ruggiu et al. 1997; Saunders et al. 2003).

To the contrary, on a pure BL6 genetic background, female germ cell numbers are not affected in *Dazl* knockout gonads throughout embryonic development and birth, whereas in male *Dazl* knockout gonads, germ cell loss occurs as early as E14.5 (Y. Lin et al. 2008; Y. Lin and Page 2005). Interestingly, loss of DAZL leads to impaired germ cell differentiation. Male *Dazl* knockout germ cells fail to upregulate NANOS2, do not arrest in G1/G0 and do not re-methylate their DNA, while also maintaining expression of pluripotency genes NANOG, STELLA, and OCT4. Female *Dazl* knockout germ cells fail to initiate meiosis, as judged by the lack of chromosome condensation, a failure to upregulate *Stra8* and *Dmc1* and absence of meiotic markers such as yH2AX and SCP3 (at E15.5) (Y. Lin et al. 2008). Further, female *Dazl* knockout germ cells maintain the expression of pluripotency genes, which, under normal circumstances, are downregulated upon entry into meiosis (Y. Lin et al. 2008).

Based on these observations, the authors proposed a model in which expression of DAZL in gonadal germ cells licenses germ cells to transition to "gametogenesis competent cells"(Gill et al. 2011; Y. Lin et al. 2008). Only these competent germ cells have the ability to respond to extrinsic signals and initiate meiosis or spermatogenesis (Y. Lin et al. 2008; Gill et al. 2011). However considering the fact that on a mixed genetic background, *Dazl* knockout cells were able to initiate meiosis and some progressed up to the early pachynema stage (Ruggiu et al. 1997; Saunders et al. 2003), the role of DAZL seems to be more complex. Further work is needed to determine the role of DAZL during initiation of meiosis.

Of note, genetic background effects on observed germ cell phenotypes are not unique to DAZL. Genetic background specific differences of knockout phenotypes have also been described for germline genes *Stra8* (Baltus et al. 2006; E. L. Anderson et al. 2008; Dokshin et al. 2013) and *Dnd1* (Cook et al. 2011), for instance.

1.1.4.2. Sex determination – XX or XY

At the point of genital ridge entry, PGCs are bipotential and capable of developing either into oocytes or sperm. Sex determination is independent of the sex chromosome constitution of germ cells, but relies on the extrinsic signals from the surrounding gonadal environment (Adams and McLaren 2002; A. McLaren and Southee 1997).

In the male genital ridge, somatic cells start to express the Y chromosome linked sex determining region y (*Sry*) gene between E10.5-E12.5 (Gubbay et al. 1990; Koopman et al. 1991). SRY expression leads to upregulation of the transcription factor *Sox9*, which drives differentiation of somatic precursor cells into Sertoli cells (Sekido et al. 2004; Sekido and Lovell-Badge 2008). Sertoli cells direct germ cell development away from the female program and initiate the male differentiation program and testis formation (Windley and Wilhelm 2015). From E12.5 onwards, male germ cells are committed to spermatogenesis and meiotic entry is blocked (Adams and McLaren 2002). Upon SOX9 expression, Sertoli cells produce the ligand FGF9, which signals to both Sertoli cells and germ cells (Y. Kim et al. 2006). In Sertoli cells, FGF9 induces the expression of the P450 enzyme CYP26B1 (autocrine signalling), which is involved in the repression of meiosis via degradation of retinoic acid (RA) (see 1.1.5, p. 33) (Bowles et al. 2006; Koubova et al. 2006). In differentiating germ cells, FGF9 signalling eventually induces the expression of key germ cell specific gene *Nanos2* from E13.5 onwards (A. Suzuki and Saga 2008; Tsuda et al. 2003; Barrios et al. 2010). NANOS2 is a RNA-binding protein and has been shown to bind meiosis specific *Stra8* and *Sycp3* mRNAs, amongst others, and hence further represses meiotic initiation (Figure 1.1) (A. Suzuki et al. 2010).

Of note, masculinizing signals during testis differentiation develop in a centre-to-pole pattern. SRY expression in the gonad is first observed in somatic cells of the central region, before extending to the anterior and posterior poles within approximately 4 hours (by E11.5) (Bullejos and Koopman 2001). Subsequently, SRY expression rapidly decreases in the central region and becomes restricted to the posterior end, before completely disappearing by E12.5 (Bullejos and Koopman 2001). Following the SRY expression pattern, the downstream Sertoli-cell derived ligand FGF9 is also first detected in the central region of the gonad, from which it can diffuse to the poles and further support masculinization (Hiramatsu et al. 2010).

Together, expression of SRY and downstream signalling events lead to the expression of male germ cell specific genes such as *Nanos2* (as described above), maintenance of pluripotency markers (from E13.5 onwards) (Maurizio Pesce et al. 1998; Bowles et al. 2010)

and repression of meiosis (Bowles et al. 2006; Koubova et al. 2006; A. Suzuki et al. 2010; Windley and Wilhelm 2015). Male germ cells exit the cell cycle and enter G1/G0 mitotic arrest between E12.5 and E14.5 (Western et al. 2008). After birth, XY germ cells resume mitotic proliferation and develop into spermatogonial progenitor cells. These cell will eventually enter meiosis in order to complete gametogenesis (Figure 1.2) (Kocer et al. 2009).

In contrast, the female sex specification program is mainly driven by the WNT/β-catenin signalling pathway. Absence of SRY expression in the female gonad leads to the differentiation of somatic cells into pre-granulosa cells, which produce the germ cell extrinsic factors WNT4 and RSPO1 (Kocer et al. 2009; Vainio et al. 1999; Parma et al. 2006). These signalling factors drive the female differentiation program in part by downregulating *Sox9* in surrounding somatic cells (Chassot et al. 2008; Y. Kim et al. 2006). Female differentiation involves downregulation of pluripotency markers by E13.5 and entry into meiosis (Figure 1.1) (Maurizio Pesce et al. 1998; Borum 1961).

1.1.4.3. Initiation of meiosis in female germ cells

Between E12.5 and E16.5, female germ cells start to express genes involved in meiosis: The first gene, expressed from E12.5 onwards, is the stimulated by retinoic acid gene 8 (*Stra8*) (Menke, Koubova, and Page 2003). STRA8 is essential for entering meiosis and mice lacking *Stra8* are infertile – female germ cells fail to replicate their DNA prior to meiosis initiation and subsequently do not enter meiotic prophase I, whereas male germ cells are able to replicate their DNA but fail to enter prophase I, in both scenarios meiosis cannot be initiated (Baltus et al. 2006; E. L. Anderson et al. 2008).

At E13.5, expression follows of *Sycp3* (synaptonemal complex protein 3) and *Rec8* (yeast meiotic recombination protein REC8 homolog), two proteins involved in the synaptonemal complex and cohesion complex, respectively (Di Carlo, Travia, and De Felici 2000; J. Lee et al. 2003). Loading of both proteins onto the chromosomes marks the beginning of meiotic prophase I, first detected at E13.5 (Borum 1961). Of note, expression of many additional meiosis genes, such as *Spo11* and *Dmc1*, is induced. These two proteins are involved in the formation of double strand breaks and homologous recombination during prophase I (Handel and Schimenti 2010).

Importantly, female germ cells initiate meiosis asynchronously, in an anterior to posterior fashion. Genes such as *Stra8*, *Sycp3* and *DmC1* are first expressed in germ cells at the anterior pole only, followed by expression throughout the gonad and subsequently only in germ cells

at the posterior end, as visualized using whole-mount RNA in situ hybridizations (Menke, Koubova, and Page 2003; Bullejos and Koopman 2004). At the same time, downregulation of the pluripotency marker Oct4 exhibited the same wave-like pattern (Bullejos and Koopman 2004; Menke, Koubova, and Page 2003).

During meiotic prophase I, homologous chromosomes condense, pair and recombine. Female germ cells progress through the meiotic stages leptotene, zygotene, and pachytene until arresting in the diplotene of prophase I (Borum 1961). Only during puberty and after a surge of gonadotropins will female germ cells resume meiosis and complete the first division (under extrusion of the first polar body) during which the homologous chromosomes are separated. During meiosis II, sister chromatids are divided, and the resulting cells are haploid germ cells. Female germ cells arrest in metaphase II and complete the second meiotic division only after fertilization (and under extrusion of another polar body) (Figure 1.2) (Handel and Schimenti 2010).

1.1.5. Signalling in the gonad

Upon genital ridge entry, PGCs undergo many changes regarding their morphology, DNA methylation levels, gene expression and cell fate (entering meiosis vs mitotic arrest). It is still not entirely clear whether these changes are due to an intrinsic clock (cell autonomous) or because of some inductive signalling from the new gonadal environment or a combination of both (Anne McLaren 2003).

Signalling events underlying sexual differentiation and initiation of meiosis in females versus entering mitotic arrest in males have been intensively studied.

Early observations showed that ectopic germ cells in adrenal glands of XX and XY embryos enter meiosis in the absence of a genital ridge environment (Zamboni and Upadhyay 1983). In addition, isolated XY germ cells cultured on embryonic lung cells (A. McLaren and Southee 1997) and germ cells cultured in vitro on a feeder layer also enter meiosis (Chuma and Nakatsuji 2001). These studies suggest that either there is an intrinsic mechanism which triggers meiosis in germ cells at a certain time by default without any external signal. Alternatively, a widely expressed meiosis-inducing signal (MIS) exists and an intrinsic mechanism regulates when germ cells respond to that extrinsic signal.

Retinoic acid (RA) has been suggested to be such a putative meiosis-inducing signal. RA is produced by the mesonephros and diffuses into the gonad (Bowles et al. 2006). In organ

culture experiments, addition of exogenous RA (non-physiological levels) to XY urogenital ridges (genital ridge and mesonephros) induced expression of meiotic markers *Stra8*, *Scp3* and *Dmc1*. Alternatively, addition of RA receptor antagonist to XX urogenital ridges decreased expression of *Stra8, Scp3*, and *Dmc1* and reduced the number of meiotic cells (Koubova et al. 2006; Bowles et al. 2006). This led to the suggested model of retinoic acid as a meiosis-inducing signal, triggering *Stra8* expression and initiation of meiosis. In the male gonad, the RA degrading enzyme CYP26B1 (expressed in Sertoli cells) metabolises retinoic acid and therefore prevents any RA signalling to male germ cells (Bowles et al. 2006). In line with that is the observation that *Cyp26b1* deletion leads to increased expression of *Stra8* and *Sycp3* in XY testis, with some meiotic cells present (Bowles et al. 2006; MacLean et al. 2007).

However, the role of RA signalling during sex determination and initiation of meiosis is still controversial. Kumar and colleagues have demonstrated that *Stra8* can be upregulated independently of retinoic acid. Analysis of *Raldh2* $^{-/-}$ mutant mice, which lack RA synthesis and signalling, shows that *Stra8* expression is maintained in the absence of RA in female gonads. Chemical inhibition of CYP26B1 in *Raldh2* $^{-/-}$ male testis leads to RA independent induction of *Stra8* when the mesonephros remains attached (Kumar et al. 2011). Further, in organ culture experiments of E11.5 male genital ridges supplemented with exogenous RA or CYP26B1 inhibitors, only about 1% of germ cells are meiotic and the rest develop as male germ cells. The authors concluded that RA signalling or CYP26B1 activity is able to induce aberrant gene expression in male germ cells (*Stra8* expression), however this does not lead to initiation of meiosis or change of sexual fate (Best et al. 2008).

Overall, with contradicting evidence, RA remains only a putative meiosis-inducing signal and further work is needed to disentangle direct effects of RA on germ cells and indirect effects due to changes in the somatic environment of the genital ridge during organ culture experiments. Alternatively, the existence of a meiosis preventing substance (MPS) in the male gonad has been suggested to underlie male germ cells entering mitotic arrest instead of meiosis, and/or possibly a combination of MIS and MPS signalling (Kocer et al. 2009).

Sexual differentiation and hence, sexual fate, is highly driven via signals from surrounding Sertoli or granulosa cells (amongst other somatic cells) and changes in their survival, proliferation or differentiation can have indirect effects on germ cells, sexual differentiation and initiation of meiosis.

One example of how impaired development of the surrounding somatic cells can affect sex determination has been shown in mice lacking components of the insulin signalling

pathway. Deletion of all three insulin receptor tyrosine kinase family members (*Ir, Igfr1, Irr*) or just *Ir* and *Igfr1* leads to a reduction in the proliferation rate of surrounding somatic cells prior to sex determination (Nef et al. 2003; Pitetti et al. 2013). Males fail to upregulate *Sry* and *Sox9* in Sertoli precursor cells, and subsequently testis determination and sex differentiation is impaired, resulting in male to female sex reversal. In contrast, females fail to activate the ovarian programme and stay in a prolonged undifferentiated state (Pitetti et al. 2013).

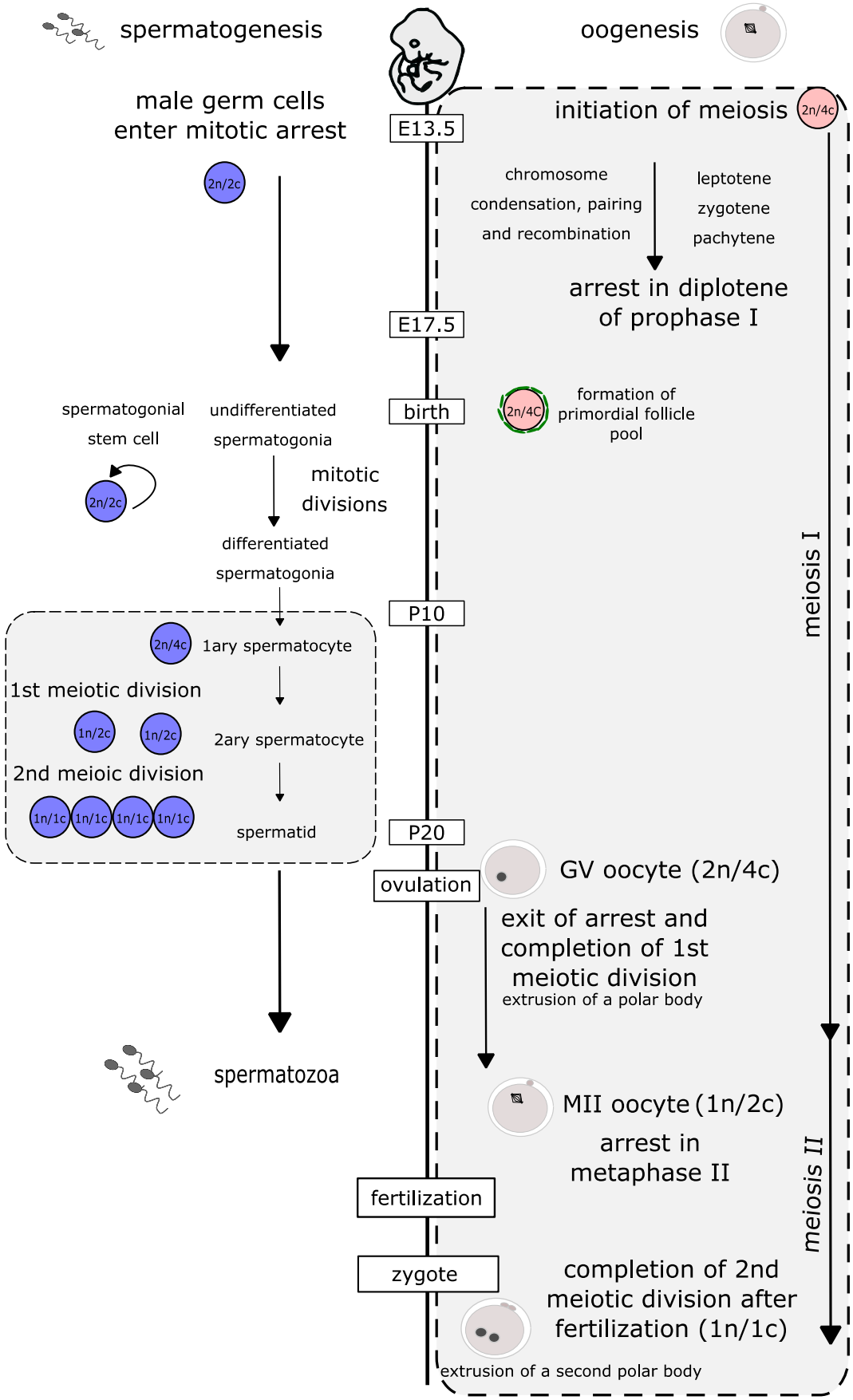
spermatogenesis
oogenesis
male germ cells
enter mitotic arrest
2n/2c
E13.5
initiation of meiosis
2n/4c
chromosome
condensation, pairing
and recombination
leptotene
zygotene
pachytene
arrest in diplotene
of prophase I
E17.5
spermatogonial
stem cell
undifferentiated
spermatogonia
birth
2n/4C
formation of
primordial follicle
pool
mitotic
divisions
differentiated
spermatogonia
P10
meiosis I
2n/4c
1ary spermatocyte
1st meiotic division
1n/2c
1n/2c
2ary spermatocyte
2nd meioic division
1n/1c
1n/1c
1n/1c
1n/1c
spermatid
P20
ovulation
GV oocyte (2n/4c)
exit of arrest and
completion of 1st
meiotic division
extrusion of a polar body
spermatozoa
MII oocyte (1n/2c)
arrest in
metaphase II
meiosis II
fertilization
zygote
completion of 2nd
meiotic division after
fertilization (1n/1c)
extrusion of a second polar body

Figure 1.2: Timing of key events during spermatogenesis and oogenesis.

At embryonic day 13.5, male germ cells enter mitotic arrest, whereas female germ cells undergo DNA replication and initiate meiosis. Male germ cells resume mitotic cell divisions after birth and develop into undifferentiated spermatogonia. These cells can either self-renew (called spermatogonial stem cells) or further develop into differentiated spermatogonia, giving rise to spermatocytes. Spermatocytes undergo two meiotic divisions and give rise to haploid spermatids, which transform into mature spermatozoa. Female germ cells, on the other hand, arrest during their first meiotic division at diplotene in prophase I around E17.5. After birth, germ cell cysts break down and the primordial follicle pool is established, each follicle containing one arrested oocyte surrounded by granulosa cells. From puberty onwards, meiosis is resumed in a subset of oocytes each month after a surge of gonadotropins. The first meiotic division is completed and oocytes arrest again in metaphase II of the second meiotic division. Upon fertilization, the second division is fully completed. 2n=diploid cells, 2 set of chromosomes; 1n=haploid cells, one set of chromosomes; c=number of chromatids

1.1.6. On the importance of translational regulation during murine germ cell development

Post-transcriptional regulation of gene expression can occur at several different levels affecting processes such as mRNA processing (polyadenylation, capping, and splicing), mRNA export and localization, mRNA decay, and mRNA translation. The sum of these regulatory mechanisms controls if, where, and how efficiently a specific mRNA transcript is translated into a protein (Lackner and Bähler 2008).

Hence, translational regulation lies at the core of post-transcriptional regulation. Translational regulation can either occur at the global level, affecting the majority of mRNAs of the cell, or can be restricted to a specific subset of mRNAs (Gebauer and Hentze 2004; Lackner and Bähler 2008). Global translation rates are frequently regulated by phosphorylation (activation) or proteolysis of key translational initiation factors, affecting the rate-limiting step of translational initiation. In contrast, mRNA specific translation is mediated to a large part by proteins (or miRNAs) which recognize and bind to certain sequence elements of the RNA transcript (Gebauer and Hentze 2004; Lackner and Bähler 2008). Such regulatory sequences define the translational fate of mRNAs and include the CAP structure (5'UTR), the poly(A) tail (3'UTR), internal ribosome entry sequences (IRESs), upstream open reading frames (uORFs), secondary or tertiary RNA structures and specific binding sequences for regulatory proteins (Gebauer and Hentze 2004).

RNA binding proteins (RBPs) and their interplay with mRNAs are central to post-transcriptional regulation and modulate every step of RNA metabolism, from RNA processing (alternative splicing and polyadenylation) to mRNA stability, localization and translation (Abaza and Gebauer 2008).

Regulation at the translational level is rapid and usually reversible, and allows fine tuning of gene expression (many genes have been shown to be regulated at the transcriptional and translational level – e.g. TNF-α) (Lackner and Bähler 2008). Post-transcriptional gene regulation is of particular importance when transcriptional control is not possible (Lackner and Bähler 2008). Such transcriptional quiescent phases occur at distinct times during mammalian germ cell development, in both male and female germ cells:

During female germ cell development, maturing oocytes are transcriptionally inactive - this state is maintained through fertilization and in the early embryo, until zygotic gene activation occurs in the 2-cell stage embryo (Clarke 2012). In fact, RNA synthesis could not be detected in the maturing oocytes (G. P. Moore et al. 1974), RNA polymerase II activity is absent (G. P. M. Moore 1975), and total poly (A) content does not increase in the early embryo (Levey, Stull, and Brinster 1978). Further, RNA synthesis inhibitors do not affect the observed changes in the protein synthesis pattern (Braude et al. 1979). All these observations indicate post-transcriptional regulation of gene expression

Transcriptionally active growing oocytes accumulate large amounts of mRNAs, which are stored for later use to support oocyte maturation and oocyte-to-zygote transition (Clarke 2012). In fact, accumulated mRNAs are remarkably stable (estimated half-life of 8-12 days) (Brower et al. 1981), however, 90% are degraded after the first embryo division (Hamatani et al. 2004). Given that maturing oocytes and the zygote must undergo several important processes during the transcriptional quiescent phase, tight post-transcriptional regulation of available mRNAs is likely.

Interestingly, mouse oocytes can re-enter meiosis in the presence of protein synthesis inhibitor cycloheximide, however for meiotic progression de novo protein synthesis is necessary (Fulka et al. 1986; Hampl and Eppig 1995; Reddy et al. 2009; Han et al. 2012). Global analysis of mRNA translation in the (transcriptionally silent) maturing oocyte revealed that although a considerable destruction of mRNA transcripts take place, 25% of the transcripts are stable while being repressed (J. Chen et al. 2010).

A recent study investigated how the pool of actively translated mRNAs changes on a global level at the onset of embryogenesis (Potireddy et al. 2006). Using sucrose gradient centrifugation, free ribonucleoproteins (RNPs) were separated from polyribosomes and the associated pools of translationally inactive (RNPs) and active mRNAs were analysed using microarray. Indeed, the profiles of transcripts being actively translated changes during the transition of MII oocytes to zygotes, with a translational switch from transcripts encoding proteins involved in the homeostatic process to biosynthetic processes (Potireddy et al. 2006).

The mechanism of how oocytes store, translate and degrade huge quantities of mRNAs have been intensively studied (reviewed in (Clarke 2012)). In lower organisms, such as *Drosophila* or *Xenopus* oocytes, post-transcriptional regulation mechanisms are well characterized and rely heavily on the function of RBPs (reviewed in (Bianchi and Sette 2011)). In mammalian oocytes and early embryos, although several RBPs are highly conserved and abundant (for instance, CPEB1 protein), much less is known about their function, the underlying mechanism or mRNA targets (Bianchi and Sette 2011; Gunter and McLaughlin 2011). Knockout or knockdown of several RBPs leads to impaired oocyte maturation and fertility. For instance, deletion of the RNA binding protein embryonic poly A binding protein (EPAB) results in a failure to translationally activate key transcripts (Guzeloglu-Kayisli et al. 2012), further supporting a critical role of translational control.

In male germ cells, several studies indicate a critical role of translational regulation during transcriptional quiescence. During spermatogenesis, two phases of transcriptional quiescence occur: The first phase is during early meiosis in leptotene and zygotene spermatocytes when DNA breaks are repaired following homologous recombination. The second phase is during the transition of spermatids to mature spermatozoa after histone replacement by transition proteins (TNP) and eventually protamines (PRM) (Braun 1998; Kleene 2001).

Recent transcriptome analyses of different, highly purified cell populations during spermatogenesis (separated via FACS sorting) revealed a gap between the transcriptional activation of genes and the time of expected function (da Cruz et al. 2016). For instance, pachytene cells (meiotic cells) already express many genes involved in post-meiotic processes such as sperm motility and sperm-egg recognition (da Cruz et al. 2016). Further, a proteomic study comparing mRNA levels from published datasets with protein levels at distinct cell stages during spermatogenesis described a set of mRNAs which were

translationally repressed in pachytene cells and de-repressed in round spermatids (Gan et al. 2013), further supporting a role for translational regulation (Gan et al. 2013).

Such translational delay during spermatogenesis has been described by several studies (Kleene 2001; Braun 1998; Licatalosi 2016). Different post-transcriptional regulatory mechanisms have been reported such as mRNA sequestration into free ribonucleoproteins particles (Iguchi, Tobias, and Hecht 2006), regulation of poly A tail length (Idler and Yan 2012), repressor protein binding to UTRs of specific transcripts (Cullinane, Chowdhury, and Kleene 2015), a role of microRNAs, piRNAs (Yadav and Kotaja 2014) and antisense long non-coding RNAs (Bao et al. 2013), amongst others.

Timely (delayed) expression of proteins during transcriptional quiescence is crucial and early production can have detrimental effects, as exemplified by experiments inducing premature translation of protamine 1 or transition protein 2 (TNP2) (K. Lee et al. 1995; Tseden et al. 2007). It is thought that the majority of germ cell mRNAs are translationally repressed and activation of select mRNAs occurs at specific stages of development (Licatalosi 2016). Most of the translational repression is likely mediated through RNA binding proteins. For example, NANOS2 has been implicated in the repression of spermatogonial stem cell differentiation via selectively repressing the translation of differentiation-promoting mRNAs through recruitment into mRNP complexes (Z. Zhou et al. 2015). Further, NANOS2 associates with the CCR4-NOT deadenylation complex, likely promoting deadenylation of mRNAs and subsequent degradation (A. Suzuki et al. 2012).

In summary, during transcriptional quiescent times in germ cell development, regulation of gene expression relies on post-transcriptional mechanisms. The observed changes in the pool of actively translated mRNAs during these transcriptionally inactive phases indicate tight post-transcriptional regulation. Studies demonstrating impaired or arrested germ cell development upon precocious translation, inhibition of global protein synthesis, or deletion of RBPs all support the idea that translational regulation during transcriptionally quiescent phases of germ cell development plays an important role. Further work is needed to understand the underlying molecular mechanisms in more detail. Of note, very little is currently known about the role of translational regulation during transcriptionally active phases of germ cell development, such as in primordial germ cells.

1.2. Epigenetic reprogramming

A key feature of primordial germ cell development is epigenetic reprogramming. In early germ cells, the epigenetic landscape is drastically remodelled to allow cells to re-acquire a naïve epigenetic state. This epigenetic state underlies the ability of mature oocytes and sperm to give rise to a totipotent zygote. Reprogramming events occur in two distinct phases: the first one occurs at the beginning of migration and the second one once primordial germ cells have entered the genital ridge (Figure 1.1).

1.2.1. Phase I – Reprogramming events in migratory PGCs

Migratory PGCs undergo a first wave of epigenetic reprogramming directly following specification. Starting as early as E7.5, there is a reduction in H3 lysine 9 dimethylation (H3K9me2), followed by an increase in histone H3 lysine 27 trimethylation (H3K27me3) from E8.5 onwards. During these changes, PGCs are in cell cycle arrest at the G2 phase and have repressed transcriptional activity (Seki et al. 2005, 2007). In addition, an increase of H3K4me and H3K9Ac is observed (Hajkova et al. 2008).

At E10.5, an accumulation of H2A/H4 arginine 3 di-methylation (H2A/H4R3me2s) can be observed in PGCs compared to surrounding somatic cells. The enzyme responsible for this modification is an arginine-specific histone methyl transferase called PRMT5 and its expression increases from E8.5 onwards. BLIMP1 and PRMT5 have been suggested to form a complex in PGCs which mediates this modification, based on co-localization in PGCs using immunofluorescence and co-immunoprecipitation in 293T cells (Ancelin et al. 2006).

In addition to chromatin changes, a first wave of DNA demethylation occurs in PGCs between E8.0-E9.0 (Seki et al. 2005; Guibert, Forné, and Weber 2012). By E9.5, global methylation levels are already reduced to 30%, mostly affecting gene bodies, intergenic regions and promoters. In contrast, methylation levels of retrotransposons, imprint control regions and germline gene promoters are maintained (Seisenberger et al. 2012; Guibert, Forné, and Weber 2012).

Of note, the process of X reactivation in female PGCs is also initiated in migratory PGCs via decreased expression of *Xist*. However, complete reactivation is only achieved a few days later in gonadal PGCSs (Sugimoto and Abe 2007; de Napoles, Nesterova, and Brockdorff 2007; Chuva de Sousa Lopes et al. 2008).

1.2.2. Phase II – Reprogramming events in gonadal PGCs

Once migrating PGCs have entered the genital ridge at E10.5, the second wave of reprogramming occurs, including extensive global DNA demethylation at germline promoters, repetitive elements and imprinted genes (Hajkova et al. 2002; Seisenberger et al. 2012; Guibert, Forné, and Weber 2012; Hill et al. 2018). Erasure of parental imprints is essential to establish new sex-specific imprints during gametogenesis (Bartolomei and Ferguson-Smith 2011). Following this reprogramming event, genome-wide DNA methylation levels reach the lowest point observed at any time during development (Hill, Amouroux, and Hajkova 2014). This hypomethylated state is long lived in female germ cells, which only start to re-methylate their DNA after birth. To the contrary, male germ cells reacquire DNA methylation a few days after the global reprogramming at around E16.5 (Seisenberger et al. 2012).

The molecular mechanism underlying the observed global loss of DNA methylation has been a subject of debate, with both active, replication-independent and passive, replication-dependent models being proposed (Hackett, Zylicz, and Surani 2012).

In replicating cells, DNA methylation patterns are typically maintained through the activity of DNMT1, a maintenance DNA methyl transferase. DNMT1 is recruited to hemi-methylated DNA and associates with replication forks via binding to UHRF1 and PCNA, respectively (Bostick et al. 2007; Sharif et al. 2007; Chuang et al. 1997). Subsequently, the newly synthesized DNA strand is methylated by DNMT1 activity. Loss of this maintenance methylation, as demonstrated in systems lacking DNMT1 or UHRF1, results in passive DNA demethylation, characterized by a gradual depletion of 5mC over several mitotic cell divisions (Bostick et al. 2007; Sharif et al. 2007).

Interestingly, de novo methyl transferases (Dnmt3a, Dnmt3b) and Uhrf1, which is crucial for DNMT1 recruitment, are transcriptionally repressed in PGCs upon their specification until E13.5. Of note, the maintenance methyl transferase (Dnmt1) is robustly expressed throughout this time (Yabuta et al. 2006; Kurimoto et al. 2008; Kagiwada et al. 2013). Consistent with the gene expression data, immunofluorescence analysis shows no UHRF1 signal in PGCs between E9.5 and E12.5 and impaired DNMT1 recruitment to replication forks (Kagiwada et al. 2013).

At selected imprinted foci, the observed demethylation rates do not exceed the expected rates from replication coupled dilution (based on an estimated PGC doubling time of 12.6h

after E9.5) (Kagiwada et al. 2013). In combination with the observed downregulation of the methyl transferase machinery, a passive replication-based DNA demethylation model (particularly at imprinted loci) has been proposed (Kagiwada et al. 2013).

Alternatively, several groups have proposed active, replication independent DNA demethylation mechanisms in PGCs, driven by enzymes which can chemically convert 5mC or its derivatives.

One such enzyme family consists of the ten-eleven translocation (TET) dioxygenases. TET enzymes catalyse the oxidation of 5mC to 5-hydroxymethyl cytosine (5hmC) and its higher oxidative derivatives 5-formylcytosine (5fC) and 5-carboxylcytosine (5caC) (Tahiliani et al. 2009; Ito et al. 2011; He et al. 2011). 5hmC is a crucial intermediate which can be reversed to unmethylated cytosine via different routes, including active, replication independent (Popp et al. 2010; Hajkova et al. 2010) and passive, replication dependent mechanisms (Yamaguchi, Hong, et al. 2013; Hackett et al. 2013):

A passive dilution model of TET generated 5hmC has been put forward based on the low enzymatic activity of the maintenance methyl transferase DNMT1 towards 5hmC, as demonstrated for human DNMT1 (Valinluck and Sowers 2007). Of note, UHRF1 has been shown to bind 5hmC with similar affinity than 5mC in vitro (Frauer et al. 2011).

Such a passive dilution model is further supported by the observation that rates of 5hmC demethylation, as determined by Glu-qPCR at selected imprinted loci (Peg3, Peg10) and the *Dazl* promoter, correlate well with the predicated rate of replication-dependent demethylation (Hackett et al. 2013). In addition, 5hmC staining of chromosome spreads revealed enrichment of 5hmC on several chromosomes at E11.5, while at E12.5 decreased signal was observed due to only one of the sister chromatids being enriched for 5hmC (Yamaguchi, Hong, et al. 2013). Of note, 5hmC derivatives 5fC and 5caC were not enriched upon loss of 5hmC, as determined through IF stainings, further supporting passive dilution of 5hmC (Hackett et al. 2013; Yamaguchi, Hong, et al. 2013).

However, there are also several observations which are inconsistent with this proposed model. Although 5mC and 5hmC cannot be distinguished in bisulphite sequencing (Y. Huang et al. 2010), conversion of 5mC to 5hmC followed by passive dilution would be observable as gradual signal loss during Bis-Seq. However, rapid signal loss is observed in Bis-Seq datasets from gonadal PGCs, arguing against gradual 5hmC dilution (Seisenberger

et al. 2012). Furthermore, absolute levels of 5hmC are very low in PGCs, further arguing against 5mC conversion to 5hmC followed by passive dilution (Hill et al. 2018).

Alternatively, active, replication independent dilution of 5hmC or its derivatives have been proposed, involving DNA glycosylases such as thymine DNA glycosylase (TDG), MBD4 or a yet unidentified glycosylase. The resulting abasic site will trigger the base excision repair (BER) pathway, resulting in the reinstatement using an unmethylated cytosine (Messerschmidt, Knowles, and Solter 2014). TDG has been shown to recognize and excise 5caC, as demonstrated in *in vitro* assays and HEK293T cell lines (He et al. 2011). Further, deletion of TDG in mESCs leads to an increase in 5caC and 5fC(Shen et al. 2013).

In PGCs, TDG transcript and protein (as judged by IF studies) was not detected between E10.5-E13.5 (Hajkova et al. 2010). On the contrary, two other reports clearly detected *Tdg* transcripts in PGCS with highest levels observed at E9.5, followed by a continued decrease thereafter until E12.5 and E13.5 (Kagiwada et al. 2013; Hackett et al. 2013). Activation of the BER machinery is observed in PGCs around this time though (Hajkova et al. 2010). Further work needs to be done to support the proposed model of TDG-mediated base excision repair to remove 5hmC.

Overall, TET driven DNA demethylation during epigenetic reprogramming has been intensively studied. The fact that PGCs express *Tet1* and at a lower level *Tet2*, supports TET driven DNA demethylation models (Hajkova et al. 2010; Kagiwada et al. 2013; Hackett et al. 2013). In addition, 5hmC was observed at genomic imprints undergoing DNA demethylation, indicating a role for TET1 and 5hmC in imprint erasure (Hackett et al. 2013).

Interestingly, recent quantitative analysis of global 5mC and 5hmC levels using LC-MS/MS did not show a correlation between 5hmC levels and the extent of 5mC/5hmC signal decrease due to epigenetic reprogramming in E10.5 and E11.5 PGCs (Hill et al. 2018). Hence, the loss of 5mC does not result in the reciprocal 5hmC increase, arguing against a TET1-mediated global DNA demethylation mechanism (Hill et al. 2018). More importantly, loss of TET1 in PGCs does not impair genome-wide DNA demethylation (Yamaguchi, Shen, et al. 2013; Hill et al. 2018). However, DNA methylation levels on some meiotic gene promoters and imprint control regions were increased in *Tet1* knockout PGCs (Yamaguchi, Shen, et al. 2013; Yamaguchi et al. 2012). Furthermore, mice deficient for TET1 or TET1/TET2 show a fertility phenotype in line with defective imprinting (Dawlaty et al. 2011; Yamaguchi, Shen, et al. 2013), suggesting defective reprogramming of imprinted genes. However, a proportion of embryos show a normal methylation pattern of imprints and survive until adulthood

(Dawlaty et al. 2011). A recent study has proposed that TET1 drives removal of aberrant residual (or de novo) DNA methylation following the global DNA demethylation wave during epigenetic reprogramming, rather than acting on a global scale (Hill et al. 2018).

Apart from TET enzymes, another family of enzymes implicated in active DNA demethylation mechanisms are the deaminases activation-induced cytidine deaminase (AID) and apolipoprotein B mRNA-editing, enzyme-catalytic, polypeptide 1 (APOBEC1) (Messerschmidt, Knowles, and Solter 2014). AID/APOBEC1 can catalyse the deamination of 5mC to uracil, as demonstrated *in vitro* and in *E.Coli* (Morgan et al. 2004). The resulting T:G mismatches could further trigger TDG or MBD4 mediated excision and repair through the BER pathway Additionally, AID can also convert TET generated 5hmC to 5-hydroxymethyluridine (5hmU), which has been shown to be a target of TDG (Cortellino et al. 2011).

To what extent AID-triggered DNA demethylation acts as an active mechanism during PGC reprogramming is still a matter of debate. Loss of AID leads to impaired genome wide 5mC demethylation in PGCs by E13.5, supporting a role (at least in part) of AID in 5mC erasure in PGCS (Popp et al. 2010). However, despite AID deficiency in mutant PGCs, 5mC methylation levels still decrease significantly to 22% (male) and 20% (females) compared to 74% in E13.5 embryonic soma (Popp et al. 2010). In wild-type PGCs 5mC methylation levels decrease to 18% (male) and 8% (female) by E13.5 (Popp et al. 2010).

Further, *Aid* expression in PGCs has only been detected from E12.5 onwards (Popp et al. 2010; Hajkova et al. 2010), while another report observed no expression between E9.5 to E13.5 (Kagiwada et al. 2013). Of note, *Apobec1* expression was detected either at very low levels between E9.5-E13.5 or almost absent by E11.5 (Kagiwada et al. 2013; Hajkova et al. 2010). The low expression levels of the AID/APOBEC deaminases around the time of global DNA demethylation argue against an active AID-mediated DNA demethylation mechanism in murine PGCs.

In view of the current findings, it is apparent that the process of DNA demethylation in PGCs is complex and likely involves a combination of active and passive processes. Also, it is possible that additional to date unidentified pathways exist (Hackett, Zylicz, and Surani 2012).

In addition to global loss of DNA methylation, changes in the nuclear architecture and extensive remodelling of the chromatin landscape occur. The nuclear size increases, along with decondensation of heterochromatin and loss of chromocenters (Hajkova et al. 2008). Further, genome-wide histone replacement leads to the loss of numerous histone modifications. Repressive histone marks H3K9me3 and H3K27me3 are transiently lost, along with the disappearance of linker histone H1 and histone variant H2Z (Hajkova et al. 2008).

In summary, developing PGCs erase epigenetic information on all layers (methylation and histone modifications). Following the reprogramming step, the epigenome reaches the most naïve state during development. Recently, reprogramming events have been linked to the PGC-to-gonocyte transition through enabling activation of key genes involved in gametogenesis and meiosis (Hill et al. 2018).

1.3. mTOR signalling pathway

The mechanistic target of rapamycin (mTOR, also known as mammalian target of rapamycin) signalling pathway is a key regulator of cellular growth, proliferation and survival. Extracellular signals as well as intracellular signals are integrated via the mTOR signalling pathway to either promote anabolic or catabolic processes, depending on the cell's energy status (Laplante and Sabatini 2009).

mTOR signalling plays pivotal roles in metabolism and maintenance of organismal homeostasis, particularly during nutrient shortage. Many diseases are characterised by deregulated mTOR signalling, such as type II diabetes, neurodegenerative disease and cancer. Inhibitors of mTOR are used in clinics as anti-cancer drugs and immunosuppressants after kidney transplantation (Laplante and Sabatini 2012). In addition, inhibition of mTOR signalling increases life span in many model organisms (*C.Elegans*, *drosophila* and *mouse*), implicating its role during aging (Laplante and Sabatini 2012).

1.3.1. mTOR and its protein complexes mTORC1 & mTORC2

mTOR is a highly conserved serine/threonine kinase and part of the PI3K-related kinase family. It was discovered in the 1990s as a direct target of rapamycin (Sabatini et al. 1994; Brown et al. 1994; Sabers et al. 1995), a macrolide which was first purified from bacteria found in soil on the Easter Islands (Vézina, Kudelski, and Sehgal 1975). Rapamycin had broad anti-proliferative effects and was shown to bind to the intracellular receptor FKBP12, an immunophilin of the FK506-binding protein (FKBP) family that binds immunosuppressants (Bierer et al. 1990). Eventually, biochemical studies identified mTOR as the direct target of the rapamycin-FKB12 complex (Sabatini et al. 1994; Brown et al. 1994; Sabers et al. 1995).

mTOR nucleates two structurally and functionally distinct multi-protein complexes, namely the rapamycin sensitive mTOR complex 1 (mTORC1) and the rapamycin insensitive mTOR complex 2 (mTORC2) (Figure 1.3) (Laplante and Sabatini 2009). Deletion of *Mtor*, and therefore ablation of both complexes, leads to embryonic lethality shortly after implantation, around E5.5-E6.5, due to defective cell proliferation in embryonic and extraembryonic tissues (Murakami et al. 2004; Gangloff et al. 2004).

In the next two sections I will describe the structure, biological functions and input signals of these two complexes, with a particular focus on mTORC1.

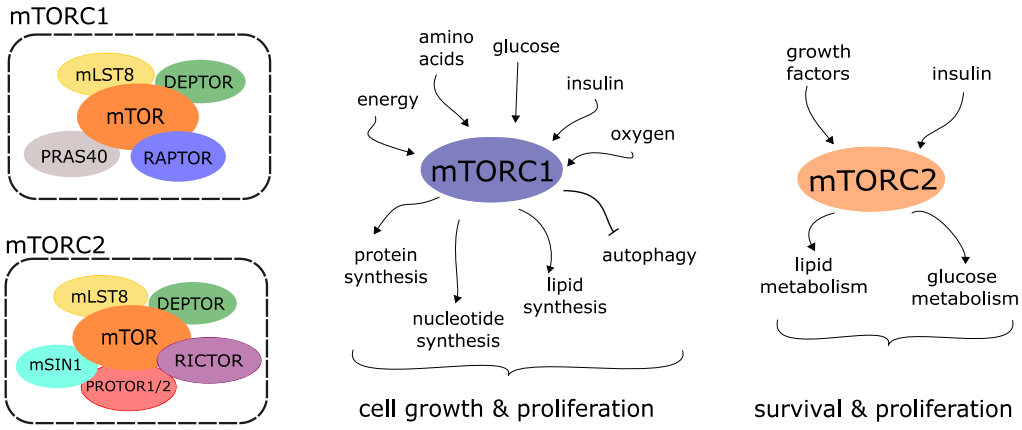

Figure 1.3: mTORC1 and mTORC2 signalling complexes.

Distinct input signals leading to activation of mTORC1 or mTORC2 and downstream biological functions are shown.

1.3.1.1. mTORC1

mTORC1 consists of 5 proteins: mTOR, RAPTOR (regulatory associated protein of mTOR), PRAS40 (proline-rich Akt substrate 40kDa), mLST8 (mammalian lethal with Sec13 protein 8) and DEPTOR (DEP-domain-containing mTOR-interacting protein) (Figure 1.3) (Laplante and Sabatini 2009).

DEPTOR and PRAS40 are negative regulators of mTORC1, whereas mTOR is the catalytic subunit (Laplante and Sabatini 2009) The rapamycin-FKBP12 complex blocks substrate recruitment and access into the catalytic cleft of the mTOR kinase domain (H. Yang et al. 2013). However, such allosteric inhibition affects some substrates more than others, leading only to partial inhibition in some cases (Choo and Blenis 2009).

mTORC1 is a master regulator of cell growth. Active mTORC1 signalling promotes anabolic processes for *de novo* synthesis of proteins, lipids, nucleotides and organelles, while inhibiting catabolic processes such as autophagy (Figure 1.3) (Laplante and Sabatini 2009). Perhaps not surprising given these many biological functions, ablation of mTORC1 signalling via deletion of *Raptor* is also embryonic lethal shortly after implantation (Guertin et al. 2006).

Four major signals can activate mTORC1 - growth factors (e.g. insulin), nutrients (e.g. amino acids, especially leucine and arginine), intracellular energy status (high ATP: AMP ratio) and oxygen levels. Additional signals include WNT signalling, inflammation and genotoxic stress (Figure 1.3) (reviewed in Laplante and Sabatini 2009).

mTORC1 is widely distributed in the cell cytoplasm and, upon nutrient availability, translocates to the lysosomal surface. This translocation is mediated via activation of RagGTPases (RAS-related GTP-binding protein (RAG) family of small GTPases). At the lysosomal surface, mTORC1 is activated via the small GTPase RHEB (RAS homologue enriched in brain) (Figure 1.4) (Saxton and Sabatini 2017).

Many upstream signal transduction pathways, such as the phosphoinositide 3-kinase (PI3K)–AKT pathway and the RAS-ERK pathway, converge on the negative regulator of mTOR called Tuberous Sclerosis Complex (TSC) (Saxton and Sabatini 2017). The Tuberous Sclerosis Complex (TSC1/2) is the GTPase-activating protein for RHEB. Phosphorylation of the TSC complex via upstream kinases, such as AKT or ERK, lead to its inhibition and GTP-bound, active RHEB can subsequently activate mTORC1 at the lysosomal surface (Figure 1.4) (Saxton and Sabatini 2017).

1.3.1.2. mTORC2

mTORC2 consists of three proteins shared with mTORC1, namely mTOR, mLST8 and DEPTOR, and three unique proteins, RICTOR (rapamycin insensitive companion of mTOR), mSIN1 (mammalian stress-activated protein kinase interacting protein 1) and PROTOR-1 (protein observed with Rictor-1) (Figure 1.3) (Laplante and Sabatini 2009).

mTORC2 has distinct functions from mTORC1. Ablation of the mTORC2 signalling complex via deletion of *Rictor* is embryonic lethal around mid-gestation (~ E10.5-E11.5), possibly due to vasculature defects. Importantly, these knockout studies present the first *in vivo* evidence of AKT being a direct target of mTORC2 (Guertin et al. 2006; Shiota et al. 2006). Previous biochemical and *in vitro* studies in cancer cells and adipocytes showed that mTORC2 can phosphorylate AKT at the Ser473 site (Hresko and Mueckler 2005; Sarbassov et al. 2005). For full activation AKT requires phosphorylation at two distinct sites - Ser473 and Thr308, the latter is mediated by PDK1 (Figure 1.4) (Alessi et al. 1997; Stephens et al. 1998; J. Yang et al. 2002; Scheid, Marignani, and Woodgett 2002). In addition, mTORC2 can localize to actively translating ribosomes and co-translationally phosphorylate nascent AKT, promoting stability of the nascent AKT peptide (Oh et al. 2010).

AKT is a central signalling hub and its regulation via mTORC2 links mTORC2 signalling to cell survival, metabolism and proliferation (Laplante and Sabatini 2009). In addition, mTORC2 signalling has also been reported to be involved in cytoskeletal organization (Figure 1.3) (Jacinto et al. 2004; Sarbassov et al. 2004)

However, many open questions remain regarding its function and input signals as mTORC2 is less studied than mTORC1. Growth factors are considered to be an upstream signal and subsequently, the PI3K signalling pathway leads to activation of mTORC2 and increased AKT Ser473 phosphorylation (Figure 1.3) (P. Liu et al. 2015).

Of note, mTORC2 is insensitive to rapamycin under acute treatment/inhibition (Jacinto et al. 2004). However, prolonged rapamycin treatment can also lead to mTORC2 inhibition due to failed complex assembly (Sarbassov et al. 2006).

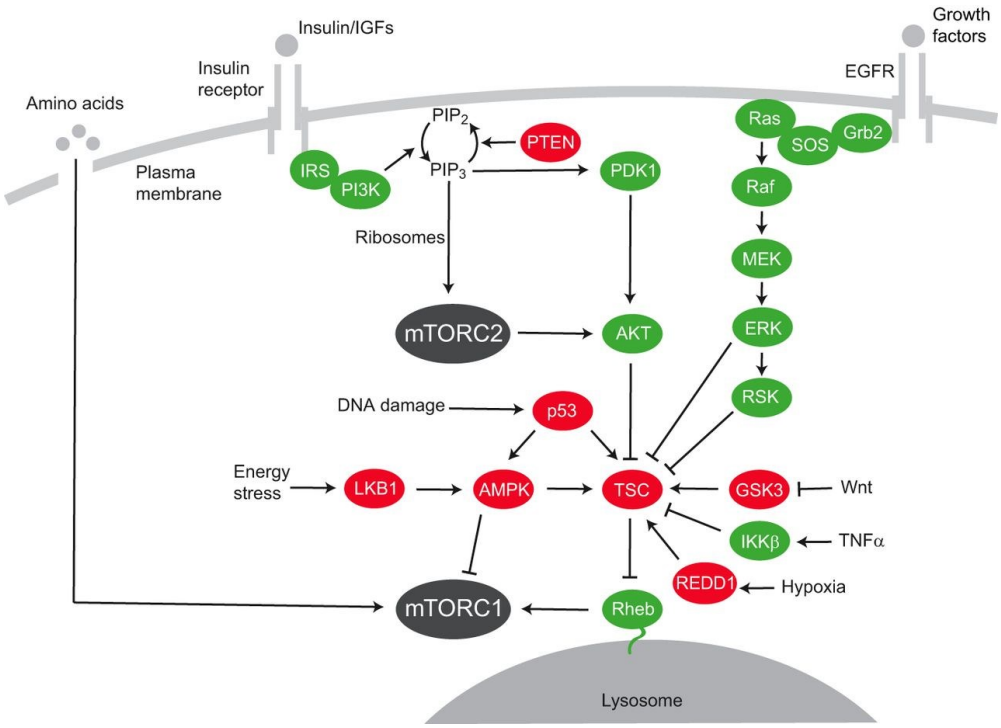

Figure 1.4: Overview of signalling pathways regulating mTORC1 and mTORC2.

Insulin signals via the insulin receptor and activates insulin receptor substrates (IRS), which further activate PI3K. PI3K stimulates phosphorylation of PIP2 to PIP3. PIP3 recruits PDK1 and AKT to the plasma membrane, stimulating phosphorylation of AKT at the Thr308 site by PDK1. MTORC2 can further activate AKT via phosphorylation at the Ser473 site. Activated AKT inhibits the TSC complex (via inhibition of the GAP activity), which further activates RHEB. Activated RHEB can phosphorylate and activate mTORC1 at the lysosomal surface. Translocation to the lysosomal surface is mediated via RAG GTPases in the presence of nutrients (amino acids). In addition, growth factors can signal through the RAS-MAPK pathway, activating ERK and its downstream substrate RSK, to inhibit the TSC complex. Other non-classical input signals are WNT signalling, TNFα signalling, oxygen levels and DNA damage. Green shows positive regulators, red shows negative regulators of mTOR; This figure is adapted from (D. Meng, Frank, and Jewell 2018)

1.3.2. Downstream targets of mTORC1

As a central regulator of cellular growth, mTORC1 signalling is involved in many downstream biological processes, which are described in more detail below.

1.3.2.1. Lipid, nucleotide, and glucose metabolism

New membrane formation and expansion requires *de novo* lipid synthesis, which is driven to a large part by the sterol responsive element binding proteins (SREBPs). These transcription factors induce the expression of genes involved in cholesterol and fatty acid synthesis if sterol levels are low (Rawson 2003; Espenshade and Hughes 2007). Interestingly, in addition to canonical activation of this pathway, mTORC1 signalling can also activate SREBPs separately (Porstmann et al. 2008). mTORC1-dependent activation is mediated either through the activation of the downstream target S6K1 (Düvel et al. 2010) or through phosphorylation and inhibition of LIPIN1, a negative regulator of SREBP in the absence of mTORC1 signalling (Peterson et al. 2011).

In addition to lipid synthesis, mTORC1 signalling also facilitates growth by promoting nucleotide synthesis required for ribosome biogenesis and DNA replication in proliferating cells. mTORC1-dependent activation of the transcription factor ATF4 induces purine synthesis via increased expression of MTHFD2, a component of the tetrahydrofolate cycle which provides one-carbon units (in mitochondria) (Ben-Sahra et al. 2016). Furthermore, the mTORC1 target S6K1 activates its downstream target carbamoyl-phosphate synthase (CAD) via phosphorylation, an important component in the *de novo* synthesis of pyrimidines (Robitaille et al. 2013; Ben-Sahra et al. 2013).

Lastly, mTORC1 signalling promotes a shift from oxidative phosphorylation to glycolysis through increased translation of HIF1a, which further drives the expression of several glycolytic enzymes (Düvel et al. 2010). In addition, mTORC1 activated SREBPs increase the expression of the rate-limiting enzyme *G6pd* of the oxidative pentose phosphate pathway (PPP), leading to increased flux. The PPP pathway utilizes glucose to generate NADPH and ribose needed for biosynthetic processes and nucleotide synthesis (Düvel et al. 2010).

1.3.2.2. Regulation of protein turnover

In addition to promoting anabolic processes, mTORC1 signalling also suppresses catabolic processes, most notably autophagy. One of the first steps in autophagy is the formation of the autophagosome, which is driven by the kinase ULK1. ULK1 is usually activated by AMPK under low energy levels. Active mTORC1 phosphorylates ULK1 and prevents its activation through AMPK, inhibiting successful autophagy induction (J. Kim et al. 2011). Further, mTORC1 can phosphorylate and subsequently inhibit the nuclear translocation of the transcription factor TFEB, which induces expression of genes crucial for the autophagy machinery and lysosomal biogenesis (Martina et al. 2012; Settembre et al. 2012; Roczniak-Ferguson et al. 2012).

Apart from autophagy, mTORC1 has also been linked to another major protein turnover pathway, namely the ubiquitin-proteasome system (UPS) (Zhao et al. 2015; Rousseau and Bertolotti 2016). Following covalent ubiquitination of selected targets, modified proteins are degraded by the 20S proteasome (Glickman and Ciechanover 2002). Acute mTORC1 inhibition (with rapamycin and/or TORIN1) lead to either an increase in protein ubiquitination (Zhao et al. 2015) or an increased abundance of proteasomal chaperones through ERK5 inhibition (Rousseau and Bertolotti 2016), both scenarios resulted in a rapid increase of proteolysis. Of note, an earlier study reported that upon hyperactivation of mTORC1 signalling (via genetic ablation of TSC2), proteasome activity increased due to elevated expression of genes encoding proteasome subunits downstream of NRF1 (Zhao et al. 2015).

1.3.2.3. Regulation of protein synthesis

Most importantly, and of particular interest to this thesis, is the regulation of protein translation through mTORC1. The first characterised targets and the most studied ones are the two downstream effector families, ribosomal S6 kinases and 4E-binding proteins (Burnett et al. 1998; Ma and Blenis 2009).

1.3.2.3.1 S6 kinases (S6Ks)

Ribosomal S6 kinases are serine/threonine kinases and belong to the ACG kinase family (Laplante and Sabatini 2009). Two distinct genes *Rps6kb1* and *Rps6kb2* encode for ribosomal S6 kinase 1 (S6K1) and ribosomal S6 kinase 2 (S6K2) (Magnuson, Ekim, and Fingar 2012).

Both kinases share 84% amino acid sequence homology in their kinase domains, including many regulatory phosphorylation sites (Lee-Fruman et al. 1999).

S6K1 exists in 4 isoforms due to alternative start sites or splicing variants: p85, p70, p60, p31. S6K2 exists in 2 isoforms, p56 and p54. Isoforms differ in their cellular localization (constitutively located in the nucleus vs shuttling between nucleus and cytoplasm) and expression patterns (Magnuson, Ekim, and Fingar 2012; Pardo and Seckl 2013). From now on, S6K1 and S6K2 will refer to the most common variants p70S6K1 and p54S6K2, with a special focus on S6K1.

S6 kinases are activated via phosphorylation at several sites in response to various upstream signals such as growth factors and nutrients (Magnuson, Ekim, and Fingar 2012). Active mTORC1 signalling directly phosphorylates S6K1 at the Thr389 residue and S6K2 at the Thr388 residue (Isotani et al. 1999; Burnett et al. 1998). For full activation, however, further phosphorylation at the Thr229 (S6K1) or Thr229 (S6K2) is essential (Weng et al. 1998). This is carried out by PDK1 in an mTORC1 independent manner (Alessi et al. 1998; Pullen et al. 1998; Lee-Fruman et al. 1999).

Fully activated S6K1 phosphorylates and activates several downstream proteins involved in ribosome biogenesis and protein synthesis (Figure 1.5). The best characterised downstream target is ribosomal protein S6 (rpS6), a subunit of 40s ribosomal complex (Ma and Blenis 2009; Shimobayashi and Hall 2014). Other substrates, which are not part of the translational machinery, include upstream targets such as mTOR and insulin receptor substrate 1 (IRS1), forming important negative feedback loops (Holz and Blenis 2005; Harrington et al. 2004).

Of note, like activation of S6 kinases, many downstream targets of S6 kinases, including rpS6, are not solely phosphorylated in an mTORC1-dependent manner via mTORC1-S6K1 signalling. Other MAP-ERK activated p90 ribosomal kinases can also phosphorylate and activate these proteins and together regulate many cellular processes (Figure 1.4) (Magnuson, Ekim, and Fingar 2012).

Mice lacking S6K1 or S6K2 are viable and fertile. $S6K1^{-/-}$ mice show reduced size and bodyweight, and their growth retardation already starts and is most pronounced during embryogenesis (Shima et al. 1998). $S6K2^{-/-}$ mice seem slightly larger than wild-type controls, possibly due to compensatory effects from S6K1 (Pende et al. 2004). However, combined deletion of S6K1 and S6K2 results in a more severe phenotype, with perinatal lethality possibly due to hypoxic stress. Very few $S6K1^{-/-}S6K2^{-/-}$ double mutant mice survived day 1

after delivery. However, mice that did survive reached adulthood and were fertile (Pende et al. 2004).

Overall, the described knockout studies demonstrate that S6 kinases are mediators of cellular growth. Subsequent characterisation of *S6k1*$^{-/-}$ mice showed that they are protected from diet-induced obesity (Um et al. 2004) and are long-lived (Selman et al. 2009), implicating S6 kinases in the regulation of obesity and aging.

1.3.2.3.2 4E-binding proteins (4E-BPs)

Eukaryotic initiation factor 4E – binding proteins (4E-BPs) are a family of translational repressors consisting of three paralogues 4E-BP1, 4E-BP2 and 4E-BP3, each encoded by a separate gene (C. Hu et al. 1994; T. A. Lin et al. 1994; Pause et al. 1994; Poulin et al. 1998).

4E-BP3 was originally identified and cloned in human cells. Although several mouse expressed sequence tags (ESTs) were identified, predicted to encode for a protein highly homologous to the human 4E-BP3 protein (Poulin et al. 1998), currently very little is known about 4E-BP3 expression and function in the mouse.

4E-BP1 and 4E-BP2, on the other hand, have been extensively studied in the mouse. The two proteins show 56% identity at the amino acid level, have key phosphorylation sites conserved and are regulated via their phosphorylation state (Pause et al. 1994; T. A. Lin and Lawrence 1996; Fonseca et al. 2014). 4E-BPs are widely expressed and differ in their relative tissue expression patterns – 4E-BP1 is particularly enriched in adipose and pancreatic tissue, and 4E-BP2 is the predominant expressed isoform in the brain (Tsukiyama-Kohara et al. 2001; Banko et al. 2005).

mTORC1 signalling has been shown to directly phosphorylate and inactivate 4E-BPs (Brunn et al. 1997; Burnett et al. 1998), positively regulating initiation of translation (Figure 1.5).

Translation initiation requires the formation of the translation initiation complex at the 5′ cap structure of mRNAs. The eukaryotic initiation factor 4F (eIF4F) complex recognizes the cap structure and together with eIF4B, mRNA secondary structure is unwound to facilitate binding of the 43S pre-initiation complex (Figure 1.5) (Aitken and Lorsch 2012).

4E-BPs can bind to eIF4E, which is part of eIF4F complex, and prevent its assembly. Subsequently, binding of 43s pre-initiation complex to mRNA is inhibited and initiation of translation is blocked (Mader et al. 1995; Marcotrigiano et al. 1999; Siddiqui et al. 2012).

Hierarchical phosphorylation of 4E-BP1 at several residues via active mTORC1 signalling leads to the dissociation from eIF4E, allowing the formation of the initiation complex (Gingras et al. 1999, 2001) and 5'cap dependent mRNA translation (Musa et al. 2016).

Mice lacking 4E-BPs show largely a metabolic phenotype, but the severity of the phenotype depends on the genetic background of the mutants. Overall, loss of 4E-BP1 or 4E-BP2 or both have no effect on viability or fertility (Tsukiyama-Kohara et al. 2001; Banko et al. 2005). 4E-BP1 mutants have reduced adipose tissue, hypoglycemia and males have a higher metabolic rate (Tsukiyama-Kohara et al. 2001). 4E-BP2 mutant mice show compromised memory, special learning and synaptic plasticity (Banko et al. 2005). Double knockout mice suffer from increased sensitivity to diet induced obesity, insulin resistance and over activation of the S6K1 signalling axis (Le Bacquer et al. 2007).

1.3.3. Regulation of translation by 4E-BPs and S6 kinases

Regulation of translation via mTORC1 has been extensively studied via characterizing its mediators S6 kinases and 4E-binding proteins. While the mTORC1-4E-BP1 signalling axis generally promotes cell proliferation, the mTORC1-S6K1-S6 signalling axis promotes cell growth (Dowling et al. 2010; Ruvinsky et al. 2005; Pende et al. 2004; Shima et al. 1998). Both mediators are involved in the regulation of translation, which partly underlies these distinct functions and will be discussed in more detail in the next sections.

1.3.3.1. The role of 4E-binding proteins

4E-binding proteins are translational repressors – they bind to eIF4E, which ablates assembly of the eukaryotic initiation factor 4F (eIF4F) complex and inhibits subsequent binding of the pre-initiation complex and translational initiation. Phosphorylation of 4E-BPs by mTORC1 sequesters these factors away from eIF4E and allows initiation of translation (see 1.3.2.3.2, p. 55).

Several studies showed that the mTOR-4E-BP1-eIF4E axis controls global translation rates to a certain degree. However, in recent years it has become apparent that 4E-BP1 specifically regulates translation of subsets of mRNAs (Roux and Topisirovic 2018; Masvidal et al. 2017).

TOP mRNAs. One subclass are TOP mRNAs containing a 5′ terminal oligopyrimidine motif (5′TOP) or related "top-like" motifs. The 5′TOP motif consists of a cytidine, followed by an uninterrupted sequence of 4-14 pyrimidines, immediately after the 5'cap. TOP mRNAs

largely contain gene products involved in protein synthesis, such as ribosomal proteins, elongation factors and translation initiation proteins (Meyuhas and Kahan 2015).

Ribosome profiling studies showed that under acute chemical inhibition of mTORC1 signalling, translation of TOP mRNAs was greatly suppressed due to impaired initiation (Thoreen et al. 2012; Hsieh et al. 2012), while global translation rates were only moderately affected with a mean reduction of 61% (Thoreen et al. 2012). Knockdown of 4E-BP1 and 4E-BP2 in PC3 prostate cancer cells (Hsieh et al. 2012) and double knockout of 4E-BP1/4E-BP2 in MEFs (Thoreen et al. 2012) rendered the cells resistant to mTORC1 inhibition and subsequent TOP mRNA suppression, suggesting that 4E-binding proteins are the key mediators of TOP mRNA translational regulation downstream of mTORC1 signalling (Hsieh et al. 2012; Thoreen et al. 2012).

However, another study found that under physiological stress conditions (oxygen deprivation, amino acid starvation), translation of TOP mRNAs is repressed via mTOR in an 4E-BP1 independent manner (Miloslavski et al. 2014). In line with that, overexpression of eIF4F does not affect translational repression of TOP mRNAs in mouse erythroleukemia (MEL) cells (Shama et al. 1995).

In summary, these studies demonstrate that many open questions remain regarding translational regulation of TOP mRNAs. It seems likely that mTORC1 can regulate translation in a 4E-BP1-dependent and a 4E-BP1-independent manner (Figure 1.5).

Non-TOP mRNAs. Another subclass of mRNAs sensitive to mTORC1-4E-BP1-eIF4F signalling are non-TOP mRNAs or "eIF4E sensitive mRNAs". These mRNAs are sensitive to changes in 4E-BP1 activity and/or eIF4E levels and divide into two groups based on their 5'UTR regions (Gandin et al. 2016; Masvidal et al. 2017).

One group is characterised by highly structured and long 5' UTRs, which need unwinding via the eIF4F complex. EIF4E is responsible for recruiting the helicase eIF4A into the eIF4F complex, leading to efficient unwinding. This group mainly encodes for proteins involved in cell proliferation, cell-cycle and survival (Gandin et al. 2016). The second group of non-TOP mRNAs is characterised by very short 5'UTRs (<50nt). These mRNAs mainly include genes involved in mitochondrial function and the respiratory chain complex (Gandin et al. 2016). Of note, mRNAs with an intermediate 5'UTR length (70-150 nt) are less sensitive to eIF4E and mostly include housekeeping genes (Roux and Topisirovic 2018).

Overall, the mTOR-4E-BP1 signalling axis seems to specifically regulate translation of mRNA subclasses characterised by specific 5'UTR regions (length and complexity) or by presence of a TOP motif. These subclasses contain genes encoding ribosomal proteins and proteins involved in proliferation and survival, and in the context of cancer, proteins involved in cell invasion and metastasis (Figure 1.5) (Hsieh et al. 2012; Thoreen et al. 2012; Gandin et al. 2016; Roux and Topisirovic 2018; Masvidal et al. 2017).

1.3.3.2. The role of S6 kinases

The first identified target of S6 kinases was rpS6, which is part of the ribosome. Subsequently, many initial studies on mTORC1 mediated regulation of translation focused on the S6K1-S6 signalling axis.

In S6K1$^{-/-}$/S6K2 $^{-/-}$ mice, phosphorylation of rpS6 was reduced but translation of 5'TOP mRNAs was not affected and remained rapamycin sensitive (Pende et al. 2004). In line with that, rpS6$^{P-/-}$ knock-in mice expressing a phospho-mutant rpS6 protein (serine to alanine substitutions) phenocopy growth defects observed in S6K1$^{-/-}$/S6K2 $^{-/-}$ mice. However, 5'TOP mRNA translation was not affected. Surprisingly, incorporation of ribosomes into polysomes in liver tissue of rpS6$^{P-/-}$ mice and the incorporation of labelled methionine and cysteine in isolated rpS6$^{P-/-}$ MEFs was increased compared to wild-type cells. This indicates that global rates of protein synthesis are actually increased in rpS6$^{P-/-}$ mice (Ruvinsky et al. 2005). Eventually, the S6K1-S6 signalling axis has been implicated in the regulation of the transcriptional program of ribosome biogenesis, with 78% of ribosome biogenesis mRNAs being downregulated in S6K1$^{-/-}$/S6K2 $^{-/-}$ mice and to a lesser extend in rpS6$^{P-/-}$ mice (Chauvin et al. 2014). The authors note that possible compensatory mechanisms could sustain global translation rates, based on observations of increased levels of phosphorylated 4E-BP1 in mutant cells (Chauvin et al. 2014).

Overall, knockout studies of components of the mTORC1-S6K1-pS6 signalling axis showed that S6 kinases and rpS6 are mediators of cell growth. They are dispensable for the regulation of global translation rates and 5'TOP mRNAs but regulate ribosome biogenesis at the transcriptional level (Figure 1.5).

Of note, S6 kinases also phosphorylate many other downstream proteins of the translational machinery, including proteins involved in translational initiation (eIF4B and PDCD4) and elongation (eEF2K) (Figure 1.5) (Raught et al. 2004; Dorrello et al. 2006; X. Wang et al. 2001; Dennis, Jefferson, and Kimball 2012).

In addition, S6K1 has been suggested to enhance translation of spliced mRNAs via forming a complex with SKAR (Aly/REF-like target)(Ma et al. 2008; Richardson et al. 2004). Splicing of mRNA transcripts can also be enhanced by S6K1 via phosphorylation of CBP80, a subunit of the nuclear RNA cap-binding complex promoting cap-dependent RNA splicing (Wilson, Wu, and Cerione 2000).

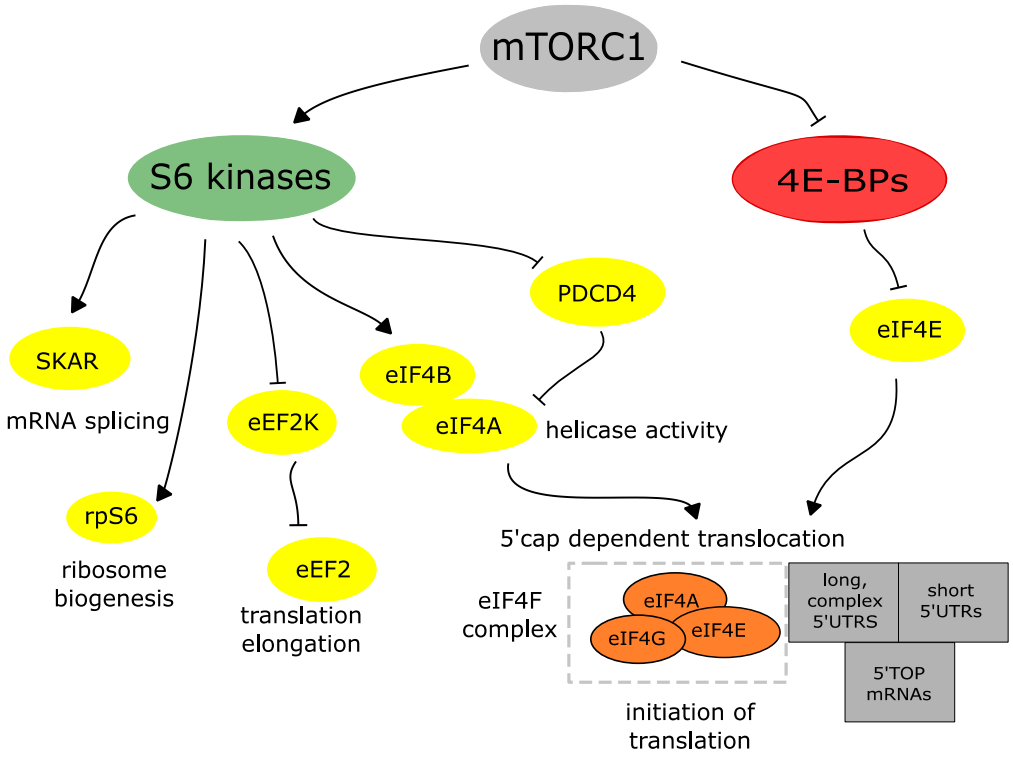

Figure 1.5: Regulation of translation via mTORC1.

S6 kinases and 4E-binding proteins are the key downstream effectors of mTORC1 and regulate protein synthesis. 4E-BPs are translational repressors and bind eIF4E, sequestering it away from the eIF4F complex and preventing initiation of translation. Phosphorylation of 4E-BPs via mTORC1 leads to the dissociation from eIF4E, allowing formation of the initiation complex and 5'cap dependent translation. 4E-BPs regulate global translation levels to a certain degree, however, specific subsets of mRNAs are most affected by mTORC1-4E-BP1-eIF4E signalling axis. S6 kinases on the other hand can phosphorylate rpS6, which is involved in transcriptional regulation of ribosome biogenesis. In addition, S6 kinases phosphorylate many proteins of the translational machinery, including proteins involved in initiation of translation such as eIF4B and PDCD6, and eEF2K, a protein involved in translational elongation. Further, S6 kinases can enhance mRNA splicing via forming a complex with SKAR.

1.4. mTOR signalling during embryonic and germ cell development

The PI3K/AKT/mTOR signalling axis has been the focus of many studies regarding diseases such as cancer and diabetes or cellular processes such as aging (Saxton and Sabatini 2017). However, its role during early development, especially at the molecular level, is less clear.

The disruption of many core components of the PI3K/AKT/mTOR signalling axis results in embryonic lethality, precluding detailed investigation of the role of this signalling pathway, as reviewed in (Yu and Cui 2016). However, *in vitro* systems such as embryonic stem cells (ESC) and conditional knockout approaches have shed some light on mTOR signalling during embryonic and germ cell development in recent years.

1.4.1. The role of mTOR during early development

Mtor deletion leads to embryonic lethality shortly after implantation, around E5.5-E6.5. Blastocysts are able to implant, however, trophoblast outgrowth and proliferation is impaired and the inner cell mass fails to proliferate (Gangloff et al. 2004; Murakami et al. 2004).

Loss of mTORC1 specific protein *Raptor* leads to a similar phenotype (Guertin et al. 2006), suggesting that early lethality in *Mtor*$^{-/-}$ mice is due to the loss of mTORC1 signalling (Guertin et al. 2006). Loss of the mTORC2 specific protein *Rictor* leads to a slightly delayed embryonic lethality at around E10.5-E11.5, possibly due to impaired development of the cardiovascular system (Guertin et al. 2006; Shiota et al. 2006), indicating distinct functions of the two mTOR complexes during development.

No ES cell clones could be derived from the ICM of *Mtor* $^{-/-}$ blastocysts (Gangloff et al. 2004; Murakami et al. 2004). Ablation of mTOR signalling in wild-type embryonic stem cells via either chemical inhibition (Rad001, rapamycin analogue) or genetic disruption of the *Mtor* kinase domain resulted in decreased proliferation rates and cell size (Gangloff et al. 2004; Murakami et al. 2004), underlining the essential role of mTOR in regulating proliferation.

1.4.2. The role of mTOR in pluripotency

Pluripotent cells are characterised by indefinite self-renewal capacity and the ability to contribute to all three germ layers (mesoderm, ectoderm and endoderm) (Nichols and Smith

2009). *In vivo*, pluripotency is a transient state found in epiblast cells of the pre-implantation blastocyst. Via derivation of embryonic stem cells from those pre-implantation epiblast cells, pluripotency can be captured *in vitro*.

In mESC, increased mTOR signalling upon knockdown of *Deptor*, a negative regulator of mTORC1 and mTORC2, promotes differentiation. This is characterised via decreased expression of pluripotency markers, changed cell morphology and expression of differentiation markers (Agrawal et al. 2014). Removal of LIF from embryonic stem cell cultures also leads to increased mTOR signalling. LIF is known to promote pluripotency in mESC cultures and withdrawal leads to mESC differentiation - whether increased mTOR signalling underlies differentiation remains to be shown though (Cherepkova, Sineva, and Pospelov 2016). mESC differentiation to mesoderm involves activation and correct localization of the mTORC2 complex via the serine/ threonine phosphatase calcineurin variant CNAB1 (Gómez-Salinero et al. 2016), further indicating active mTOR signalling in driving differentiation of mESCs.

In vivo, a reversible developmental arrest induced by unfavourable conditions, called embryonic diapause, is an exception to the transient nature of pluripotency. Diapause delays implantation and leads to a dormant state with preserved pluripotency (Renfree and Fenelon 2017).

Recently, inhibition of mTOR has been shown to induce a reversible diapause-like pluripotent state in blastocysts cultured *ex vivo.* In line with that, naturally induced diapaused blastocysts have reduced mTOR activity (Bulut-Karslioglu et al. 2016). In addition, treatment of embryonic stem cells with mTOR inhibitors INK128 and RapaLink-1 also induces a paused state, characterised by reduced transcription, reduced translation and maintained pluripotency (Bulut-Karslioglu et al. 2016). Of note, inhibition of mTORC1 and mTORC2 is necessary to induce the paused state, as treatment with rapamycin alone has no effect (Bulut-Karslioglu et al. 2016).

Overall, these studies suggest that low levels of mTOR signalling are necessary to maintain pluripotency *in vivo* and *in vitro* and upregulation of mTOR signalling promotes differentiation.

1.4.3. mTOR signalling during spermatogenesis

Spermatogenesis is the continuous process during which spermatogonial stem cells form spermatozoa (mature sperm) in the adult testis. Initially, a mitotic proliferation and differentiation phase occurs, followed by meiotic reduction and morphological transformation into functional spermatozoa (Figure 1.2) (Griswold 2016).

Clinical observations of reversible infertility in male patients treated with sirolimus (rapamycin analogue) after transplant surgery first suggested mTOR as an important regulator during spermatogenesis. These patients had decreased testosterone levels (produced by Leydig cells) and reduced sperm counts (Huyghe et al. 2007). Since then, mTOR signalling has been shown to play important roles in germ cells and surrounding somatic cells such as Sertoli cells and Leydig cells, in addition to regulating the blood-testis-barrier (Jesus et al. 2017; Oliveira, Cheng, and Alves 2017). Here, I will focus particularly on the role of mTOR signalling in germ cells.

1.4.3.1. mTOR and spermatogonial stem cells – self-renewal versus differentiation

In the past few years, several groups have reported a central role for mTOR signalling in spermatogonial stem cells. Spermatogonial stem or progenitor cells (SSC/SPC) form from quiescent gonocytes in the mouse testis during postnatal development, starting as early as day 1 after birth. These cells possess self-renewal potential and a pool of spermatogonial progenitor or stem cells is maintained throughout adult life, underlying the continuous production of differentiating spermatogonia (Figure 1.2). Hence, the decision of self-renewal versus differentiation into progenitor cells is key and any deviation can result in germ cell tumours or exhaustion of the SSC pool (Kanatsu-Shinohara and Shinohara 2013).

Extrinsic factors produced by surrounding Sertoli cells such as the growth factor glial cell-derived neurotrophic factor (GDNF) are essential for SSC maintenance, as well as intrinsic factors such as the transcription factor promyelocytic leukemia zinc finger (PLZF) (X. Meng et al. 2000; Buaas et al. 2004; Costoya et al. 2004; Kanatsu-Shinohara and Shinohara 2013). At the molecular level, PLZF has been shown to induce expression of REDD1 which inhibits mTORC1 activity and promotes self-renewal (Hobbs et al. 2010). Loss of *Plzf* and subsequent increased mTORC1 activity induces a negative feedback loop involving the GDNF receptor, rendering the cells unable to respond to niche signals such as GDNF (Hobbs et al. 2010).

In line with the above study, hyperactivation of mTORC1 signalling via conditional deletion of its negative regulators *Tsc1* or *Tsc2* leads to differentiation at the expense of self-renewal and germ line maintenance in SPCs (Hobbs et al. 2015; C. Wang et al. 2016). Increased differentiation eventually leads to germline degeneration in adult testis and subfertility due to partial spermatogenic/meiotic arrest and excessive germ cell loss (C. Wang et al. 2016).

The reciprocal experiments, during which mTOR signalling was either inhibited using rapamycin or ablated via genetic deletion of *Mtor* lead to impaired spermatogonial proliferation and blocked differentiation (Busada, Niedenberger, et al. 2015; Serra et al. 2017). Mice lacking Mtor are unable to produce sperm in adult testis, however, some undifferentiated spermatogonia remain, indicating that the undifferentiated germ cell pool is maintained (Serra et al. 2017).

Retinoic Acid and mTORC1. RA is essential in driving spermatogonial differentiation (Teletin et al. 2017). In undifferentiated spermatogonia, exogenous retinoic acid can induce precocious translation of mRNAs encoding for proteins required during germline differentiation such as SOHLH1, SOHLH2 and KIT (Busada, Chappell, et al. 2015). This increased translation is mediated via the PI3K/AKT/mTOR signalling pathway, as rapamycin treatment resulted in repressed translation of these mRNAs (Busada, Chappell, et al. 2015; Busada, Niedenberger, et al. 2015). The suggested model is that certain genes are transcribed in undifferentiated spermatogonia, however, only after RA signalling and activation of the PI3K/AKT/mTOR pathway, these mRNAs can be efficiently translated and protein products then drive differentiation (Busada, Chappell, et al. 2015; Busada, Niedenberger, et al. 2015).

To conclude, the described studies show that mTOR signalling is dynamic, changes throughout different stages of postnatal development and needs to be fine-tuned for normal development to proceed. Further studies are needed to depict the exact molecular mechanism and downstream targets.

1.4.4. mTOR signalling during oogenesis

In the developing mouse embryo, female germ cells (oogonia) enter meiosis at around E13.5 and arrest in the diplotene stage of meiotic prophase I at around E17.5. After birth, germ cell cysts start to break apart resulting in the formation of primordial follicles, each containing one primary oocyte surrounded by a layer of granulosa cells (Pepling 2006). The established pool of primordial follicles is kept in a dormant, quiescent state (meiotic arrest) until sexual

maturity and maintains a continuous supply of oocytes throughout the female reproductive life. From puberty onwards, during each oestrous cycle, some primordial follicles are activated and folliculogenesis, the process of follicle maturation to produce a mature oocyte, is initiated (Figure 1.2) (Pepling 2006)

Key events during oogenesis are primordial follicle activation, oocyte maturation and completion of meiosis. The mTOR signalling pathway plays a critical role during granulosa cell proliferation and differentiation, primordial follicle survival and activation and completion of meiosis (Makker, Goel, and Mahdi 2014). I will particularly focus on the role of mTOR signalling in primordial follicles.

1.4.4.1. mTOR and primordial follicles – quiescence versus activation

Follicular activation is the process that recruits dormant, quiescent primordial follicles into the pool of growing follicles. The TSC-mTOR signalling axis is essential for maintaining the primordial follicle pool (Adhikari et al. 2009, 2010).

Overactivation of mTOR signalling via deletion of *Tsc1* or *Tsc2* (using the GDF9-Cre line) in primordial follicles leads to premature activation of all primordial follicles, followed by premature ovarian failure due to follicular depletion and subsequent infertility (Adhikari et al. 2009, 2010). Rapamycin injections in *Tsc1*$^{-/-}$ mice, starting from post-natal day 4, is able to reverse the premature activation of primordial follicles (Adhikari et al. 2010). At the molecular level, hyper-activation of mTORC1 leads to increased phosphorylation of downstream targets 4E-BP1, S6K1 and rpS6 (Adhikari et al. 2010). Subsequent conditional knockout studies have identified another signalling pathway, the PI3K-PDK1 signalling axis (upstream of mTORC1), which can phosphorylate and activate S6K1 at distinct sites in an mTORC1 independent manner (Reddy et al. 2008, 2009).

Taken together, the maintenance of the quiescent state of primordial follicles involves the combined and synergistic repression of mTORC1 via TSC and PDK1 via PTEN, both ensuring low phosphorylation levels of S6K1. Follicle activation is triggered via activation of the S6K1 – rpS6 signalling axis, possibly leading to increased translation (Adhikari et al. 2010).

1.4.5. mTOR signalling in primordial germ cells

Very little is known about mTOR signalling in PGCs. On the search for possible signalling cascades activated in PGCs between E8.5 and E11.5, a targeted immunostaining approach revealed activation of AKT signalling, as determined by pAKT1 (Peter Hill, personal communication). While at E8.5 only 1 out of 58 germ cells was positive for pAKT1, at E9.5 roughly 20% of germ cells stained positive for pAKT1. By E10.5, the percentage of pAKT1 positive germ cells further increased to 50% (n=103/205) and stayed relatively constant until E11.5 (Peter Hill, personal communication). Interestingly, the transient activation of AKT signalling at E10.5 coincides with germ cell entry into the genital ridge and the onset of epigenetic reprogramming.

Analysis of possible AKT downstream targets indicated activation of mTORC1 signalling, as determined by p4E-BP as a readout for mTORC1 activity. At E9.5, phosphorylated 4E-BP1 was only detected in 13% of germ cells (n=7/51) (Peter Hill, personal communication). However, upon genital ridge entry at E10.5, 72% of germ cells exhibited a strong nuclear and cytoplasmic staining for p4E-BP1 (n=42/58), which was maintained until E11.5 (Peter Hill, personal communication).

Hence, 4E-BP1 phosphorylation dynamics correlate well with observed AKT signalling dynamics (as determined by pAKT1 staining) in PGCs, possibly indicating the activation of the AKT-mTORC1-4E-BP1 signalling axis from E10.5 onwards in PGCs. However, these preliminary observations require further detailed investigation.

1.5. Hypothesis

Signalling events between developing germ cells and their surrounding tissues lie at the heart of germ cell development: WNT/BMP signalling is important for germ cell induction, SDF1-CXCR4 and KIT ligand-C-KIT signalling is important for germ cell survival, proliferation and migration, SRY-SOX9-FGF9 signalling in males vs WNT/RSPO1 signalling in females during sexual differentiation and potentially RA signalling for initiation of meiosis.

Upon entry into the genital ridge, PGCs undergo many key developmental processes such as epigenetic reprogramming (including global DNA demethylation), induction of germline specific genes (*Mvh* and *Dazl*) and sexual differentiation. Whether or to what level the new gonadal environment plays a role in initiating these processes via production of inductive signals, in addition to intrinsic signals, is still largely unknown.

mTOR signalling integrates and senses many signals from the surrounding environment and regulates cell growth and proliferation, partly via regulating protein biosynthesis and translation. Translational regulation during distinct (transcriptionally silent) phases of germ cell development is tightly regulated. Further, in primordial germ cells and gonocytes, many key germ cell specific proteins (such as LIN28, DAZL, MVH, NANOS2, amongst others) are RNA-binding proteins, indicating that primordial germ cells possibly regulate developmental processes not only at the transcriptional level, but also at the translational level.

Conditional knockout studies in germ cells from E15.5 onwards demonstrated that the right level of mTOR signalling is essential during oogenesis and spermatogenesis, mainly driving differentiation and activation at the loss of pluripotency and maintenance in the adolescent gonad.

However, the role of mTOR signalling during early germ cell development is completely unknown. Recent unpublished work indicated the activation of the AKT-mTORC1-4E-BP1 signalling axis in gonadal germ cells from E10.5 onwards (Peter Hill).

Based on these initial observations, I set out to analyse the role of mTOR signalling during early germ cell development. Our hypothesis was that intrinsic mTOR signalling is activated in PGCs and that it plays a critical role during early germ cell development.

2. Materials and Methods

2.1. Mice

2.1.1. Ethics statement

All animal experiments were carried out in a UK Home Office designated facility (Imperial College London) under a UK Home Office Project license (Prof Dominic Withers - 20/6466; Prof Petra Hajkova - 70/8946). Experiments conformed to the UK Animals (Scientific Procedures) Act 1986.

2.1.2. General husbandry & identification

Mice were kept under pathogen-free conditions within individually ventilated cages with same-sex littermates in groups of two to four. Mice had ad libitum access to water and chow and a 12 hour light/dark cycle. At approximately 2 weeks of age, pups were earmarked for identification purposes and to determine their genotype. The ear biopsy was used for DNA extraction.

2.1.3. DNA extraction for genotyping

Collected ear biopsies or embryo tails were digested using alkaline hydrolysis. 300µl (ear biopsy) or 150µl (embryo tissue) of 0.06M NaOH was added to the tissues and the samples were incubated at 100^{o}C for 10-15 minutes. Following cooling down of the sample to room temperature, the reaction was neutralized by adding 50µl (ear biopsy) or 25µl (embryo tissue) of 1M Tris-HCL pH 8.0. After briefly vortexing the samples, a 10 second centrifugation step at 12000 x g followed. 1µl of the supernatant was used for the PCR reaction. The remaining sample was stored at 4^{o}C.

2.1.4. Timed matings

Timed matings were set up for timed pregnancies and collection of primordial germ cells at defined stages. Females from breeding duos or trios were checked each morning for a vaginal plug. Appearance of a vaginal plug was defined as embryonic day (E) 0.5. Plugged females were separated from males at E0.5 and housed in separate cages.

For analysis of wild-type PGCs, mixed background GOF18ΔPE-EGFP (Yeom et al. 1996; Yoshimizu et al. 1999) transgenic males were crossed with C57BL/6 females (purchased from Charles River). For analysis of genetically modified PGCs, see further details regarding mating strategy for each mouse line separately in the next section.

2.1.5. Genetically modified mouse lines

2.1.5.1. Global S6K1 knockout mouse line

Genetic modification. The global S6K1 knockout mouse line was established in Prof Withers' group. Initially, a floxed S6K1 mouse line was generated, which has been previously described (Smith et al. 2015). To establish the global S6K1 knockout mouse line, germline deletion was accomplished via crossing the floxed S6K1 mouse line with the Nestin-Cre mouse line (Smith et al. 2015). Subsequently, Nestin-Cre was outcrossed. Global $S6K1^{-/-}$ knockout mice have exon 3 and 4 of the S6K1 gene deleted, which results in a frame shift in the downstream exons and loss of the catalytic domain.

Genetic background and colony maintenance. The global S6K1 knockout mouse line is maintained on a pure C57BL/6 genetic background. The colony is maintained via heterozygous breeding pairs. Every second generation, heterozygous or homozygous S6K1 knockout males are outbred to C57BL/6 wild-type females.

Experimental mice. For the generation of experimental $S6K1^{-/-}$ knockout and $S6K1^{+/+}$ wild-type embryos or adult mice, timed matings (for embryos) or breeding pairs crossing a heterozygous $S6K1^{+/-}$ male with a heterozygous $S6K1^{+/-}$ female were set up. Experimental and wild-type tissues were always from the same litter.

Genotyping protocol. S6K1 genotypes were identified using the primers listed in **Table 2.1**. Two separate reactions with different primer combinations (25+26 or 25+30) were set up for each sample using the OneTaq® Hot Start Quick-Load® 2X Master Mix (New England Biolabs, M0488S). PCR reactions were run using the following cycling conditions: 94°C for 3 minutes, followed by 5 cycles of 94°C for 30 seconds, 64°C for 30 seconds and 72°C for 1 minute. This was followed by further 31 cycles of 94°C for 30 seconds, 60°C for 30 seconds and 72°C for 1 minute. A final extension at 72°C for 5 minutes was performed, followed by 18°C for 10 minutes. Primers 25 and 26 amplify the wild-type allele, corresponding to a band at 250 base pairs. The floxed S6K1 allele is amplified by primers 25 and 30, corresponding to a band at 400 base pairs.

2.1.5.2. Global S6K1 and S6K2 knockout mouse line

Genetic Modification. The global S6K1/S6K2 double knockout mouse line was established in Prof Withers' group by crossing the previously described global S6K1 knockout mouse line (Shima et al. 1998) with a global S6K2 knockout mouse line. The global S6K2 knockout

mouse line was generated using targeted ESC cells purchased from KOMP (Project ID: CSD33372). The targeted mutation ($Rps6kb2^{tm1a(KOMP)Wtsi}$) is a knockout first allele containing a lacZ reporter and neomycin cassette inserted between exon 4 and 5. ESCs were injected by the LMS Transgenics Facility. The targeted S6K1 allele contains a neomycin resistance cassette replacing 1.2 kb of the genomic sequence including the conserved Ser/Thr kinase catalytic sub-domains VIII–X (Shima et al. 1998).

Genetic background and colony maintenance. The global S6K1/S6K2 knockout mouse line is maintained on a pure C57BL/6 genetic background. $S6K1^{+/+}$ $S6K2^{+/+}$ wild-type mice are maintained as a separate colony through wild-type breeding pairs. Due to the high perinatal lethality of $S6K1^{-/-}$ $S6K2^{-/-}$ double knockout mice, experimental mice are maintained using breeding pairs heterozygous for the S6K1 allele and homozygous for the S6K2 allele ($S6K1^{-/+}$ $S6K2^{-/-}$ x $S6K1^{-/+}$ $S6K2^{-/-}$).

Experimental mice. For the generation of experimental $S6K1^{-/-}$ $S6K2^{-/-}$ double knockout and $S6K1^{+/+}$ $S6K2^{+/+}$ wild-type embryos, two separate timed matings (for embryos) of wild-type or heterozygous ($S6K1^{-/+}$ $S6K2^{-/-}$) breeding pairs were set up. Experimental and wild-type tissues were from different litters.

Genotyping protocol - S6K1 allele. S6K1 genotypes were identified using the primers listed in **Table 2.1**. PCR reactions were set up using Qiagen Taq DNA Polymerase (Qiagen, 201203). PCR reactions were run using the following cycling conditions: 94°C for 3 minutes, followed by 5 cycles of 94°C for 30 seconds, 65°C for 30 seconds and 72°C for 1 minute. This was followed by further 35 cycles of 94°C for 30 seconds, 62°C for 30 seconds and 72°C for 1 minute. A final extension at 72°C for 5 minutes was performed, followed by 18°C for 10 minutes. The presence of a wild-type allele corresponds to a band at 375 base pairs. The presence of the mutant allele corresponds to a band at 175 base pairs.

Genotyping protocol - S6K2 allele. S6K2 genotypes were identified using the primers listed in **Table 2.1**. PCR reactions were set up using the ThermoPrime 2x ReddyMix PCR Master Mix (ThermoFischer, AB0575DCLDB). PCR reactions were run using the following cycling conditions: 94°C for 3 minutes, followed by 5 cycles of 94°C for 30 seconds, 64°C for 30 seconds and 72°C for 1 minute. This was followed by further 35 cycles of 94°C for 30 seconds, 62°C for 30 seconds and 72°C for 1 minute. A final extension at 72°C for 5 minutes was performed, followed by 18°C for 10 minutes. The presence of a wild-type allele corresponds to a band at 574 base pairs. The presence of the mutant allele corresponds to a band at 352 base pairs.

2.1.5.3. Global 4E-BP1 knockout mouse line

Genetic Modification. The global 4E-BP1 knockout mouse line was established in Prof Withers' group. Briefly, targeted ESC cells were purchased from EUCOMM (Project ID: 67566). The targeted mutation (Eif4ebp1$^{tm1a(EUCOMM)Wtsi}$) is a KO first allele containing a lacZ reporter and neomycin cassette inserted between exon 1 and 2. Targeted ESC cells were injected by the LMS Transgenics Facility.

Genetic background and colony maintenance. 4E-BP1 knockout mice are maintained as heterozygotes (4E-BP1$^{+/-}$) on a mixed genetic background (50% 129/Sv x 50% C57BL/6). Every third generation, 4E-BP1$^{-/-}$ knockout mice are outbred to either C57BL/6 or 129/Sv wild-type mice (purchased from Jackson Laboratory).

Experimental mice. For the generation of experimental 4E-BP1$^{-/-}$ knockout and 4E-BP1$^{+/+}$ wild-type embryos or adult mice, timed matings (for embryos) or breeding pairs crossing a heterozygous 4E-BP1$^{+/-}$ male with a heterozygous 4E-BP1$^{+/-}$ female were set up. Experimental and wild-type tissues were always from the same litters.

Genotyping protocol. 4E-BP1 genotypes were identified using the primers listed in **Table 2.1**. PCR reactions were set up using ThermoPrime 2x ReddyMix PCR Master Mix (ThermoFischer, AB0575DCLDB). PCR reactions were run using the following cycling conditions: 94^{o}C for 2 minutes, followed by 5 cycles of 94^{o}C for 30 seconds, 64^{o}C for 30 seconds and 72^{o}C for 1 minute. This was followed by further 35 cycles of 94^{o}C for 30 seconds, 62^{o}C for 30 seconds and 72^{o}C for 1 minute. A final extension at 72^{o}C for 5 minutes was performed, followed by 18^{o}C for 10 minutes. The presence of a wild-type allele corresponds to a band at 458 base pairs. The presence of the mutant allele corresponds to a band at 339 base pairs.

2.1.5.4. Global 4E-BP1 and 4E-BP2 knockout mouse line

Genetic Modification. The global 4E-BP1/4E-BP2 double knockout mouse line was established through crossing global 4E-BP1$^{-/-}$ knockout mice (described in the previous section) with global 4E-BP2$^{-/-}$ knockout mice. The global 4E-BP2$^{-/-}$ knockout mouse line was generated in Prof Withers' group. Briefly, targeted ESC cells were purchased from KOMP (Project ID: 45628). The targeted mutation (Eif4ebp2$^{tm1a(KOMP)Wtsi}$) is a KO first allele containing a lacZ reporter and neomycin cassette inserted between exon 1 and 2. Targeted

ES cells were injected by the LMS Transgenic Facility. The 4E-BP2 knockout mouse line is maintained on a pure C57BL/6 genetic background.

Genetic background and colony maintenance. The global 4E-BP1/4E-BP2 double knockout mouse line is maintained on a mixed genetic background (129/Sv x C57Bl/6). Wild-type 4E-BP1$^{+/+}$ 4E-BP2$^{+/+}$ control mice are maintained as a separate colony through wild-type breeding pairs. Global 4E-BP1$^{-/-}$ 4E-BP2$^{-/-}$ double knockout mice are maintained via homozygous breeding pairs.

Experimental mice. For the generation of experimental 4E-BP1$^{-/-}$ 4E-BP2$^{-/-}$ knockout and 4E-BP1$^{+/+}$ 4E-BP2$^{+/+}$ wild-type embryos or adult mice, two separate timed matings (for embryos) or breeding pairs were set up, using either wild-type or homozygous mice. Experimental and wild-type tissues were from different litters.

Genotyping protocol - 4E-BP1 allele. See details section above (2.1.5.3, p. 72).

Genotyping protocol - 4E-BP2 allele. 4E-BP2 genotypes were identified using the primers listed in **Table 2.1**. PCR reactions were set up using the Qiagen Taq DNA Polymerase (Qiagen, 201203). PCR reactions were run using the following cycling conditions: 94^{o}C for 3 minutes, followed by 5 cycles of 94^{o}C for 30 seconds, 66^{o}C for 30 seconds and 72^{o}C for 1 minute. This was followed by further 30 cycles of 94^{o}C for 30 seconds, 64^{o}C for 30 seconds and 72^{o}C for 1 minute. A final extension at 72^{o}C for 1 minutes was performed, followed by 18^{o}C for 10 minutes. The presence of a wild-type allele corresponds to a band at 545 base pairs. The presence of the mutant allele corresponds to a band at 679 base pairs.

2.1.5.5. Global rpS6 phospho-mutant mouse line

Genetic Modification. The global rpS6 phospho-mutant knock-in mouse line has been previously described (Ruvinsky et al. 2005). Briefly, the targeted rpS6 allele contains alanine residues at position 235, 236, 240, 244, 247 instead of phosphorylatable serine residues.

Genetic background and colony maintenance. Global rpS6 phospho-mutant mice were maintained as heterozygotes on a pure C57BL/6 genetic background by Darran Hardy.

Experimental mice. For the generation of experimental rpS6p$^{-/-}$ knock-in and rpS6p$^{+/+}$ wild-type embryos, timed matings of heterozygous breeding pairs were set up. Experimental and wild-type tissues were from the same litters.

Genotyping protocol. Genotypes of global rpS6 phospho-mutant knock-in mice were identified using the primers listed in **Table 2.1**. PCR reactions were set up using the OneTaq® Hot Start Quick-Load® 2X Master Mix (New England Biolabs, M0488S). PCR reactions were run using the following cycling conditions: 94°C for 3 minutes, followed by 5 cycles of 94°C for 30 seconds, 63°C for 30 seconds and 72°C for 1 minute. This was followed by further 30 cycles of 94°C for 30 seconds, 60°C for 30 seconds and 72°C for 1 minute. A final extension at 72°C for 5 minutes was performed, followed by 18°C for 10 minutes. The resulting PCR product of 639 base pairs was digested with EcoRV for 3 hours or overnight at 37°C. Following digestion, the presence of a wild-type allele corresponds to a band at 639 base pairs, while the mutant allele corresponds to two bands at 305 and 355 base pairs.

2.1.5.6. Floxed mTOR mouse line

Genetic Modification. The floxed mTOR mouse line has been previously described (Risson et al. 2009). Briefly, loxP sites are flanking the region between the promoter and exon 5 (see 6.2.1, p. 202, Figure 6.1, p. 203). Floxed mTOR mice were obtained from Jackson Laboratory (Stock no 011009).

Genetic background and colony maintenance. Floxed mTOR mice were maintained as homozygotes on a pure C57BL/6 genetic background.

Experimental mice. For the generation of *Mtor*$^{-/-}$ conditional knockout mice, homozygous *Mtor*$^{fl/fl}$ males were crossed with newly generated, heterozygous *Blimp1-iCre* females (F4) in the first breeding step. Subsequently, male offspring (*Mtor*$^{fl/+,}$ Tg(*Blimp1-iCre*)/+) were bred with homozygous *Mtor*$^{fl/fl}$ females (see 6.2.1, p. 202, Figure 6.1, p. 203).

Genotyping protocol. The genotype of floxed mTOR mice was identified using the primers listed in **Table 2.1**. PCR reactions were set up using the Qiagen Taq DNA Polymerase (Qiagen, 201203). PCR reactions were run using the following cycling conditions: 94°C for 2 minutes, followed by 6 cycles of 94°C for 30 seconds, 63°C for 30 seconds and 72°C for 1 minute. This was followed by further 26 cycles of 94°C for 30 seconds, 60°C for 30 seconds and 72°C for 1 minute. A final extension at 72°C for 5 minutes was performed, followed by 18°C for 10 minutes. The presence of the mTOR wild-type allele corresponds to a band at 331 base pairs, whereas the presence of the floxed mTOR allele corresponds to a band at 520 base pairs.

Table 2.1: List of primers used for genotyping.

gene	primer name	Primer Sequences 5'-3'
S6K1 (Taconic)	25 (forward)	TCC-ACC-CAC-CAG-TAA-AGA-GC
	26 (reverse)	CCT-CAG-TCT-CCT-GAG-TGT-TAA-GG
	30 (reverse)	TCA-AGG-CCA-GCC-TGG-ACT-AC
S6K1	9580 (forward)	CAT-CTT-TAC-TGA-AGG-AGC-TAC-TGG
(Pende et al, 2004)	9957 (reverse)	AGC-AGG-CTG-GAC-TCA-AAC-TCA-TAG
	Neo (reverse)	TTC-GCA-GCG-CAT-CGC-CTT-CTA-TC
S6K2	14902 (forward)	GCA-CAC-CAG-GGG-CTA-CATA-ATG
	22572 (reverse)	GCA-CTG-CAT-ACA-ATC-TTG-GCC-TAG
	15254 (Lar3)	CAC-AAC-GGG-TTC-TGT-TAG-TCC
4E-BP1	Eif4ebp1 (reverse)	CCA-ACC-TGA-CCA-CAT-CCC-TGG-TCC
	Eif4ebp1 (forward)	GAG-GTC-AGG-AGG-AAT-GGG-ACT-GGC
	LAR2	CAA-CGG-GTT-CTT-CTG-TTA-GTCC
4E-BP2	5′arm (forward)	GTC-TGT-AAC-TCC-AGT-TCC-AGA-GGC-TC
	CSD-Eif4ebp2-tt (reverse)	CAT-GGG-GTG-TCT-CTG-AGT-GAA-GAG-G
	CSD-neo (forward)	GGG-ATC-TCA-TGC-TGG-AGT-TCT-TCG
rpS6	rpS6_52 (forward)	GTC-ATC-CAG-CAT-GGG-TGC-TG
	rpS6_11 (reverse)	GGC-TGA-TAC-CTT-TTG-GGA-CAG
mTOR	mTOR (forward)	GAT-AAT-TGC-AGT-TTT-GGC-TAG-CAG
	mTOR (reverse)	CTC-CTT-CTG-TGA-CAT-ACA-TTT-CCT
Z/EG	Zeg (forward)	CCT-CTG-CCA-AAA-ATT-ATG-GGG
	Zeg (reverse)	ACT-ATG-GTT-GCT-GAC-TAA-TTG
Blimp1-iCre	iCre (forward)	ACC-TGG-AAG-ATG-CTC-CTG-TC
	iCre (reverse)	AGA-TCT-CCT-GTG-CAG-CAT-GT

2.2. Dissection techniques

2.2.1. Embryo dissection to obtain PGCs

Following timed matings, appearance of a vaginal plug in the morning was defined as embryonic day (E) 0.5. For analysis of primordial germ cells, embryo trunks (E9.5 & E10.5) and genital ridges (E11.5-E15.5) were dissected out from embryos between E9.5 and E15.5. The embryo tail was collected for DNA isolation and genotyping. The sex of embryos from E12.5 onwards was determined by visual inspection of the gonads.

2.2.2. Adult tissue dissection to obtain adult ovaries and testes

For analysis of adult gonads, testis and ovaries were dissected from adult global S6 kinase or 4E-BP wild-type and knockout mice. Males have been mated and primed prior to tissue collection. Whenever possible, wild-type and knockout tissues were collected from littermates.

2.3. Histology

2.3.1. Cryosections followed by immunofluorescence stainings

Freshly dissected embryonic trunks (E9.5 & E10.5) or genital ridges (E11.5-E15.5) were fixed with 2% PFA for 30 minutes at 4°C, followed by three 20 minute PBS washes. Whole embryos and placentas were fixed in 4% PFA for 2-4 hours, followed by three 20 minute PBS washes. Samples were equilibrated in 30% sucrose (in PBS) at 4°C overnight and subsequently embedded in OCT Embedding Matrix (VWR), flash frozen using liquid nitrogen and stored at -80°C for later processing.

Using a Leica CM 1950 cryostat, samples were cut into 10 µm thick sections and consecutive sections were collected on 4-6 polylysine coated slides (Thermo Scientific) or Superfrost slides (Thermo Scientific) per genital ridge. Sections were post-fixed for 2 minutes in 2% PFA, followed by three 5 minute washes with PBS. After incubation with blocking buffer (PBS with 1% BSA and 0.1% Triton TX-100) for 30 minutes at room temperature to permeabilize the tissue and block any non-specific signal, primary antibodies (see **Table 2.2**) diluted in blocking buffer were added overnight at 4°C. The next day, sections were washed three times with 1% BSA / 0.1% Triton in PBS for 5 minutes. Secondary antibodies (see **Table 2.3**) diluted in blocking buffer were added for 1 hour at room temperature in the dark. Subsequently, slides were protected from light for the following steps. After three washes

with PBS for 5 minutes, cell nuclei were stained with DAPI (1µg/µl; Severn Biotech) diluted in PBS for 20 minutes at room temperature. For p4E-BP1 stainings, an additional staining step was performed using HCS CellMask Deep Red (Invitrogen, H32721), following the manufacturer's protocol. After a final 5 minute PBS wash, slides were mounted with Vectorshield Mounting agent for Fluorescence (H-1000, Vector Laboratories), surrounded with nail polish, and imaged using a SP5 confocal microscope.

SP5 acquisition settings were kept constant for each imaged slide and were chosen as follows: HCX PL APO CS 40.0x1.25 OIL UV objective, 2.5x zoom, 1024x1024 format, scanning speed 400Hz, pinhole (53.10µm), argon laser power 15%. For each fluorophore, the following laser lines for excitation and spectral detection ranges for detection were used: DAPI - 405 laser (spectral detection range 415-480), Alexa 488 fluorophore - 488 laser (spectral detection range of 503-551), Alexa 568 fluorophore - 561 laser (spectral detection range 571-674), Alexa 647 fluorophore - 633 laser (spectral detection range 643-715), CellMask Dark red – 643 laser (spectral detection range 649-705); Excitation laser power was 15% and PMT detectors were used for detection.

For direct comparison of wild-type and knockout tissues or comparison of different time points in wild-type tissue (without further quantification), the voltage has been kept constant within each experiment/replicate. If quantification followed, the voltage (gain) has been occasionally adjusted within an experiment for increased image quality and improved downstream processing (due to slight variations in antibody staining quality between microscope slides).

Total fluorescence (red channel) was measured using a half-automated pipeline in CellProfiler (Chad Whilding): Germ cells were automatically identified using the green channel (Oct4-GFP expression). For each analysed image, the correct identification of germ cells was manually (visually) checked and if necessary, adjusted (e.g. to remove wrongly identified PGCs or in case of doublets). Further, somatic cells were identified based on the DAPI staining in combination with the red channel (in 4E-BP1 stainings) or in combination with a HCS CellMask Deep Red staining (in p4E-BP1 stainings). For each analysed image, 10-20 correctly identified somatic cells were manually chosen. The total fluorescence of each PGC was divided by the average total fluorescence of the 10-20 somatic cells. The resulting total fluorescence measured in PGCs is therefore relative to somatic cells and corrects for different voltages between images. Statistical analysis was performed using the Graphpad software.

At time points E9.5-E11.5, on average about 7 sections were imaged and analysed per replicate and at time points E12.5-E14.5, about 5 sections were imaged and analysed per replicate.

2.3.2. PGC single cell immunofluorescence staining

For PGC single cell staining, freshly dissected genital ridges were trypsinized and the single cell suspension was incubated on poly-L-Lysine treated slides for 30min. Following cell attachment, the slides were washed with PBS and fixed with 4% PFA in PBS for 15 min at room temperature. The subsequent immunofluorescence staining steps are the same as for cryosections.

Table 2.2: Primary antibodies used for immunofluorescence staining.

germ cell proteins, pluripotency factors, meiosis markers						
name	company	cat nr	lot nr	type	host	IF dilution
GFP	Abcam	ab5450	GR244481-1	p (IgG)	goat	1 in 1000
DAZL	Abcam	ab34139	GR265350-2	p (IgG)	rabbit	1 in 300
MVH (mouse)	Abcam	ab27591	AP:422776 AP:424621 AP:314079	m (IgG1, κ)	mouse	1 in 300
MVH (rabbit)	Abcam	ab13840	AP:173265	p (IgG)	rabbit	1 in 300
SSEA1 (Tg1)	gifted by Dr P Beverly via Dr G Durcova Hills			m (IgM)	mouse	1 in 1
Oct4 (mouse)	Biosciences	611202	-	m (IgG1, κ)	mouse	1 in 200
Oct4 (rabbit)	Abcam	ab181557	-	m (IgG)	rabbit	1 in 200
SOX2	Abcam	ab15830	AP:480146	p (IgG)	rabbit	1in200
Stra8	Abcam	ab49602	GR275803-2	p (IgG)	rabbit	1 in 250
SCP3	Abcam	ab15093	GR180746-2 318655-3	p (IgG)	rabbit	1 in 500
AKT/mTor signalling						
name	company	cat nr	lot nr	type	host	IF dilution
Akt	Cell Signalling	4691	20	m(IgG)	rabbit	1 in 400
p-AKT (S473)	Cell Signalling	4060	23	m (IgG)	rabbit	1 in 400
p-Akt1 (S473)	Abcam	ab81283	GR240003-44	m(IgG)	rabbit	1 in 200
p-AKT (T308)	Cell Signalling	13038	5	m(IgG)	rabbit	1 in 800
mTOR	Cell Signalling	2983	16	m(IgG)	rabbit	1 in 400
p-mTOR (S2448)	Cell Signalling	5536	-	m(IgG)	rabbit	1:50
S6	Cell Signalling	2217	7	m(IgG)	rabbit	1 in 200
p-rpS6 (S240/244)	Cell Signalling	5364	6	m(IgG)	rabbit	1 in 400
4E-BP1	Cell Signalling	9644	-	m(IgG)	rabbit	1 in 1500
p-4E-BP1 (Thr37/46)	Cell Signalling	2855	20	m(IgG)	rabbit	1 in 300

p - polyclonal, m - monoclonal

Table 2.3: Secondary antibodies used for immunofluorescence staining.

reactivity	type	raised in	Alexa Fluor	cat nr
a-rabbit	IgG (H+L)	donkey	568	A10042
a-goat	IgG (H+L)	donkey	488	A11055
a-rabbit	IgG (H+L)	goat	488	A11034
a-mouse	IgM	goat	647	A21238
a-rabbit	IgG (H+L)	donkey	488	A21206
a-mouse	IgG (H+L)	donkey	488	A21202
a-mouse	IgG (H+L)	donkey	568	A10037
a-mouse	IgG (H+L)	goat	488	A11029
a-rabbit	IgG (H+L)	goat	568	A11036

2.3.3. H&E stainings

Adult testis and ovaries were fixed in 4% PFA for 20-24 hours at 4°C, followed by three 10 minute PBS washes. Samples were stored in 70% EtOH until paraffin infiltration using the Tissue TEK VIP Processor (Sakura). The following program was used to dehydrate tissues and infiltrate them with wax: 70% EtOH – 45 minutes, 80% EtOH – 45 minutes, 90% EtOH – 30 minutes, 96% EtOH – 45 minutes, 100% EtOH – 30 minutes, 100% EtOH – 60 minutes, 100% EtOH – 60 minutes, xylene – 30 minutes, xylene – 45 minutes, xylene – 60 minutes, wax – 45 minutes, wax – 60 minutes, wax – 30 minutes, wax – 30 minutes. After wax infiltration, tissues were embedded in paraffin blocks using HistoEmbedder (Leica) and stored at room temperature until further processing. Using a microtome MicromHM355S (ThermoScientific), tissue blocks were cut into 8 µm thick sections. After the tissue sections were dried overnight at 42°C, rehydration of the tissue followed. Slides were incubated three times for 5 minutes in Xylene (#534056, Sigma), followed by two times in 100% EtOH for 1 minute each, followed by two times 95% EtOH for 1 minute each and a final 1 minute incubation in 80% EtOH. Tissues were rinsed in tap water for 1 minute and stained with Mayer's Haematoxylin (#MHS32-1L, Sigma Aldrich) for 7 minutes following the progressive staining technique. Excess stain was removed by rinsing slides in running tap water, and the stain was blued in Scott's tap water substitute (0.25M Sodium Bicarbonate, 30 mM Magnesium Sulphate in ddH_2O) for 5 minutes. After a 1 minute incubation in 95% EtOH, female sections were additionally stained with Eosin Y (alcoholic, #HT110132-1L, Sigma Aldrich) for 7 minutes. Rapid dehydration was performed via a 1 minute incubation at 95% EtOH, followed by two 1 minute incubations in 100% EtOH and three 5 minute incubations in Xylene. Tissue sections were mounted using DPX mounting medium (#D/5319/05, Fischer) and imaged using a Zeiss upright microscope with a CANON EOS 40D camera attached.

2.4. Generation of new *Blimp1-iCre* mouse line

2.4.1. Synthesis of new *Blimp1-iCre* BAC transgene

The bacterial artificial chromosome (BAC) transgene was generated by Philip Hublitz at the University of Oxford, Genome Engineering Service (see 5.2.1. p.181, Figure 5.1, p. 182). Bacterial plates containing correct and sequence verified BAC and one purified BAC DNA sample were sent to our lab.

2.4.2. Bacterial cultures and glycerol stocks

Single colonies of BAC containing bacteria cells (DH10b) were picked using sterile pipette tips and incubated in 3ml Luria-Bertani (LB) broth containing 12.5µg/ml Chloramphenicol (Sigma, C0378). The cells were grown at 37°C with shaking (RPM 225) overnight or for 8 hours. For large preparations and subsequent BAC isolation, 0.5mls of a starter culture were inoculated into 250ml of LB broth containing 12.5µg/ml Chloramphenicol and incubated at 37°C for a further 12-16 hours. To generate glycerol stocks for long term storage, 800µl bacterial culture were combined with 200µl 80% glycerol (80% glycerol in dH_20) and stored at -80°C.

2.4.3. Isolation and purification of BAC transgene from E.coli

The circular BAC transgene was isolated using the Qiagen Large Construct Kit (Qiagen, 12462) according to the manufacturer's instructions including the exonuclease III treatment. Wide bore pipette tips were used and any vortexing or excess pipetting was avoided to reduce shear forces and breaking of the BAC transgene. The DNA pellet was gently dissolved in 50µl nuclease free ddH_20 overnight at 4°C. DNA concentration was determined using Nanodrop.

2.4.4. Linearization of the circular, purified BAC transgene

Restriction enzyme digestion. For linearization, 2µg of purified BAC sample were digested with the restriction enzyme SgrAI (NEB, R0603S) for 1 hour at 37°C. The reaction was heat inactivated via incubation at 65°C for 20 minutes. In addition, control digestions using different enzymes (HindIII, SpeI, AdHI) (NEB, R0104S, R3133S, R0584S)) with several cutting sites on the BAC transgene were performed to check the integrity and quality of the BAC preparation. Digested control samples were run on a 0.5% agarose gel for 2 hours at 60V

using standard gel electrophoresis to confirm the digestion reaction and assess the quality of the BAC preparation (appearance of sharp bands).

Phenol/chloroform extraction. The linearized BAC sample was purified using phenol/chloroform extraction and Pellet Phase Lock Gel heavy tubes (5Prime, #2302830). To each sample, 1 volume of room temperature phenol/chloroform/isoamyl alcohol (ph8, Invitrogen, 15593031) was added and tubes were inverted several times to mix the solutions. A 10 minute centrifugation step at 12.000 x g followed. The aqueous upper phase was carefully pipetted off into a new tube. Another extraction with phenol/chloroform/isoamyl alcohol followed. The third round of extraction was performed by adding 1 volume of chloroform alone, in order to remove any leftover phenol. The aqueous phase containing the dissolved DNA was transferred into a microcentrifuge tube and a tenth of the volume of 3M sodium acetate (pH 5.2) was added. The DNA was precipitated by adding 2 volumes of 100% ethanol. Following a 10 minute centrifugation step at 13.000 x g, the supernatant was discarded and the DNA pellet was washed with 1ml of 70% ethanol. Another centrifugation step of 3 minutes at 13.000 x g followed. The supernatant was discarded, any residual liquid removed and the DNA pellet was air-dried for 5-10 minutes. DNA was re-dissolved in 30µl TE buffer (10mM Tris, 1mM EDTA, pH 8.0) or microinjection buffer (10mM Tis-HCL pH7.5, 0.1mM EDTA, 30µM spermine, 7µM spermidine, 100mM NaCl). The DNA concentration was measured using Nanodrop.

Pulse-field gel electrophoresis. Due to the large size of the circular or linearized BAC (~100.000kb), pulse-field gel electrophoresis (PFGE) was performed to confirm successful sample digestion (CHEF-DRII system – Biorad). A 1% agarose gel (MegaSieve agarose) was prepared. 1µl of liquid circular and linear BAC sample was run for 14 hours at the following conditions: 14ºC, 6V/cm field, angle 120ºC, linear ramping time (switch time) 5-15 seconds; Following PFGE, the agarose gel was stained for 3 hours with 1x SybrSafe (Invitrogen, S33102) and analysed using UV light.

2.4.5. Pro-nuclei injections and generation of founders

Purified circular or linear BAC DNA was diluted in microinjection buffer (10mM Tis-HCL pH7.5, 0.1mM EDTA, 30µM spermine, 7µM spermidine, 100mM NaCl) (1.5ng/µl). The samples were injected into pronuclei by the LMS Transgenics Facility and the EMBO Transgenics Facility in Monterotondo, Rome (see 5.2.2, p. 183, Table 5.1, p. 184).

2.4.6. Generation of founders, germline transmission and iCre expression

Positive founder mice carrying the Blimp1-iCre transgene were identified using PCR (see 2.4.7, p. 83). Germline transmission was tested via mating each positive founder with C57BL/6 wild-type mice (see 5.2.3, p. 184, Table 5.2, p. 185). iCre expression and recombination efficiency was tested using two reporter strains: Z/EG (Novak et al. 2000) and R26RGOF (Madisen et al. 2010; Yoshimizu et al. 1999; Yeom et al. 1996) (see 5.2.4, p. 186, Table 5.3, p. 189).

Genotyping protocol - Z/EG allele. Genotypes were identified using the primers listed in **Table 2.1**. PCR reactions were set up using Qiagen Taq DNA Polymerase (Qiagen, 201203). PCR reactions were run using the following cycling conditions: 94^{o}C for 1 minutes, followed by 29 cycles of 94^{o}C for 30 second, 55^{o}C for 30 seconds and 72^{o}C for 1:30 minutes. A final extension at 72^{o}C for 10 minutes was performed, followed by 18^{o}C for 10 minutes. The presence of the reporter allele corresponds to a band at 750 base pairs.

Genotyping protocol - R26R allele. The R26RGOF reporter mice were homozygous for the R26R reporter (Madisen et al. 2010) and the GOF transgene (Yoshimizu et al. 1999; Yeom et al. 1996). Therefore, the genotype was not determined using PCR, as all embryos were heterozygous for both transgenes.

2.4.7. Blimp1-iCre colony – strain #555309

Genetic background and colony maintenance. The Blimp1-iCre (#555309) founder female was on a pure FVB background. A colony has been established by crossing the founder female with C57BL/6 wild-type mice (purchased from Charles River). The Blimp1-iCre colony is maintained via breeding pairs of heterozygous Blimp1-iCre males and C57BL/6 wild-type females. So far, the colony has been backcrossed to C57BL/6 for 6 generations.

Experimental mice. Female Blimp1-iCre (F4) mice were used to cross with male floxed mTOR$^{fl/fl}$ mice for experiments (due to time constraints and availability) (see 6.2.1, p. 202, Figure 6.1, p. 203).

Genotyping protocol. The presence of the iCre transgene was identified using the primers listed in **Table 2.1**. PCR reactions were set up using the OneTaq® Hot Start Quick-Load® 2X Master Mix (New England Biolabs, M0488S). PCR reactions were run using the following

cycling conditions: 95°C for 5 minutes, followed by 34 cycles of 95°C for 30 seconds, 60°C for 30 seconds and 72°C for 1:30 minutes. A final extension at 72°C for 10 minutes was performed, followed by 18°C for 10 minutes. Presence of the iCre transgene corresponds to a positive band at 186 base pairs.

3. Chapter 3 - Characterisation of mTOR signalling in wild-type primordial germ cells.

3.1. Introduction

3.1.1. Signalling events in mouse developing primordial germ cells

As described in chapter 1, signalling events are crucial during germ cell development. WNT/BMP signals from the surrounding somatic environment induce PGC specification in a subset of epiblast cells (Lawson et al. 1999; Ying and Zhao 2001; Ying et al. 2000; de Sousa Lopes et al. 2004; Tremblay, Dunn, and Robertson 2001; Chu et al. 2004; H. Chang and Matzuk 2001; Ohinata et al. 2009). Migrating PGCs rely on SDF1-CXCR4 and KIT ligand - C-KIT signalling for germ cell survival, proliferation and correct migration (Ara et al. 2003; Molyneaux et al. 2003; Y. Gu et al. 2009; Runyan et al. 2006). Gonadal germ cells undergo sex determination driven by SRY-SOX9-FGF9 signalling in males and WNT/RSPO1 signalling in females and initiation of meiosis is potentially dependent on RA signalling (Kocer et al. 2009).

Our current understanding of signalling events in primordial germ cells is reflected in our ability to modulate some of the above described developmental processes *in vitro.* Via the addition of defined agonists or antagonist of underlying signalling pathways, specification can be induced in epiblast cells of cultured embryonic fragments (Hayashi et al. 2011; Ohinata et al. 2009), migration can be manipulated in migratory PGCs during embryo slice culture (Molyneaux et al. 2003) and sex determination pathways can be directed towards the male or female pathway during urogenital ridge culture experiments *in vitro* (Bowles et al. 2006; Koubova et al. 2006; Bowles et al. 2010).

In fact, specification of germ cells can be recapitulated starting from embryonic stem cells via first differentiating ESCs into epiblast-like cells (EpiLCs) through the addition of basic fibroblast growth factor (bFGF) and Activin A for 48 hours (Hayashi et al. 2011). EpiLCs can be further induced to form PGC like cells (PGCLCs) via the addition of BMP4, LIF, SCF and EGF over a 7 day period (Hayashi et al. 2011). PGCLCs closely resemble *in vivo* migratory PGCs, sharing many properties at the transcriptional and epigenetic level, such as expression of germ cell specific genes and pluripotency genes, histone modifications and methylation levels (Hayashi et al. 2011). PGCLCs are able to progress further through gametogenesis and differentiate into mature egg or sperm when co-cultured with either somatic gonadal cells (Ishikura et al. 2016; Q. Zhou et al. 2016; Hikabe et al. 2016; Morohaku et al. 2016) or when transplanted back into intact gonads lacking endogenous germ cells (Hayashi et al. 2011) or a combination of both (Hayashi et al. 2012). However, unless mixed with somatic cells,

PGCLCs cannot progress beyond the point of resembling migratory PGCs under defined culture conditions *in vitro* (Hayashi et al. 2011).

Efforts to culture PGCs *in vitro* have been relying on undefined culture conditions such as serum or the use of feeders, in addition to further growth factors (Leitch, Tang, and Surani 2013). To date, long term *in vitro* culture of PGCs has been unsuccessful as cells usually undergo apoptosis after a few days or reprogram into embryonic germ cells (EGCs). EGCs are considered pluripotent cells that share many characteristics with embryonic stem cells (Leitch, Tang, and Surani 2013; M De Felici and McLaren 1983; Donovan 1994; Donovan and de Miguel 2003; Leitch et al. 2013).

Although we can re-capitulate or modulate some of the key processes of PGC development *in vitro*, successful culturing conditions still rely heavily on the use of undefined media, feeders and/or the use of somatic cells, demonstrating that there is still a lot to learn about signalling pathways in foetal germ cells, especially upon their entry into the genital ridge.

In vivo, gonadal PGCs initiate a second wave of epigenetic reprogramming (including global DNA demethylation), induce expression of germline specific genes (MVH and DAZL) and undergo sexual differentiation including initiation of meiosis in females. It is still largely unknown, whether or to what extent the new gonadal environment plays a role in initiating these processes via production of inductive signals.

3.1.2. AKT – mTORC1 signalling axis

Our current understanding of the AKT-mTORC1 signalling axis is based on studies using many different cell types. Binding of extracellular signals, such as insulin and various growth factors, to receptor tyrosine kinases (RTK) leads to activation of these receptors at the cell surface (Manning and Toker 2017). Activated RTKs further activate intracellular adaptor proteins such as insulin receptor substrate (IRS) proteins in the case of insulin-like growth factor 1 receptor (IGF1R) signalling. Such adaptor proteins can activate PI3K, which stimulates phosphorylation of PIP2 to PIP3 and leads to recruitment of PDK1 and AKT to the plasma membrane (Figure 1.4) (Manning and Toker 2017). PDK1 subsequently phosphorylates AKT at the Thr308 site. To be fully activated, AKT can be further phosphorylated at the Ser473 site by mTORC2 (Manning and Toker 2017). AKT is a central signalling hub within the cell with many downstream targets, regulating many biological functions such as proliferation, survival, growth and metabolism (Manning and Toker 2017). One downstream target is the TSC1/2 complex, and its inhibition leads to activation of

mTORC1 signalling (Figure 1.4). Alternatively, AKT can also directly phosphorylate the inhibitory mTORC1 subunit PRAS40, leading to mTORC1 activation (Manning and Toker 2017; J. Huang and Manning 2009). mTORC1 regulates many downstream biological functions through activation of different downstream targets. The two mTORC1 downstream effectors S6 kinases and 4E-binding proteins specifically regulate translation and protein synthesis (Laplante and Sabatini 2009).

In germ cells, the PI3K-AKT signalling axis has been implicated in regulating cell proliferation and survival. Germ cell specific deletion of PTEN, a negative regulator of AKT, leads to increased proliferation of germ cells *in vivo*, causing testicular teratomas in male mice (Kimura et al. 2003). Most of the acquired data, however, is from *in vitro* experiments of short-term cultured primordial germ cells or conversion of PGCs to EGCs (Leitch, Tang, and Surani 2013). Overexpression of AKT in cultured primordial germ cells results in increased proliferation and survival (De Miguel et al. 2002). In this study, mTORC1 has been suggested as a possible downstream mediator of AKT in promoting cell proliferation based on two observations. Culturing wild-type PGCs in the presence of the mTORC1 inhibitor rapamycin for 7 days decreased cell proliferation. Further, overexpression of AKT in cultured PGCs resulted in the detection of phosphorylated S6K1 (downstream of mTORC1). It should be noted though that these observations were *in vitro* and phosphorylated S6K1 was not detected in PGCs unless AKT was overexpressed (De Miguel et al. 2002).

In vivo, very little is known about the role of AKT-mTORC1 signalling during early germ cell development.

In this chapter, mTOR signalling was characterised in wild-type PGCs *in vivo* using an immunofluorescence-based approach. The aims were to identify the exact timing of mTORC1 signal activation in germ cells and to determine the preferred signalling axis downstream of mTORC1 (S6 kinases vs 4E-binding proteins). In addition, the role of AKT signalling was analysed as a possible mTORC1 activator in PGCs.

3.2. Results

3.2.1. mTOR signalling in wild-type PGCs

3.2.1.1. Gene expression of mTOR and mTORC1 downstream targets

mTOR is part of two structurally and functionally different multi-protein complexes – mTORC1 and mTORC2 (Laplante and Sabatini 2009). To analyse mTOR signalling in wild-type PGCs, I first analysed gene expression levels of *Mtor* and its associated proteins forming the mTORC1 or mTORC2 signalling complex in foetal germ cells (Figure 3.1 A). For this, existing RNA-Seq data from wild-type PGCs collected at three different time points during embryonic development (E10.5, E12.5 male and female, E14.5 male and female) was used (Hill et al. 2018).

Mtor and all subunits of mTORC1 and mTORC2 were expressed *in vivo* in foetal germ cells with FPKM values (Fragments Per Kilobase of transcript per Million mapped reads) up to ~10 (Figure 3.1 B-C). *Mtor* gene expression levels increased from E10.5 to E14.5, with no apparent difference in expression levels between male and female germ cells. Regarding the two other proteins present in both complexes, *Deptor* gene expression peaked at E12.5 in female PGCs, whereas *Mlst8* expression was higher in male PGCs at E12.5 and E14.5 (Figure 3.1 B-C). Interestingly, mTORC1 specific subunits *Rptor* (RAPTOR) and *Akt1s1* (PRAS40) were expressed at lower levels compared to mTORC2 specific subunits *Rictor*, *Mapkap1* (mSIN1) and *Prr5* (PROTOR1/2) (Figure 3.1 B-C). In fact, *Rictor* had about 4-fold higher average gene expression levels compared to *Rptor*.

Next, I checked gene expression levels of mTORC1 downstream targets involved in the regulation of translation (Figure 3.2 A). S6 kinases, consisting of *Rps6kb1* (S6K1) and *Rps6kb2* (S6K2), were expressed at a fairly constant level over the analysed time period of E10.5 to E14.5. *Rps6kb1* was the higher expressed gene compared to *Rps6kb2* in wild-type foetal germ cells (< 10 FPKM vs < 3.5 FPKM, respectively) (Figure 3.2 B). The 4E-binding protein family consists of three isoforms and *Eif4ebp1* (4E-BP1) (< 100 FPKM) was by far the highest expressed gene compared to *Eif4ebp2* (4E-BP2) (<4.5 FPKM) and *Eif4ebp3* (4E-BP3) (< 0.5 FPKM). In fact, *Eif4ebp1* was the highest expressed mTORC1 downstream target among S6 kinases and 4E-binding proteins, with fairly constant expression at E10.5 and E12.5 (~70 FPKM) and comparably low expression at E14.5 in female (< 20 FPKM) versus high expression in male PGCs (< 100 FPKM) (Figure 3.2 B).

The main downstream effector of 4E-BPs, *Eif4e* was very highly expressed (< 250 FPKM) at a fairly constant level (Figure 3.2 C). Ribosomal protein S6 (*Rps6*), a downstream effector of S6 kinases, was expressed at even higher levels in wild-type germ cells, peaking at E14.5 (~ 480 FPKM) (Figure 3.2 C).

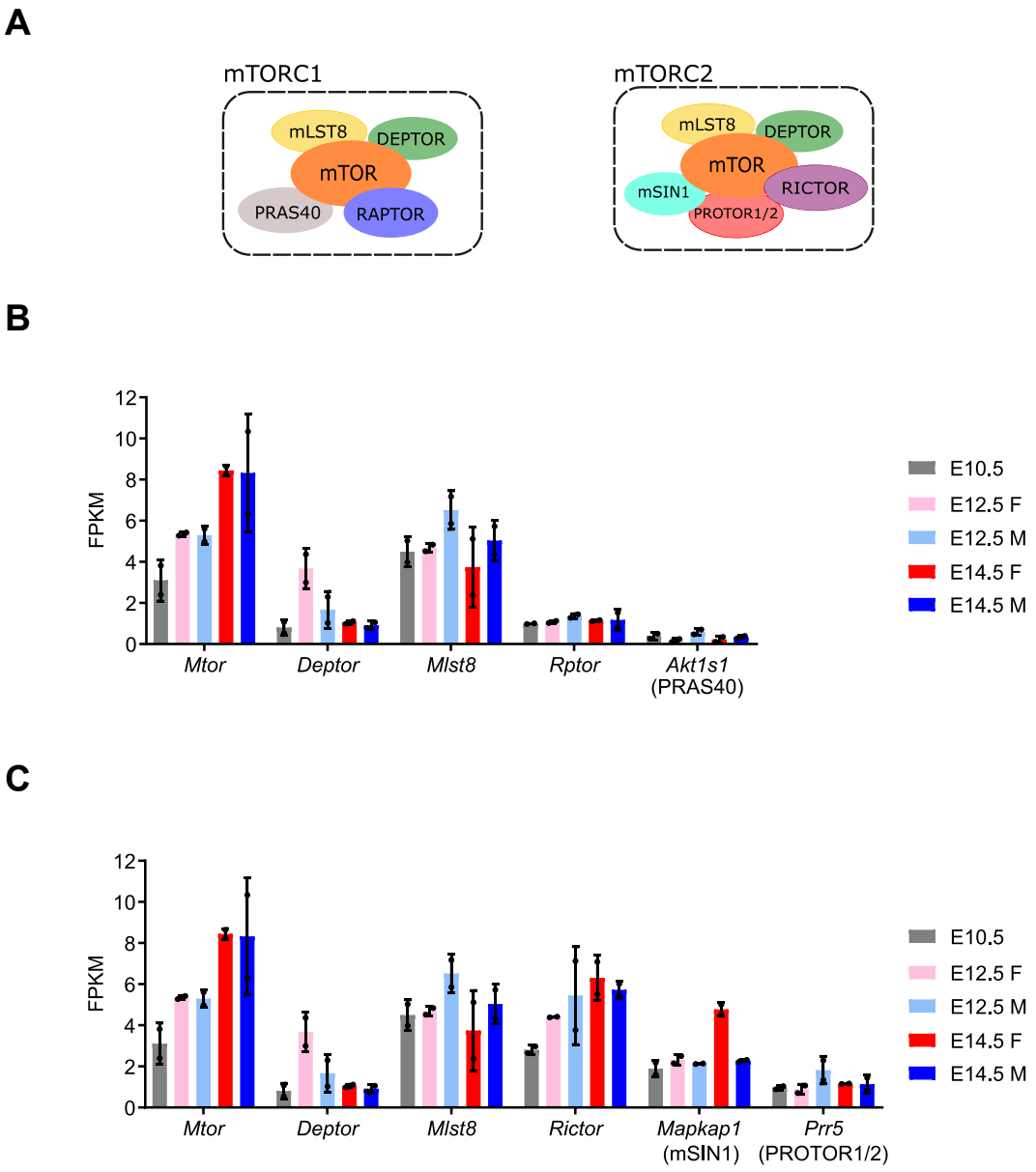

Figure 3.1: Gene expression of mTORC1 and mTORC2 subunits in wild-type PGCs.

RNA-Seq data from E10.5, E12.5 female and male and E14.5 female and male PGCs. **A** Schematic of mTORC1 and mTORC2 multi protein complexes. **B** Gene expression of mTORC1 subunits. **C** Gene expression of mTORC2 subunits. Gene names are depicted, protein names are in brackets. FPKM values are shown, n=2, error bars = standard deviation; RNA-Seq data were generated and analysed by Peter Hill.

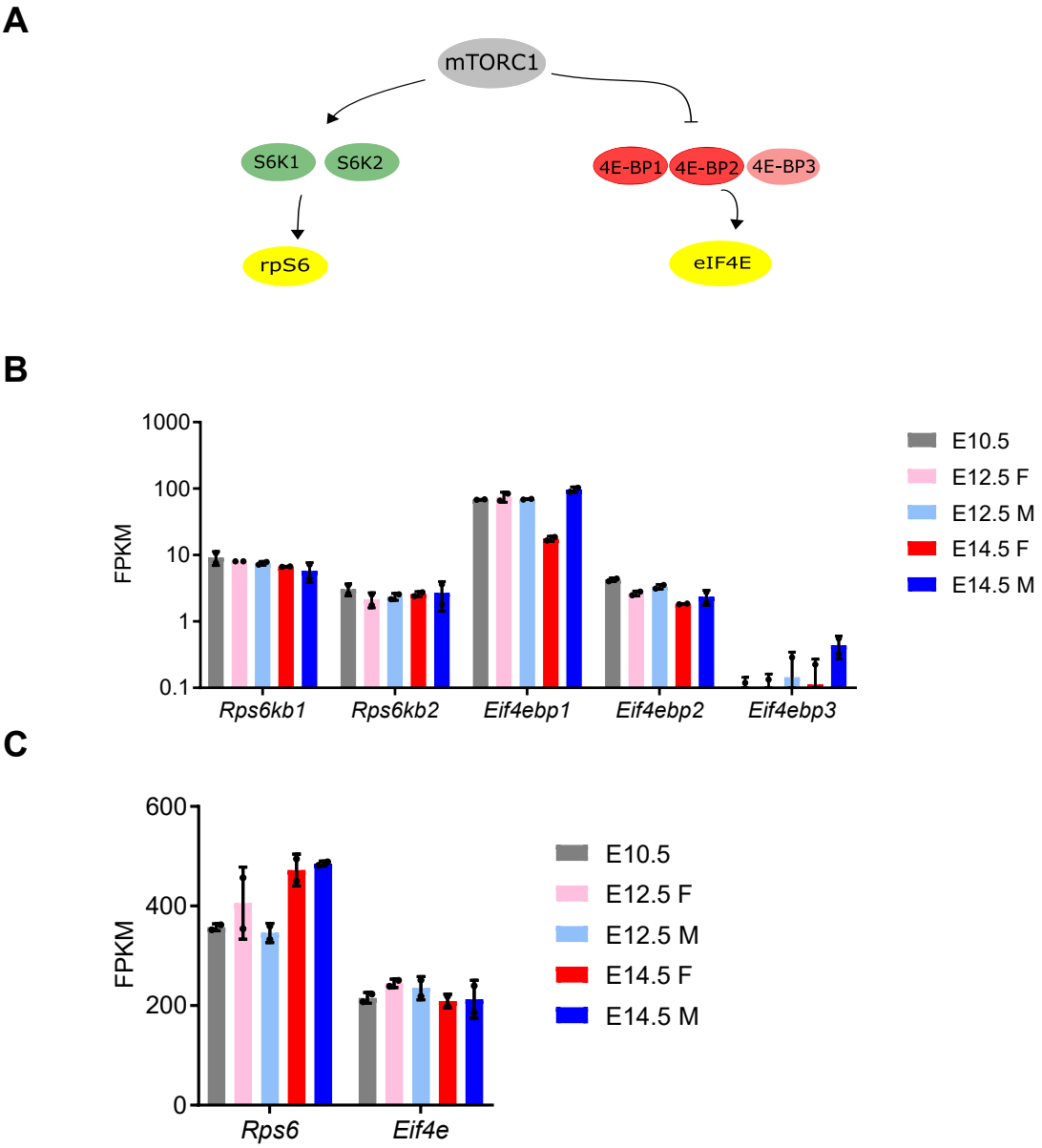

Figure 3.2: Gene expression of downstream targets of mTORC1 signalling in wild-type PGCs.

A Simplified schematic of the signalling cascade downstream of mTORC1. The two main downstream targets (S6 kinases and 4E-binding proteins) involved in the regulation of translation are shown. S6 kinases are activated via mTORC1 signalling and subsequently phosphorylate ribosomal protein S6 (amongst others). 4E-binding proteins are phosphorylated upon mTORC1 signalling and phosphorylation inhibits binding to eIF4E, enabling formation of translation initiation complex. **B** Gene expression of S6 kinases and 4E-binding proteins. **C** Gene expression data of downstream effectors *Rps6* and *Eif4e*. Gene names are depicted. FPKM values are shown, n=2, error bars = standard deviation; RNA-Seq data were generated and analysed by Peter Hill.

Taken together, gene expression analysis showed that *Mtor* and all subunits of the mTORC1 and mTORC2 complexes are expressed in foetal germ cells, however, mTORC2 specific subunits are expressed at higher levels compared to mTORC1 specific subunits. Downstream of mTORC1, *Rps6kb1* (S6K1) and *Eif4ebp1* (4E-BP1) are the highest expressed genes among their families, and *Eif4ebp1* is the highest expressed downstream target overall. Further, downstream effectors *Rps6* and *Eif4e* are both highly expressed compared to S6 kinases and 4E-binding proteins.

3.2.1.2. Protein levels and activation status of downstream mTORC1 effectors

Gene expression levels do not necessarily correlate with protein levels (Y. Liu, Beyer, and Aebersold 2016). In addition, overall protein levels do not indicate the activation status of proteins or signalling pathways. To complement our gene expression data and to get an actual readout of mTORC1 signalling in wild-type germ cells, a targeted immunostaining approach was used. Due to the lack of a satisfactory antibody against phosphorylated mTOR kinase, activation levels of the mTORC1 catalytic subunit could not be analysed. Further, mTOR can be part of both signalling complexes (mTORC1 and mTORC2) (Laplante and Sabatini 2012) and therefore phosphorylated mTOR levels will not accurately reflect activation of the mTORC1 signalling complex. Therefore, levels of mTORC1 signalling were assessed using a functional readout of mTORC1 mediated phosphorylation of downstream effectors.

I focused on the mTORC1 effectors S6K1 and 4E-BP1, since these isoforms were the highest expressed isoforms among their protein families at the mRNA level. Total protein levels and phosphorylated protein levels were analysed between E9.5 to E14.5. Changes in the protein activation status will determine the exact timing of mTORC1 signalling activation and identify which downstream signalling axis is activated upon mTORC1 signalling in germ cells.

For all the following experiments, embryonic trunks (E9.5 and E10.5), genital ridges (E11.5) and gonads (E12.5 – E14.5) from C57BL6 x GOF18ΔPE-EGFP embryos, in which germ cells express EGFP driven by an *Oct4* promoter and distal enhancer, were collected (Yeom et al. 1996; Yoshimizu et al. 1999). This allows easy and accurate identification of germ cells using an antibody against GFP.

3.2.1.2.1 mTORC1 - S6 kinase - S6 signalling axis

To analyse mTORC1 signalling via S6 kinases, I initially wanted to check total and phosphorylated protein levels of S6K1, since it was the highest expressed isoform at the mRNA level. However, no satisfactory antibodies against total and phosphorylated S6K1 were available for IF stainings on cryosections (data not shown). Alternatively, ribosomal protein S6, a downstream effector of S6 kinases, was analysed as a readout for mTORC1-S6 kinase signalling. RpS6 is a subunit of the 40s ribosomal complex and was also highly expressed in foetal germ cells in our RNA-Seq data (Figure 3.2 C).

In wild-type tissues from E9.5 to E13.5, S6 was localized to the cytoplasm of cells, as expected given that S6 is a subunit of the 40s ribosomal complex (Figure 3.3). PGCs as well as somatic cells stained positive for total S6 and signal intensities seemed to be fairly evenly distributed by eye with no specific enrichment of total S6 protein in either germ cells or somatic cells (Figure 3.3). Some variation in signal intensity was observed throughout the tissue, sometimes with slightly higher staining intensity towards the edge of the tissue (at E12.5, and E13.5F), possibly due to technical reasons (Figure 3.3).

To determine whether mTORC1-S6 kinase signalling is activated in germ cells, phosphorylated S6 levels were analysed. Ribosomal protein S6 has 5 phosphorylation sites and can be phosphorylated via the mTORC1-S6 kinase signalling pathway and via the MAP-ERK pathway (Meyuhas 2015; Pende et al. 2004; Roux et al. 2007). For a detailed read out reflecting mTORC1-S6K1 signalling only, phosphorylated S6 protein levels specifically at the Serine 240/244 phosphorylation sites were analysed, which have been shown to be solely phosphorylated by the mTORC1-S6 Kinase signalling pathway (Pende et al. 2004; Roux et al. 2007).

First, the pS6 (S240/244) antibody was validated using *Rps6*$^{P-/-}$ knock-in mice expressing a S6 protein which cannot be phosphorylated. Control stainings of E11.5 tissue from phospho-mutant *Rps6*$^{P-/-}$ knock-in mice showed complete lack of pS6 (S240/244) staining, demonstrating the specificity of the antibody used (Figure 3.4 A). As expected, total S6 protein could be detected in the *Rps6*$^{P-/-}$ tissue, indicating the presence of non-phosphorylated S6 protein, although at lower levels compared to wild-type tissues (Figure 3.4 A).

Following antibody validation, wild-type germ cells were analysed. pS6 (S240/244) was also localized to the cytoplasm and the observed staining pattern showed heterogeneous signal

intensities throughout the tissue, with low and high levels present in somatic cells and primordial germ cells (Figure 3.4 B-C). Again, no clear enrichment of pS6 signal could be detected in either PGCs or somatic cells. However, male tissues seemed to have more and higher overall pS6 signal compared to female tissues at E13.5 by eye (Figure 3.4 B-C). The enriched pS6 signal in male tissues was restricted to the gonad, while the attached mesonephros showed similar staining intensity between males and females (Figure 3.4 B).

Taken together, there is no clear enrichment of total or pS6 in germ cells or somatic cells, suggesting that the mTORC1-S6 kinase-S6 signalling axis is not specifically activated in foetal germ cells over the examined time period, but rather active at varying levels in a subset of somatic and germ cells throughout the tissue. Interestingly, at E13.5 male tissues seem to have higher overall levels of mTORC1-S6K1-S6 signalling compared to females.

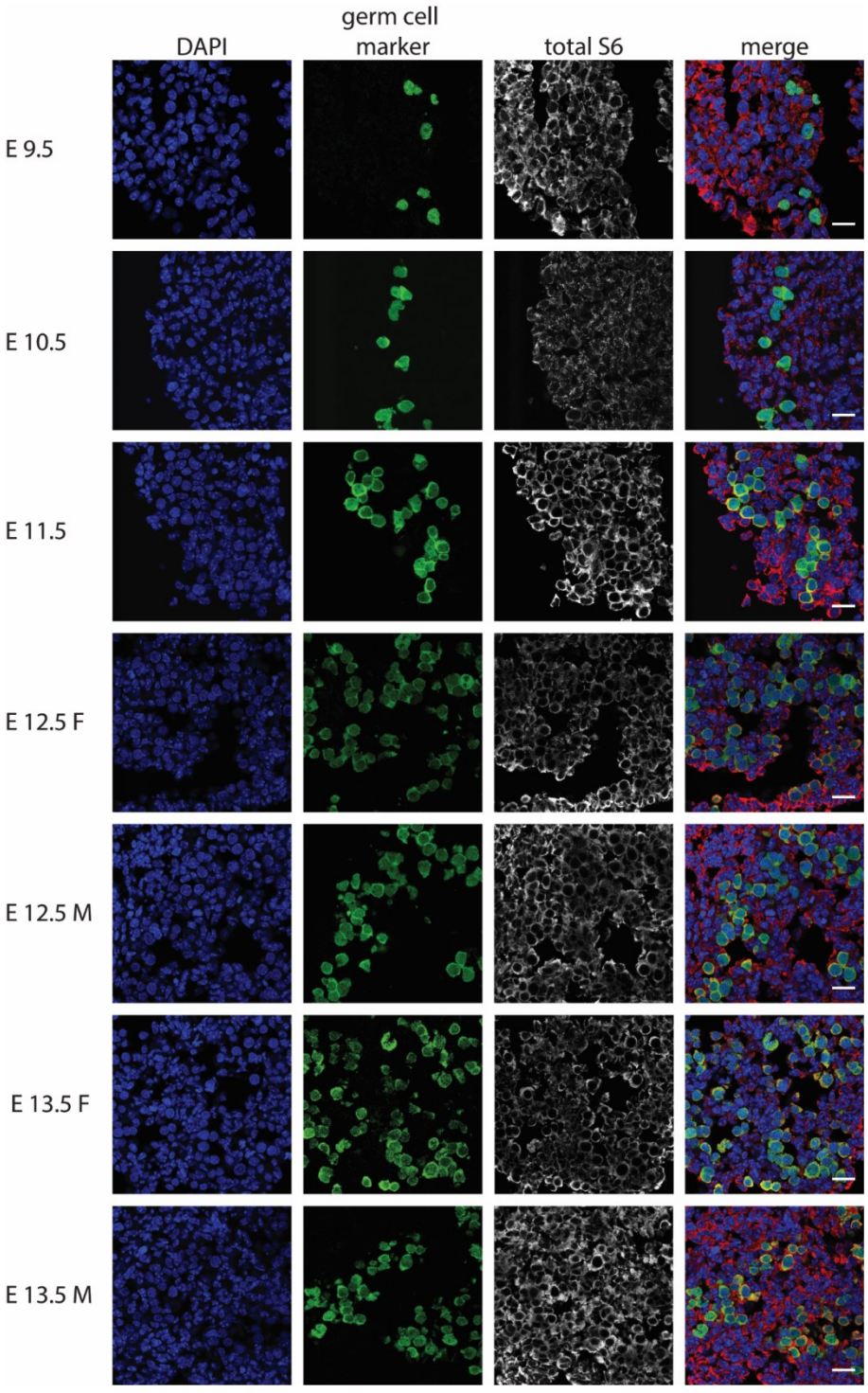

Figure 3.3: Total S6 protein levels in wild-type germ cells.

Immunofluorescence stainings of wild-type germ cells from E9.5-E13.5. Total S6 protein levels are shown. Germ cells were identified via GFP expression driven by the *Oct4* promoter (green), nuclei were stained with DAPI (blue). Representative images shown, n=3 (embryos), scale bar = 20μm

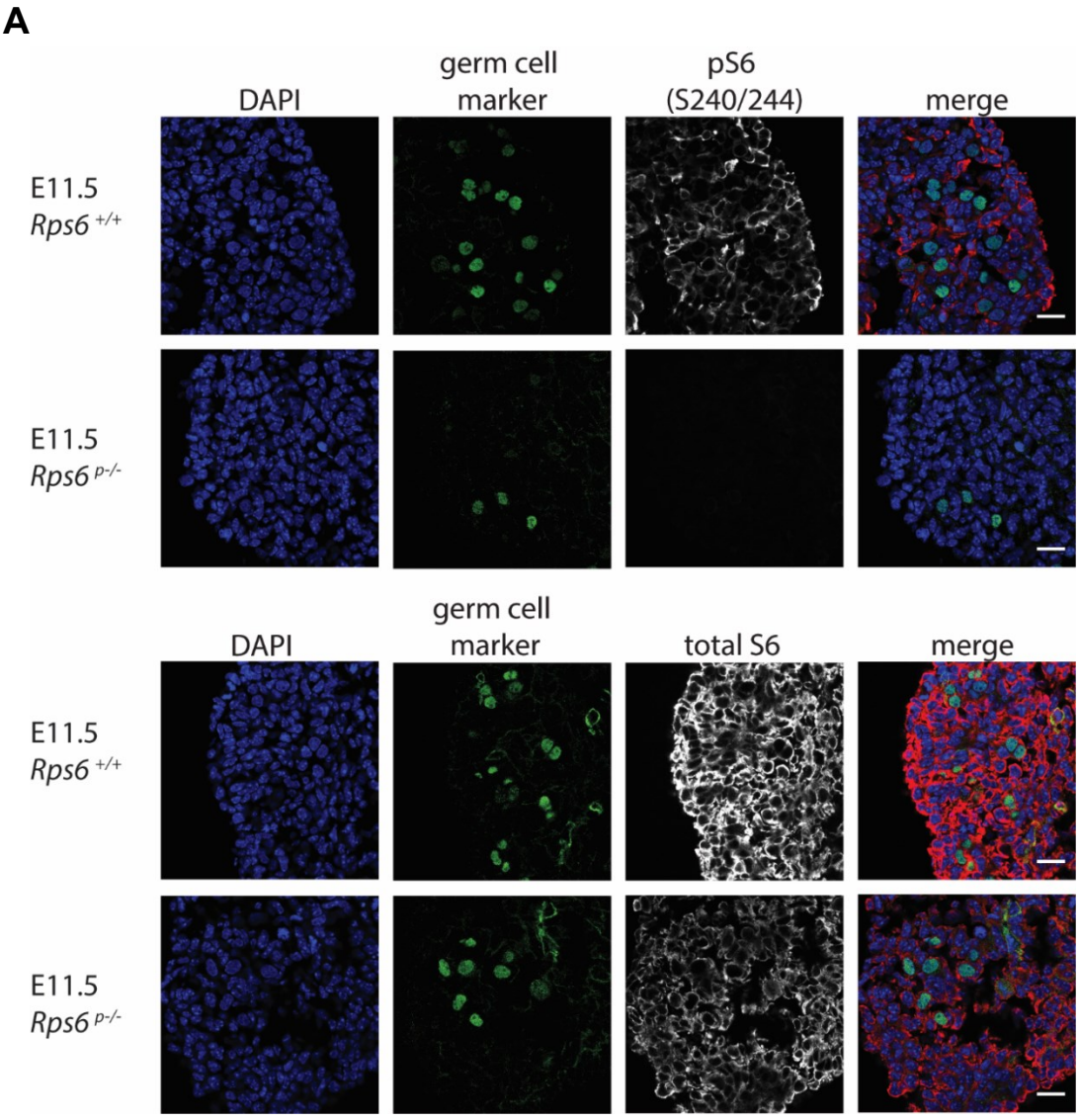
A
DAPI
germ cell marker
pS6 (S240/244)
merge
E11.5 Rps6 +/+
E11.5 Rps6 p-/-
DAPI
germ cell marker
total S6
merge
E11.5 Rps6 +/+
E11.5 Rps6 p-/-

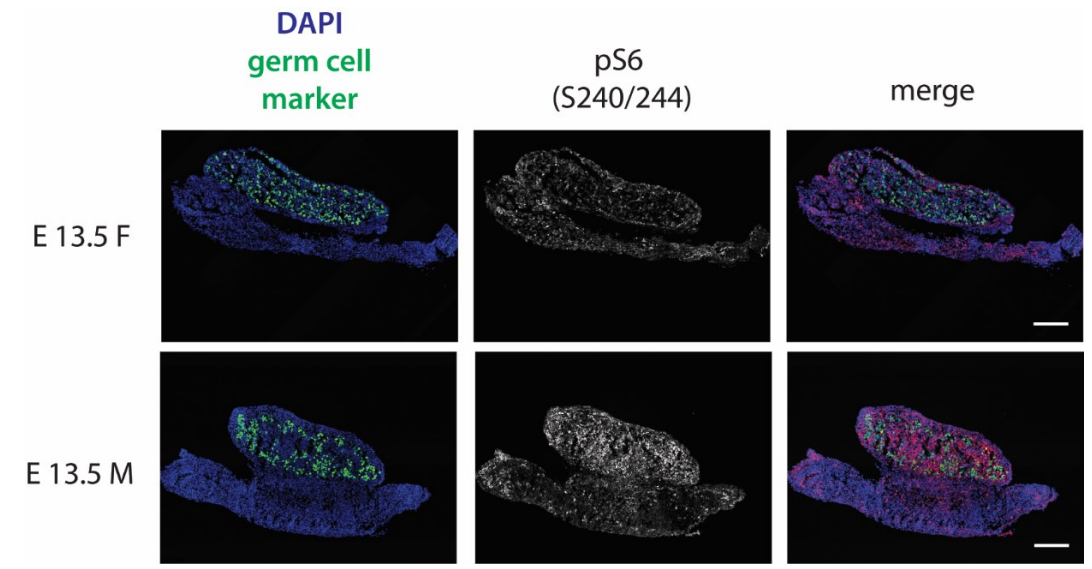
B
DAPI
germ cell marker
pS6 (S240/244)
merge
E 13.5 F
E 13.5 M

C

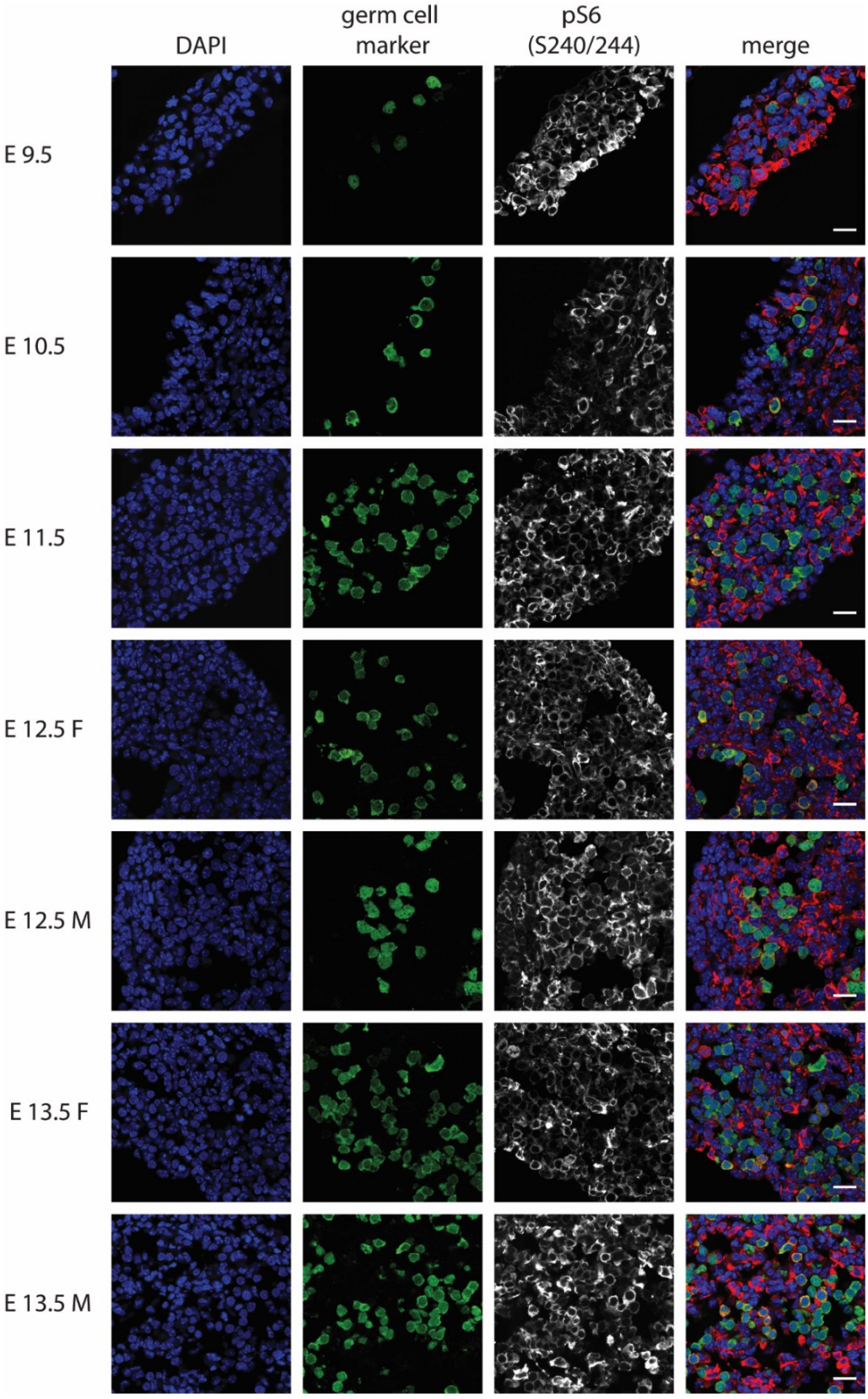
DAPI
germ cell marker
pS6 (S240/244)
merge
E 9.5
E 10.5
E 11.5
E 12.5 F
E 12.5 M
E 13.5 F
E 13.5 M

Figure 3.4: Activation status of the S6K1-S6 signalling axis in wild-type PGCs.

Immunofluorescence staining of wild-type germ cells from E9.5-E13.5. Germ cells were identified via GFP expression driven by the *Oct4* promoter (green), nuclei were stained with DAPI (blue). **A** pS6 (240/244) antibody validation. Control stainings of E11.5 wild-type tissue (*Rps6*$^{+/+}$) and phospho-mutant tissue (*Rps6*$^{p-/-}$) to confirm pS6 (240/244) antibody specificity. Germ cells were identified via OCT4 expression. Expression of pS6 (240/244) and total S6 protein is shown. Representative images shown, n=1 (embryo per genotype), scale bar = 20µm; Wild-type and knock-in tissue were from litter mates. Genotype was identified via PCR. **B** Tile scans of whole female and male genital ridges at E13.5 showing phosphorylated S6 (S240/244) staining. Scale bar = 200µm. **C** Phosphorylated S6 (S240/244) protein levels in wild-type germ cells. Representative images shown, n=3 (embryos), scale bar = 20µm

3.2.1.2.2 mTORC1 - 4E-BP1 signalling axis

Gene expression data revealed that 4E-BP1 was not only the highest expressed isoform among 4E-binding proteins, but also the highest expressed downstream target among S6Ks and 4E-BPs. Preliminary data suggesting activation of the mTORC1-4E-BP1 signalling axis was based on IF stainings of p4E-BP1 over a short time period of E9.5-E11.5 (Peter Hill, personal communication).

To validate these observations in addition to acquiring a detailed understanding of mTORC1-4E-BP1 signalling in foetal germ cells, total and phosphorylated protein levels of 4E-BP1 in wild-type tissues were analysed over a wider time period (E9.5-E14.5).

First, antibody specificity was validated using global 4E-BP1$^{-/-}$ knockout tissues. At E11.5, wild-type genital ridges stained positive for total 4E-BP1 or phosphorylated 4E-BP1 (T37/46) protein. In contrast, global 4E-BP1$^{-/-}$ knockout genital ridges showed no signal (total 4E-BP1) or loss of the characteristic staining pattern (p4E-BP1), respectively, demonstrating antibody specificity (Figure 3.5).

Following antibody validation, wild-type germ cells were analysed. Overall, total 4E-BP1 signal was detected mainly in the cytoplasm of cells, although female PGCs at E13.5 also showed strong nuclear staining (Figure 3.6 A). 4E-BP1 protein levels were semi-quantitatively measured via comparing signal intensities of primordial germ cells relative to signal intensities of somatic cells of the gonad (Figure 3.6). At E9.5, total 4E-BP1 levels were low throughout the tissue. Interestingly, a significant increase in protein levels was detected specifically in primordial germ cells from E9.5 onwards (Kruskal-Wallis test, $p<0.0001$) (Figure 3.6 A-B). At E11.5, a peak was reached with the total 4E-BP1 median fluorescence being roughly 1.8 fold higher in PGCs compared to surrounding somatic cells (Figure 3.6 B).

From E12.5 onwards, 4E-BP1 protein levels decreased again, with a more pronounced and rapid decrease observed in male germ cells (Figure 3.6 A-B). While in males, the relative 4E-BP1 median fluorescence dropped significantly from E12.5 to E13.5 (1.71 vs. 1.27 relative fluorescence) (Kruskal-Wallis test, $p<0.001$), reaching a plateau, female samples reached similarly low protein levels only one day later at E14.5 (Figure 3.6 B). Of note, male samples showed an enrichment of 4E-BP1 signal intensities in somatic cells closely surrounding PGCs at E13.5, with an even more pronounced enrichment at E14.5 (Figure 3.6 A).

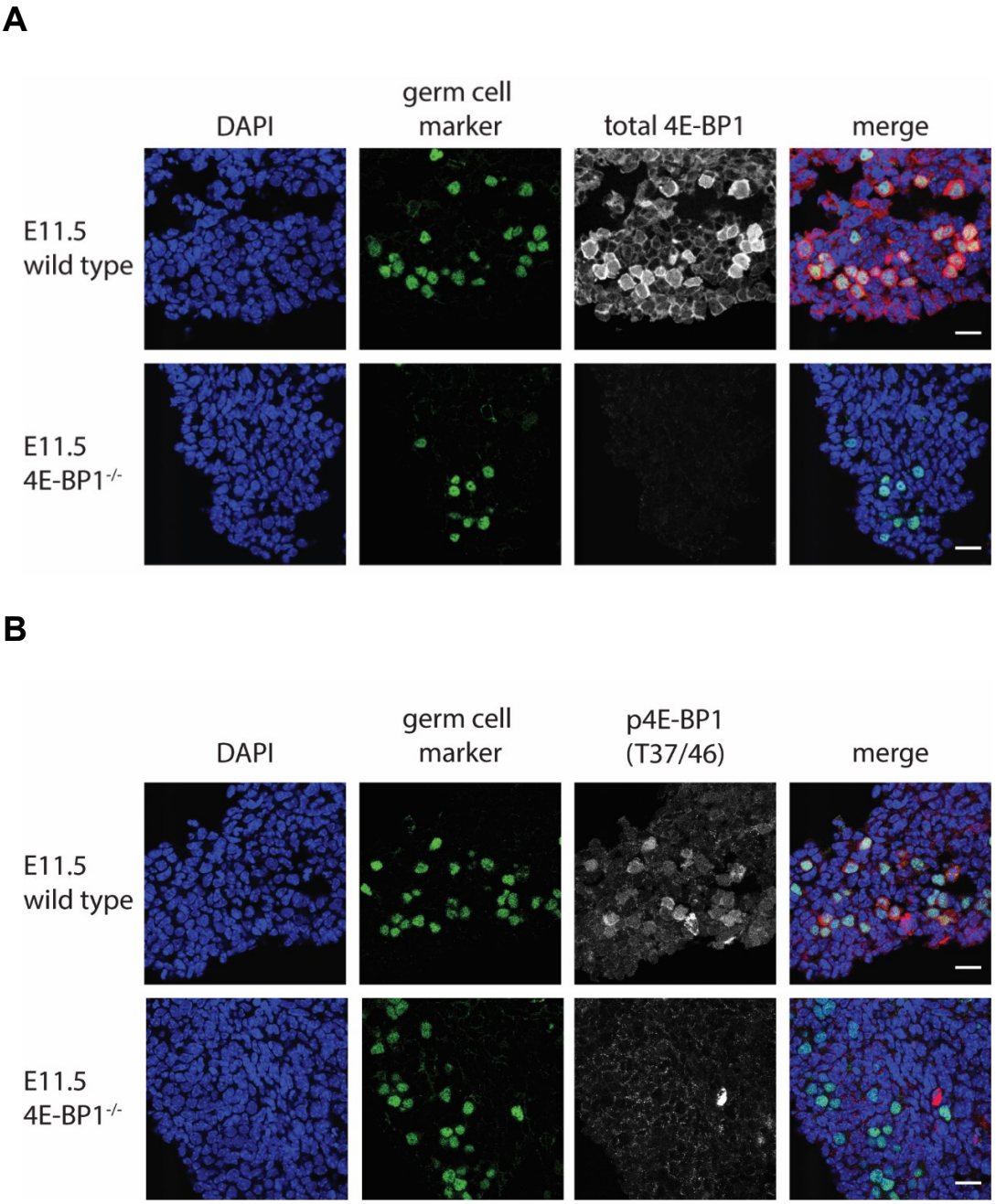

Figure 3.5: Total 4E-BP1 and p4E-BP1 antibody validation in global 4E-BP1$^{-/-}$ knockout tissues.

Immunofluorescence control stainings of E11.5 wild-type and 4E-BP1$^{-/-}$ knockout tissues to confirm 4E-BP1 antibody specificity. Germ cells were identified via OCT4 expression, nuclei were stained with DAPI (blue). **A** Total 4E-BP1 antibody staining shown. Representative images shown, n=1 (embryo), scale bar = 20µm **B** p4E-BP1 (T37/46) antibody staining shown. Representative images shown, n=1 (embryo), scale bar = 20µm; Wild-type and 4E-BP1$^{-/-}$ knockout tissues were from littermates. Genotype was identified via PCR.

A

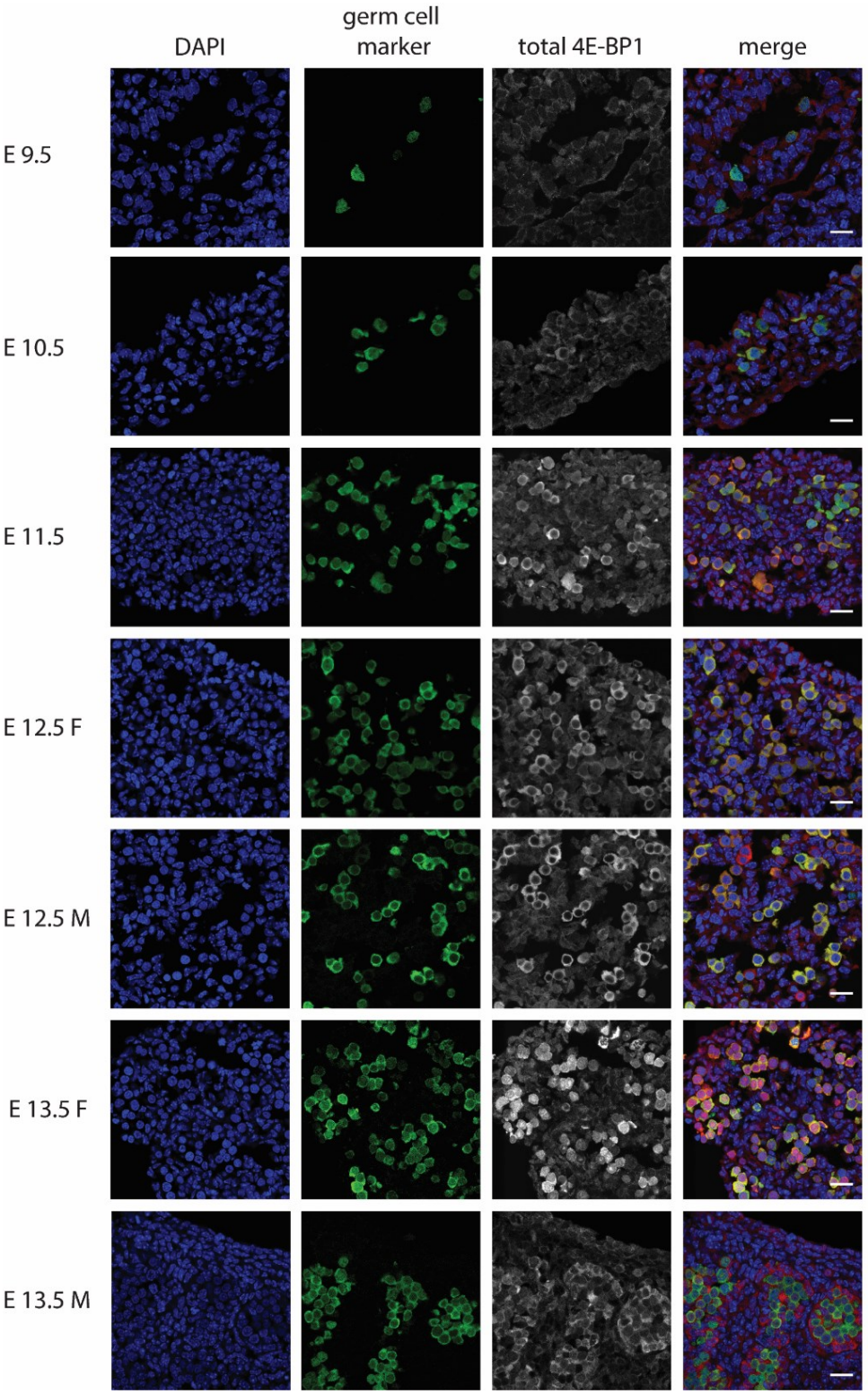
DAPI
germ cell marker
total 4E-BP1
merge
E 9.5
E 10.5
E 11.5
E 12.5 F
E 12.5 M
E 13.5 F
E 13.5 M

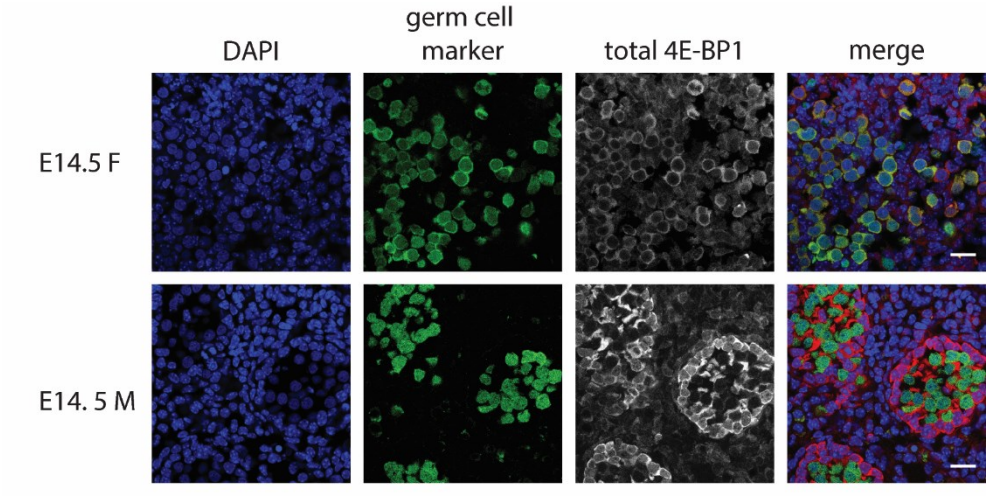

B

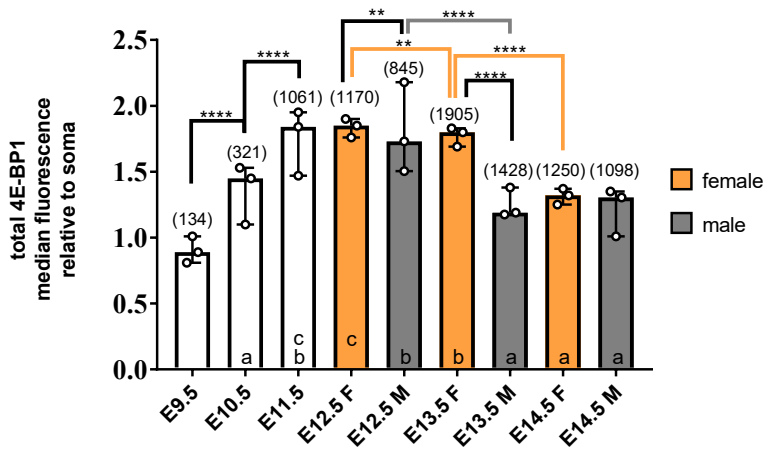

Figure 3.6: Total 4E-BP1 protein levels in wild-type PGCs from E9.5 to E14.5.

Immunofluorescence stainings of wild-type germ cells from E9.5-E14.5. Germ cells were identified via GFP expression driven by the *Oct4* promoter (green), nuclei were stained with DAPI (blue). **A** Total 4E-BP1 protein expression in wild-type germ cells. Representative images shown, n=3 (embryos), scale bar = 20µm; **B** Quantification of 4E-BP1 signal intensity in germ cells relative to somatic cells. Relative median fluorescence is depicted with error bars showing the 95% confidence intervals (CI). Female samples are depicted in orange, male samples in grey. Data points represent the median from three independent experiments (n=3 embryos), (n) is the total number of quantified germ cells for each time point. Significance was analysed across cells by the non-parametric Kruskal-Wallis Test, followed by Dunn's multiple comparisons test. **** $p<0.0001$, ** $p<0.01$; Medians with the same letter are not significantly different.

To determine activation of the mTORC1-4E-BP1 signalling axis, p4E-BP1 levels were analysed from E9.5-E13.5 (Figure 3.7). In line with total 4E-BP1 levels, p4E-BP1 levels were low or not detected at E9.5. At E10.5, a few germ cells started to stain positive for p4E-BP1 resulting in a non-significant increase in relative signal intensity (Figure 3.7 A-B). Interestingly, from E10.5 onwards, p4E-BP1 levels significantly increased specifically in gonadal germ cells reaching a peak at E11.5 (Kruskal-Wallis test, $p<0.0001$), with a 2.3 fold relative increase in median signal intensity compared to surrounding somatic cells (Figure 3.7 A-B). Intriguingly, the signal appeared mainly nuclear at this time point (Figure 3.7 B). At E12.5, p4E-BP1 levels were decreased again, with male germ cells having similar levels to E10.5 (Figure 3.7 A-B). In female germ cells, a peak of p4E-BP1 signal was detected at E13.5, while male germ cells showed significantly lower p4E-BP1 levels (Kruskal-Wallis Test, $p<0.0001$) (Figure 3.7 A-B). However, total protein levels were also significantly lower in male germ cells compared to female germ cells at E13.5 (Kruskal-Wallis test, $p<0.0001$) (Figure 3.7 A-B). Of note, at E13.5, male samples showed increased p4E-BP1 levels in surrounding somatic cells, in line with the observed total 4E-BP1 protein levels (Figure 3.7 A, Figure 3.5 A).

For direct comparison of mRNA levels, total 4E-BP1 and p4E-BP1 levels, relevant selected time points were replotted in Figure 3.8. While gene expression data showed increased expression of 4E-BP1 mRNA at E14.5 in male samples compared to female samples, these differences were not reflected at the protein level (Figure 3.8 A-B). In fact, relative median fluorescence levels at E14.5 did not significantly differ between males and females and were similar to E10.5 protein levels (Kruskal-Wallis test, $p>0.05$). (Figure 3.8A-B). In addition, while total protein levels were significantly increased in male and female samples at E12.5 compared to E10.5, p4E-BP1 signal intensities were only significantly increased in female samples at E12.5 (Kruskal-Wallis test, $p<0.0001$) (Figure 3.8 B-C).

Taken together, using validated antibodies, I showed that total 4E-BP1 protein levels increase specifically in germ cells, reaching a peak at E11.5 and subsequently decreasing from E12.5 onwards. The observed decrease is more pronounced and rapid in male germ cells (Figure 3.6 A-B). In comparison, p4E-BP1 levels peak specifically in PGCs at E11.5 and in female germ cells at E13.5 (Figure 3.7 A-B). These observations confirm previous data on activation of the mTORC1-4E-BP1 signalling axis in foetal germ cells. More importantly, the highly germ cell specific expression and activation pattern of 4E-BP1 suggest a potential role of the mTORC1-4E-BP1 signalling axis during germ cell development.

A

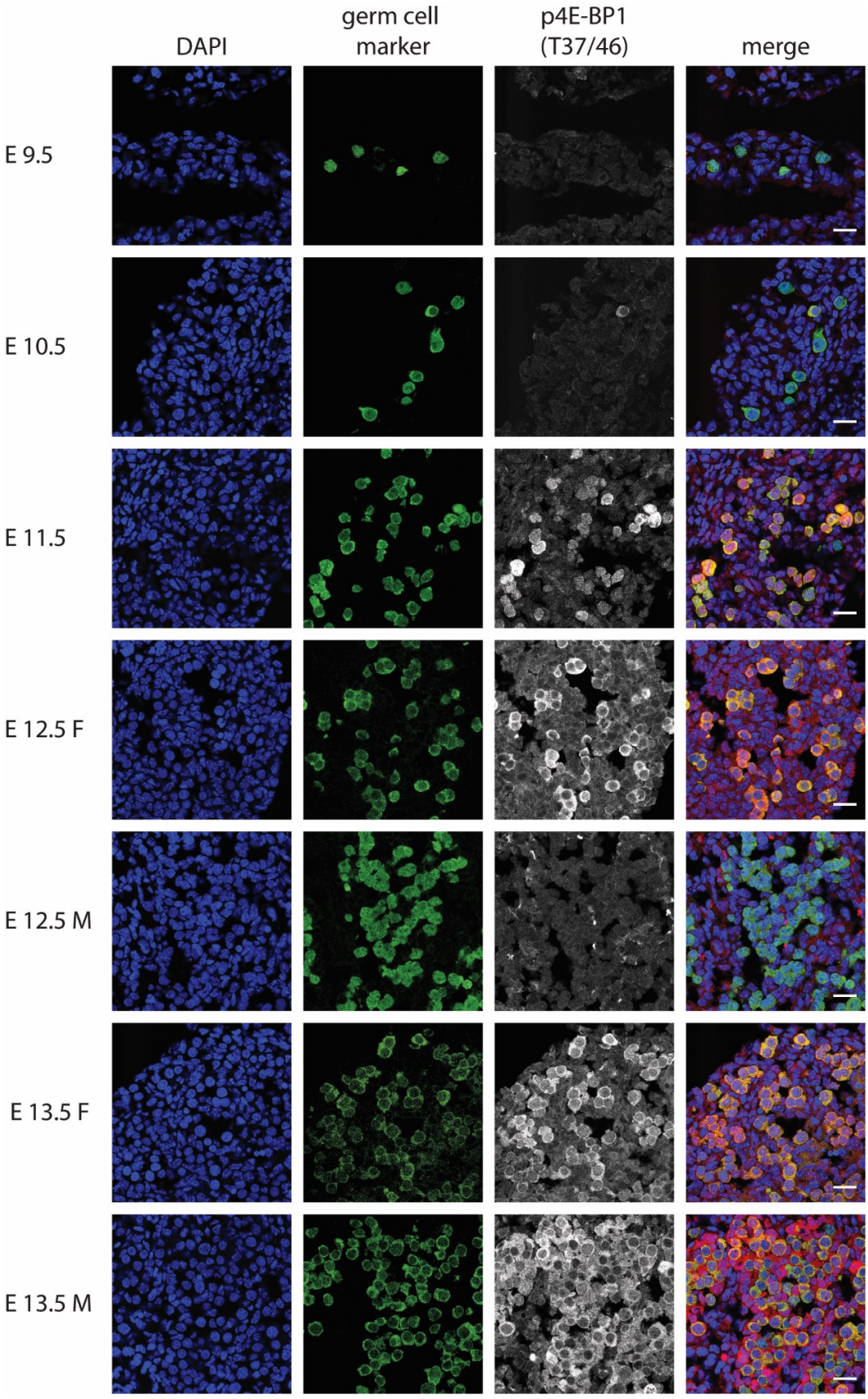
DAPI
germ cell marker
p4E-BP1 (T37/46)
merge
E 9.5
E 10.5
E 11.5
E 12.5 F
E 12.5 M
E 13.5 F
E 13.5 M

B

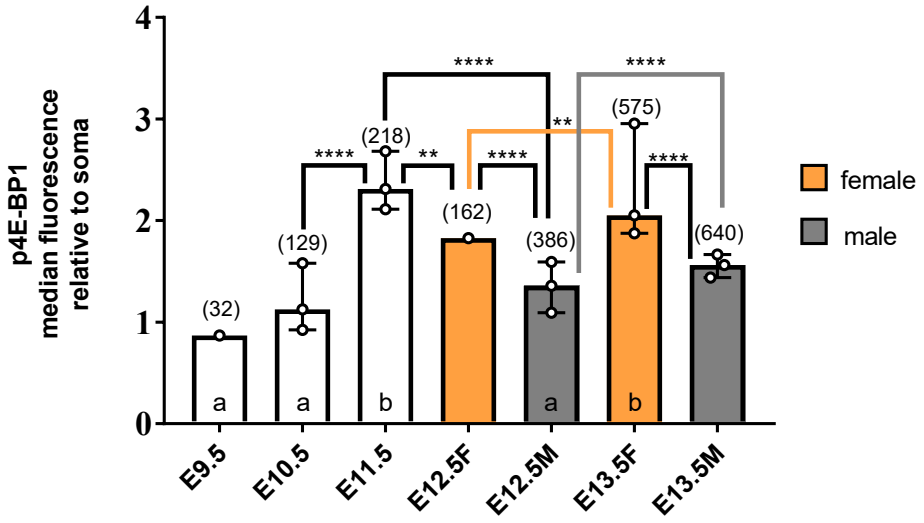

Figure 3.7: p4E-BP1 protein levels in wild-type PGCs.

Immunofluorescence stainings of wild-type germ cells from E9.5-E14.5. Germ cells were identified via GFP expression driven by the *Oct4* promoter (green), nuclei were stained by DAPI (blue). **A** Phosphorylated 4E-BP1 protein levels in wild-type germ cells (E9.5-E13.5). Representative images shown, n=1-3 (embryos), scale bar = 20µm **B** Quantification of p4E-BP1 signal intensity in germ cells relative to somatic cells. Relative median fluorescence is depicted with error bars showing the 95% confidence intervals (CI). Female samples are depicted in orange, male sample in grey. Data points represent the median from independent experiments (n=1-3 embryos), (n) is the total number of quantified germ cells for each time point. Significance was analysed across cells by the non-parametric Kruskal-Wallis Test, followed by Dunn's multiple comparisons test (**** $p<0.0001$, ** $p<0.01$). Medians with the same letter are not significantly different.

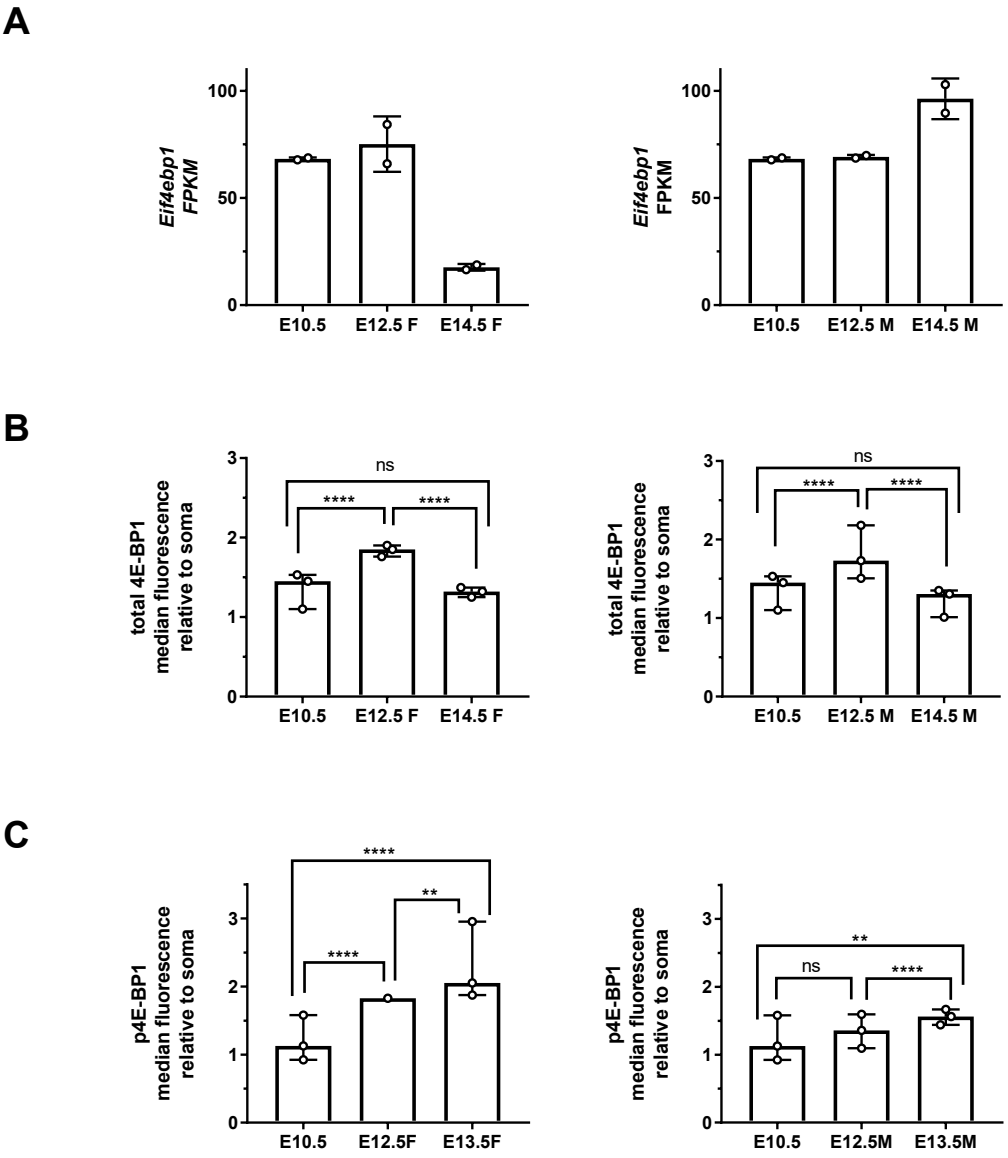

Figure 3.8: 4E-BP1 gene expression and protein levels in wild-type PGCs replotted for comparison.

A Gene expression data from Fig1.2 replotted to show *Eif4ebp1* expression at E10.5, E12.5 and E14.5. FPKM values are shown, n=2, error bars = standard deviation; **B** Total 4E-BP1 protein levels replotted from Fig1.4B at the same time points. Relative median fluorescence is depicted with error bars showing the 95% confidence intervals (CI). Data points represent the median from independent experiments, (n) is the total number of quantified germ cells for each time point. **C** p4E-BP1 fluorescent signal intensity replotted from Fig1.5B at time points E10.5, E12.5 and E13.5 for comparison. Significance was analysed across cells by the non-parametric Kruskal-Wallis Test, followed by Dunn's multiple comparisons test. **** $p<0.0001$, ** $p<0.01$;

3.2.2. AKT signalling in wild-type PGCs

To complement the above observations showing activation of mTORC1-4E-BP1 signalling, AKT signalling upstream of mTORC1 was analysed next. Active AKT can phosphorylate and inhibit the TSC1/2 complex, a major negative regulator of mTORC1 (Figure 3.9 A). Inhibition of TSC1/2 leads to activation of RHEB and subsequent phosphorylation and activation of mTORC1 at the lysosomal surface (Figure 3.9 A) (Saxton and Sabatini 2017).

The AKT protein family consists of three isoforms (AKT1, AKT2, AKT3), each encoded by a separate gene (Martelli et al. 2012). AKT isoforms have tissue specific expression patterns and functions, however they can be highly redundant in their functions (Razquin Navas and Thedieck 2017). Based on these observations, I first checked gene expression levels of all three AKT isoforms in wild-type foetal germ cells, using existing RNA-Seq data (Hill et al. 2018) (Figure 3.9 B).

Gene expression of all three *Akt* isoforms was detected, with *Akt1* being the highest expressed isoform at E10.5 and E12.5, followed by *Akt2* and *Akt3* respectively (Figure 3.9 B). At E14.5, female germ cells express all three isoforms at similar levels, whereas in male germ cells *Akt2* expression is the highest (Figure 3.9 B).

Next, I analysed AKT protein levels and activation status in wild-type tissues from E9.5-E13.5 using an immunofluorescence-based approach with antibodies recognizing all three isoforms (Figure 3.10). Total AKT protein was detected mainly in the cytoplasm throughout the analysed time points. At early time points (E9.5 and E10.5), AKT was observed at similar levels throughout the tissue (Figure 3.10 A). From E11.5 onwards, total AKT signal was enriched in the surrounding gonadal somatic cells compared to PGCs (Figure 3.10 A). Quantification of the median fluorescent intensity of AKT in PGCs relative to somatic cells showed a significant decrease in AKT signal from E10.5 to E13.5 in male samples (Kruskal-Wallis test, $p<0.0001$), with the lowest levels of fluorescence being 0.5 fold relative to somatic cells (Figure 3.10 B). In comparison, in female germ cells AKT levels decreased significantly between E10.5 and E11.5, followed by a less pronounced decrease compared to males germ cells from E12.5 onwards (Kruskal-Wallis test, $p<0.0001$) (Figure 3.10 B). Of note, the observed relative decrease likely reflects the increase in AKT signal in the surrounding somatic cells, rather than a decrease in overall protein levels in PGCs (Figure 3.10 A). These data suggest that AKT protein levels are low and fairly constant in PGCs, while somatic cells increase total AKT levels from E11.5 onwards.

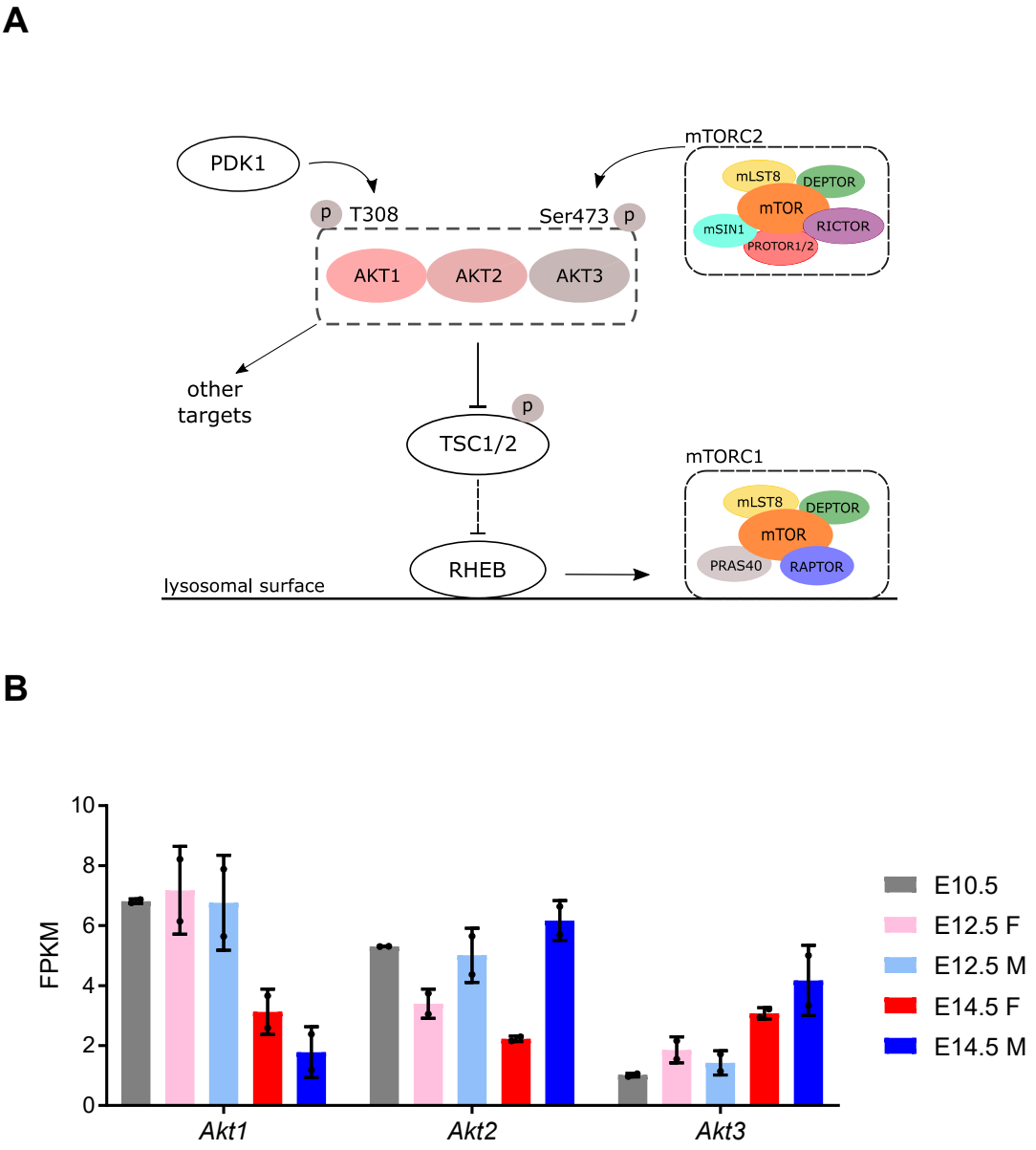

Figure 3.9: Gene expression of *Akt* isoforms in wild-type PGCs.

A Simplified schematic of AKT signalling. The three AKT isoforms and their two phosphorylation sites are depicted. Upstream kinases required for phosphorylation of specific sites and subsequent full activation are shown. Activated AKT inhibits the TSC1/2 complex, which further activates RHEB. Activated RHEB can phosphorylate mTORC1 at the lysosomal surface. **B** Gene expression data of *Akt* isoforms in wild-type PGCs at E10.5, E12.5 and E14.5. FPKM values are shown, n=2, error bars = standard deviation; RNA-Seq data were generated and analysed by Peter Hill.

A

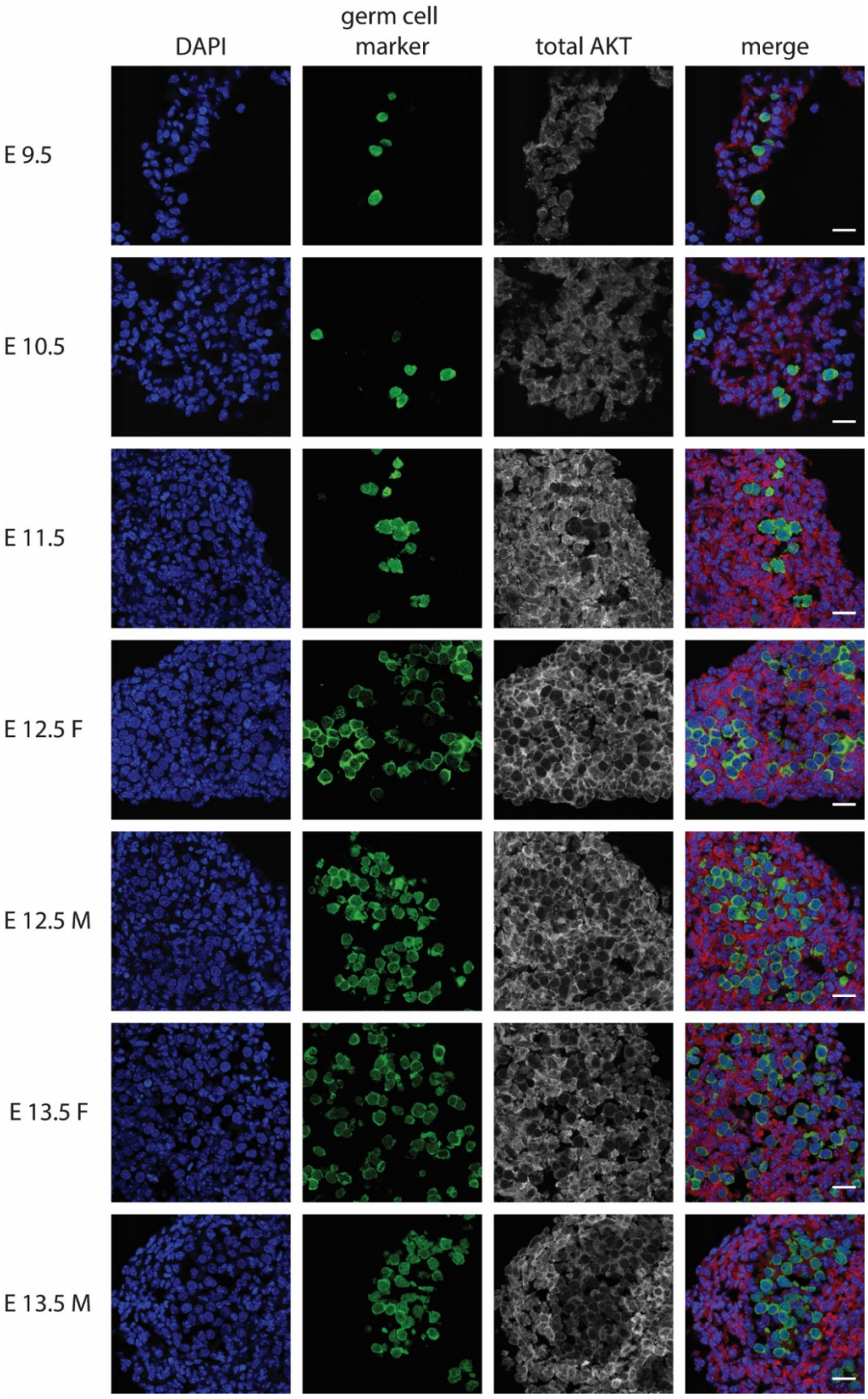
DAPI
germ cell marker
total AKT
merge
E 9.5
E 10.5
E 11.5
E 12.5 F
E 12.5 M
E 13.5 F
E 13.5 M

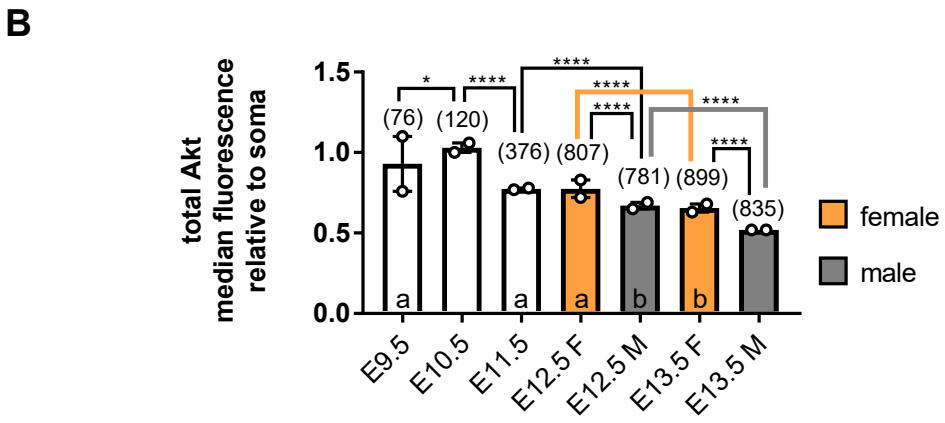

Figure 3.10: Total AKT protein levels in wild-type PGCs.

Immunofluorescence stainings of wild-type germ cells from E9.5-E13.5. Germ cells were identified via GFP expression driven by the *Oct4* promoter (green), nuclei were stained with DAPI (blue). **A** Total AKT (all three isoforms recognized) protein levels in wild-type germ cells. Representative images shown, n=2 (embryos), scale bar = 20µm; **B** Quantification of total AKT signal in PGCs relative to somatic cells. Relative median fluorescence is depicted with error bars showing the 95% confidence intervals (CI). Female samples are depicted in orange, male samples in grey. Data points represent the median of two independent experiments (n=2 embryos). (n) is the total number of quantified germ cells for each time point. Significance was analysed across cells by the non-parametric Kruskal-Wallis Test, followed by Dunn's multiple comparisons test. ****p<0.0001, * p<0.05; Medians with the same letter are not significantly different.

For full activation, AKT requires phosphorylation at two distinct sites, T308 and Ser473, mediated by PDK1 and mTORC2 respectively (Manning and Toker 2017). To analyse the activation status of AKT signalling, pAKT at the Ser473 site was examined. pAKT was detected specifically in a subset of PGCs from E10.5 onwards and the percentage of pAKT positive PGCs increased between E11.5 to E12.5 from 14% to around 40% (Figure 3.11 A-B). No pAKT signal was detected in surrounding somatic cells (Figure 3.11 A). This data suggests that AKT signalling is activated in a subset of PGCs between E11.5 and E12.5.

Intriguingly, total AKT was enriched in the cytoplasm, whereas pAKT signal was detected in the nucleus. Nuclear pAKT has been observed in a variety of cancers and AKT isoforms are known to either reside in the nucleus or translocate to the nucleus upon a wide range of stimuli such as insulin, insulin like growth factors and nerve growth factor (Martelli et al. 2012).

At the time, no positive control tissue or AKT knockout tissue was available to further support our observations, so instead another pAKT (Ser473) antibody from a different

company (Abcam) was used. At E12.5, the same nuclear staining pattern was detected specifically in PGCs, in line with the previous observations (Figure 3.11 C).

In addition, single cell staining of germ cells and somatic cells was performed. For this, E12.5 genital ridges were trypsinized and a single cell suspension (containing PGCs and somatic cells) was spotted onto a microscope slide, fixed and immediately stained. In some cases, this technique can greatly improve overall staining quality by reducing unspecific background staining. Both pAKT (Ser473) antibodies (Cell Signalling and Abcam) showed a nuclear staining pattern in PGCs in line with observations from immunostainings on cryosections. In addition, some somatic cells showed a cytoplasmic staining pattern (Figure 3.11 D).

Additionally, an antibody against the T308 phosphorylation site was tested in order to complement the above findings. However, only very weak cytoplasmic signal, comparable to unspecific background levels, was detected. This could be due to the antibody not working on cryosections, a complete lack of pAKT (T308) protein in germ cells or very low levels of pAKT (T308) protein which cannot be detected by this specific antibody. Due to the fact that the antibody is likely to be technically deficient, this data is not presented.

Taken together, total AKT protein levels are low and fairly constant in PGCs, while somatic cells increase total AKT levels from E11.5 onwards (Figure 3.10). AKT signalling seems to be activated in a subset of PGCs between E11.5 and E12.5 (Figure 3.11). Efforts to perform control experiments supporting our pAKT (Ser473) findings using different antibodies worked only partly in demonstrating the same nuclear staining pattern of pAKT (Ser473) with two independent antibodies on cryosections and single cell PGC staining (Figure 3.11). Additional work is currently being carried out to clearly determine the specificity of the pAKT antibody using chemical inhibitors against AKT, either during organ culture or in a cell culture based system such as cultured embryonic stem cells.

A

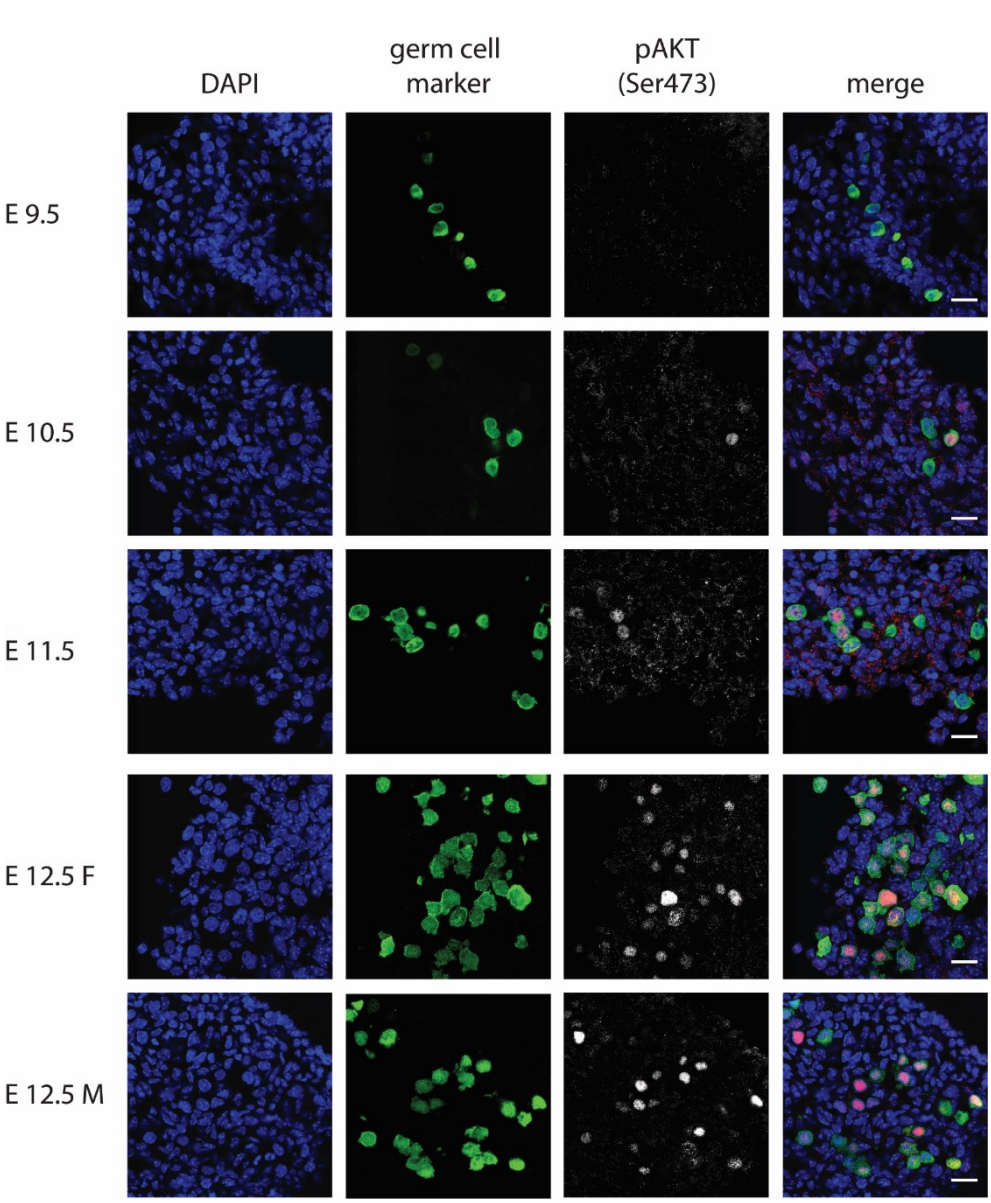
DAPI
germ cell marker
pAKT (Ser473)
merge
E 9.5
E 10.5
E 11.5
E 12.5 F
E 12.5 M

B

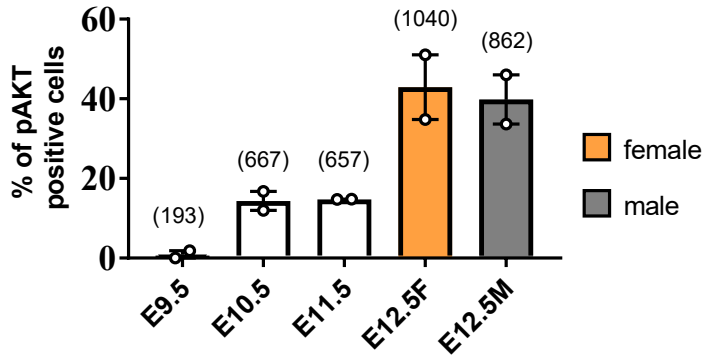
% of pAKT positive cells
60
40
20
0
(193)
(667)
(657)
(1040)
(862)
E9.5
E10.5
E11.5
E12.5F
E12.5M
female
male

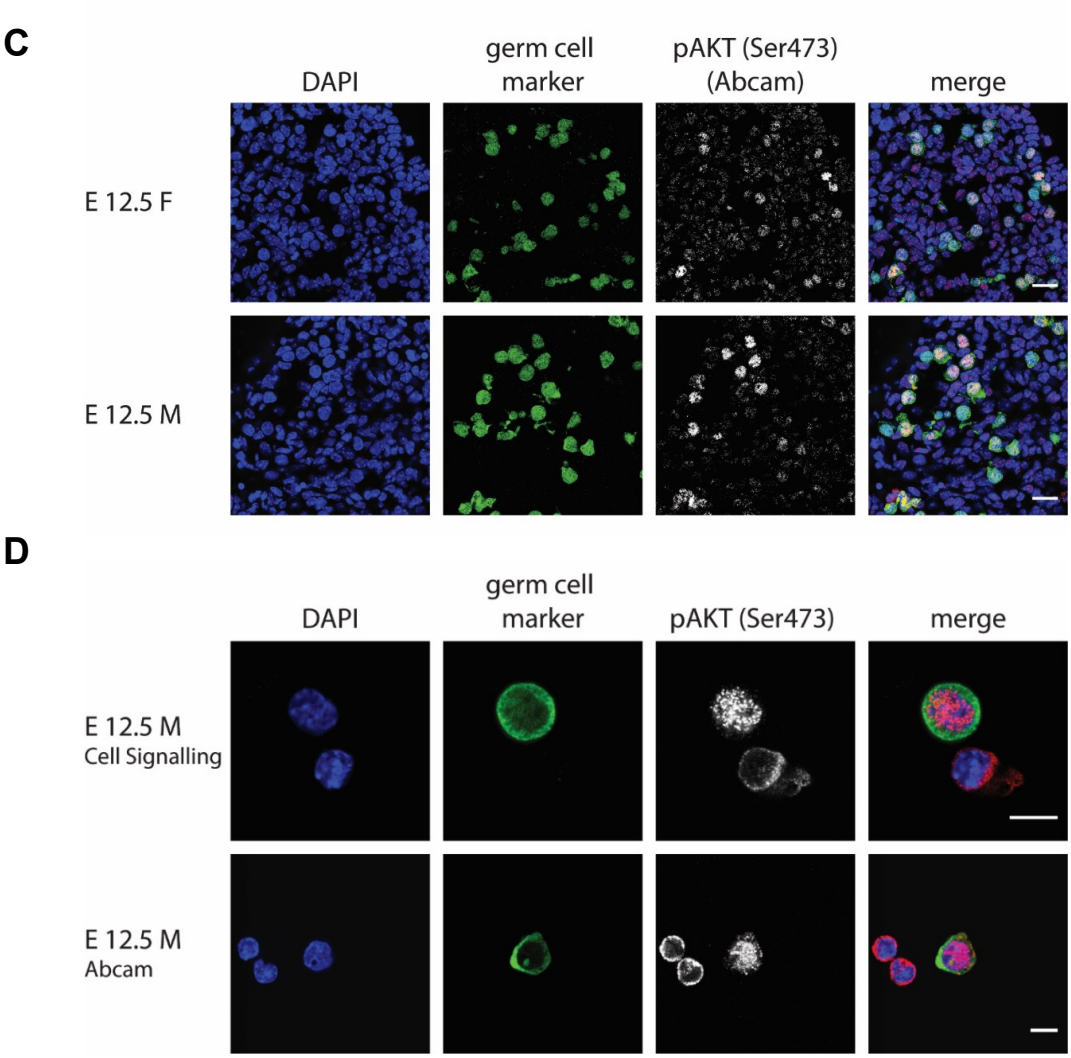

Figure 3.11: pAKT protein expression in wild-type PGCs

Immunofluorescence stainings of wild-type germ cells from E9.5-E13.5. Germ cells were identified via GFP expression driven by the *Oct4* promoter (green), nuclei were stained with DAPI (blue). **A** Phosphorylated AKT (Ser473) protein levels in wild-type germ cells (E9.5-E12.5). Representative images shown, n=2 (embryos), scale bar = 20µm, AB source = Cell Signalling **B** Quantification of pAKT positive germ cells. Percentage of pAKT positive germ cells is depicted. Female samples are depicted in orange, male samples in grey. Data points represent percentage of pAKT positive germ cells from two independent experiments (n=2 embryos). Total number of quantified germ cells (n) shown above each time point. Data is preliminary and due to the low n number, no statistical test has been performed. **C** pAKT (Ser473) stainings of E12.5 wild-type tissue with an antibody from a different company (Abcam). Representative images shown, n=1 (embryo), scale bar = 10µm **D** pAKT (Ser473) single cell PGC staining using both antibodies (Cell Signalling and Abcam). Representative images shown, n=1 (embryo), scale bar = 10µm;

3.3. Discussion

3.3.1. mTOR signalling in wild-type PGCs

Gene expression data revealed that all subunits of mTORC1 and mTORC2 are expressed in PGCs, with mTORC2 specific subunits being more abundant than mTORC1 specific subunits at the mRNA level. To what extent these expression patterns are reflected at the protein level, and more importantly, to what degree mTOR associates with specific subunits to form functional mTORC1 and/or mTORC2 complexes in PGCs remains unknown and warrants future studies.

Downstream of mTORC1, the two main signalling axes (S6 kinases and 4E-BPs) involved in the regulation of translation were analysed. Highly germ cell specific expression and activation pattern of 4E-BP1 was observed, suggesting that mTORC1 signals mainly via 4E-BP1 in foetal germ cells (as judged by p4E-BP1 levels). In contrast, no clear enrichment of total or pS6 was detected in germ cells. In E13.5 male tissues, higher overall pS6 signal (somatic cells + PGCs) was observed compared to female tissues. On the other hand, total and p4E-BP1 levels were higher in female PGCs at E13.5 compared to males, suggesting possible sex specific differences in mTORC1 downstream signalling.

3.3.1.1. mTORC1 - S6 kinase signalling axis

Varying levels of pS6 in a subset of somatic and germ cells throughout the tissue suggest the mTORC1-S6 kinase-S6 signalling axis is not specifically activated in foetal germ cells over the examined time period. However, a lack of signal enrichment specifically in germ cells does not exclude critical functions of mTORC1-S6 kinase-S6 signalling during PGC development. S6 is phosphorylated by S6K1 and S6K2, and for full phosphorylation, both kinases are required, with S6K2 playing a dominant role (Pende et al. 2004). Global knockout studies in mice have implicated the mTORC1-S6K1-S6 signalling axis in mediating body size and cellular growth (increase in cell volume or mass) (Shima et al. 1998; Pende et al. 2004; Ruvinsky et al. 2005; Dowling et al. 2010).

It should be noted that S6 kinases have many additional substrates beside S6 through which they regulate various aspects of translation (Magnuson, Ekim, and Fingar 2012). It is likely that the mTORC1-S6 kinase signalling axis also signals via different downstream effectors in wild-type PGCs. It would be interesting to know how the differential mRNA expression of the two isoforms (Figure 3.2 B) translates to protein levels and activation status of S6K1 and

S6K2 in wild-type PGCs. The functional role of S6 kinases during PGC development is described in the next chapter (see 4.2.1, p. 130).

3.3.1.2. mTORC1 - 4E-BP1 signalling axis

The observation of highly germ cell specific expression and activation pattern of 4E-BP1 suggests a possible role of mTORC1-4E-BP1 signalling during PGC development and is interesting for several reasons.

First, the mTORC1-4E-BP1 signalling axis generally promotes cell proliferation (Dowling et al. 2010; Musa et al. 2016). Based on studies in wild-type and 4E-BP knockout MEFs and HEK cells, it has been proposed that cell proliferation is mediated via selective translation of transcripts involved in cell cycle progression such as ornithine decarboxylase (ODC), cyclin D3 and VEGF upon mTORC1-4E-BP1 signalling (Dowling et al. 2010). Primordial germ cells undergo proliferation during the migratory and gonadal stages. From E10.5 to E13.5, germ cell number increases roughly from ~1000 cells to ~26.000 cells (P. P. L. Tam and Snow 1981), before males enter mitotic arrest and females initiate meiosis. The mTORC1-4E-BP1 signalling axis could (partly) underlie this increase in proliferation, however, further work is needed to test this hypothesis.

Second, 4E-BP1 is a translational repressor. In its non-phosphorylated state, 4E-BP1 binds eIF4E, sequestering it away and preventing assembly of the eIF4F complex and subsequently inhibiting translational initiation (Musa et al. 2016). Upon phosphorylation of 4E-BP1 via active mTORC1 signalling, 4E-BP1 dissociates from eIF4E, allowing initiation of translation (Musa et al. 2016). The mTORC1-4E-BP1-eIF4E signalling axis can regulate global translation rates to a certain degree. However, certain subsets of mRNAs characterised by distinct 5'UTR regions are specifically sensitive to mTORC1 signalling (Musa et al. 2016). These subclasses include mRNAs encoding proteins involved in protein synthesis, proliferation and survival, and mitochondrial metabolism (see 1.3.3.1, p. 56) (Musa et al. 2016).

Activation of the mTORC1-4E-BP1 signalling axis specifically in PGCs suggests a possible role of mTORC1 signalling in the regulation of translation during PGC development. Currently, very little is known about translational regulation and how global translation rates change in primordial germ cells with time. One study has shown that E13.5 gonadal germ cells have elevated levels of translation compared to somatic cells based on HPG incorporation (Percharde, Wong, and Ramalho-Santos 2017). The same study also showed that PGCs exhibit global hyper transcription compared to surrounding somatic cells from

E9.5 to E13.5 (Percharde, Wong, and Ramalho-Santos 2017). Interestingly, ribosomal proteins and proteins involved in rRNA processing were among the hypertranscribed genes (Percharde, Wong, and Ramalho-Santos 2017). Many mRNA subsets sensitive to mTORC1-4E-BP1 regulation also encode ribosomal proteins (Musa et al. 2016). The mTORC1-4E-BP1 signalling axis could be a possible mechanism of tightly regulating translation in germ cells with global hypertranscription. The germ cell specific increase of total 4E-BP1 from E10.5 onwards could allow repression of translation, which is removed via bursts of p4E-BP1 signalling, leading to increased translation when needed. To date, this remains a hypothesis and requires further work.

To what extend the observed mTORC1-4E-BP1 signalling affects translational rates of either global mRNA or subsets of mRNA in foetal germ cells is not known. A nascent mRNA translation assay based on HPG incorporation to measure the global translation rates of PGCs compared to soma could help to shed light on this process (in progress) (Percharde, Wong, and Ramalho-Santos 2017). It would be interesting to compare early time points such as E10.5, which show minimal p4E-BP1 signal, to E11.5 or E13.5 female samples when p4E-BP1 signal peaks. In addition, RNA-Seq comparing ribosome loaded versus total mRNAs would allow to determine the extent of translational regulation during PGC development, however, optimization of the mRNA pulldown for small cell numbers is currently a bottleneck.

Third, activation of 4E-BP1 signalling coincides with key germ cell processes. The observed peaks in p4E-BP1 at E11.5 and E13.5 (females only) coincide with two key developmental processes in gonadal germ cells, epigenetic reprogramming and initiation of meiosis respectively. This correlation suggests a possible role of translational regulation via the mTORC1-4E-BP1 signalling pathway underlying these processes. In view of that, the functional role of 4E-BP1 during foetal germ cell development was analysed using global knockout mice (see 4.2.2. p. 146).

Fourth, activation of the mTORC1-4E-BP1 signalling axis poses the question of what the upstream activating signals are. The mTORC1 signalling pathway integrates four major intracellular and extracellular signals: energy status, growth factors, oxygen and amino acids. Many of these signals converge on the negative mTORC1 regulator TSC1/2 (Laplante and Sabatini 2009).

While the upregulation of total 4E-BP1 protein levels coincide with entry into the genital ridge at E10.5, active mTORC1-4E-BP1 signalling is detected at specific time points (E11.5,

E12.5 F, E13.5 M & F), suggesting presence of upstream activating signals at those time points. Of note, high p4E-BP1 levels are present only in females at E12.5 and higher in females compared to males at E13.5. Sex specific differences in 4E-BP1 signalling might reflect changes in the surrounding gonadal environment during sex determination. Female sex determination is driven by WNT/β-catenin signalling, with gonadal somatic cells producing the WNT4 ligand (Kocer et al. 2009; Vainio et al. 1999). Interestingly, WNT is also a non-classical signal upstream of mTORC1 and WNT signalling leads to mTORC1 activation via inhibition of GSK3 (Inoki et al. 2006). Whether WNT signalling, among others, is involved in the activation of mTORC1-4E-BP1 in gonadal germ cells requires further investigation.

Of note, although 4E-BP1 is one of the best studied downstream targets of mTORC1 and generally an accepted readout for mTORC1 activity, recent studies have reported mTORC1 independent phosphorylation of 4E-BP1 (Batool, Aashaq, and Andrabi 2017). In different biological contexts, several other protein kinases have been implicated in 4E-BP1 phosphorylation at different sites, including (but not limited to) GSK-3β, p38 MAP kinase, ERK, PIM kinases, ATM and Cdc2/CDK1 (Batool, Aashaq, and Andrabi 2017). Especially in cancer cells, mTORC1 independent phosphorylation of 4E-BP1 is commonly observed and contributes to their resistance to mTOR kinase inhibitors (Y. Zhang and Zheng 2012). Therefore, mTORC1-independent activation of 4E-BP1 signalling in PGCs cannot be excluded at this point.

3.3.2. AKT signalling in primordial germ cells

Analysis of AKT signalling has revealed that AKT protein levels are fairly constant in PGCs, while increasing in surrounding somatic cells from E11.5 onwards. AKT signalling, as determined by pAKT (Ser473), is activated specifically in a subset of PGCs between E11.5 and E12.5. Although the pAKT data are still preliminary, and currently experiments are undertaken to demonstrate specificity of the pAKT (Ser473) antibody *in vivo*, these observations are interesting for several reasons.

3.3.2.1. AKT – a possible upstream activator of mTORC1 signalling in PGCs?

AKT lies upstream of mTORC1 and AKT signalling can active mTORC1 signalling either via inhibition of the TSC1/2 complex or via direct phosphorylation of the inhibitory subunit

PRAS40 (Manning and Toker 2017). Preliminary data suggested activation of the AKT-mTORC1-p4E-BP1 axis, based on pAKT and p4E-BP1 signal observed at the same time points (Peter Hill, personal communication).

However, detailed analysis of AKT signalling over a longer time period suggest that AKT signalling might not activate the mTORC1-4E-BP1 signalling axis in germ cells. This is based on several observations:

First, I detected AKT signalling in PGCs at E12.5, whereas activation of mTORC1-4E-BP1 signalling (p4E-BP1) was observed one day earlier, from E11.5 onwards. This discrepancy on timing compared to our preliminary data is likely due to the different genetic background of the embryos used. Secondly, while p4E-BP1 signal is detected in the majority of germ cells at varying levels, pAKT signal is only detected in up to 40% of PGCs. Third, the mTORC1 signalling complex has been shown to be localized mainly to the cytoplasm (Rosner and Hengstschlager 2008; Sancak et al. 2008), whereas the pAKT signal was detected in the nucleus. Overall, the timing, extent of signal activation and localization suggests that mTORC1 is activated via an AKT independent pathway. In fact, many other pathways, such as the RAS-ERK pathway, can regulate mTORC1 signalling via modulating TSC1/2 function (Saxton and Sabatini 2017).

However, the possibility of mTORC1 activation via pAKT in germ cells cannot be excluded, since attempts to analyse levels of phosphorylated AKT at the T308 site were unsuccessful, likely due to the antibody not working on cryosections. For full activation, AKT requires phosphorylation at T308 in the catalytic domain and Ser473 in the hydrophobic motif (Manning and Toker 2017). However, partially phosphorylated AKT at the T308 site can still phosphorylate some of its substrates, including the TSC1/2 complex, as demonstrated in *Rictor* knockout MEFs lacking the mTORC2 complex (Guertin et al. 2006).

To summarize, based on our observations, it is possible that mTORC1-4E-BP1 signal activation is activated in an AKT-independent way via alternative routes and activation of AKT signalling may have an mTORC1 independent role during germ cell development. However, a role of AKT signalling in mTORC1 activation cannot be excluded at this point and further work is required to determine upstream activators of mTORC1 signalling in foetal germ cells.

3.3.2.2. AKT signalling seems to be tightly controlled in PGCs *in vivo*

The observations that AKT levels are kept at fairly low and constant levels in PGCs and signalling is only activated in up to 40% of PGCs suggest that AKT signalling is tightly controlled in PGCs *in vivo.*

In line with that, germ cell deletion of PTEN, a negative regulator of AKT, results in testicular teratoma formation in male new born mice (Kimura et al. 2003). In ES cells, deletion of PTEN results in the accumulation of PIP3 and subsequent activation of the downstream effector AKT (Sun et al. 1999). *PTEN* $^{-/-}$ mice also showed hyper activation of AKT signalling in germ cells and early teratomas (Kimura et al. 2003). Teratoma formation was suggested to be due to de-differentiation of germ cells into pluripotent cells or increased proliferation and impaired differentiation of immature germ cells, likely driven by AKT hyperactivation (Kimura et al. 2003).

In fact, wild-type PGCs, although lineage committed, have been suggested to be able to de-differentiate (acquiring broader developmental potential) based on two observations: First, PGCs transplanted into adult testis can give rise to teratomas (Stevens 1984, 1967) and PGCs cultured *in vitro* under specific culture conditions can reprogram into pluripotent embryonic germ cells (Resnick et al. 1992; Yasuhisa Matsui, Zsebo, and Hogan 1992). However, in wild-type mice and under normal circumstances, testicular tumours are very rare (Stevens 1967).

In vitro, conditional deletion of PTEN, as well as forced expression of AKT, enhance germ cell colony formation efficiency (Kimura et al. 2003, 2008; Y. Matsui et al. 2014). Primordial germ cells can be reprogrammed into embryonic germ cells via addition of a combination of growth factors and over activation of AKT likely enhances bFGF and LIF signalling, playing a crucial role in the acquisition of pluripotency (Y. Matsui et al. 2014).

Based on our observations and the current literature, it is possible that AKT levels are tightly controlled in PGCs *in vivo* in order to prevent aberrant germ cell differentiation/de-differentiation leading to tumour formation. This is a hypothesis though and further work is required to characterise AKT signalling *in vivo.*

3.3.2.3. Upstream kinases activating AKT

Phosphorylation of the Ser473 site is attributed to different kinases depending on the context and cell type. Upon growth factor stimulation, AKT (Ser473) is phosphorylated via mTORC2

(Sarbassov et al. 2005), whereas in the context of DNA damage (double strand breaks), AKT is phosphorylated by DNA protein kinase (DNA-PK) (Bozulic et al. 2008).

pAKT (Ser473) signal was localized to the nucleus and the nuclear staining pattern was confirmed with a different antibody. Although most of the machinery required to phosphorylate AKT is present in the nucleus, such as PI3K, PDK1 and mTORC2, it has not been shown yet if AKT can be phosphorylated in the nucleus (Martelli et al. 2012). In fact, it is not entirely clear how AKT translocates to the nucleus to start with and if activity and phosphorylation status influences the nuclear translocation (Martelli et al. 2012).

Detection of pAKT (Ser473) combined with RNA-Seq data showing expression of all mTORC2 subunits in PGCs, actually at higher levels compared to mTORC1 specific subunits, may indicate a possible role of mTORC2 signalling in PGCs. In fact, mTORC2 has been located to the nucleus and cytoplasm (Rosner and Hengstschlager 2008). Although mTORC2 is the main kinase for pAKT (Ser473) phosphorylation under normal circumstances, in some cases the presence of pAKT (Ser473) is a more accurate marker of upstream PI3K activity rather than accurately reflecting mTORC2 activity (J. Huang and Manning 2009). In addition, in the context of DNA double strand breaks, AKT is phosphorylated by DNA protein kinase (DNA-PK), rather than mTORC2, promoting survival via upregulation of DNA damage induced transcription of p21 (Bozulic et al. 2008; Bozulic and Hemmings 2009). Hence, further work is needed to determine how mTORC2 mRNA levels translate to protein levels and subsequently, to functional mTORC2 complexes, and whether mTORC2 signalling is involved in activating AKT during foetal germ cell development.

Regarding possible upstream signals, the KIT ligand/c-KIT signalling pathway has been shown to activate AKT, likely in a PI3K independent way, in PGCs *in vitro* (De Miguel et al. 2002). However, *in vivo* KIT ligand is expressed from E7.5 until E11.5 (Runyan et al. 2006; Y. Gu et al. 2009) and activation of AKT was observed between E11.5-E12.5.

3.3.2.4. Conclusion

To conclude, timing of the observed AKT signalling and activation in only a subset of PGCs, combined with its nuclear localization, suggest that MTORC1-4E-BP1 signalling is not activated via upstream AKT signalling, rather AKT may have an mTORC1-independent function. Based on our observations and current literature, AKT signalling seems to be tightly regulated *in vivo* and possible downstream functions may include proliferation, survival and germ cell differentiation. However, extensive future studies are needed to determine the role of AKT signalling in PGCs *in vivo.*

3.3.3. Some general comments

It should be noted that the applied immunofluorescence-based approach to study mTOR signalling in wild-type PGCs has some limitations.

Firstly, in the experimental design, the assumption was made that expression and activation patterns of proteins of interest (S6, 4E-BP1, AKT) are randomly distributed within PGCs in the hindgut and/or gonad. Although by eye no obvious spatial bias regarding the staining pattern was detected (data not shown), acquired images and quantification thereof originated from random locations within sections. Given the fact that during germ cell development, some processes do occur with a clear spatial bias, such as entry into meiosis in females (anterior to posterior wave) (Menke, Koubova, and Page 2003; Bullejos and Koopman 2004) or male gonad sex determination (centre to pole wave) (Bullejos and Koopman 2001; Hiramatsu et al. 2010), a possible spatial distribution pattern of mTOR signalling proteins within gonads cannot be excluded.

Secondly, inferring protein levels from fluorescent signal and antibody binding has some caveats. Antibody binding can be influenced by differences in antigen accessibility at different developmental time points. Antigen accessibility can change due to post-translational modifications or due to the target protein being part of different protein complexes (Saper 2009).

Thirdly, occasionally variations in fluorescent signal are observed within experiments and between sections due to technical reasons. For cell quantification, the chosen normalization method of using surrounding somatic cells corrects for differences in staining quality (due to technical reasons) between images. This approach, however, assumes that the antibody binding and antigen accessibility is the same in both cell populations. Hence, it cannot be

excluded that any observed changes in the relative signal are due to changes in somatic cells. For this reason, interpretation of the quantified fluorescent signal (and changes thereof) in combination with the observed staining pattern in IF images, which allows to detect (by eye) any big changes in somatic cells, has been applied to allow a more accurate interpretation of observed changes.

4. Chapter 4 – Functional validation of mTOR signalling using global knockout mouse models.

4.1. Introduction

Analysis of wild-type germ cells revealed increased expression of 4E-BP1 protein specifically in germ cells and activation of the mTORC1-4E-BP1 signalling axis from E10.5 onwards (as judged by phosphorylated 4E-BP1) (Chapter 3). In contrast, mTOR-S6 kinase-S6 signalling was detected in germ and somatic cells throughout the genital ridge (Chapter 3). These observations suggest a possible role for mTOR signalling during germ cell development, likely via 4E-binding proteins.

To test possible biological functions of mTOR signalling, global knockout mouse lines were analysed. Since global *Mtor* deletion or deletion of mTORC1 specific protein *Raptor* leads to embryonic lethality around E5.5-E6.5 (Murakami et al. 2004; Gangloff et al. 2004; Guertin et al. 2006), mouse lines lacking downstream effectors S6 kinases or 4E-binding proteins were analysed. An immunofluorescence-based screening approach was used to identify any aberrant change in early germ cell development upon deletion of mTOR effectors. For this, wild-type and knockout genital ridges were collected at two chosen time points: E13.5 and E15.5.

The first time point (E13.5) was chosen because by that time germ cells have already completed several critical steps of development. First, a founder population of primordial germ cells specifies from epiblast cells at around E7.25 upon inductive BMP signalling. A distinct transcriptional program is initiated leading to the repression of somatic genes and expression of germ cell specific and pluripotency genes. While OCT4 is continuously expressed, SOX2 and NANOG expression is regained (Saitou and Yamaji 2012). Following specification, primordial germ cells proliferate and migrate through the hindgut and mesentery towards the genital ridges (Molyneaux et al. 2001; Richardson and Lehmann 2010; Saitou and Yamaji 2012). Gonadal germ cells undergo epigenetic reprogramming including genome wide DNA demethylation (Saitou and Yamaji 2012). At the same time, expression of key germ cell genes such as *Mvh* and *Dazl* is induced (Toyooka et al. 2000; Cooke et al. 1996; Seligman and Page 1998). In addition, the bipotential genital ridge and germ cells within undergo sex determination. Male genital ridges start to express SRY at E10.5, subsequently inducing Sox9 signalling and Sertoli cell differentiation. Sertoli cells drive testis differentiation – the earliest morphological sign being testis cord formation at around E12.5 (Spiller and Bowles 2015; Kocer et al. 2009). Testis cords are the precursors of seminiferous tubules of adult testis, which contain germ cells surrounded by Sertoli cells, an outer layer of peritubular myoid cells (PMCs) and an extra cellular matrix (ECM) (Svingen and

Koopman 2013). In comparison, lack of SRY expression in the female genital ridge drives the female program via WNT/β-catenin signalling (Spiller and Bowles 2015; Kocer et al. 2009). Morphological changes are less apparent, and by E13.5, the female gonad is smaller, less organized with no clear structure compared to the male gonad. Importantly, female germ cells start to express *Stra8* and initiate meiosis, while downregulating pluripotency factors such as *Oct4* and *Sox2*. In contrast, male germ cells enter mitotic arrest at E13.5 and maintain expression of pluripotency markers (Maurizio Pesce et al. 1998; Feng, Bowles, and Koopman 2014).

Hence, close examination of E13.5 genital ridges is a good starting point to pick up possible phenotypes developing between germ cell specification and sex determination. Morphological changes of the genital ridge as well as expression of characteristic germ cell proteins were analysed across 4E-BP1$^{-/-}$ or S6K1$^{-/-}$ single knockout and 4E-BP1$^{-/-}$ 4E-BP2$^{-/-}$ or S6K1$^{-/-}$S6K2$^{-/-}$ double knockout tissues. More specifically, at E13.5, successful induction and expression of key germ cell proteins DAZL and MVH was examined. Further, the changing differentiation status of germ cells was analysed via expression of the cell surface marker stage specific antigen 1 (SSEA1) and the pluripotency factors OCT4 and SOX2 (Figure 4.1). SSEA1 is an established marker for ESCs, embryonic carcinoma cells and undifferentiated PGCs from their specification onwards. From E12.5/E13.5 onwards, SSEA1 expression is gradually downregulated and can almost not be detected at E15.5, as cells progress in their sexual differentiation (Fox et al. 1981).

At E15.5, initiation of meiosis in female germ cells and the successful inhibition of meiosis in male germ cells was assessed. The majority of female germ cells will have entered meiosis by E15.5, given expression of key meiosis genes is already induced from E12.5 onwards. Expression of STRA8, a protein necessary for pre-meiotic DNA replication and SCP3, a protein which is part of the synaptonemal complex, were used as meiosis markers to examine correct initiation or inhibition of meiosis (Figure 4.1).

To start with, global knockout mice were analysed rather than germ cell specific knockouts for several reasons: First, most of the analysed lines were already established mouse colonies in Prof Withers' laboratory and hence, available to use straight away (with some exceptions, further details see 4.2.2, p. 146). Second, generation of germ cell specific knockouts using the existing *Prdm1-Cre* driver line is extremely challenging and time consuming due to very small litter sizes (Ohinata et al. 2009; Mikedis and Downs 2017). Hence, a broad screen of single and double knockout tissues would allow to determine which mTOR downstream

target plays the biggest role during germ cell development. Once identified, a more focused analysis of that protein can be undertaken using a germ cell specific knockout system.

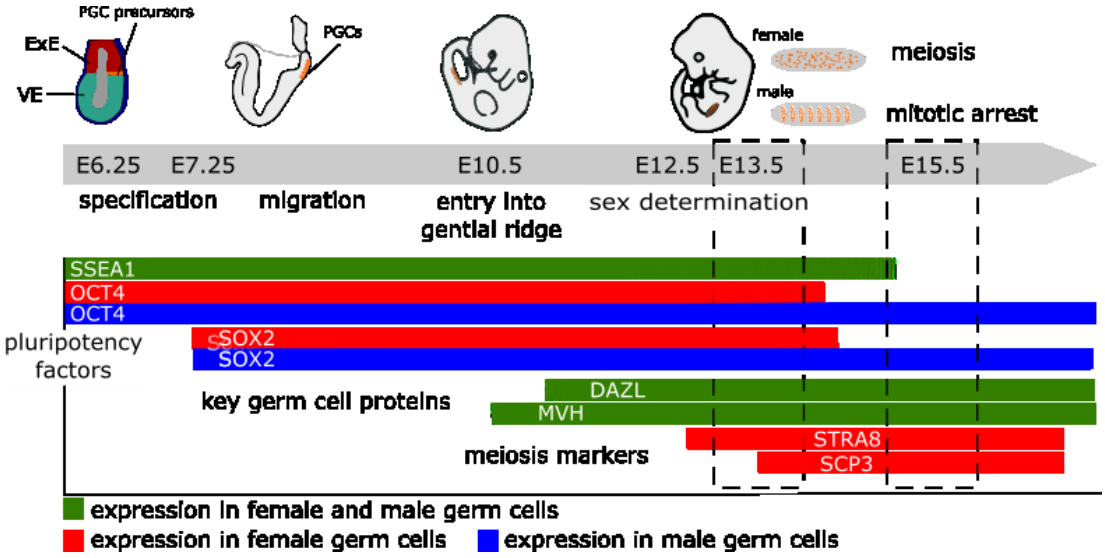

Figure 4.1: Overview of germ cell development and expression pattern of analysed proteins.

Key events of germ cell development between specification and E15.5 are shown, along with expression pattern of selected proteins: Germ cells specify from epiblast cells upon inductive BMP signalling. At embryonic day (E) 7.25, a founder population of ~40 germ cells starts to migrate along the developing hindgut towards the mesoderm until they eventually colonize the genital ridges at E10.5. Gonadal germ cells start to express DAZL and MVH, undergo epigenetic reprogramming and enter sex differentiation at around E12.5. At E13.5, male and female genital ridges can be distinguished by their distinct morphology. Female germ cells induce meiosis genes such as STRA8 and SCP3 (among others) and initiate meiosis, while male germ cells enter mitotic arrest. Expression pattern of germ cell proteins chosen for the immunofluorescence-based screen is shown. If expression pattern differs between sexes, expression of the protein is shown separately for males and females. Genital ridges at selected time points E13.5 and E15.5 (dashed boxes) were analysed.

4.2. Results

4.2.1. The role of S6 kinases during germ cell development

4.2.1.1. Characterisation of foetal germ cells lacking S6 kinases

To analyse possible functions of S6 kinases during germ cell development, global knockout mice lacking only S6K1 or both S6 kinases (S6K1 and S6K2) were analysed.

For analysis of S6K1, wild-type ($S6K1^{+/+}$) and knockout ($S6K1^{-/-}$) tissues were obtained from the same litter via matings between heterozygous ($S6K1^{+/-}$) males and females. Using the above described immunofluorescence approach, preliminary observations (n=1) showed no obvious difference between wild-type genital ridges and $S6K1^{-/-}$ knockout genital ridges at E13.5 and E15.5. Tissue morphology, approximate germ cell number, expression of key germ cell proteins (DAZL, MVH), expression of pluripotency markers (OCT4, SSEA1) and expression of meiosis markers (STRA8, SYCP3) were all as expected and similar between genotypes (n=1, data not shown). The only exception was an increased number of SSEA1 positive germ cells in male $S6K1^{-/-}$ global knockout tissues at E13.5 (Figure 4.2). While about 27% of wild-type germ cells stained positive for SSEA1, 92% of $S6K1^{-/-}$ knockout germ cells were positive for SSEA1 (Figure 4.2). However, these are preliminary observations only and need to be confirmed.

Although S6K1 was the highest expressed isoform among S6 kinases at the mRNA level, expression of S6K2 was also detected in wild-type PGCs (see 3.2.1.1, p. 90, Figure 3.2, p. 92). Hence, it is possible that the very mild phenotype observed during preliminary analysis of $S6K1^{-/-}$ knockout germ cells is due to functional compensation via S6K2. In fact, the genes encoding S6K1 and S6K2 share a high degree of homology (Shima et al. 1998). In a previously published $S6K1^{-/-}$ knockout mouse model, S6K2 mRNA was upregulated and based on the mild phenotype, a compensatory mechanisms has been suggested by the authors (Shima et al. 1998).

To rule out any compensatory effect of S6K2 during germ cell development, further analysis focused on $S6K1^{-/-}S6K2^{-/-}$ double knockout embryos (Pende et al. 2004). Wild-type ($S6K1^{+/+}S6K2^{+/+}$) and double knockout tissues were obtained from separate breeding colonies subject to the same colony maintenance. $S6K1^{+/-}S6K2^{-/-}$ males were crossed with $S6K1^{+/-}S6K2^{-/-}$ females to generate double knockout embryos, as the majority of $S6K1^{-/-}S6K2^{-/-}$ double knockout mice are not viable. Most pups are born dead or die shortly after birth, with very few exceptions developing to adulthood (Pende et al. 2004). Mendelian ratios are

normal until E18.5 though, so tissue collection at E13.5 and E15.5 was possible. The only reported phenotype at that stage is a growth retardation as measured via decreased body weight of up to 30% at E12.5 (Pende et al. 2004).

First, E13.5 genital ridges were co-stained for two key germ cell proteins DAZL and MVH. Both proteins are known to be robustly expressed in all wild-type PGCs at E13.5 and are absolutely critical for normal germ cell development. All wild-type and S6K1$^{-/-}$S6K2$^{-/-}$ knockout germ cells stained positive for DAZL and MVH (Figure 4.3). Further, no difference in expression levels was observed between wild-type and knockout tissues, suggesting S6 kinases are not essential for DAZL and MVH expression in germ cells. Both proteins were subsequently used as markers to identify germ cells.

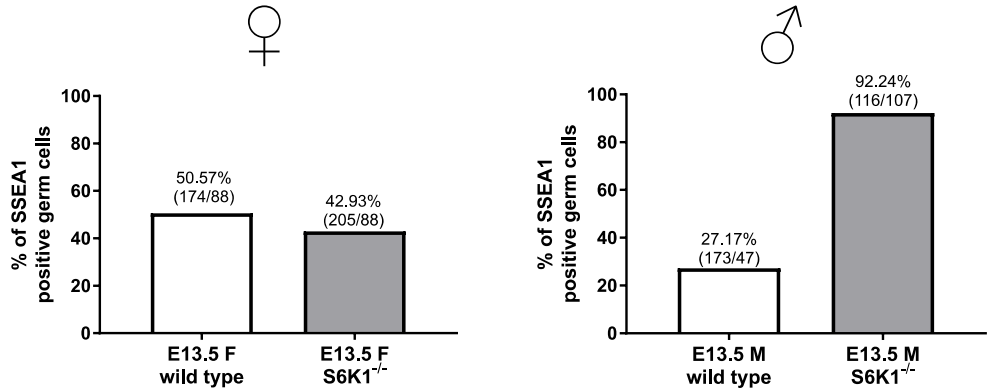

Figure 4.2: Expression of SSEA1 in global S6K1$^{-/-}$ knockout germ cells at E13.5.

Quantification of immunofluorescence stainings of female and male genital ridges at E13.5. In each tissue section of wild-type and S6K1$^{-/-}$global knockout genital ridges, total germ cells were identified via DAZL expression. The number of DAZL positive and SSEA1 positive germ cells were counted. Average percentages of SSEA1 positive germ cells across different tissue sections are shown. (n/n) above each bar = total number of germ cells counted/SSEA1^{+} germ cells; biological replicate = 1 embryo per genotype; Wild-type and S6K1$^{-/-}$ knockout tissues were from littermates. Genotype was identified via PCR. This is preliminary data and due to n=1, no statistical test has been performed.

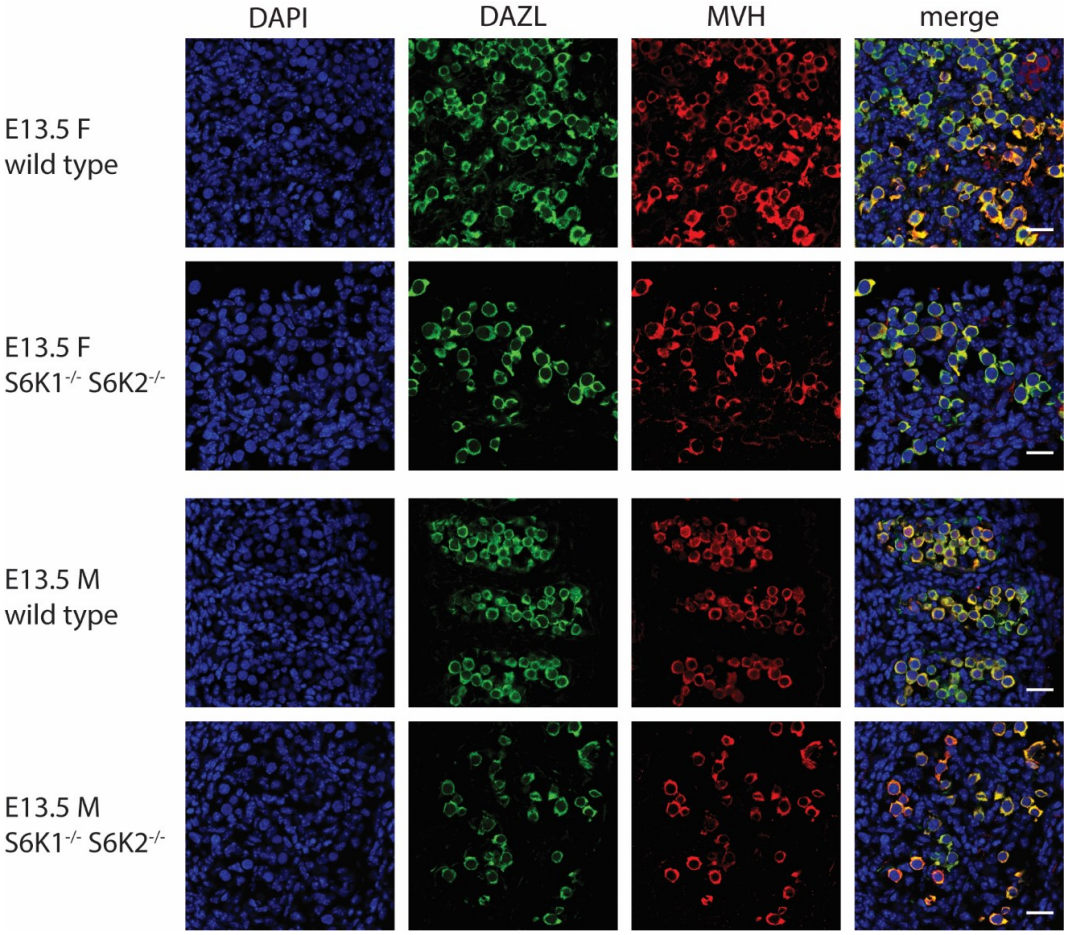

Figure 4.3: Expression of key germ cell proteins in wild-type and global S6K1$^{-/-}$S6K2$^{-/-}$ knockout germ cells.

Immunofluorescence stainings of female and male genital ridges at E13.5. Germ cells were stained for DAZL and mouse Vasa homologue (MVH), nuclei were stained with DAPI (blue). Representative images shown, n=2 (embryos per genotype), scale bar = 20µm; Wild-type and S6K1$^{-/-}$S6K2$^{-/-}$ knockout tissues were from separate litters. Genotype was identified via PCR.

4.2.1.1.1 Morphological characterisation of S6K1$^{-/-}$S6K2$^{-/-}$ knockout gonads

At the tissue level, some morphological differences were observed between S6K1$^{-/-}$S6K2$^{-/-}$ knockout genital ridges and wild-type controls.

Female wild-type genital ridges showed the characteristic morphology with no clear visible structure and germ cells being less organized compared to male wild-type genital ridges at E13.5 (Figure 4.4 A). As expected, compared to a long and thin bipotential wild-type genital ridge at around E10.5/E11.5, the E13.5 wild-type genital ridge appeared more compact and was shorter. In comparison, global S6K1$^{-/-}$S6K2$^{-/-}$ knockout genital ridges at E13.5 were longer and contained fewer germ cells (observation only, not quantified) compared to their wild-type controls (Figure 4.4 A). Two days later, at E15.5, the wild-type gonad has an even more rounded shape, while S6K1$^{-/-}$S6K2$^{-/-}$ knockout genital ridges were still elongated and thin in comparison, with fewer germ cell numbers (observation only, not quantified) (Figure 4.4 A). The overall length of the knockout genital ridge has decreased from E13.5 to E15.5, indicating a slow progression in development (Figure 4.4 A). However, taken together, the observed morphology of the S6K1$^{-/-}$S6K2$^{-/-}$ knockout genital ridges at both time points resembled earlier developmental stages of female genital ridges more closely than control tissues at the same stage, suggesting a possible delay in development at the tissue level.

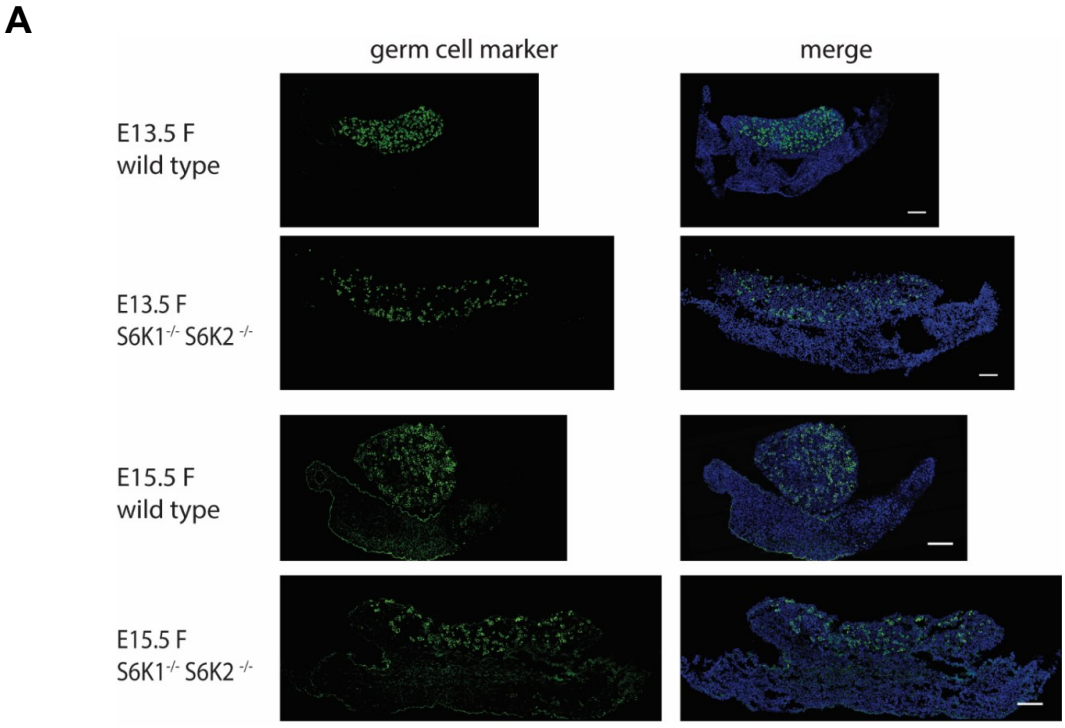

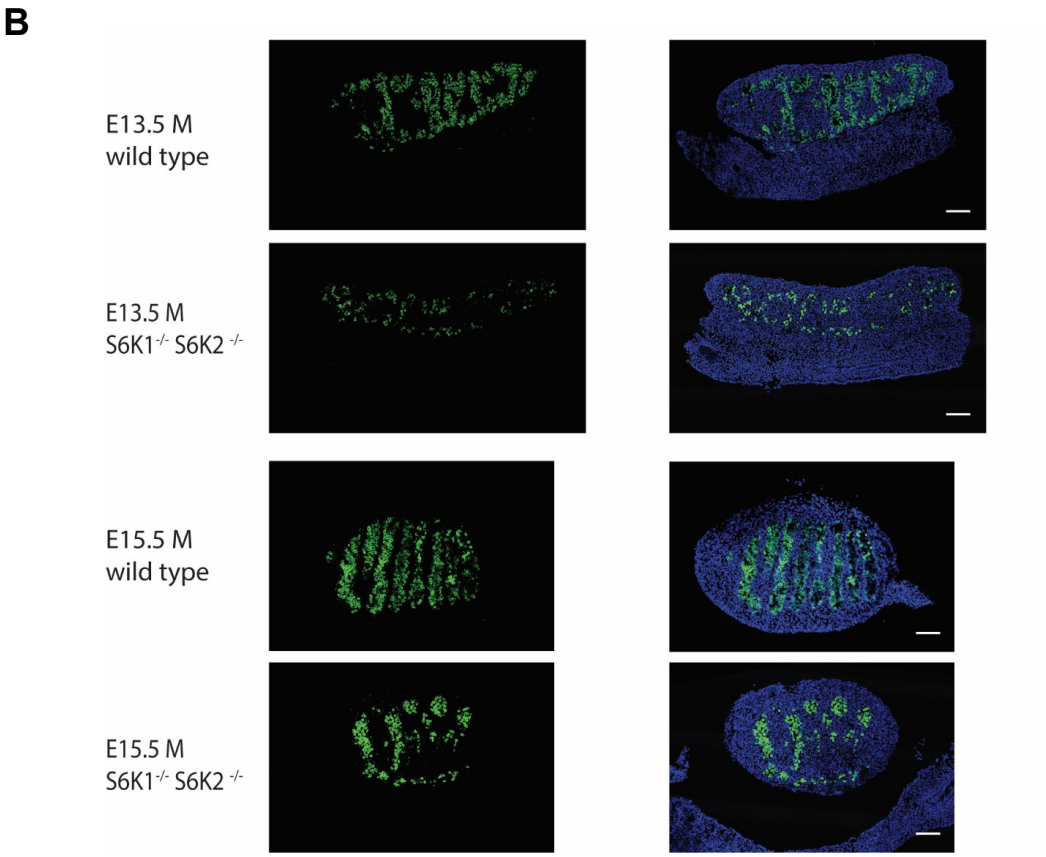

Figure 4.4: Morphology of wild-type and global S6K1$^{-/-}$S6K2$^{-/-}$ knockout genital ridges.

Tile scans of immunofluorescence stainings of female **(A)** and male **(B)** genital ridges at E13.5 and E15.5. Germ cells were identified via DAZL expression (germ cell marker), nuclei were stained with DAPI (blue). Representative images shown, n=2 (embryos per genotype), scale bar = 100µm; Wild-type and S6K1$^{-/-}$S6K2$^{-/-}$knockout tissues were from separate litters. Genotype was identified via PCR.

Male wild-type genital ridges showed the characteristic morphology of differentiating testis at E13.5 (Figure 4.4 B). A thickening in width was observed compared to the long and thin bipotential genital ridges at E11.5. Testis cords were present, as visualised by the organised and compartmentalized location of germ cells within the gonad (Figure 4.4 B). In comparison, global S6K1$^{-/-}$S6K2$^{-/-}$ knockout genital ridges appeared thinner compared to wild-type controls at E13.5 (Figure 4.4 B). Overall germ cell numbers seemed reduced (observation only, not quantified) and testis cords were not as obvious as in wild-type genital ridges (Figure 4.4 B). This could be due to the reduced germ cell number making cords less visible or a delayed cord formation.

Overall, the observed morphology of the male S6K1$^{-/-}$S6K2$^{-/-}$ knockout genital ridge closely resembled a more immature male genital ridge, possibly around E11.5 or E12.5, rather than the E13.5 control genital ridge. By E15.5, the wild-type male genital ridge further increased in width, having a characteristic round shape (Figure 4.4 B). Testis cords were clearly visible based on the localization of germ cells. Surprisingly, S6K1$^{-/-}$S6K2$^{-/-}$ knockout gonads looked very similar to the wild-type controls at this stage regarding the rounded shape and testis cord organization (Figure 4.4 B). A possible reduction in germ cell numbers was less obvious compared to E13.5, suggesting that a possible developmental delay at E13.5 was possibly compensated by E15.5. Of note, exact germ cell numbers were not determined at either stage.

Taken together, overall morphology of global S6K1$^{-/-}$S6K2$^{-/-}$ knockout genital ridges at E13.5 and E15.5 suggests a possible delay in development at the tissue level, which is more pronounced in females. It is likely that the observed possible developmental delay is linked to the reported growth retardation of S6K1$^{-/-}$S6K2$^{-/-}$ knockout embryos (Pende et al. 2004).

4.2.1.1.2 Characterisation of E13.5 S6K1$^{-/-}$ S6K2$^{-/-}$ knockout germ cells

In order to get a more detailed understanding on the developmental stage of germ cells within the genital ridge, expression of pluripotency factors was analysed at E13.5. Expression of pluripotency genes is downregulated in female germ cells as meiosis is initiated, while male germ cells maintain expression for until after birth (Figure 4.1) (Maurizio Pesce et al. 1998; Feng, Bowles, and Koopman 2014).

At E13.5, preliminary observations showed heterogeneous OCT4 expression in female wild-type germ cells, with only a subset of cells staining positive for OCT4 (Figure 4.5 A). In global S6K1$^{-/-}$S6K2$^{-/-}$ knockout germ cells a similar staining pattern was observed with no obvious difference compared to wild-type germ cells. In comparison, almost all male germ cells were positive for OCT4 in wild-type and S6K1$^{-/-}$S6K2$^{-/-}$ knockout gonads during preliminary analysis (Figure 4.5 A). By E15.5, OCT4 expression was absent in male and female germ cells of wild-type and S6K1$^{-/-}$S6K2$^{-/-}$ knockout tissues (Figure 4.5 B). Further, preliminary data on SOX2 expression, another pluripotency factor, revealed no difference between control and S6K1$^{-/-}$S6K2$^{-/-}$ knockout tissues in male and female germ cells (Figure 4.5 C). In addition, about 10% of female and 21% of male wild-type germ cells also stained positive for the cell surface antigen SSEA1, suggesting that the majority of germ cells have already downregulated the marker by E13.5 (Figure 4.5 C-D). In contrast, the percentage of SSEA1 expressing germ cells was increased in global S6K1$^{-/-}$S6K2$^{-/-}$ knockout genital ridges. 77% of female germ cells and 81% of male germ cells were positive for SSEA1 in double knockout

genital ridges (Figure 4.5 C-D). The observations in the male genital ridge are in line with previous preliminary observations showing an increase in SSEA1 positive male germ cells in S6K1$^{-/-}$ global knockout genital ridges (Figure 4.2).

Taken together, expression of OCT4 and SOX2 is not altered in S6K1$^{-/-}$S6K2$^{-/-}$ knockout germ cells. However, expression of the cell surface antigen SSEA1 was observed in a higher percentage of S6K1$^{-/-}$S6K2$^{-/-}$ knockout germ cells compared to wild-type germ cells, indicating a possible delay in downregulation of this pluripotency marker.

A

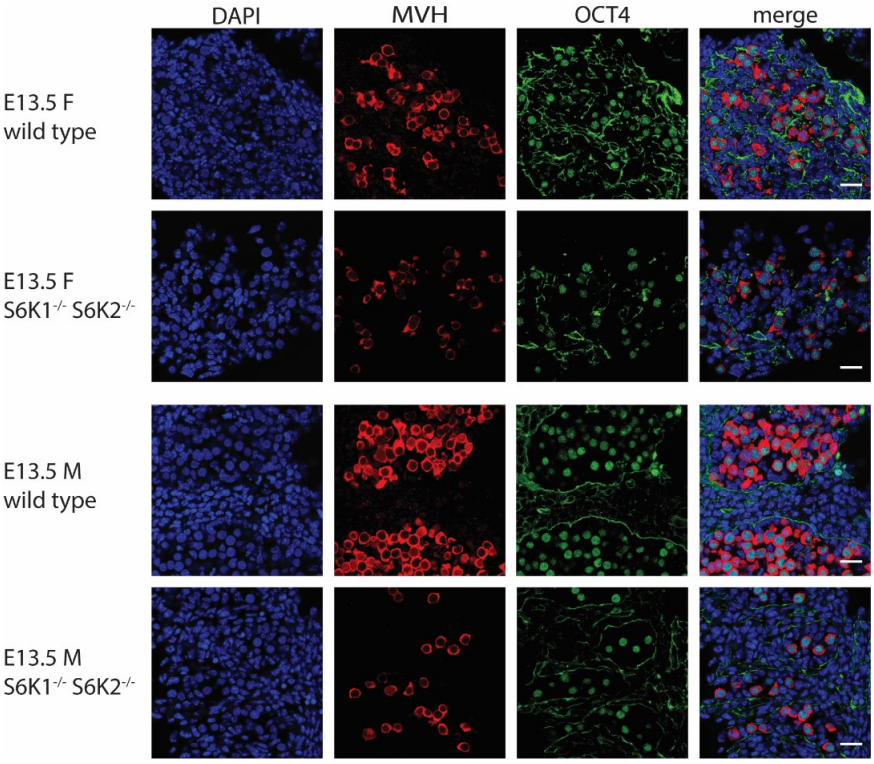
DAPI
MVH
OCT4
merge
E13.5 F
wild type
E13.5 F
S6K1-/- S6K2-/-
E13.5 M
wild type
E13.5 M
S6K1-/- S6K2-/-

B

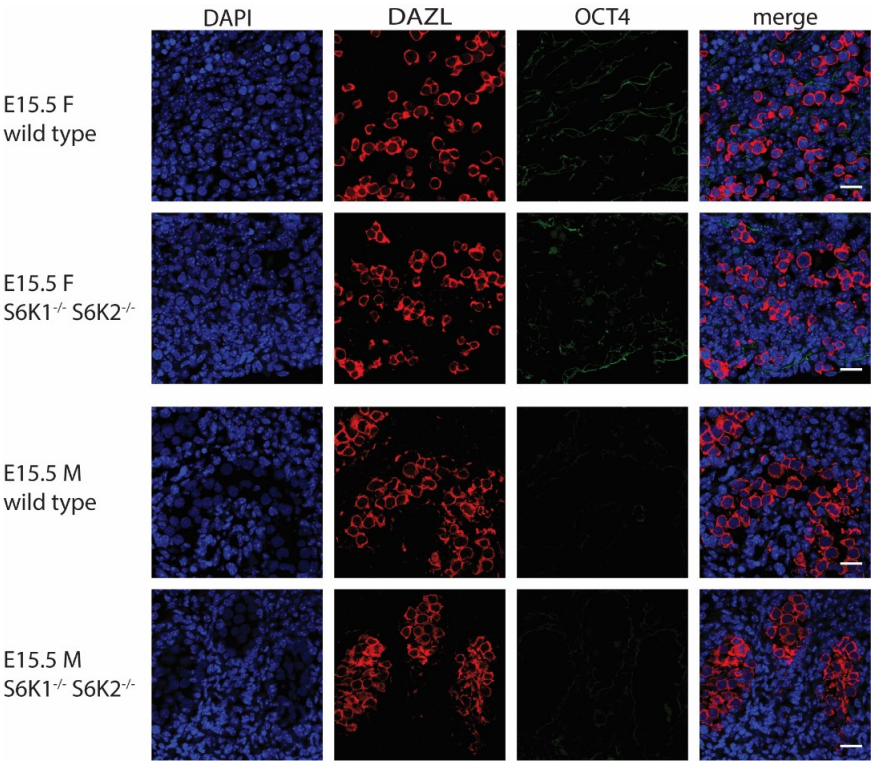
DAPI
DAZL
OCT4
merge
E15.5 F
wild type
E15.5 F
S6K1-/- S6K2-/-
E15.5 M
wild type
E15.5 M
S6K1-/- S6K2-/-

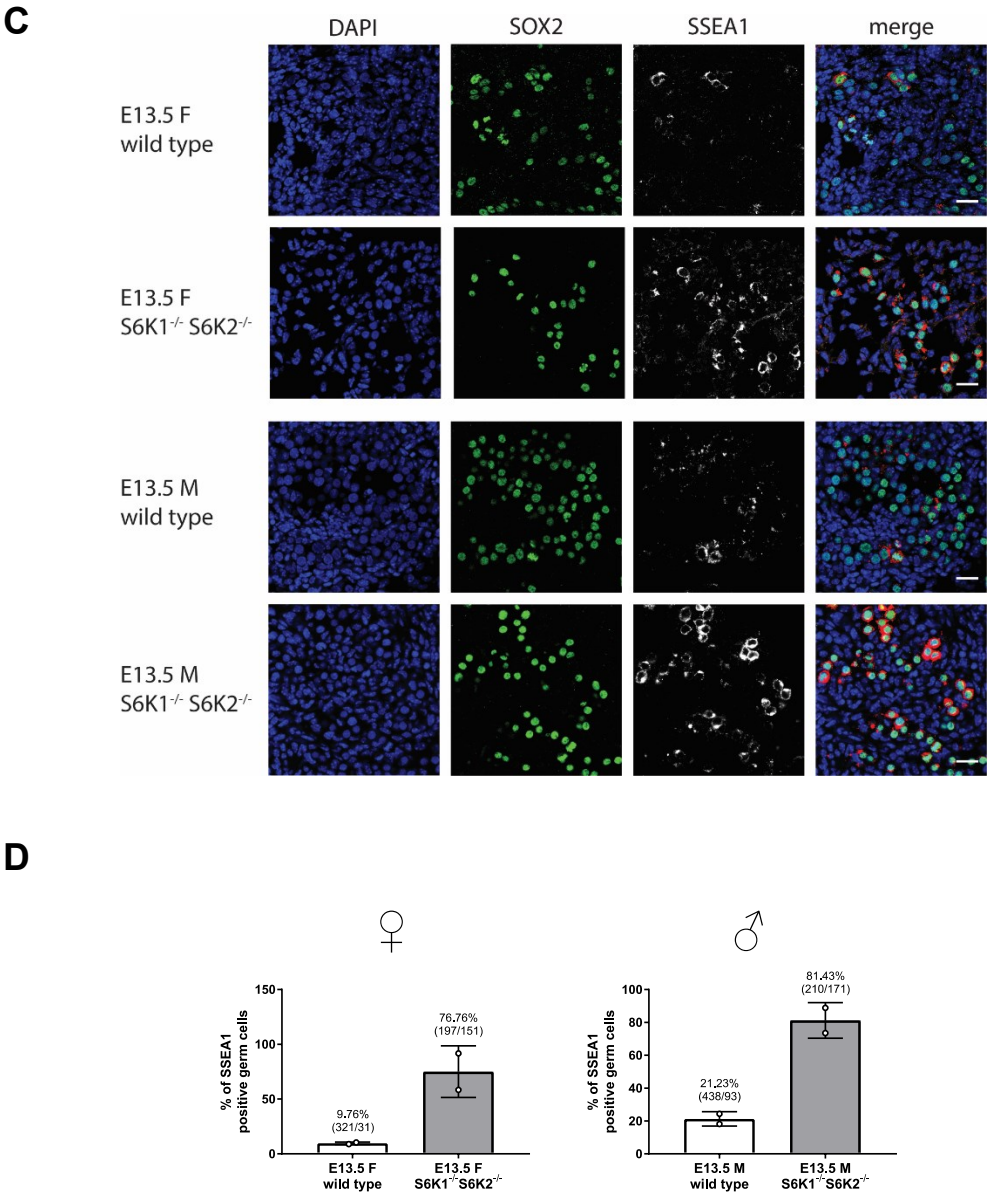

Figure 4.5: Expression of pluripotency factors in wild-type and global S6K1$^{-/-}$S6K2$^{-/-}$ knockout germ cells.

Immunofluorescence stainings of female and male genital ridges at E13.5. Nuclei were stained with DAPI (blue). **A** Expression of OCT4 in male and female germ cells at E13.5. Germ cells were identified using MVH as a germ cell marker. Representative images shown, n=1 (embryos per genotype), scale bar = 20µm **B** Expression of OCT4 in male and female germ cells at E15.5. Germ cells were identified using DAZL. Representative images shown, n=1 (embryos per genotype), scale bar = 20µm **C** Expression of SOX2 and SSEA1 in male and female germ cells. Representative images shown, n=1 (embryo per genotype) for Sox2, n=2 (embryos per genotype) for SSEA1, scale bar = 20µm **D** Quantification of SSEA1 positive germ cells in immunofluorescence stainings of wild-type and S6K1$^{-/-}$S6K2$^{-/-}$ global knockout genital ridges shown in (**C**). Average percentages of SSEA1 positive germ cells across biological replicates is shown. Data points represent percentage of SSEA1 positive germ cells from independent experiments (n=2 embryos per genotype). Germ cells were identified either via Sox2, DAZL or MVH. (n/n) above each bar = total number of germ cells counted/SSEA1^{+} germ cells; error bars = SD; Wild-type and S6K1$^{-/-}$S6K2$^{-/-}$ double knockout tissues were from separate litters. Genotype was identified via PCR. This is preliminary data and due to low n numbers, no statistical test has been performed.

4.2.1.1.3 Characterisation of E15.5 S6K1$^{-/-}$S6K2$^{-/-}$ knockout germ cells

By E15.5, the majority of female germ cells will have entered meiosis, whereas male germ cells are mitotically arrested. To test the normal developmental progression, the expression of two meiotic markers (STRA8 and SYCP3) was analysed in S6K1$^{-/-}$S6K2$^{-/-}$ knockout germ cells.

First, DAZL and MVH expression was checked again at E15.5 in male and female germ cells to confirm continuous expression in S6K1$^{-/-}$S6K2$^{-/-}$ knockout germ cells and validate the use of either protein as a robust germ cell marker. Consistent with data from E13.5, both proteins are robustly expressed in all germ cells at E15.5 (Figure 4.5 B, Figure 4.6).

At E15.5, preliminary observations showed that 92% of female wild-type germ cells expressed STRA8 and 96% were SCP3 positive, indicating that the majority of germ cells have initiated meiosis (Figure 4.6 A-B). In comparison, 81% of S6K1$^{-/-}$S6K2$^{-/-}$ knockout germ cells stained positive for STRA8, however SCP3 expression was greatly reduced. Only 24% of MVH-positive germ cells were positive for SCP3 in global S6K1$^{-/-}$S6K2$^{-/-}$ knockout genital ridges (Figure 4.6 A-B). In contrast, male germ cells were negative for SCP3 and STRA8 as expected (Figure 4.6 C).

Taken together, while expression of STRA8 was not affected in S6K1$^{-/-}$S6K2$^{-/-}$ knockout genital ridges, SCP3 expression was greatly reduced, suggesting a possible delay in SCP3 upregulation. These preliminary observations are in line with the observed possible developmental delay of E15.5 genital ridges.

Overall, global deletion of S6 kinases resulted in a possible reduced germ cell number and a likely delay of genital ridge development at E13.5 (female and male) and E15.5 (female). In germ cells, expression of key proteins DAZL and MVH and key pluripotency factors OCT4 and SOX2 was not affected. Intriguingly, SSEA1 expression is higher in S6K1$^{-/-}$S6K2$^{-/-}$ knockout germ cells compared to wild-type germ cells at E13.5. At E15.5, female S6K1$^{-/-}$S6K2$^{-/-}$ knockout germ cells have greatly reduced SCP3 expression. These observations indicate a possible overall delay in germ cell development, in line with possible delayed genital ridge development.

A

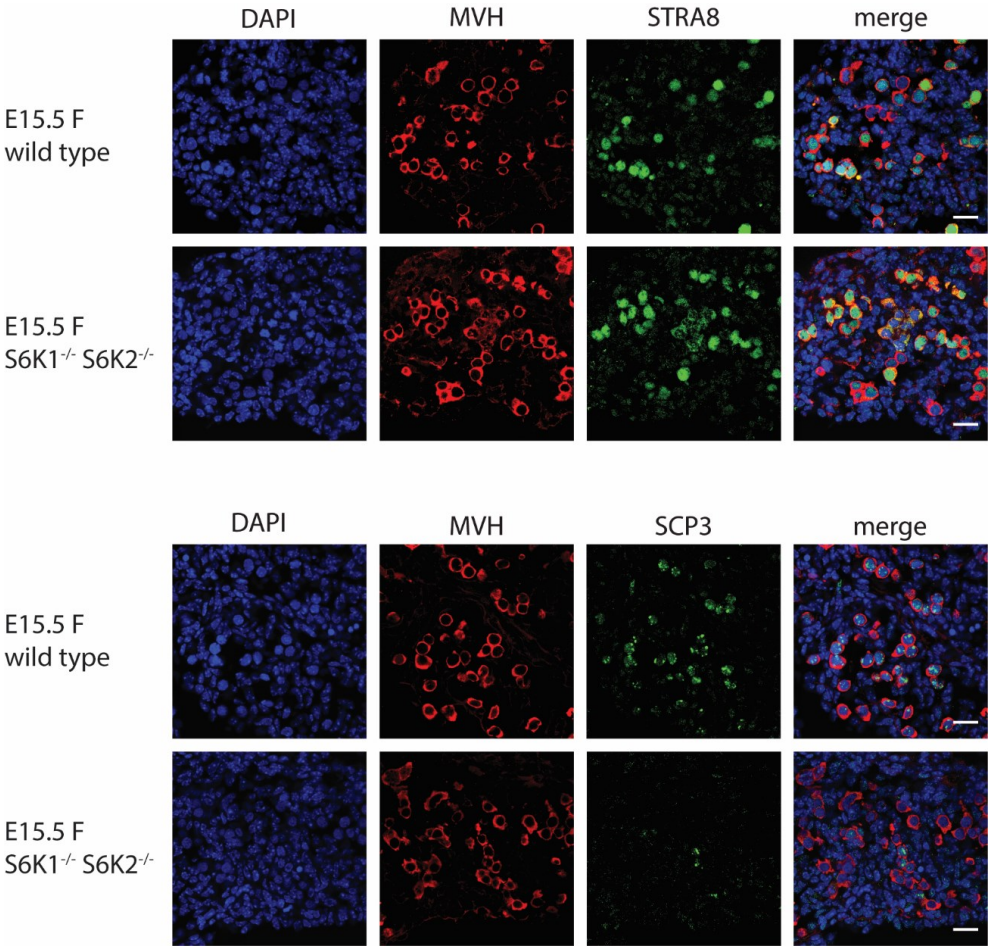
DAPI
MVH
STRA8
merge
E15.5 F
wild type
E15.5 F
S6K1-/- S6K2-/-
DAPI
MVH
SCP3
merge
E15.5 F
wild type
E15.5 F
S6K1-/- S6K2-/-

B

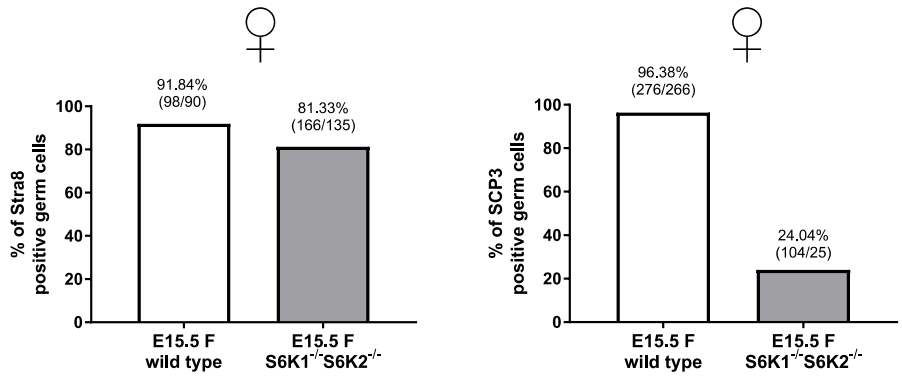
91.84%
(98/90)
81.33%
(166/135)
% of Stra8
positive germ cells
100
80
60
40
20
0
E15.5 F
wild type
E15.5 F
S6K1-/-S6K2-/-
96.38%
(276/266)
24.04%
(104/25)
% of SCP3
positive germ cells
100
80
60
40
20
0
E15.5 F
wild type
E15.5 F
S6K1-/-S6K2-/-

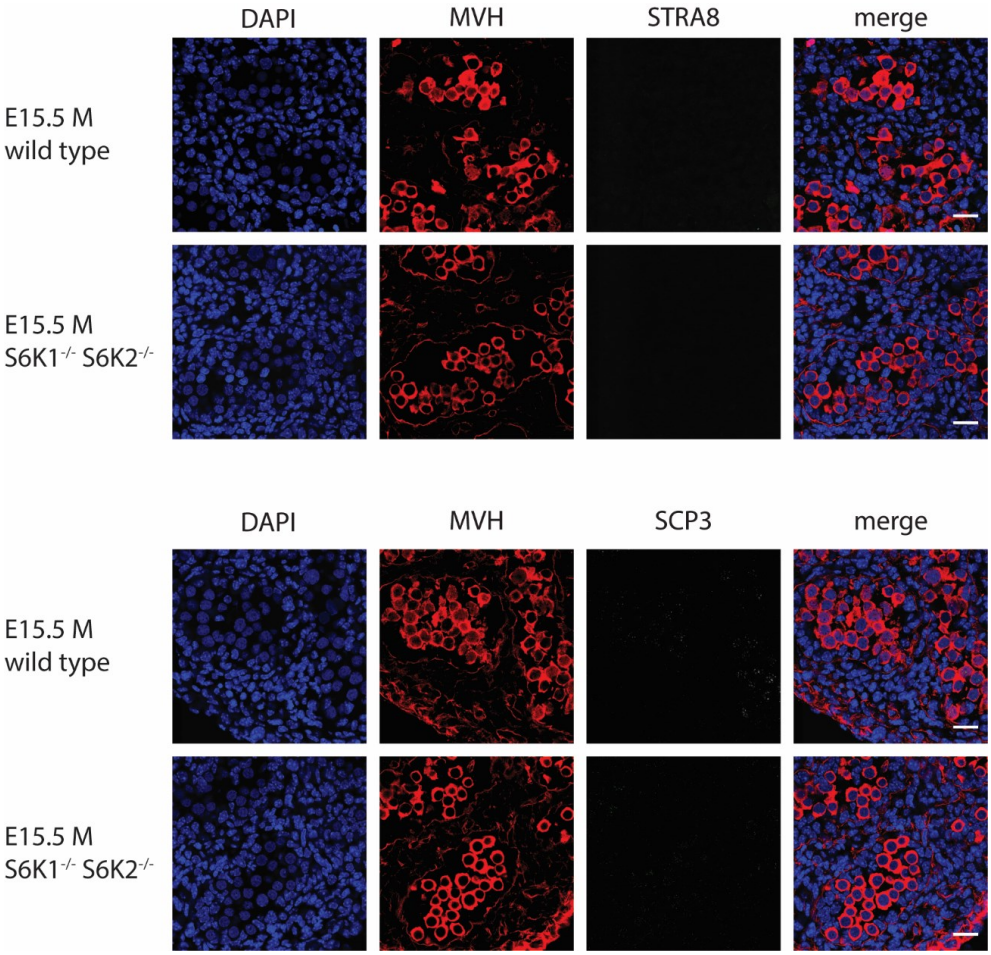

Figure 4.6: Expression of meiosis markers in wild-type and global S6K1$^{-/-}$S6K2$^{-/-}$knockout germ cells at E15.5.

Immunofluorescence stainings of female and male genital ridges at E15.5. Germ cells were identified via MVH expression, nuclei were stained with DAPI (blue). **A** Expression of STRA8 and SCP3 in E15.5 female germ cells. Representative images shown, n=1 (embryo per genotype), scale bar = 20µm **B** Quantification of STRA8 and SCP3 positive germ cells in immunofluorescence stainings of wild-type and S6K1$^{-/-}$S6K2$^{-/-}$knockout tissues shown in (**A**). Average percentages of STRA8 or SCP3 positive germ cells across different tissue sections is shown. Germ cell were identified via MVH expression. (n/n) above each bar = total number of germ cells counted/SCP3^{+} or STRA8^{+} germ cells; biological replicate = 1 embryo per genotype **C** Expression of STRA8 and SCP3 in E15.5 male germ cells. Representative images shown, n=2 (embryos per genotype), scale bar = 20µm; Wild-type and S6K1$^{-/-}$S6K2$^{-/-}$double knockout tissues were from separate litters. Genotype was identified via PCR. This is preliminary data and due to low n numbers, no statistical test has been performed.

4.2.1.1. Histological analysis of adult gonads lacking S6 kinases

In order to further complement the observations on foetal germ cells, adult (> 8 week old) wild-type and global S6K1$^{-/-}$ single and S6K1$^{-/-}$S6K2$^{-/-}$ double knockout gonads were collected for histological analysis. Since the vast majority of S6K1$^{-/-}$S6K2$^{-/-}$ double knockout mice die shortly after birth or in the womb (Pende et al. 2004), only one pair of double knockout ovaries and testes could be obtained for histological analysis. Any late arising phenotypes during foetal development after E15.5 or postnatally will be detected this way.

In females, wild-type and S6K1$^{-/-}$ knockout ovaries were of similar size (Figure 4.7 A). Histological tissue sections of ovaries revealed no apparent difference between genotypes. Follicles at different stages of development were present in examined ovaries, from the earliest stages of primordial follicles all the way to antral follicles, characterised by presence of fluid-filled cavities (arrows, Figure 4.7 A). Further, multiple corpora lutea were found, indicating successful ovulation (*, Figure 4.7 A). Of note, global S6K1$^{-/-}$ knockout females were fertile and litter sizes appeared normal when mated with wild-type males (observation only) (average litter size KO x WT breedings = 8±0 SEM (n = 2 litters), average litter size HET x HET breedings = 8±0.7 SEM (n = 5 litters), Student's t-test, t=5, df=5, p=0.99). Surprisingly, tissue sections of S6K1$^{-/-}$S6K2$^{-/-}$ double knockout ovaries also displayed similar morphology to wild-type control ovaries (Figure 4.7 B). Follicles of different stages could be detected, as well as corpora lutea (Figure 4.7 B).

In males, wild-type and S6K1$^{-/-}$ knockout testes were of similar size (Figure 4.8 A). S6K1$^{-/-}$ knockout tissue sections stained with hematoxylin appeared similar to control sections (Figure 4.8 A). Seminiferous tubules containing different stages of male germ cells were observed. Seminiferous tubules typically consist of round immature spermatogonia on the basal lamina (edge of the tubule), followed by layers of different stages of spermatocytes and spermatids. Some tubules contain elongated spermatids towards the luminal surface of the tubule (Ahmed and de Rooij 2009). Tubules with elongated haploid spermatids lying at the luminal surface with their tails extending into the lumen could be detected (Figure 4.8 A), indicating that S6K1$^{-/-}$ germ cells can undergo all different stages of spermatogenesis. Further, no apparent difference was observed between wild-type and S6K1$^{-/-}$S6K2$^{-/-}$ double knockout testis sections (Figure 4.8 A), in line with observations in S6K1$^{-/-}$ knockout testis. Of note, detailed staging of different tubules or sperm counts were not determined. However, S6K1$^{-/-}$ knockout males were fertile and litter sizes appeared normal when mated with wild-type females (observation only) (average litter size KO x WT breedings = 8 (n = 1 litter), average litter size HET x HET breedings = 8±0.7 SEM (n = 5 litters)).

In summary, no gross differences could be detected between wild-type and S6K1$^{-/-}$ single and S6K1$^{-/-}$S6K2$^{-/-}$ double knockout adult gonads. In combination with the weak observed phenotype in foetal germ cells and genital ridges, these observations suggest that S6 kinases are not essential for germ cell development in the mouse.

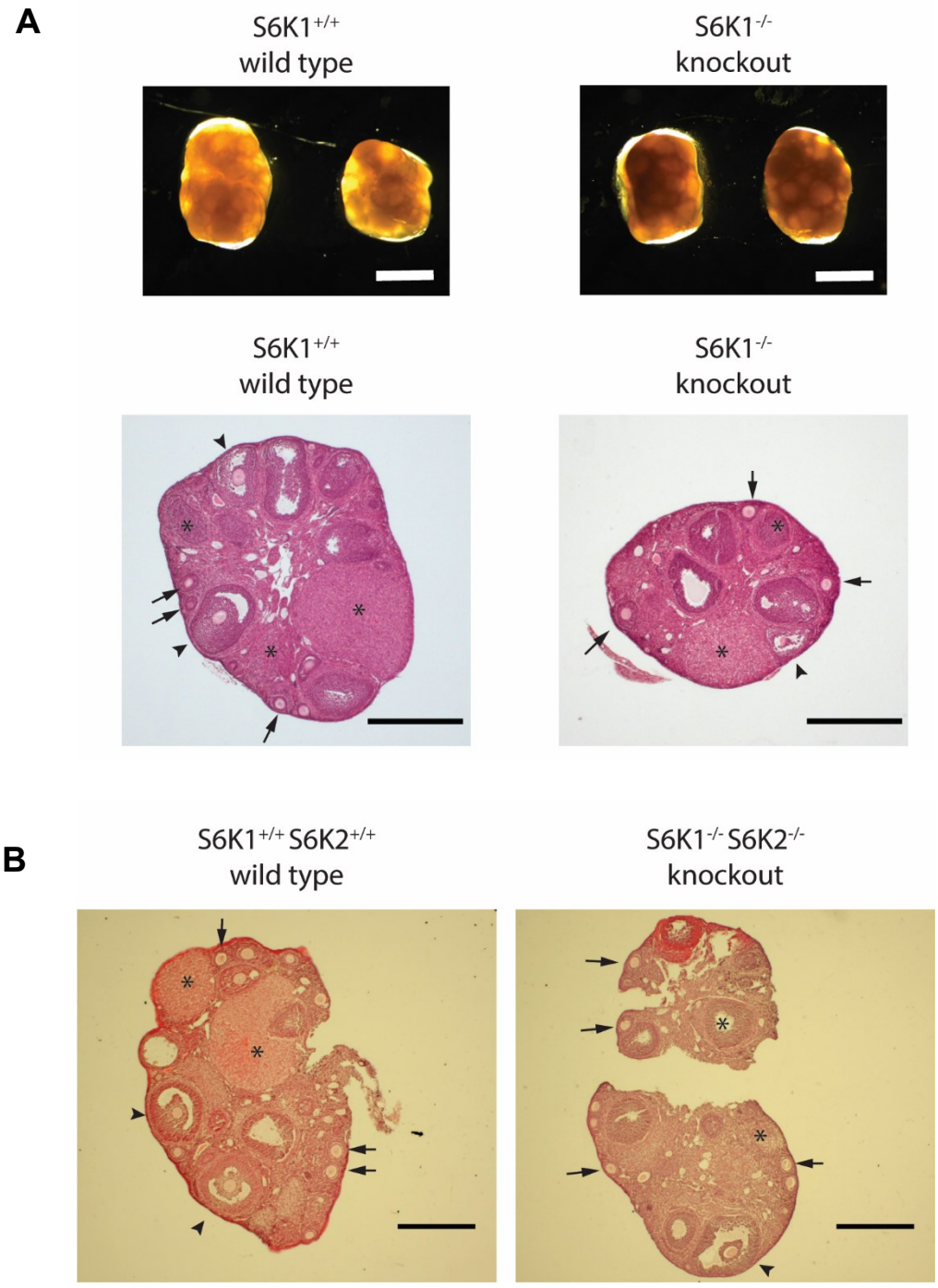

Figure 4.7: Histological analysis of S6K1$^{-/-}$ single and S6K1$^{-/-}$S6K2$^{-/-}$ double knockout adult ovaries.

A Wild-type and S6K1$^{-/-}$ single knockout ovaries from littermates at 8 weeks. Representative images of whole ovaries shown, n=2 (mice per genotype), scale bar = 1mm; Representative images of Haematoxylin and Eosin stained sections of same ovaries. n=2 (mice per genotype), scale bar = 500µm, zoom = 2.5x; **B** Haematoxylin and Eosin stained sections of wild-type and S6K1$^{-/-}$S6K2$^{-/-}$ double knockout ovaries. Wild-type control = 14 weeks, double knockout = 21 weeks; Control and double knockout ovaries are from separate litters. Representative images shown, n=1 (mouse per genotype), scale bar = 500µm, zoom = 2.5x; * denote corpus lutea, arrows point to secondary follicles, arrow heads depict antral follicles;

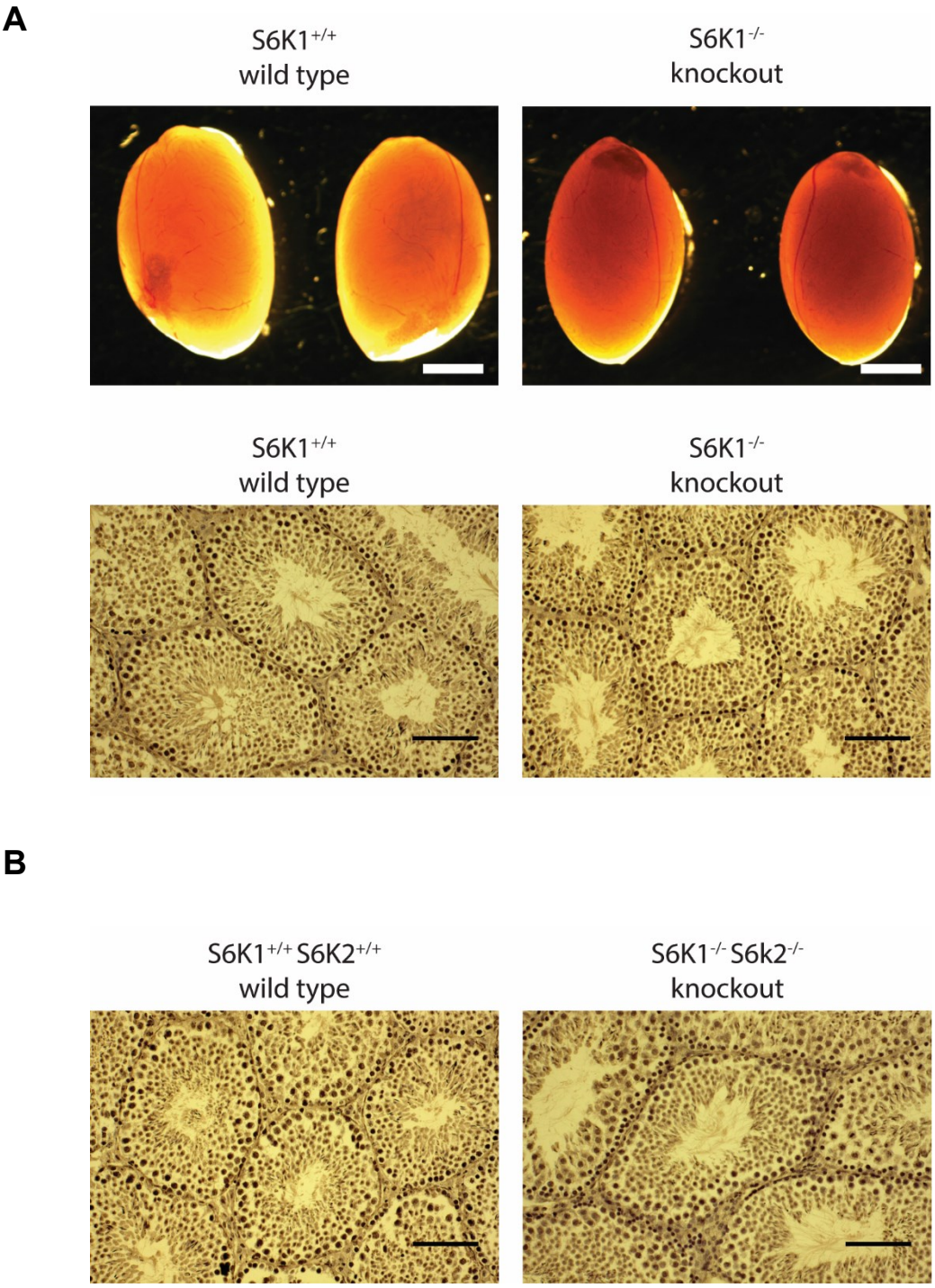

Figure 4.8: Histological analysis of S6K1$^{-/-}$ single and S6K1$^{-/-}$S6K2$^{-/-}$ double knockout adult testes.

A Wild-type and S6K1$^{-/-}$ single knockout adult testes from littermates at 9 weeks. Representative images of whole testes shown**.** n=2 (mice per genotype), scale bar = 2mm; Representative images of Haematoxylin stained sections of same testes. n=2 (mice per genotype), scale bar = 80µm, zoom = 20x; **B** Haematoxylin stained sections of wild-type and S6K1$^{-/-}$S6K2$^{-/-}$ double knockout testes at 10 weeks. Control and double knockout testes are from separate litters. Representative images shown, n=1 (mouse per genotype), scale bar = 80µm, zoom = 20x;

4.2.2. The role of 4E-BPs during germ cell development

Analysis of wild-type germ cells revealed activation of the mTORC1-4E-BP1 signalling axis from E10.5 onwards. To analyse possible functions of 4E-binding proteins during germ cell development, global knockout mice lacking only 4E-BP1 or 4E-BP1 and 4E-BP2 were analysed.

Given that 4E-BP1 was the highest expressed isoform at the mRNA level and an enrichment in total 4E-BP1 protein was observed specifically in germ cells, 4E-BP1$^{-/-}$ germ cells were analysed first. Wild-type (4E-BP1$^{+/+}$) and knockout tissues were obtained from the same litter via mating of heterozygous (4E-BP1$^{+/-}$) males and females. At the same time, the 4E-BP1$^{-/-}$4E-BP2$^{-/-}$ double knockout colony was established by crossing 4E-BP1$^{-/-}$ mice with 4E-BP2$^{-/-}$ mice. Wild-type control mice (4E-BP1$^{+/+}$4E-BP2$^{+/+}$) were maintained as a separate colony. Hence, wild-type and 4E-BP1$^{-/-}$4E-BP2$^{-/-}$ double knockout tissues were obtained from separate litters and subsequently analysed to rule out any compensation by 4E-BP2 in our initial results.

4.2.2.1. Characterisation of primordial germ cells lacking 4E-BPs

First, E13.5 genital ridges were co-stained for two key germ cell proteins DAZL and MVH. All wild-type and 4E-BP1$^{-/-}$ knockout germ cells robustly expressed DAZL and MVH (Figure 4.9 A). Further, no consistent difference in expression levels was observed between wild-type and knockout tissues by eye, suggesting 4E-BP1 is not essential for DAZL and MVH expression. At the tissue level, no obvious difference was observed between wild-type genital ridges and knockout genital ridges regarding tissue morphology and approximate germ cell numbers (not quantified) (Figure 4.9 A). In line with these observations, 4E-BP1$^{-/-}$ 4E-BP2$^{-/-}$double knockout germ cells also expressed DAZL and MVH, with no apparent morphological difference to wild-type genital ridges at E13.5 (Figure 4.9 B). Both proteins were subsequently used to identify germ cells.

A

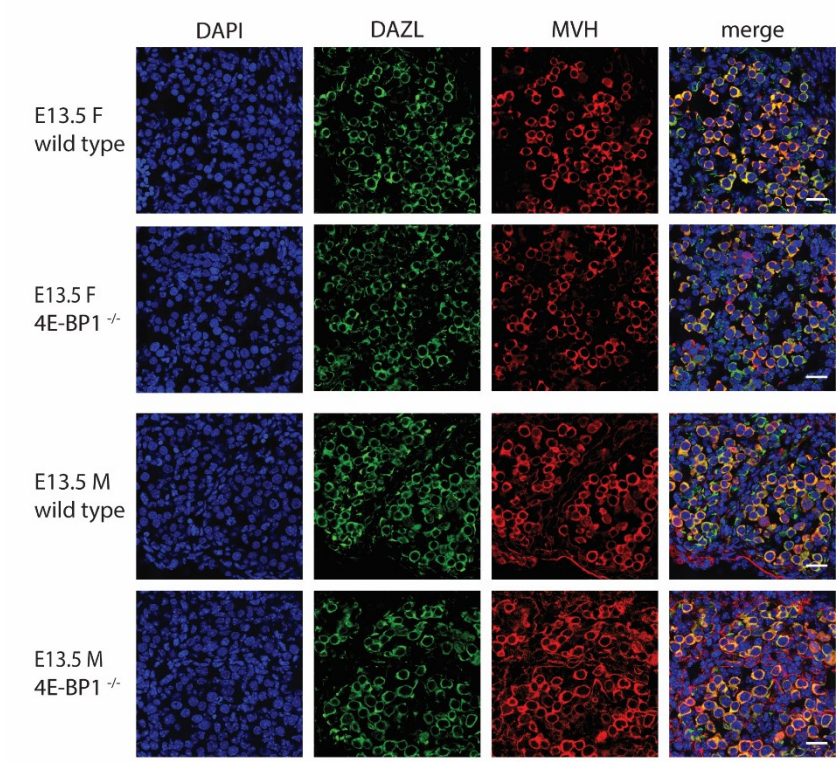
DAPI
DAZL
MVH
merge
E13.5 F
wild type
E13.5 F
4E-BP1 -/-
E13.5 M
wild type
E13.5 M
4E-BP1 -/-

B

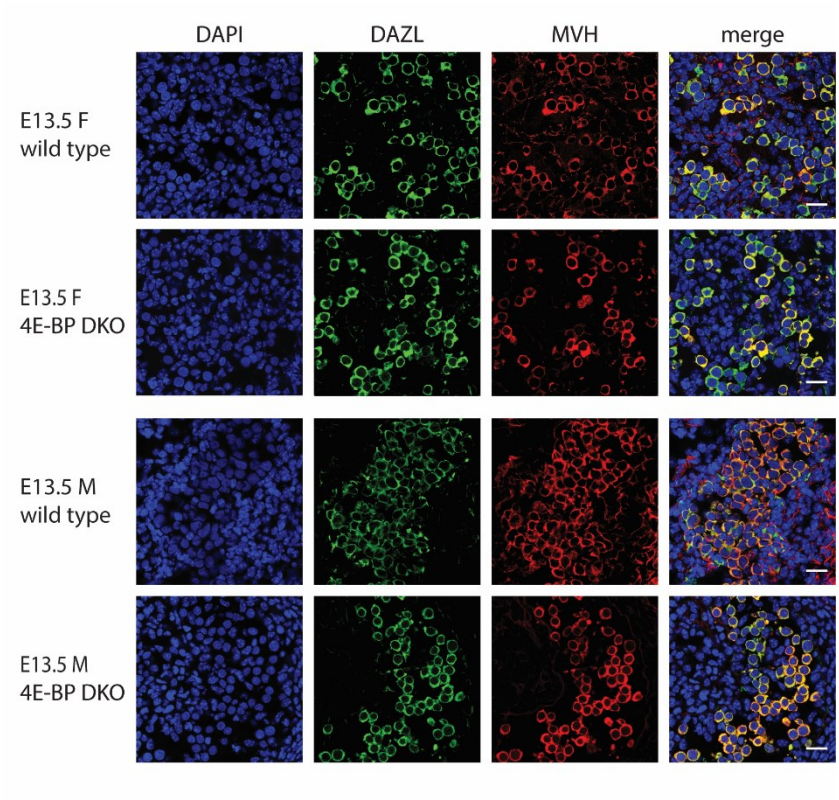
DAPI
DAZL
MVH
merge
E13.5 F
wild type
E13.5 F
4E-BP DKO
E13.5 M
wild type
E13.5 M
4E-BP DKO

Figure 4.9: Expression of key germ cell proteins at E13.5 in wild-type and global 4E-BP single and double knockout germ cells.

Immunofluorescence stainings of female and male genital ridges at E13.5. Germ cells were stained for DAZL and mouse Vasa homologue (MVH), nuclei were stained with DAPI (blue). **A** DAZL and MVH expression 4E-BP1$^{-/-}$ knockout germ cells. Representative images shown, n=2 (embryos per genotype), scale bar = 20µm; Wild-type and 4E-BP1$^{-/-}$ knockout tissues were from littermates. Genotype was identified via PCR. **B** DAZL and MVH expression in E13.5 in 4E-BP1$^{-/-}$ 4E-BP2$^{-/-}$ double knockout germ cells. Representative images shown, n=3 (embryos per genotype), scale bar = 20µm; Wild-type and 4E-BP1$^{-/-}$ 4E-BP2$^{-/-}$ double knockout tissues were from separate littermates. Genotype was identified via PCR.

4.2.2.1.1 Characterisation of E13.5 4E-BP single and double knockout germ cells

In order to get a more detailed understanding on the developmental stage of 4E-BP1$^{-/-}$ single and 4E-BP1$^{-/-}$4E-BP2$^{-/-}$ double knockout germ cells, the above described immunofluorescence-based approach was applied to E13.5 genital ridges (Figure 4.1).

At E13.5, only a subset of female germ cells stained positive for OCT4. The heterogeneous expression pattern was observed in wild-type and 4E-BP1$^{-/-}$ global knockout tissues with no apparent difference between genotypes (Figure 4.10 A). At E15.5, control and knockout female germ cells were OCT4 negative (Figure 4.10 B). Further, robust expression of SOX2 was detected in female wild-type and 4E-BP1$^{-/-}$ knockout germ cells at E13.5. In contrast, only about 21% of wild-type and 19% of 4E-BP1$^{-/-}$ knockout female germ cells stained positive for SSEA1 at this stage (Figure 4.10 C, E). Consistent with these observations, deletion of both isoforms (4E-BP1 and 4E-BP2) did not change the percentage of SSEA1 positive germ cells in double knockout tissues compared to wild-type control tissues. About 38% of wild-type and 37% of 4E-BP1$^{-/-}$4E-BP2$^{-/-}$ double knockout germ cells stained positive for SSEA1 (Figure 4.11 B-C). Further, expression of other pluripotency markers (OCT4, SOX2) were similar between of 4E-BP1$^{-/-}$4E-BP2$^{-/-}$ double knockout and wild-type germ cells (Figure 4.11 A-B). Of note, a difference in overall percentages of SSEA1 positive germ cells was observed between the single knockout and double knockout tissues. The two colonies have slightly different mixed genetic backgrounds (see 2.1.5.3, p. 72), which could underlie the observed difference.

In contrast, the majority of male germ cells were positive for OCT4 in wild-type and 4E-BP1$^{-/-}$ global knockout gonads at E13.5 (Figure 4.10 A). SOX2 expression was detected in germ cells of both genotypes, similar to the observations in female germ cells. Interestingly, while only about 14% of male wild-type germ cells showed SSEA1 expression, 54% of 4E-BP1$^{-/-}$

knockout germ cells stained positive for SSEA1 at E13.5 (Figure 4.10 C, E). At E15.5, male germ cells were negative for SSEA1 and OCT4 in control and 4E-BP1$^{-/-}$ knockout germ cells (Figure 4.10 B, D), suggesting a possible delay in the downregulation of SSEA1 in E13.5 male germ cells. In line with these observations, deletion of 4E-BP1 and 4E-BP2 resulted in an increase in SSEA1 positive germ cells from 15% in wild-type to 41% in knockout tissues (Figure 4.11 B-C). Expression of other pluripotency markers (OCT4, SOX2) appeared similar between wild-type and 4E-BP1$^{-/-}$4E-BP2$^{-/-}$ double knockout genital ridges (Figure 4.11 A-B).

Taken together, expression of all examined pluripotency factors (OCT4, SOX2 and SSEA1) is likely not dependent on 4E-BP1 or both 4E-BPs in female germ cells at E13.5. In male germ cells, OCT4 and SOX2 expression is unchanged upon 4E-BP1 deletion alone or in combination with 4E-BP2. However, SSEA1 is still highly expressed in 4E-BP1$^{-/-}$ knockout germ cells compared to wild-type germ cells, with a similar trend in 4E-BP1$^{-/-}$4E-BP2$^{-/-}$ knockout germ cells, indicating a possible delay in downregulation of this specific cell surface marker.

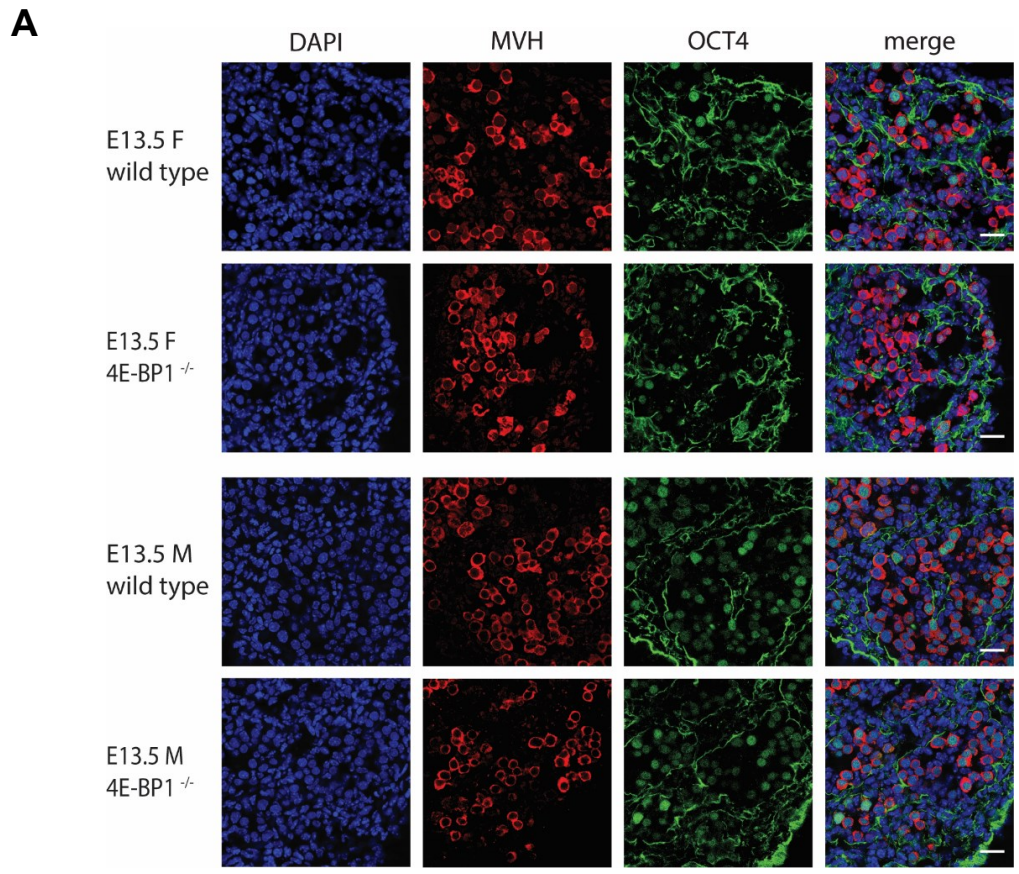

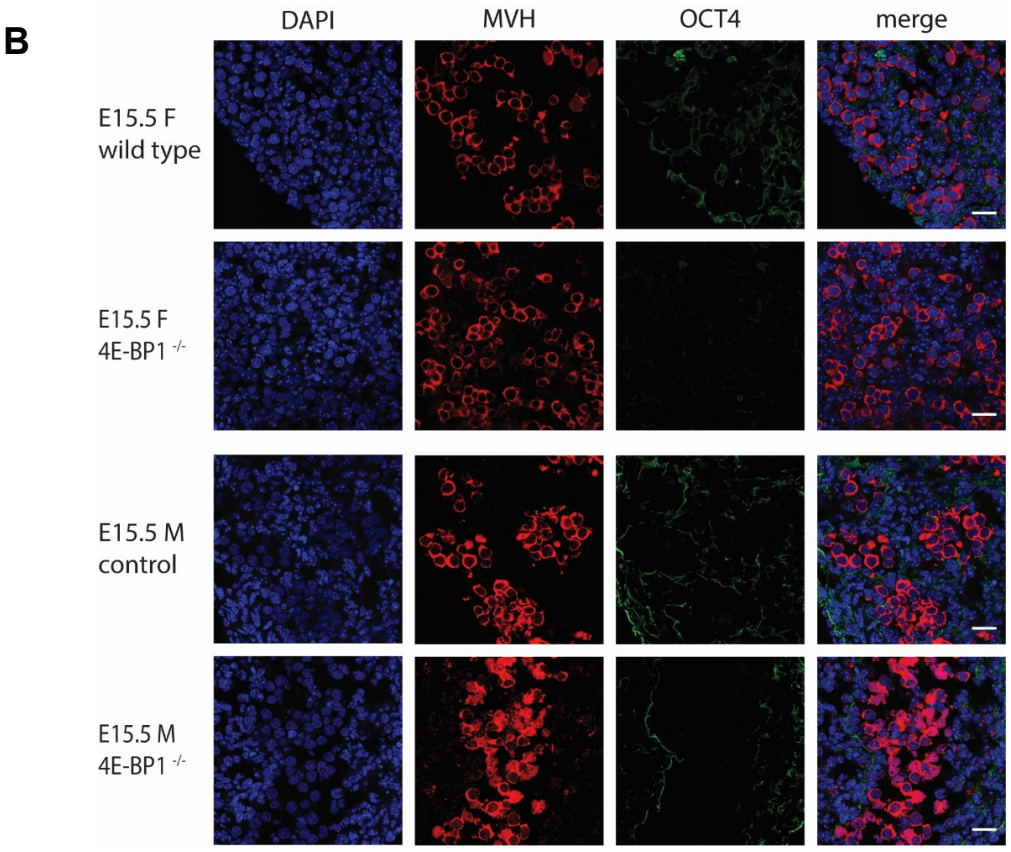
B
DAPI
MVH
OCT4
merge
E15.5 F
wild type
E15.5 F
4E-BP1 -/-
E15.5 M
control
E15.5 M
4E-BP1 -/-

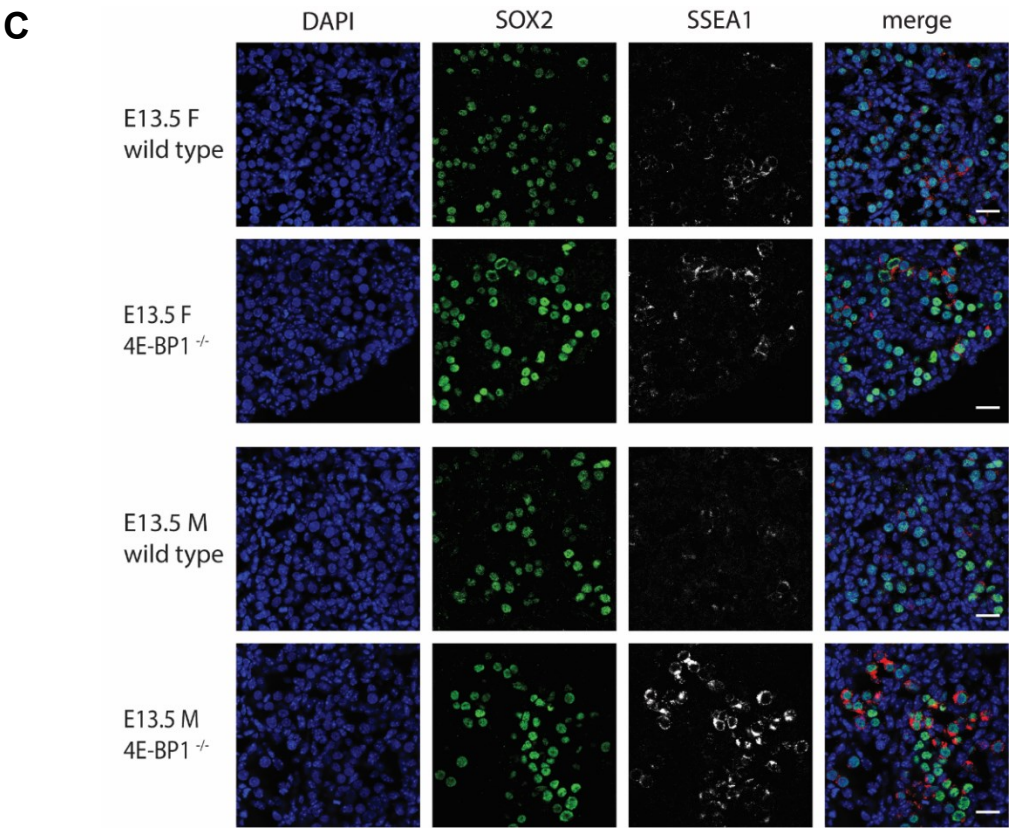
C
DAPI
SOX2
SSEA1
merge
E13.5 F
wild type
E13.5 F
4E-BP1 -/-
E13.5 M
wild type
E13.5 M
4E-BP1 -/-

D

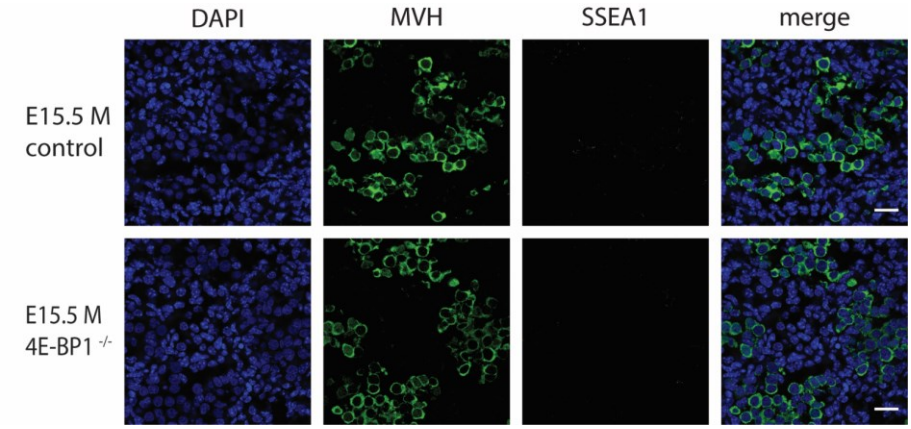

E

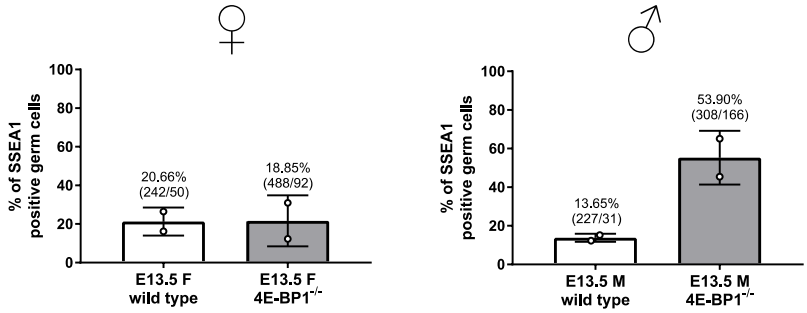

Figure 4.10: Expression of pluripotency factors in wild-type and global 4E-BP1$^{-/-}$ knockout germ cells.

Immunofluorescence stainings of female and male genital ridges at E13.5 and E15.5. Nuclei were stained with DAPI (blue). **A** Expression of OCT4 in male and female germ cells at E13.5. Germ cells were identified using MVH. Representative images shown, n=2 (embryos per genotype), scale bar = 20µm **B** Expression of OCT4 in male and female germ cells at E15.5. Germ cells were identified using MVH. Representative images shown, n=2 (embryos per genotype), scale bar = 20µm **C** Expression of SOX2 and SSEA1 in male and female germ cells at E13.5. Representative images shown; control = 4E-BP1$^{-/+}$ heterozygous tissue; n=1 (embryo per genotype) for SOX2, n=2 (embryos per genotype) for SSEA1, scale bar = 20µm **D** Expression of SSEA1 in male germ cells at E15.5. Germ cells were identified using MVH. Representative images shown; control = 4E-BP1$^{-/+}$ heterozygous tissue; n=1 (embryo per genotype), scale bar = 20µm **E** Quantification of SSEA1 positive germ cells at E13.5. Immunofluorescence stainings of wild-type and 4E-BP1$^{-/-}$ global knockout genital ridges shown in (C) were analysed. Average percentages of SSEA1 positive germ cells is shown. Data points represent percentages of SSEA1 positive germ cells from independent experiments (n=2 embryos per genotype). Germ cells were identified either via SOX2 or MVH. (n/n) above each bar = total number of germ cells counted/SSEA1^{+} germ cells; error bars = SD; Wild-type, 4E-BP1$^{-/-}$ heterozygous and 4E-BP1$^{-/-}$ knockout tissues were littermates. Genotype was identified via PCR. This is preliminary data and due to low n numbers, no statistical test has been performed.

A

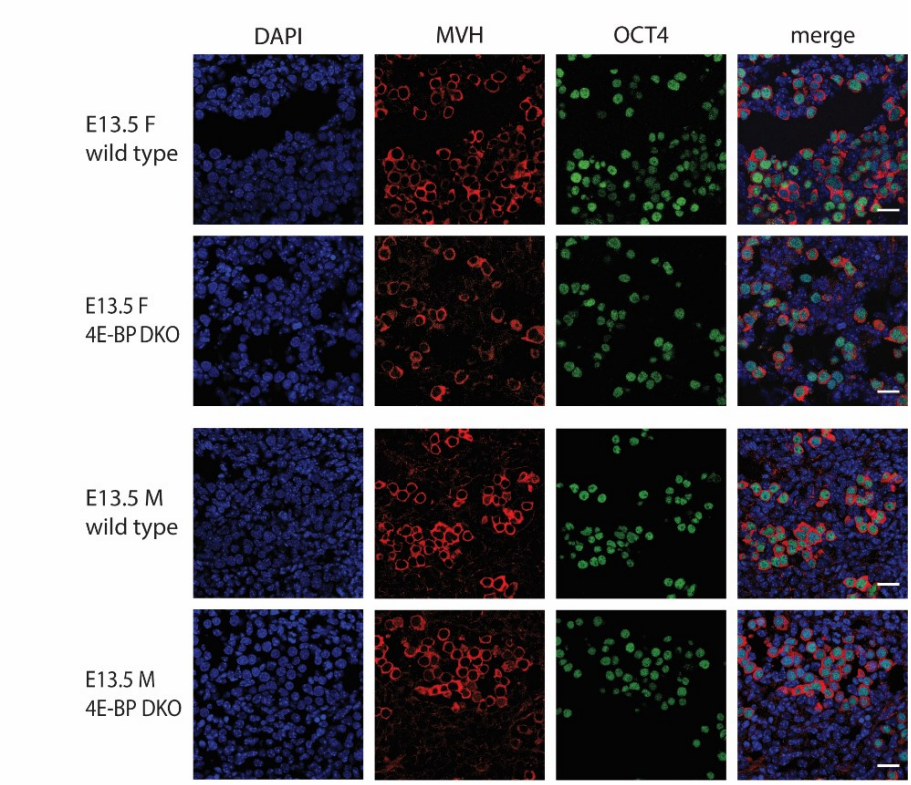
DAPI
MVH
OCT4
merge
E13.5 F
wild type
E13.5 F
4E-BP DKO
E13.5 M
wild type
E13.5 M
4E-BP DKO

B

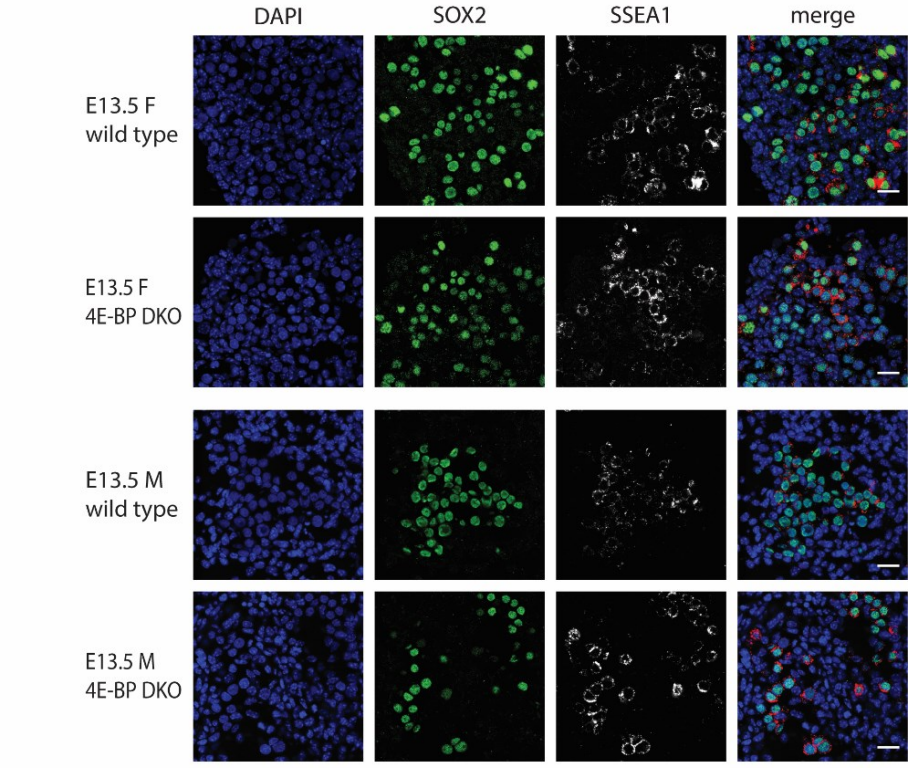
DAPI
SOX2
SSEA1
merge
E13.5 F
wild type
E13.5 F
4E-BP DKO
E13.5 M
wild type
E13.5 M
4E-BP DKO

C

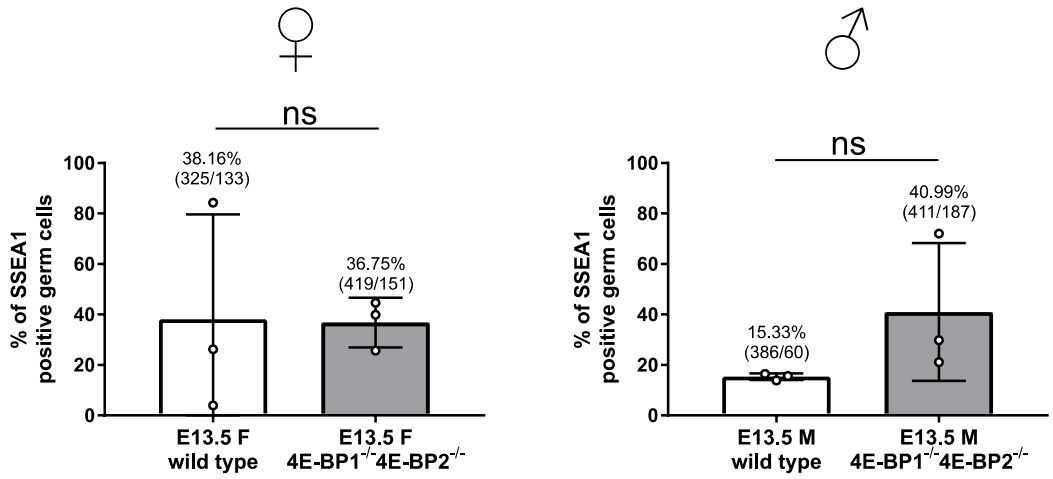

Figure 4.11: Expression of pluripotency factors in wild-type and global 4E-BP1$^{-/-}$ 4E-BP2$^{-/-}$ knockout germ cells.

Immunofluorescence stainings of female and male genital ridges at E13.5. Nuclei were stained with DAPI (blue). **A** Expression of OCT4 in male and female germ cells. Germ cells were identified using MVH. Representative images shown, n=3 (embryos per genotype), scale bar = 20µm **B** Expression of SOX2 and SSEA1 in male and female germ cells. Representative images shown; n=3 (embryo per genotype), scale bar = 20µm **C** Quantification of SSEA1 positive germ cells in immunofluorescence stainings of wild-type and global 4E-BP1$^{-/-}$ 4E-BP2$^{-/-}$ double knockout genital ridges from (B). Average percentages of SSEA1 positive germ cells are shown. Data points represent percentages of SSEA1 positive germ cells from independent experiments (n=3 embryos per genotype). Germ cells were identified via MVH or SOX2. (n/n) above each bar = total number of germ cells counted/SSEA1^{+} germ cells; error bars = SD; Significance was analysed by unpaired student's t-test. ns = not significant, $p > 0.05$; Wild-type and 4E-BP1$^{-/-}$ 4E-BP2$^{-/-}$ knockout tissues were from separate litters. Genotype was identified via PCR.

4.2.2.1.2 Characterisation of E15.5 4E-BP1 $^{-/-}$ knockout germ cells

Analysis of E15.5 genital ridges revealed that all male and female control and 4E-BP1 $^{-/-}$ knockout germ cells still expressed DAZL and MVH, validating the use of either protein as a robust germ cell marker (Figure 4.12).

By E15.5, the majority of female germ cells will have entered meiosis, whereas male germ cells are mitotically arrested. Analysis of the two meiotic markers STRA8 and SYCP3 in female germ cells showed no difference in expression between wild-type and 4E-BP1$^{-/-}$ knockout germ cells (Figure 4.13 A-B). About 59% of wild-type and 60% of 4E-BP1$^{-/-}$ knockout germ cells stained positive for STRA8. Further, about 85% of wild-type and 90% of 4E-BP1$^{-/-}$ knockout germ cells stained positive for SCP3, indicating successful initiation of meiosis (Figure 4.13 B).

In contrast, male germ cells were negative for STRA8 as expected (Figure 4.13 C). Intriguingly, some SCP3 signal above background levels was detected specifically in male 4E-BP1$^{-/-}$ knockout germ cells (Figure 4.13 C). The signal intensities were lower compared to female germ cells though. Also, the staining pattern was different. In female meiotic germ cells, SCP3 staining appears typically as fluorescent dots within the nucleus or as elongated fibers, depending on the stage of meiosis (Figure 4.13 A). In contrast, male germ cells showed no such pattern but rather an overall accumulation of fluorescent signal in the nucleus, suggesting that SCP3 protein is present, but not necessarily functional.

Taken together, expression of STRA8 and SCP3 in female germ cells is independent of 4E-BP1, suggesting entry into meiosis is not perturbed. In contrast, while male germ cells are negative for STRA8 as expected, very low signal of SCP3 can be observed in 4E-BP1$^{-/-}$ knockout tissues. These results still have to be confirmed in 4E-BP1$^{-/-}$4E-BP2$^{-/-}$ knockout germ cells.

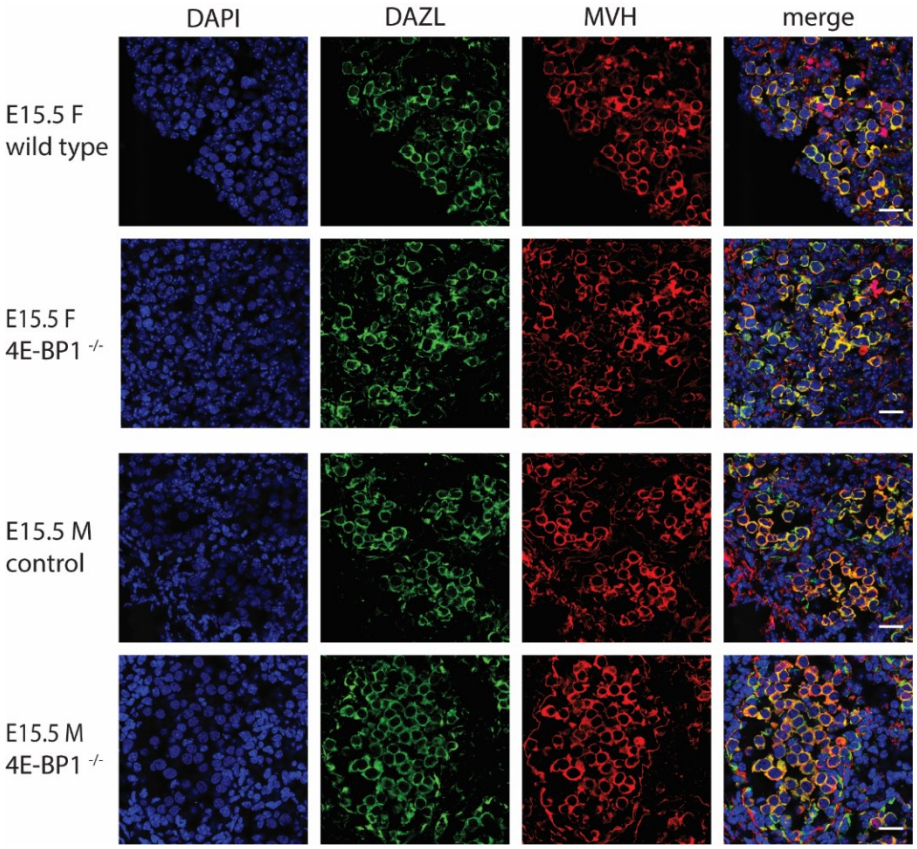

Figure 4.12: Expression of key germ cell proteins at E15.5 in control and global 4E-BP1$^{-/-}$ knockout germ cells.

Immunofluorescence stainings of female and male genital ridges at E15.5. Germ cells were stained for DAZL and mouse Vasa homologue (MVH), nuclei were stained with DAPI (blue). Representative images shown, n=1 (embryo per genotype), scale bar = 20µm; control = heterozygous tissue; Wild-type, 4E-BP1$^{-/+}$ heterozygous and 4E-BP1$^{-/-}$ knockout tissues were from littermates. Genotype was identified via PCR.

A

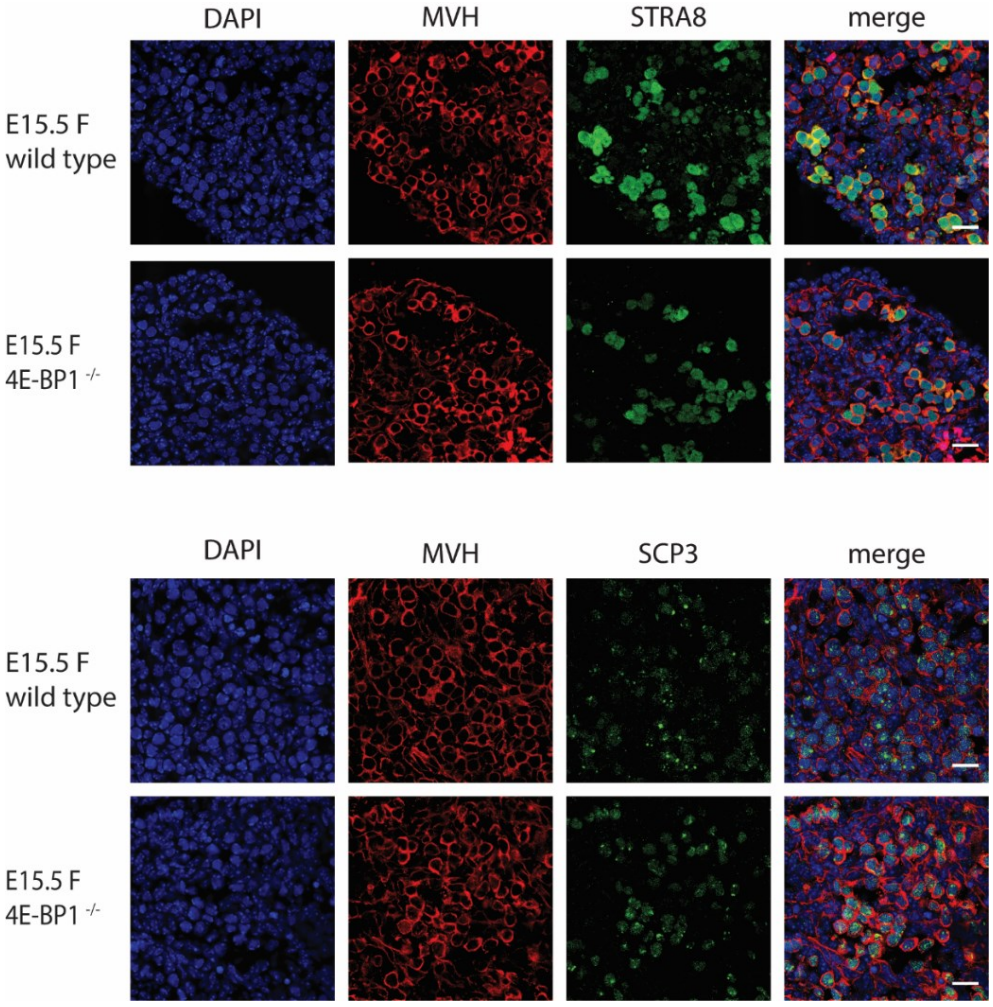
DAPI
MVH
STRA8
merge
E15.5 F wild type
E15.5 F 4E-BP1 -/-
DAPI
MVH
SCP3
merge
E15.5 F wild type
E15.5 F 4E-BP1 -/-

B

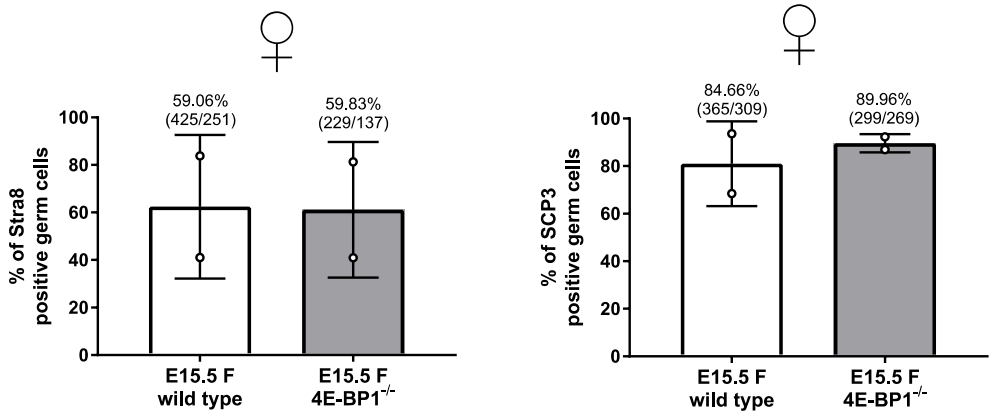
% of Stra8 positive germ cells
59.06% (425/251)
59.83% (229/137)
E15.5 F wild type
E15.5 F 4E-BP1-/-
% of SCP3 positive germ cells
84.66% (365/309)
89.96% (299/269)
E15.5 F wild type
E15.5 F 4E-BP1-/-

C

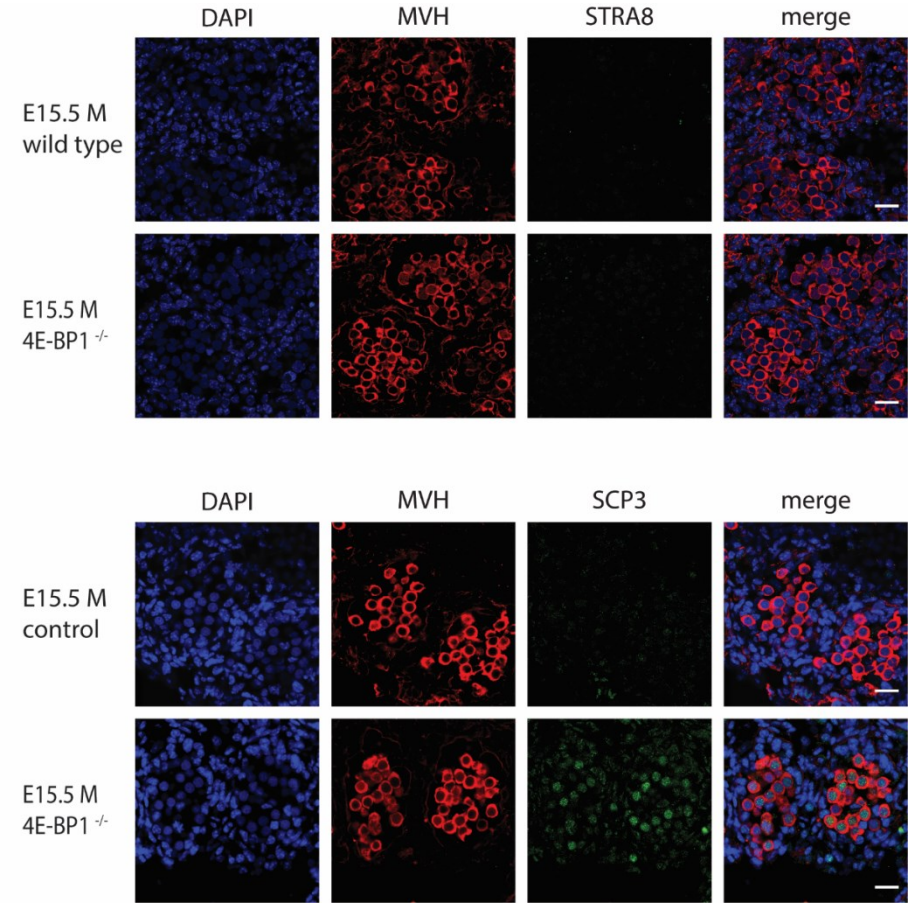

Figure 4.13: Expression of meiosis markers at E15.5 in wild-type and global 4E-BP1$^{-/-}$ knockout germ cells.

Immunofluorescence stainings of female and male genital ridges at E15.5. Germ cells were identified via MVH expression, nuclei were stained with DAPI (blue). **A** Expression of STRA8 and SCP3 in E15.5 female germ cells. Representative images shown, n= 2 (embryos per genotype), scale bar = 20µm **B** Quantification of STRA8 and SCP3 positive germ cells in immunofluorescence stainings of wild-type and 4E-BP1$^{-/-}$ knockout tissues (A). Average percentages of MVH positive cells which express either STRA8 or SCP3 is shown. Data points represent percentages of SSEA1 positive germ cells from independent experiments (n=2 embryos per genotype). (n/n) above each bar = total number of germ cells counted/SCP3^{+} or STRA8^{+} germ cells; error bars = SD; This is preliminary data and due to low n numbers, no statistical test has been performed. **C** Expression of STRA8 and SCP3 in E15.5 male germ cells, Representative images shown, n= 2 (embryos per genotype), scale bar = 20µm; control = heterozygous tissue; Wild-type, 4E-BP1$^{-/+}$ heterozygous and 4E-BP1$^{-/-}$ knockout tissues were littermates. Genotype was identified via PCR.

4.2.2.1.3 Characterisation of E10.5 4E-BP1 $^{-/-}$ knockout germ cells

Analysis of E13.5 and E15.5 germ cells lacking 4E-BP1 protein did not reveal a strong phenotype regarding tissue morphology, germ cell number and expression of analysed germ cell, pluripotency and meiosis markers (with a few exceptions).

The deletion of 4E-BP1 mimics active mTORC1-4E-BP1 signalling. 4E-BP1 is a translational repressor whose function is inhibited via phosphorylation through mTORC1 signalling, leading to initiation of translation. To exclude the possibility of an early change in mRNA translation, possibly leading to precocious protein expression, earlier embryonic stages were examined. At E10.5, primordial germ cells reach the bipotential genital ridge. Pluripotency factors are still highly expressed and expression of germ cell proteins DAZL and MVH is induced (Saitou and Yamaji 2012).

Wild-type and 4E-BP1$^{-/-}$ knockout genital ridges could not be distinguished based on size (observation only) or tissue morphology at E10.5 (Figure 4.14), in line with no differences observed at later stages. OCT4 was robustly expressed in wild-type and 4E-BP1$^{-/-}$ knockout germ cells and was used as a reliable germ cell marker (Figure 4.14). The majority of germ cells were positive for SSEA1 in wild-type and knockout tissues (Figure 4.14 A). In addition, most germ cells already expressed DAZL and MVH at high levels, with no apparent difference between wild-type and 4E-BP1$^{-/-}$ knockout tissues (Figure 4.14 B). Such strong expression at E10.5, especially of DAZL, is slightly surprising. MVH protein has been reported to be detected in some PGCs from E10.5 onwards (Toyooka et al. 2000). In contrast, *Dazl* transcript however has been reported to be first detected at E11.5 in wild-type mice on a pure C57BL/6 genetic background (Seligman and Page 1998). Given that this slight shift in timing is observed in wild-type and knockout germ cells, it is likely due to the mixed genetic background (129/BL6) of the 4E-BP1 colony. Further, possible early expression of meiosis genes STRA8 and SCP3 were tested. As expected, wild-type and knockout germ cells were negative for both meiosis markers (Figure 4.14 C).

Taken together, no obvious difference was observed between wild-type and knockout germ cells regarding pluripotency factors (OCT4, SSEA1), key germ cell proteins (DAZl, MVH) and meiosis markers (STRA8, SCP3). These observations suggest no shift in expression of key germ cell proteins at E10.5 upon deletion of 4E-BP1. However, further investigation using 4E-BP1$^{-/-}$4E-BP2$^{-/-}$ double knockout tissues is required.

A

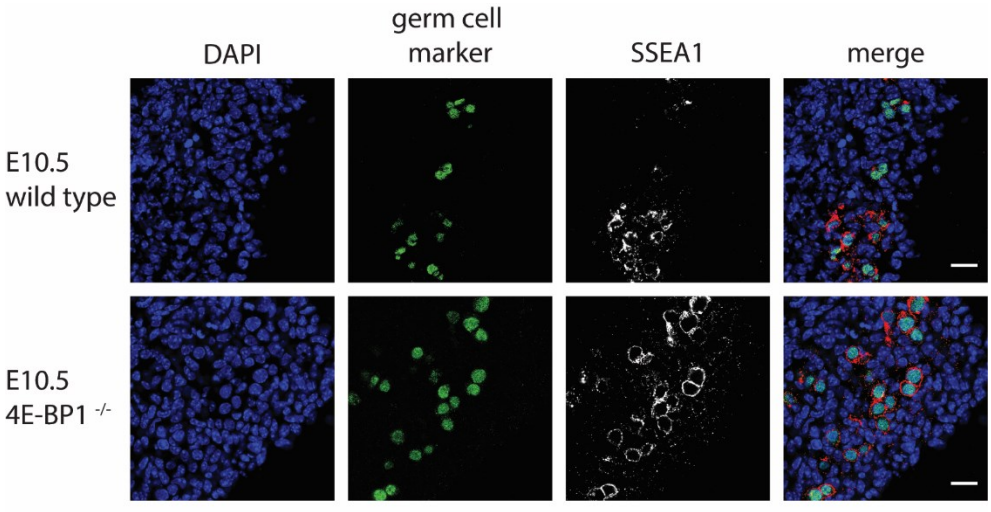
DAPI
germ cell marker
SSEA1
merge
E10.5 wild type
E10.5 4E-BP1 -/-

B

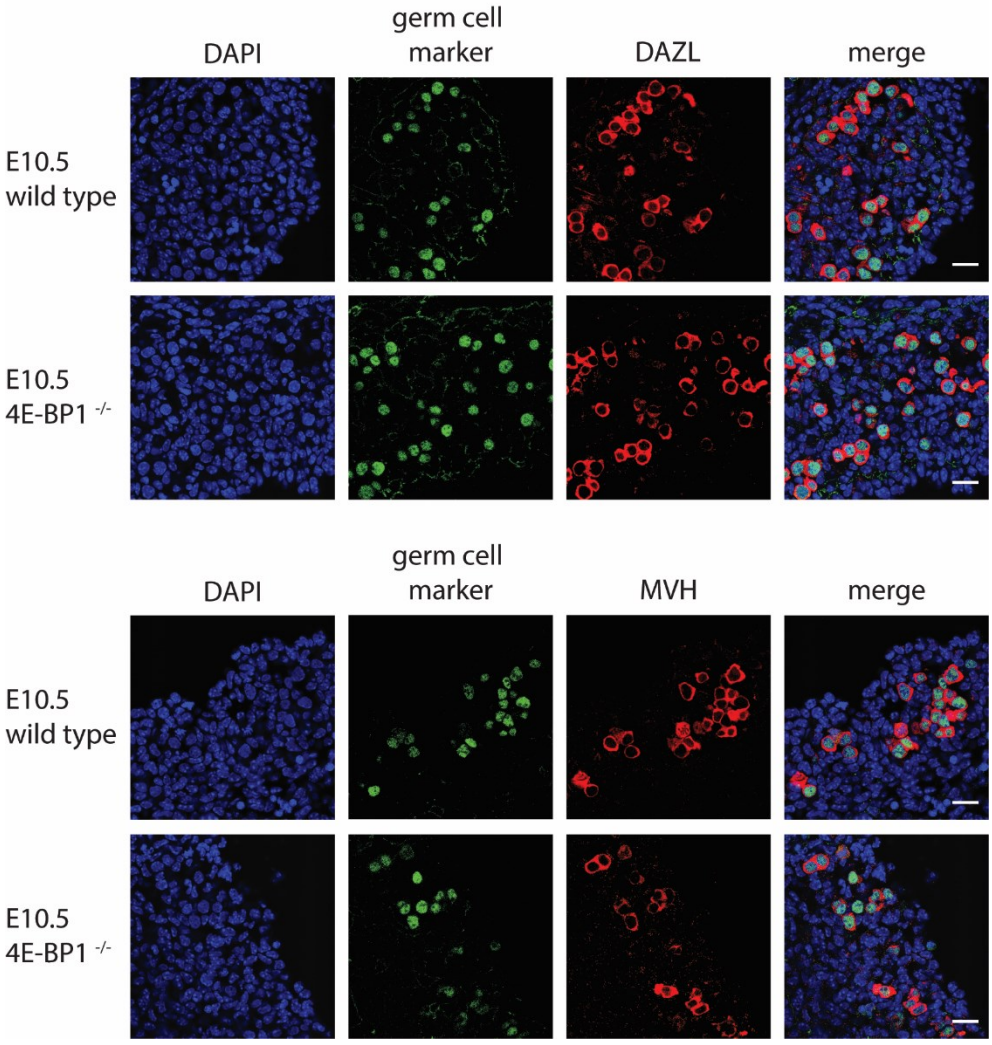
DAPI
germ cell marker
DAZL
merge
E10.5 wild type
E10.5 4E-BP1 -/-
DAPI
germ cell marker
MVH
merge
E10.5 wild type
E10.5 4E-BP1 -/-

C

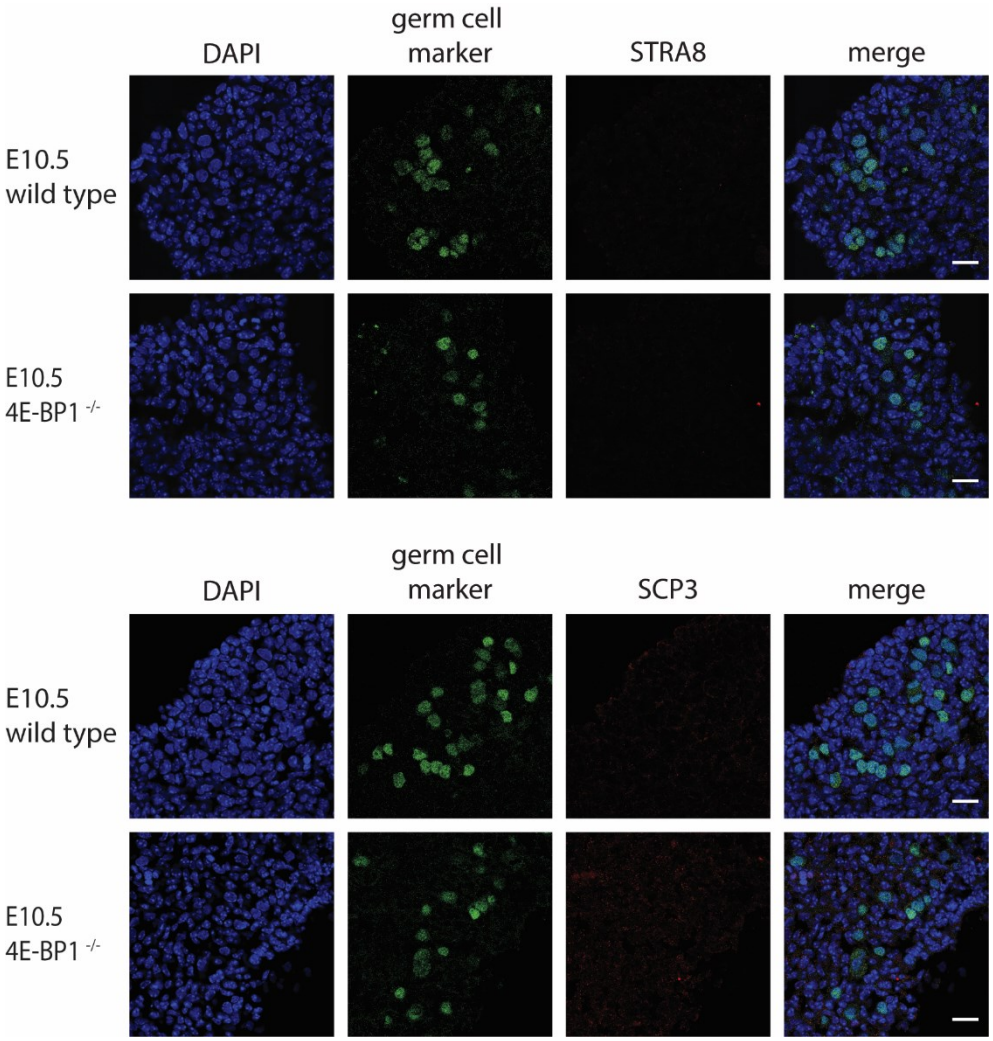

Figure 4.14: Expression of pluripotency factors and germ cell proteins at E10.5 in wild-type and global 4E-BP1$^{-/-}$ knockout germ cells.

Immunofluorescence stainings of bipotential genital ridges at E10.5. Germ cells were identified via OCT4 expression (germ cell marker), nuclei were stained with DAPI (blue). **A** Representative images of SSEA1 expression. n=1 (embryo per genotype), scale bar = 20µm; **B** Representative images of DAZL and MVH expression. n=2 (embryos per genotype), scale bar = 20µm; **C** Representative images of STRA8 and SCP3 expression. n=1 (embryo per genotype), scale bar = 20µm; Wild-type and 4E-BP1$^{-/-}$ knockout tissues were littermates. Genotype was identified via PCR.

4.2.2.2. Histological analysis of adult gonads lacking 4E-BPs

In order to further complement our data on foetal germ cells, 8 or 10 week adult wild-type and global 4E-BP1$^{-/-}$ single and 4E-BP1$^{-/-}$4E-BP2$^{-/-}$ double knockout gonads were collected for histological analysis. Adult gonads will reveal any alterations or impairment in germ cell development manifesting later during foetal or postnatal development.

In females, wild-type and 4E-BP1$^{-/-}$ knockout ovaries were of similar size (Figure 4.15 A). Haematoxylin and Eosin stained tissue sections revealed no apparent difference between genotypes. Examined ovaries contained follicles of all stages of development, including primordial follicles and antral follicles (arrows, Figure 4.15 A). Further, multiple corpora lutea were found in ovaries of both genotypes, indicating successful ovulation (*, Figure 4.15 A). In addition, tissue sections of 4E-BP1$^{-/-}$4E-BP2$^{-/-}$ double knockout ovaries also displayed similar morphology to wild-type control ovaries (Figure 4.15 B). Follicles at different stages could be detected, as well corpora lutea (Figure 4.15 B). Of note, exact numbers of follicles at different stages were not determined.

In males, wild-type and 4E-BP1$^{-/-}$ knockout testes were of similar size (Figure 4.16 A). Further, Haematoxylin stained 4E-BP1$^{-/-}$ knockout tissue sections appeared similar to control sections (Figure 4.16 A). Different seminiferous tubules containing different stages of male germ cells and Sertoli cells were observed. Seminiferous tubules with round immature spermatogonia in the basal lamina, followed by layers of spermatocytes in different stages and elongated spermatids with tails extending towards the lumen of the tubule could be observed (Figure 4.16 A), indicating successful spermatogenesis. In line with that, 4E-BP1$^{-/-}$ 4E-BP2$^{-/-}$ double knockout testis sections revealed no gross difference to wild-type control sections. (Figure 4.16 B). Of note, detailed staging of different tubules or sperm counts and analysis were not determined. However, 4E-BP1$^{-/-}$ knockout males were fertile and litter sizes appeared normal (observation only) (average litter size KO x WT breedings = 6.1 ± 0.95 SEM (n = 5 litters), average litter size HET x HET breedings = 7.16±0.92 SEM (n = 3 litters), Student's t-test, t=0.74, df=6, p=0.74).

Further, 4E-BP1$^{-/-}$4E-BP2$^{-/-}$ double knockout males and females were fertile and litter sizes appeared normal (observation only) (average litter size KO x KO breedings = 7.75 ± 0.83 SEM (n = 8 litters), average litter size WT x WT breedings = 5.429±0.86 SEM (n = 7 litters), Student's t-test, t=1.9, df=13, p=0.07).

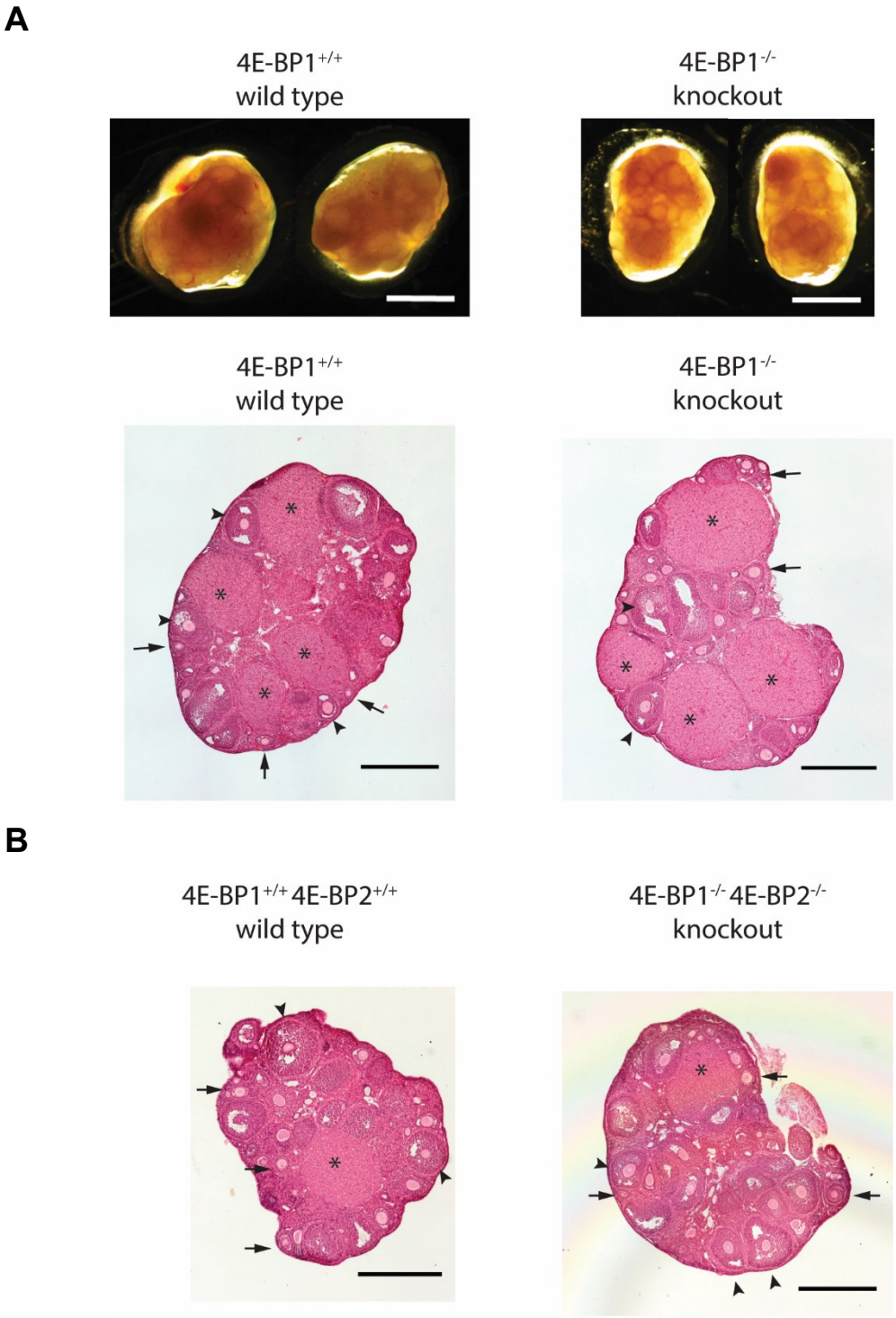

Figure 4.15: Histological analysis of 4E-BP1$^{-/-}$ single and 4E-BP1$^{-/-}$4E-BP2$^{-/-}$ double knockout adult ovaries.

A Wild-type and 4E-BP1$^{-/-}$ single knockout ovaries from littermates at 8 weeks. Representative images of whole ovaries shown, n=2 (mice per genotype), scale bar = 1mm; Representative images of Haematoxylin and Eosin stained sections of same ovaries. n=2 (mice per genotype), scale bar = 500µm, zoom = 10x, stitched image; **B** Haematoxylin and Eosin stained sections of wild-type and 4E-BP1$^{-/-}$4E-BP2$^{-/-}$ double knockout ovaries at 10 weeks. Control and double knockout ovaries are from separate litters. Representative images shown, n=2 (mice per genotype), scale bar = 500µm, zoom = 10x, stitched image; * denote corpus lutea, arrows point to secondary follicles, arrow heads depict antral follicles;

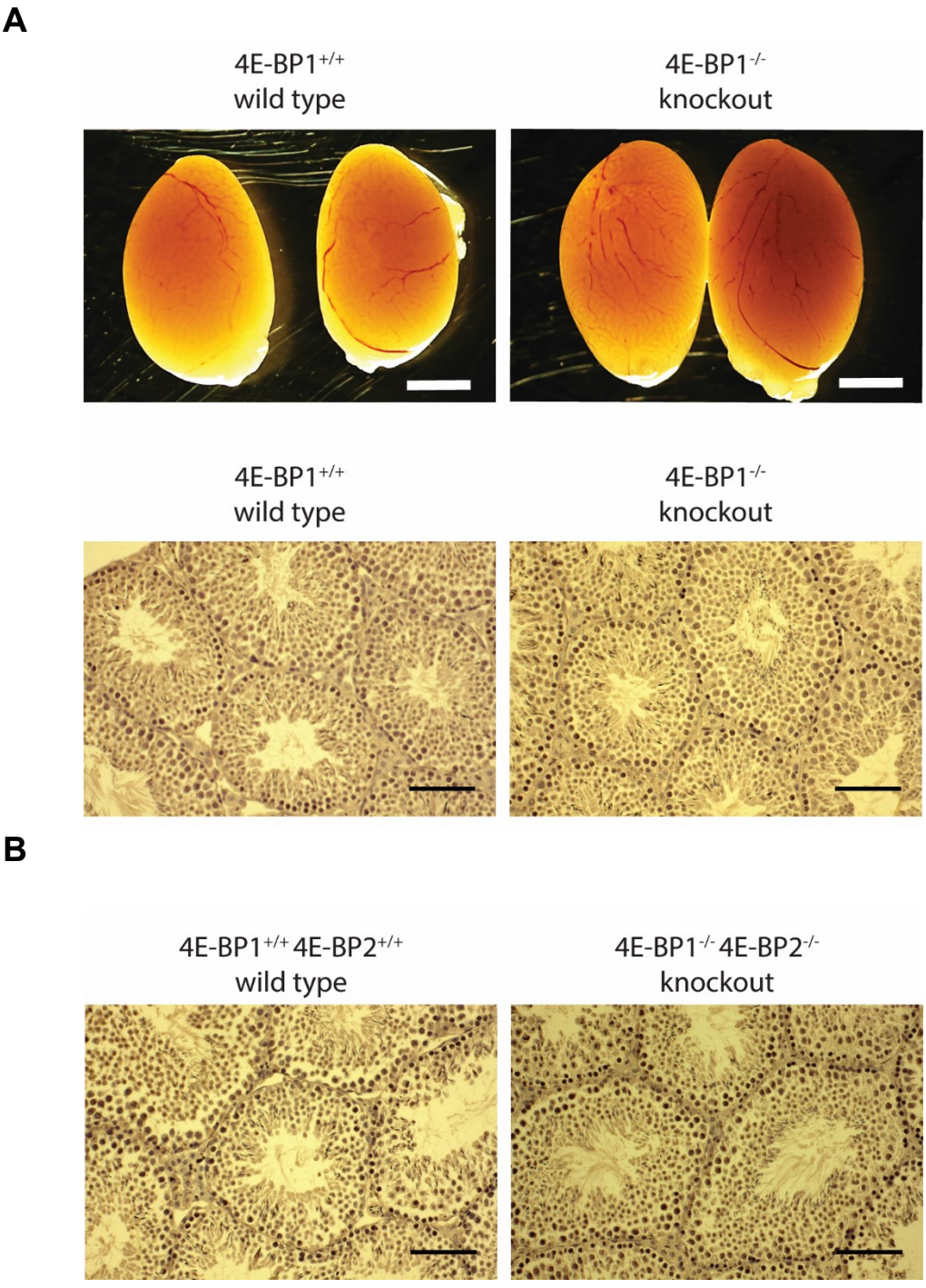

Figure 4.16: Histological analysis of 4E-BP1$^{-/-}$ single and 4E-BP1$^{-/-}$4E-BP2$^{-/-}$ double knockout adult testes.

A Wild-type and 4E-BP1$^{-/-}$ single knockout adult testes from littermates at 10 weeks. Representative images of whole testes shown**.** n=2 (mice per genotype), scale bar = 2mm; Representative images of Haematoxylin stained sections of same testes. n=2 (mice per genotype), scale bar = 80µm, zoom = 20x; **B** Haematoxylin stained sections of wild-type and 4E-BP1$^{-/-}$4E-BP2$^{-/-}$ double knockout testes. Wild-type control = 10 weeks, double knockout = 11 weeks. Control and double knockout testes are from separate litters. Representative images shown, n=2 (mice per genotype), scale bar = 80µm, zoom = 20x

4.3. Discussion

4.3.1. On the role of S6 kinases during primordial germ cell development

Overall, the deletion of S6 kinases did not result in a gross phenotype in the development of early mouse germ cells. Germ cell specification and overall migration to the genital ridge was not affected. Further, expression of the majority of analysed proteins was similar between wild-type and knockout germ cells.

At E13.5, an increased number of SSEA1 positive germ cells was observed in S6K1$^{-/-}$S6K2$^{-/-}$ knockout genital ridges compared to wild-type controls in both sexes, suggesting a possible delay in downregulation of this cell surface marker. In addition, at E15.5, female S6K1$^{-/-}$S6K2$^{-/-}$ double knockout germ cells showed decreased levels of SCP3 staining compared to wild-type germ cells, suggesting a possible delay in SCP3 upregulation.

The described phenotype of S6K1$^{-/-}$S6K2$^{-/-}$ embryos is a growth retardation, most pronounced at E12.5 with up to 30% difference in weight (Pende et al. 2004). At the overall tissue level, a possible developmental delay and potential reduction in germ cell number (observation only) was observed in S6K1$^{-/-}$S6K2$^{-/-}$ knockout genital ridges, which was more pronounced in females compared to males. It is likely that the growth retardation causes the observed possible delay in overall genital ridge development. Subsequently, the observed phenotype in germ cells (delayed SSEA1 downregulation and SCP3 upregulation) could be (partly) caused by such an overall genital ridge developmental delay. Of note, increased SSEA1 staining was also observed in preliminary data of S6K1$^{-/-}$ single knockout genital ridges which exhibit no apparent developmental delay between wild-type and knockout tissues. These preliminary observations could indicate that in male germ cells, SSEA1 upregulation might be germ cell autonomous. To tell apart which observed phenotypes are germ cell autonomous and which are non – cell autonomous, further work using germ cell specific knockout systems is needed.

Analysis of adult gonads revealed no obvious difference between wild-type and S6K1$^{-/-}$ single or S6K1$^{-/-}$S6K2$^{-/-}$ double knockout tissues. However, quantification of follicles at different stages or detailed analysis of different seminiferous tubules and sperm counts was not carried out. Therefore, it is possible that a less obvious phenotype is present in adult gonads, which was not detected. In mouse ovaries, repressed S6K1 signalling has been implicated in the maintenance of the primordial follicle pool (see 1.4.4.1, p. 64) (Adhikari et

al. 2009, 2010, Reddy et al. 2008, 2009). Activated S6K1-S6 signalling was suggested to trigger primordial follicle activation (Adhikari et al. 2010). It would be interesting to determine the number of primordial follicles and activated follicles in S6K1$^{-/-}$ single and S6K1$^{-/-}$S6K2$^{-/-}$ double knockout ovaries to see if they differ from wild-type ovaries.

It should be mentioned that S6K1$^{-/-}$ knockout mice were fertile with no apparent abnormalities (observation only), in line with published observations (Shima et al. 1998; Pende et al. 2000). In the original paper describing the S6K1$^{-/-}$S6K2$^{-/-}$ knockout mouse, it is noted that the very few viable double knockout mice were fertile, however, litter sizes were small with a high incidence of perinatal lethality (Pende et al. 2004). Whether decreased fertility underlies (partly) the decreased litter size in addition to the severe phenotype is not known.

Taken together, the observed differences are likely (in part) due to an overall delay in development caused by growth retardation upon deletion of S6K1$^{-/-}$S6K2$^{-/-}$. The lack of a gross phenotype in S6K1$^{-/-}$S6K2$^{-/-}$ double knockout embryonic germ cells and adult gonads suggests that S6 kinases are not essential for germ cell development. To confirm these observations, analysis of additional biological replicates, in combination with detailed quantification of germ cell numbers, is needed. However, to disentangle cell autonomous from non-cell autonomous effects of S6 kinases, analyses of germ cell specific knockout genital ridges are necessary. Only then, a final conclusion on the role of S6 kinases during germ cell development can be obtained.

4.3.2. On the role of 4E-BPs during primordial germ cell development

4.3.2.1. Deletion of 4E-BP1 to mimic active mTORC1-4E-BP1 signalling

Female germ cells lacking 4E-BP1, mimicking active mTOR-4E-BP1 signalling, showed no obvious difference compared to wild-type germ cells regarding genital ridge morphology, germ cell number (by eye), expression of germ cell genes (DAZL, MVH) and pluripotency markers (OCT4, SOX2, SSEA1) and expression of meiosis markers (SCP3, STRA8).

In contrast, in male 4E-BP1$^{-/-}$ knockout tissues, an increase in SSEA1 positive germ cells was observed at E13.5, further confirmed in 4E-BP1$^{-/-}$4E-BP2$^{-/-}$ double knockout genital ridges. In addition, very low levels of SCP3 were observed at E15.5 in male 4E-BP1$^{-/-}$ knockout germ cells.

4.3.2.1.1 SSEA1 – a marker for pluripotent cells

The observation that only a subset of PGCs stained positive for SSEA1 at E13.5 is in line with previous observations that SSEA1 expression is downregulated from E12.5/E13.5 as cells differentiate more (Fox et al. 1981). Intriguingly, male 4E-BP1 knockout genital ridges have a higher percentage of SSEA1 positive germ cells at E13.5 compared to wild-type genital ridges. By E15.5, SSEA1 staining was absent though, in line with published observations (Fox et al. 1981). Given the fact that SSEA1 is downregulated by PGCs as differentiation progresses, the observed slightly delayed SSEA1 downregulation points towards a possible delay in overall differentiation.

SSEA1 is an established marker for undifferentiated PGCs, embryonic stem cells and embryonic carcinoma cells. The antigenic epitope of SSEA1 is a carbohydrate structure called LewisX (Gooi et al. 1981), which is present on glycoproteins, proteoglycans and glycolipids on the cell surface (Yanagisawa 2011). Many cells in the early embryo express SSEA1, starting from the 8-cell stage onwards up to the blastocyst stage, when SSEA1 expression is restricted to the ICM. Cultured mouse embryonic stem cells are positive for SSEA1 and expression decreases upon differentiation. Of note, expression of SSEA1 is heterogeneous - only about 51.5% of undifferentiated ESCs are SSEA1 positive to start with, in line with observations in vivo (Cui et al. 2004). The reason for some cells or embryos being completely negative are not clear (Solter and Knowles 1978).

Although SSEA1 is an established marker for undifferentiated PGCs and ESCs, the biological relevance of the cell surface antigen is less clear. Proposed functions of SSEA1 are in cell-cell interactions such as adhesion and compaction of embryonic carcinoma cells and of mouse embryos at the morula stage (Eggens et al. 1989; Shade et al. 2015). However, ablation of SSEA1 via deletion of the gene encoding the responsible enzyme *Fut9* revealed that SSEA1 is not essential during embryonic development - *Fut9*$^{-/-}$ knockout mice developed normally (Kudo et al. 2004).

In germ cells, SSEA1 is expressed from specification until around E13.5, when it starts being downregulated. E13.5 genital ridges express *Fut9*, however global deletion of *Fut9* did not result in a germ cell phenotype or reduced fertility (Kudo et al. 2004).

In summary, the biological significance of the observed slightly delayed SSEA1 downregulation in PGCs *in vivo* is likely to be small. In line with that, no difference was observed in the expression of pluripotency factors (SOX2 and OCT4) and germ cell protein

expression (MVH and DAZL). It could be that the possible delay in differentiation plays a role during *in vitro* culture. Delayed differentiation could result in increased ability or efficiency of 4E-BP1$^{-/-}$ knockout primordial germ cells to convert to pluripotent embryonic germ cells, for instance. However, to this point this is just a hypothesis and requires the actual experiments to be carried out.

Of note, increased SSEA1 signal in 4E-BP1$^{-/-}$knockout germ cells can be the consequence of a cell autonomous mechanism leading to more SSEA1 being present at the cell surface (due to increased production or delayed conversion/downregulation, for instance). Alternatively, global loss of 4E-BP1 might change the surrounding somatic environment, which could cause delayed differentiation. To disentangle cell autonomous and non-cell autonomous effects of 4E-BP1 deletion, germ cell specific knockouts should be analysed.

4.3.2.1.2 SCP3 expression in male E15.5 4E-BP1$^{-/-}$ germ cells

Intriguingly, male 4E-BP1$^{-/-}$ germ cells stained weakly positive for SCP3 at E15.5. The synaptonemal complex protein 3 (SCP3) is part of the synaptonemal complex, a protein structure forming between homologous chromosome pairs in meiotic cells, which is essential for pairing, synapsis and subsequent recombination (Fraune et al. 2012).

Both female and male germ cells upregulate *Scp3* gene expression at E12.5 (Chuma and Nakatsuji 2001). At the protein level, fluorescent dots of SCP3 signal is detected in male and female germ cells at E13.5 (Di Carlo, Travia, and De Felici 2000). In female germ cells, as meiotic prophase I progresses, SCP3 staining pattern changes to fine, elongated fibers reflecting the developing alignment of homologous chromosomes starting during zygotene. In males, however, meiosis is inhibited and SCP3 downregulated, with fluorescent dots barely visible at E14.5 and absent at E15.5 (Di Carlo, Travia, and De Felici 2000).

In male 4E-BP1$^{-/-}$ germ cells, the staining pattern was weak and dispersed throughout the nucleus with a clear absence of fluorescent foci or elongated fibers. In combination with the lack of STRA8 expression, the observed SCP3 signal is likely due to a delay in SCP3 downregulation, rather than male 4E-BP1$^{-/-}$ germ cells entering meiosis. It would be interesting to explore SCP3 expression dynamics at later time points to confirm complete downregulation. Further, analysis of 4E-BP1$^{-/-}$4E-BP2$^{-/-}$ double knockout germ cells would reveal a potentially stronger phenotype in case any compensatory mechanisms mediated by 4E-BP2 are present in 4E-BP1$^{-/-}$ knockout germ cells.

It could be that active 4E-BP1 is (partly) required to repress *Scp3* mRNA translation directly or indirectly in embryonic male germ cells, leading to downregulation of SCP3 protein levels. In fact, translational regulation of SCP3 has been described in male germ cells:

During sexual differentiation, male embryonic germ cells start to express the RNA binding protein NANOS2 from E13.5 onwards (A. Suzuki and Saga 2008). NANOS2 promotes RNA degradation of target mRNAs via binding to the CCR4-NOT deadenylation complex (A. Suzuki et al. 2010, 2012). In *Nanos2* knockout mice, embryonic male germ cells abnormally enter meiosis with a clear upregulation of SCP3 at E15.5 (A. Suzuki and Saga 2008). NANOS2 has been shown to bind *Scp3* mRNA *in vivo* in E15.5 genital ridges based on immunoprecipitation assays. Deletion of *Nanos2* leads to upregulation of *Scp3* mRNAs. The authors suggest that NANOS2 either indirectly represses transcription of the *Scp3* gene or directly represses translation of the *Scp3* mRNA possibly via deadenylation and subsequent mRNA degradation (A. Suzuki et al. 2010).

In adult testis, the RNA binding protein DAZL was shown to bind *Scp3* mRNA based on immunoprecipitation assays (Reynolds et al. 2005). Further, SCP3 protein levels in *Dazl* knockout germ cells was reduced (Reynolds et al. 2007). DAZL was shown to bind to and stimulate S*cp3* mRNA translation in vitro (Reynolds et al. 2007). Hence, it was suggested that DAZL is important for enhancing Sycp3 mRNA translation, rather than being essential for translation (Reynolds et al. 2007). Of note, binding of DAZL to the *Scp3* mRNA was attributed to the presence of a 3'UTR consensus sequence (U2–10[G/C]U2–10) (Reynolds et al. 2005, 2007).

Whether and to what extent the translational repressor 4E-BP1 is repressing and subsequently downregulating SCP3 in male germ cells requires further work. So far, 4E-BP1 has been described to mainly regulate translation of mRNAs with characteristic 5'UTR motifs (see 1.3.3.1, p. 56). As a starting point, using the existing RNA Seq data of wild-type primordial germ cells, it would be interesting to check if genes involved in gametogenesis, such as SCP3, display any of those motifs.

4.3.2.1.3 Summary of 4E-BP1$^{-/-}$ germ cell analysis

Overall, deletion of 4E-BP1 caused delayed SSEA1 and SCP3 downregulation in male germ cells at 13.5 and E15.5 respectively. In comparison, female germ cells lacking 4E-BP1 did not differ from wild-type controls.

Detecting a phenotype only in male 4E-BP1$^{-/-}$ germ cells is interesting for several reasons. First, analysis of wild-type male germ cells revealed lower total and phosphorylated 4E-BP1 levels compared to female wild-type germ cells. It could be that active 4E-BP1 plays a role specifically in male germ cells, potentially via inhibiting translation of certain mRNAs. To this point this remains a hypothesis though and requires further work.

Histological analysis of adult gonads revealed no gross difference between wild-type and 4E-BP1$^{-/-}$ single or 4E-BP1$^{-/-}$4E-BP2$^{-/-}$ double knockout tissues. It is possible that a less obvious phenotype was not detected since detailed quantification of follicles or seminiferous tubule staging was not performed. 4E-BP1$^{-/-}$ single (males) or 4E-BP1$^{-/-}$4E-BP2$^{-/-}$ double knockout mice were fertile though and litter size appeared normal (observation only).

Taken together, deletion of 4E-BP1 did not reveal a strong phenotype in male or female foetal germ cells and adult gonads, suggesting that 4E-binding proteins are not essential for germ cell development. To confirm observations in male germ cells, analysis of additional biological replicates of 4E-BP1$^{-/-}$4E-BP2$^{-/-}$ double knockout genital ridges at E15.5 is needed. However, to disentangle cell autonomous from non-cell autonomous effects of 4E-binding proteins, analysis of germ cell specific knockout genital ridges is necessary.

Further, it would be interesting to test germ cell development in the absence of mTORC1-4E-BP1 signalling. For this, a conditional transgenic mouse model overexpressing a non-phosphorylatable version of 4E-BP1 (upon Cre excision of a STOP codon) can be used (Prof Wither's group). 4E-BP1 overexpression will lead to exogenous levels of active 4E-BP1 protein which can bind and sequester away eIF4E, inhibiting translation. Constitutively active 4E-BP1 mimics the absence of mTOR-4E-BP1 signalling *in vivo*.

4.3.3. Some general comments

In summary, analysis of global S6K1$^{-/-}$ single and S6K1$^{-/-}$S6K2$^{-/-}$ double knockout genital ridges as well as global 4E-BP1$^{-/-}$ single and 4E-BP1$^{-/-}$4E-BP2$^{-/-}$ double knockout genital ridges did not reveal a strong phenotype in germ cell development. Based on the distinct 4E-BP1 expression pattern in wild-type primordial germ cells with signalling peaks at E11.5 and E13.5, it seemed surprising that only a very mild phenotype was detected in global 4E-BP1$^{-/-}$ or 4E-BP1$^{-/-}$4E-BP2$^{-/-}$ double knockout tissues. Overall, these data suggest that downstream mTOR effectors S6 kinases and 4E-binding proteins are not essential during germ cell development.

The used immunofluorescence screening approach of global knockout lines has some limitations, some have already been briefly mentioned.

Firstly, the use of global knockout mouse models leaves the question open whether any observations are germ cell autonomous or non-cell autonomous. In wild-type male germ cells, for instance, total 4E-BP1 signal is enriched in surrounding somatic cells at E13.4 and E14.5 and comparably low in germ cells at E14.5. Whether described observations in 4E-BP1$^{-/-}$ germ cells are caused by a secondary effect due to 4E-BP1 loss in surrounding somatic cells (especially at E15.5) is not known. Further work analysing germ cell specific 4E-BP1$^{-/-}$ knockout genital ridges is required.

Secondly, it should be stressed that the described genetic phenotypes are inferred from low n numbers (maximum of 3 embryos analysed, mostly 2 or 1 embryos per genotype) due to time constraints. Although litter mate controls were used whenever possible, in the case of double mutant lines (S6K1/S6K2 and 4E-BP1/4E-BP2) wild-type and knockout tissue was derive from different litters. Hence, biological variation between litters caused by, for example, developmental stage (which can differ up to 12h from the time of the plug) requires analysis of several embryos to infer robust conclusions. More importantly, low n numbers can be a limiting factor regarding genetic penetrance of a phenotype. Penetrance is a measure of the frequency of affected mice (displaying a phenotype) among carriers of the mutation (Sanford et al. 2001). Genetic background is known to affect penetrance of a phenotype, with a mixed background increasing variability due to incomplete penetrance, while congenic strains usually have a more consistent phenotype (Sanford et al. 2001; Doetschman 2009). Hence, it cannot be excluded that a more severe phenotype has been missed due to the combination of a mixed genetic background and low n numbers analysed.

Thirdly, there are limitations regarding the immunofluorescence-based approach. Antibody binding can be influenced by differences in antigen accessibility between wild-type and knockout tissues, due to putative differences in post-translational modifications or the target protein being part of different protein complexes (Saper 2009). Further, only a number of specific germ cell proteins at certain time points were checked. Absolute expression levels, as well as embryonic gonadal germ cell number was not determined. Also, the experimental design assumes random distribution of germ cell number or stage of development. Although by eye no obvious spatial bias regarding the staining pattern was detected (data not shown), acquired images and quantification thereof originated from random locations within sections. It is possible that a small phenotype was missed, such as slightly reduced germ cell number/protein levels or a spatial bias thereof. However, given the fact that all analysed lines are fertile as based on previous publications and our own observations and the lack of obvious abnormalities, any possible misses are likely to be small.

More importantly, apart from technical limitations, there are several other reasons for a weak phenotype which should be mentioned:

Compensatory mechanisms. Signalling pathways are highly complex with lots of cross-talk between different pathways and high redundancy. Compensatory signalling has been reported within each mTOR effector protein family (S6 kinases versus 4E-binding proteins) as well as between protein families. The combined deletion of S6K1 and S6K2 results in a more severe phenotype with perinatal lethality compared to the single deletion of either S6K1 or S6K2 (Pende et al. 2004), suggesting some redundant functions between S6K1 and S6K2. In line with that, in $S6K1^{-/-}$ global knockout mice, S6K2 mRNA was found to be upregulated (Shima et al. 1998). Further, in $4E\text{-}BP1^{-/-}4E\text{-}BP2^{-/-}$ double knockout mice, an over activation of S6K1 signalling was observed, possibly contributing to the observed insulin resistant phenotype via feedback loop signalling (Le Bacquer et al. 2007). At an even higher level, signalling pathways apart from mTOR and its effectors have to be considered as well. For example, in $S6K1^{-/-}S6K2^{-/-}$ double knockout mice, the downstream target S6 was still found to be phosphorylated via the MAPK signalling pathway, demonstrating that several signalling pathways can affect downstream inputs and redundancy between them is likely (Pende et al. 2004).

Based on these observations, it is probably safe to assume that some compensatory signalling is at play in analysed global knockout genital ridges. It would be interesting to know how 4E-BP1 signalling changes in $S6K1^{-/-}$ single or $S6K1^{-/-}S6K2^{-/-}$ double knockout germ cells and

vice versa. Combined deletion of 4E-BPs and S6 kinases would allow to study the role of mTOR signalling via downstream translational effectors. Whether these mice would be viable though is not certain.

Genetic background of mouse lines. Upon deletion of a gene, the severity of a phenotype can vary depending on the genetic background of the used mouse model (Montagutelli 2000). In fact, different phenotypes were reported upon deletion of 4E-BP1 on different genetic backgrounds. The first published study on 4E-BP1$^{-/-}$ global knockout mice on a mixed background (129/SvJx C57BL6/J) described a 10% body weight decrease in males and no apparent phenotype in females (Blackshear et al. 1997). In contrast, 4E-BP1$^{-/-}$ global knockout mice on a different mixed background (129/SvJxBalb/c) showed reduced adipose tissue and hypoglycaemia, in addition males had an increased metabolic rate (Tsukiyama-Kohara et al. 2001). Subsequent analysis of inbred BALB/c mice lacking 4E-BP1 and 4E-BP2 (after backcrossing of 5-10 times) revealed increased body weight and fat accumulation compared to wild-type mice (Le Bacquer et al. 2007). On the contrary, deletion of 4E-BP1 or 4E-BP2 in a C57BL6/J background has the opposite effect, a lean phenotype (Le Bacquer et al. 2007; Blackshear et al. 1997).

The 4E-BP1 line used in this thesis was maintained on a mixed background (C57Bl6/J x 129/SvJ) with outcrossing to wild-type C57Bl6/J or 129/SvJ mice every second generation. 4E-BP1 single knockout mice on a pure C57Bl6 background were not viable (Silvia Pedroni, personal communication). Subsequent metabolic analysis of 4E-BP1$^{-/-}$ knockout mice on a mixed genetic background revealed no apparent metabolic phenotype (weight, insulin levels, fat tissue) (Silvia Pedroni, personal communication) in contrast to observations by Tsukiyama-Kohara and collegues (Tsukiyama-Kohara et al. 2001).

Hence, the used mixed genetic background might contribute to the very weak phenotype observed in 4E-BP1$^{-/-}$ germ cells, especially when considering the possible effect on genetic penetrance and few analysed embryos. Regardless of genetic background though, all knockout lines were reported to be fertile, no detailed analysis were performed though (Blackshear et al. 1997; Tsukiyama-Kohara et al. 2001; Banko et al. 2005).

4.4. Conclusion – Functional validation of mTOR effectors

In this chapter, global knockout genital ridges and adult gonads were analysed to determine the biological function of S6 kinases and 4E-binding proteins during germ cell development. To our surprise, overall no obvious phenotype was found. The described results, in combination with the existing literature, currently suggest a non-essential role of S6 kinase signalling or 4E-binding protein signalling in germ cells. However, possible compensatory mechanisms, genetic background effects, and cell autonomous versus non-cell autonomous causes cannot be excluded or distinguished at this point. Future work involving analysis of additional biological replicates of global knockout lines can confirm some observations and shed light on compensatory mechanisms at play. Further, analysis of germ cells which lack mTORC1-4E-BP1 signalling will reveal more information about the role of active 4E-BP1 protein during germ cell development. However, going forward, moving to a germ cell specific knockout system will allow to remove some of the described confounding factors. In the next chapter, the generation of a transgenic mouse model is described, representing a new efficient tool to achieve gene deletion specifically in primordial germ cells.

5. Chapter 5 – Development of a new *Prdm1-iCre* mouse line.

5.1. Introduction

5.1.1. Cre mouse lines available for germ cell specific knockouts

In the past 18 years, several transgenic mouse Cre lines have been generated to achieve germ cell specific gene deletion using the Cre-*loxP* system (Sauer and Henderson 1988; H. Gu et al. 1994). All these lines differ in the timing of Cre expression, the overall Cre recombination pattern and in the Cre recombination efficiency. The advantages and disadvantages of each line have to be carefully considered in order to choose the most suitable one for answering a specific biological question. In order to analyse possible biological functions of mTOR signalling during primordial germ cell development, germ cell specific gene deletion has to be achieved as early as possible and at very high efficiency during PGC development.

The first reported germ line specific Cre line was the *Tnap-Cre* line (Lomelí et al. 2000). Tissue nonspecific alkaline phosphatase (TNAP) is routinely used to identify germ cells from E7.5 onwards (Ginsburg, Snow, and McLaren 1990). *Tnap-Cre* mice were generated via inserting Cre recombinase between exon 6 and 7 of the endogenous *Tnap* gene using homologous recombination (Lomelí et al. 2000). Using Z/AP reporter mice, Cre expression and recombination was first detected at 9.5-10.5, at which point signal was specific to PGCs. At E13.5, recombination efficiency in germ cells was about 60% (Lomelí et al. 2000). Recombination was also detected in the placenta, the neural tube and the intestine at E13.5, in line with the wide expression pattern of endogenous TNAP during embryonic development (MacGregor, Zambrowicz, and Soriano 1995). Given the suboptimal recombination efficiency of only 60% in combination with a deletion only from E9.5 onwards, the *Tnap-Cre* line was not a good candidate to use in this project.

Another available germline Cre-driver line is the *Prdm1-Cre* line (Ohinata et al. 2005). *Prdm1* (or *Blimp1*) is expressed in PGC progenitor cells from E6.25 onwards and is essential for PGC specification. In primordial germ cells, *Prdm1* expression is maintained until about E13.5 (D. H. Chang and Calame 2002; Ohinata et al. 2005). *Prdm1-Cre* mice exhibit Cre expression and recombination at E7.8 in 55%-76% of PGCs, as visualized using the ROSA26-EGFP reporter strain (Ohinata et al. 2005). At E12.5, recombination efficiency is 99.23% using the R26R-EYFP reporter strain (Hirota et al. 2011). Of note, recombination is not restricted to PGCs, in line with the observed expression pattern of endogenous PRDM1 (or BLIMP1) (D. H. Chang and Calame 2002; Robertson et al. 2007; Vincent et al. 2005).

Last but not least, there is also a drug inducible transgenic Cre line under the control of *Stella* regulatory elements (Hirota et al. 2011). *Stella* (also *Dpp3* or *Pgc7*) is highly expressed in preimplantation embryos, oocytes and germ cells from E7.5 onwards until E14.5 in females and at E15.5 in males (Sato et al. 2002; Saitou, Barton, and Surani 2002). The *Dpp3* – MERP transgene consists of Cre recombinase fused to the ligand-binding domains of murine estrogen receptor (MER). In addition, the C-terminus contains a degradation signal (PEST sequence, sequence rich in proline (P), glutamic acid (E), serine (S), and threonine (T)) (Hirota et al. 2011). Intraperitoneal injections of 4-OHT result in the translocation of expressed Cre recombinase (MCM-P) to the nucleus, allowing recombination and floxed allele deletion at specific time points (Hirota et al. 2011). Using the R26R-EYFP reporter strain, recombination was detected as early as E7.5, and recombination efficiency in germ cells was about 80% at E12.5 when 4-OHT was administered at E9.5. In addition, recombination events were highly specific to PGCs (Hirota et al. 2011).

The high specificity and relatively good recombination efficiency make this line a powerful tool. However, the fact that Cre translocation depends on the presence of 4-OHT can have some disadvantages. Various tested 4-OHT concentrations have different recombination efficiencies and high 4-OHT concentrations can lead to developmental abnormalities in some embryos (~30%) (Hirota et al. 2011). Further, batch variations of 4-OHT can introduce variability. Also, no litter mate controls are possible in this system, as negative controls come from separate female mice. Subsequently, the staging of the embryos has to be very carefully determined. The day a plug is found is usually defined as E0.5, however, actual fertilization times can differ up to 12 hours.

Two additional germ cell specific Cre driver lines exist (*Nanos3-Cre* and *Vasa-Cre*), however both lines are not good candidates to use in this study: The *Nanos3-Cre* line exhibits recombination in migrating PGCs from 7.75 onwards, however, recombination efficiency is very low, estimated between 11% - 25% at E12.5 (H. Suzuki et al. 2008). The *Vasa-Cre* line has a higher recombination efficiency of 90% at E18.5, however, first recombination is detected only from E15.5 onwards (Gallardo et al. 2007).

Taken together, the *Prdm1-Cre* and *Dppa3* – MERP transgenic line are the best candidates to achieve early and robust deletion. Both lines achieve very early recombination, first detected around E7.5. Although Cre expression is highly specific to germ cells in the *Dppa3* – MERP line, the overall deletion efficiency (80% at E12.5) is not as high as the observed deletion efficiency in *Prdm1-Cre* mice (99% at E12.5). In addition, the *Prdm1-Cre* line reduces

variability as no 4-OHT injections are needed and littermate controls can be obtained. These observations make the *Prdm1-Cre* driver line ideal for studying the role of mTOR signalling during primordial germ cell development.

5.1.2. Existing *Prdm1-iCre* mouse line

The existing *Prdm1-Cre* transgenic line was generated using a modified bacterial artificial chromosome (BAC) transgene. The first and second exon of *Blimp1* were replaced with the Cre sequence (Ohinata et al. 2005).

One major technical disadvantage of the *Prdm1-Cre* line is that *Prdm1-Cre* mice have a very small litter size. This was studied in detail by Mikedis and colleagues via breeding studies of congenic and outbred *Prdm1-Cre* lines over 16 weeks (Mikedis and Downs 2017). The average litter size of congenic heterozygous *Prdm1-Cre* breeding pairs was about 2.8 pups per litter. The outbred heterozygous *Prdm1-Cre* breeding pairs had a slightly bigger litter size of about 3.9 pups per litter. In each litter, Cre positive and Cre negative pups were found at the expected Mendelian ratio (1:1) (Mikedis and Downs 2017). In contrast, control breeding couples of the *ROSA26-GFP* reporter line produced larger litters of about 6.3 pups per litter (Mikedis and Downs 2017). In line with these observations, litter sizes of males heterozygous for the *Prdm1-Cre* transgene breeding with homozygous *ROSA26-GFP* reporter females consisted of about 2.6 living conceptuses and about 3.7 resorptions per litter at E7.5-E9.0. Mendelian ratios of Cre positive and Cre negative conceptuses were as expected (1:1). In addition, no gross morphological abnormalities were detected, suggesting the few recovered embryos develop normally (Mikedis and Downs 2017).

Taken together, the similarity of small litter sizes between breeding couples of (inbred *Prdm1-Cre* line) and breeding couples of (Rosa26-GFP *x Prdm1-Cre)* indicate that litter size is associated with the *Prdm1-Cre* transgene. Further, the observation that litter sizes between E7.5-E9.5 (Rosa26-GFP *x Prdm1-Cre*) and at birth (inbred *Prdm1-Cre* line) are similar suggests that there is no embryonic lethality after E7.5. Also, in both cases the expected Mendelian ratios of Cre inheritance are observed, indicating that early embryonic lethality is independent of the genotype of the embryo and/or the Cre presence (Mikedis and Downs 2017).

BAC based transgenes, such as the *Prdm1-Cre* transgene, result in random integration into the mouse genome following pronuclei injections. BAC transgenes can integrate at various sites and at different copy numbers (Chandler et al. 2007). It is therefore possible that random

transgene insertion disrupted a specific locus, causing the small litter size associated with the *Prdm1-Cre* line. This breeding phenotype is a major disadvantage as it is very challenging and time consuming to obtain enough biological replicates of gender matched control and conditional knockout (CKO) tissues from the same litter.

Nevertheless, Cre expression driven by *Prdm1* allows for the earliest possible germ cell specific deletion of candidate genes and exhibits very high recombination efficiency. Therefore, a new *Prdm1-Cre* driver line was generated, with the aim to establish a healthy line with normal litter sizes and the same robust recombination efficiency, allowing conditional deletion in germ cells at a higher efficiency. For clarity, the original line is referred to as *Prdm1-Cre* (Ohinata et al. 2005), whereas the new line described in the next sections will be referred to as *Blimp1-iCre* from now on.

5.2. Results

The original *Prdm1-Cre* line has high recombination efficiency in germ cells and closely reflects the endogenous *Prdm1* gene expression pattern. The observed phenotype of small litter sizes is possibly due to the random integration site of the modified BAC transgene.

Based on these observations, our approach to generate a new *Blimp1-iCre* line was as follows: A new *Blimp1-iCre* BAC transgene was engineered, which shared some similarities with the original transgene (*Prdm1-Cre*) given its proven functionality. The new transgene was injected into pronuclei to generate several new founder mice with unique transgene insertion sites in the hope to generate one founder with robust Cre recombination and normal litter size.

5.2.1. Construction of a new *Blimp1-iCre* transgene

The original *Prdm1-Cre* transgene was based on a bacterial artificial chromosome (BAC) containing the *Prdm1* gene, but not other genes, and a large 150kb 5' upstream region (Ohinata et al. 2005). The first 100bp of the Cre sequence, preceded by a nuclear localization sequence (NLS), were inserted into the coding region of the first exon. The remaining Cre sequence was inserted into the second exon of the *Prdm1* gene, followed by a stop cassette (Ohinata et al. 2005). The genetic background of the BAC clone was likely NOD, Molossinus or 129sV. The exact BAC clone could not be traced back using the stated Bac ID as the company ceased to exist (personal communication, Phillip Hublitz, WIMM, University of Oxford).

To generate the new *Blimp1-iCre* transgene, we sought help from Philip Hublitz at the Weatherall Institute of Molecular Medicine (WIMM) Genome Engineering Service at the University of Oxford: A bacterial artificial chromosome (BAC) originating from a pure C57BL/6 genetic background was used as a backbone (Figure 5.1). As in the original line, the chosen BAC clone contained the *Blimp1* gene, but not any other gene, and a large (>150kb) 5' upstream region including regulatory elements. An already existing selectable cassette containing improved Cre (iCre) was inserted into exon 1 of the *Blimp1* gene, replacing ATG and deleting 14bp of the coding sequence (Figure 5.1). The removal of the selection cassette was achieved via a bacterial Flp-mediated excision. The final BAC clone was verified by sequencing.

Despite a high degree of similarity between the new *Blimp1-iCre* and old *Prdm1-Cre* transgene, differences are as follows: Codon optimised Cre (iCre) was used instead of standard Cre and no NLS sequence was added. Instead, a fully synthetic exon-intron-exon sequence precedes iCre. Further, the whole iCre sequence was inserted into exon 1 to guarantee iCre expression, in contrast to a split cDNA approach in the original line.

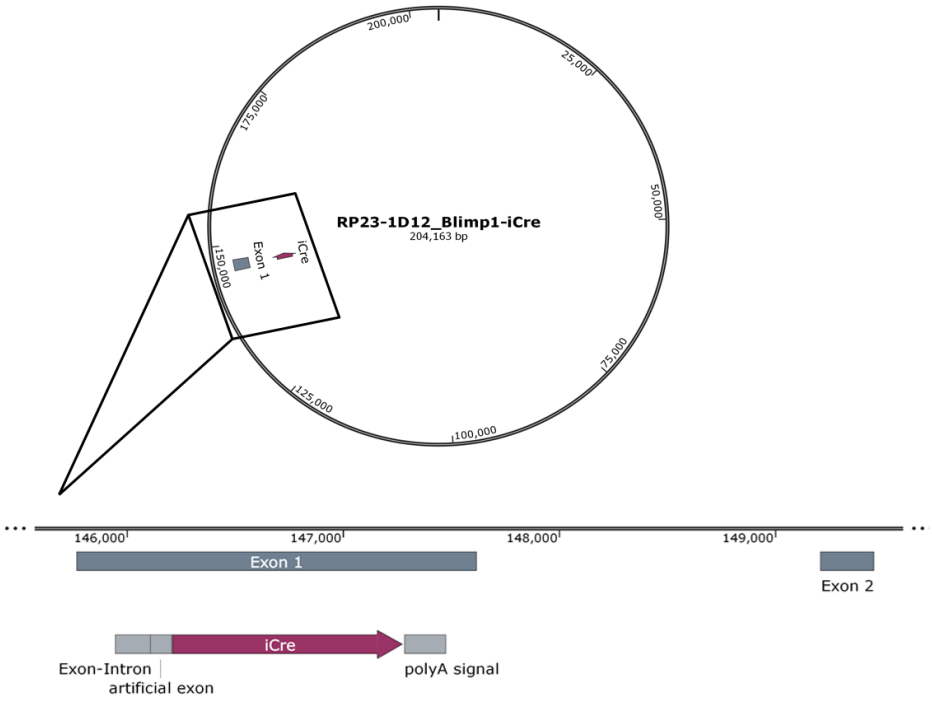

Figure 5.1: Map of modified *Blimp1-iCre* BAC transgene.

BAC clone RP23-1D12 (full C57BL/6 background) containing the *Blimp1* gene and large (>150kb) 5' regulatory elements was used. A selectable cassette (hybrid-intron-K.ATG-iCre-pA-FRT-AMP-FRT) containing iCre was inserted into exon 1 of the *Blimp1* gene. Since exon 1 is already coding, the cassette contains a hybrid intron, the endogenous ATG was replaced and 14bp of the coding sequence deleted. Removing of the selection cassette was achieved via a bacterial Flp-mediated excision. The final BAC clone was verified by sequencing. An ICSI grade modified BAC prep was prepared for pronuclei injections.

5.2.2. Pro-nuclear injections and generation of founder mice

To generate founder mice, the newly generated *Blimp1-iCre* transgene was prepared highly supercoiled and injected into the pronuclei of zygotes. Several rounds of injections were performed using slightly different conditions regarding the genetic background of zygotes, BAC concentrations and BAC structure (circular vs linear) (Table 5.1).

Initially, zygotes from a C57BL/6 background were used to maintain a pure genetic background. This would avoid future backcrossing of the newly generated founder mice to C56BL/6 wild-type mice for several generations. Two rounds of injections were performed by the LMS Transgenics Facility using the circular, supercoiled form of the transgene (Table 5.1). Using the circular transgene has the advantage of greatly reducing breakpoint expectancy, however it usually generates a lower number of insertions with lower efficiency (Philip Hublitz, personal communication). Out of 589 implanted embryos, 62 live pups were born and none of them carried the *Blimp1-iCre* transgene as identified via PCR (Table 5.1). Next, the circular transgene was linearized via restriction enzyme digestion before another round of injections proceeded (LMS Transgenics Facility). Linearization can increase the insertion efficiency of the BAC transgene (personal communication, Philip Hublitz, (Van Keuren et al. 2009)). Out of 183 implanted embryos only 7 live pups were recovered and all were negative for the *Blimp1-iCre* transgene (Table 5.1). Lastly, zygotes from a mixed genetic background (CBAxC57BL/6) were injected with the circular, supercoiled transgene at different concentrations (2ng/µl, 3ng/µl, and 5ng/µl) (LMS Transgenics Facility) (Table 5.1). During this round of injections, out of 502 implanted embryos in total, 99 live pups were born and 7 of them were identified positive for carrying the *Blimp1-iCre* transgene via PCR (Table 5.1).

In parallel, a sample of purified *Blimp1-iCre* BAC transgene was sent to the EMBO Transgenics Facility in Monterotondo (Rome) for an additional round of injections. Zygotes from an FVB background were injected with the circular transgene at a concentration of 1ng/µl. Out of 228 implanted embryos, 66 live pups were born and 2 of them carried the *Blimp1-iCre* transgene (Table 5.1).

In total, after several rounds of pronuclei injections, 9 founder mice positive for the *Blimp1-iCre* transgene were generated during two separate injections of the circular transgene. The founder mice are either from a CBAxC57BL/6 or from a FVB genetic background due to different mouse strains used for the generation of zygotes (Table 5.1). In contrast, in the

original *Prdm1-Cre* line, the transgene was linearized and microinjected into pronuclei of zygotes derived from B6CBAF1 mice.

In all newly generated founder mice, the *Blimp1-iCre* transgene has inserted randomly at unique sites in the genome and at variable copy numbers. In the next step, all founder mice were analysed for germ line transmission of the transgene.

Table 5.1: Overview of completed pronuclei injections of *Blimp1-iCre* transgene.

round	injected transgene	genetic background (zygotes)	injected zygotes	embryo transfer (implanted)	live pups	positive (%)	facility
1	*Blimp1-iCre* circular	C57BL/6	341	306	45	0 (0%)	LMS, London
2	*Blimp1-iCre* circular	C57BL/6	398	263	17	0 (0%)	LMS, London
3	*Blimp1-iCre* linear	C57BL/6	283	183	7	0 (0%)	LMS, London
4	*Blimp1-iCre* circular	CBA x C57BL/6	626	502	99	7 (7%)	LMS, London
5	*Blimp-iCre* circular	FVB	740	228	66	2 (3%)	EMBL, Monterotondo

5.2.3. Germ line transmission of the *Blimp1-iCre* transgene

Successful germline transmission of the *Blimp1-iCre* transgene was tested via mating each positive founder with C57BL/6 wild-type mice. Between 2 - 7 litters from each breeding pair or trio were genotyped for the presence of the transgene (Table 5.2). Out of the 9 founders, two founders (#1741 and #1747) did not produce a single *Blimp1-iCre* positive offspring in 2-3 litters analysed (Table 5.2). Since these founders showed no germline transmission, no further analysis was undertaken. Of the remaining 7 founders, all transmitted the transgene to the next generation, however, at different efficiencies. According to Mendelian Law, a 50% inheritance of the transgene is expected (Haruyama, Cho, and Kulkarni 2009). Founders #1752, #1820 and #1828 produced litters with less than 10% of *Blimp1-iCre* positive pups, indicating that these founders are possibly mosaic due to late transgene integration (Table 5.2). In contrast, founder #555290 transmitted the transgene to about 72% of all F1 offspring, indicating the transgene has integrated into multiple locations (Table 5.2) (Haruyama, Cho, and Kulkarni 2009). Founders #1765, #1784 and #555309 exhibited germline transmission efficiencies between 30%-58% (Table 5.2).

Most importantly, regardless of germline transmission, average litter size of all founders was in a normal range between 5.25-8.67 pups per litter (Table 5.2). In contrast, the original *Prdm1-Cre* line had average litter sizes of 2.8 pups per litter produced by congenic breeding pairs (C57BL/6) and 3.9 pups per litter produced by outbred breeding pairs (C57BL/6/CBA).

Subsequently, all 7 founders which demonstrated germline transmission were bred with C57BL/6 females to establish separate founder lines. Further detailed analysis of *Blimp1-iCre* expression was carried out for each founder.

Table 5.2: Identified founder mice and overview of germline transmission analysis.

				germline transmission				
Founder ID	sex	genetic background (F0)	BAC transgene concentration	mating (C57BL/6)	total nr of litters	total nr of pups	average litter size	positive pups (%)
1741	F	CBA/C57BL6	3ng/µl	duo	2	13	6.50	0 (0%)
1747	M	CBA/C57BL6	3ng/µl	duo	3	26	8.67	0 (0%)
1752	M	CBA/C57BL6	3ng/µl	duo	7	43	6.14	3 (6.98%)
1765	M	CBA/C57BL6	3ng/µl	duo	4	21	5.25	9 (42.86%)
1784	M	CBA/C57BL6	5ng/µl	duo	5	43	8.60	13 (30.23%)
1820	F	CBA/C57BL6	2ng/µl	duo	6	53	8.83	4 (7.55%)
1828	F	CBA/C57BL6	2ng/µl	duo	4	33	8.25	3 (9.09%)
555290	M	FVB	1ng/µl	trio	4	46	5.75	33 (71.73%)
555309	F	FVB	1ng/µl	duo	4	38	9.50	22 (57.89%)

5.2.4. *Blimp1-iCre* expression and recombination analysis using reporter mice

5.2.4.1. Characterisation of different founder lines

In order to analyse iCre expression and recombination efficiency, two different reporter strains were used: Z/EG (Novak et al. 2000) and R26RGOF (Madisen et al. 2010; Yoshimizu et al. 1999; Yeom et al. 1996).

The Z/EG reporter mice express *LacZ* throughout embryonic development and adult life. Upon Cre recombination, the *LacZ* gene is excised and a second reporter, enhanced green fluorescent protein (EGFP), will be expressed (Figure 5.2 A- B) (Novak et al. 2000). The R26RGOF mice carry two transgenes: The first transgene contains a CAG promoter-driven red fluorescent protein variant (tdTomato) inserted into the Rosa26 locus. A loxP-flanked STOP cassette between promoter and tdTomato prevents transcription. Upon successful Cre recombination, Tdtomato is expressed (Figure 5.2 A-B) (Madisen et al. 2010). In addition, the GOF18ΔPE-EGFP transgene results in GFP expression driven by the *Oct4* promoter and labels specifically germ cells (Yoshimizu et al. 1999). Both reporter strains allow detailed functional analysis of Cre expression and recombination.

For each founder line, at least one heterozygous *Blimp1-iCre* male was crossed with a homozygous reporter female, and embryos and placentas were collected at E11.5 for analysis (Table 5.3). Genotype was determined via PCR with primers against iCre and the reporter gene. The Z/EG strain was initially used for all Cre analysis experiments at the time. However, generation of experimental Z/EG females was slow and many identified plugs did not result in pregnancies, making embryo collections for Cre recombination analysis challenging. Once the R26RGOF reporter strain was available, this mouse line was used instead.

First, for each *Blimp1-iCre* founder, the germ cell recombination efficiencies were determined via quantifying the percentage of germ cells expressing the reporter gene (Figure 5.2 C, Table 5.3). Overall, founder lines exhibited different recombination efficiencies in germ cells, with levels varying from 0% to almost 100% (Figure 5.2 C). Line #1784 and #555309 both exhibited very high recombination of the Z/EG reporter transgene in germ cells. Over 98% of the identified germ cells expressed EGFP at E11.5. Founder line #1765 had a slightly lower recombination efficiency of about 88% using the R26RGOF reporter strain (Table 5.3). Further, two founder lines (#1752 and #555290) had a recombination efficiency of about 66% and 62%, respectively, as determined by crossing with the Z/EG reporter strain. Lastly,

founder lines #1820 and #1828 had a very low to no recombination efficiency of 6% and 0% (Table 5.3). The genotype of embryos analysed from line #1828 was confirmed as *Blimp1-iCre* positive and *R26R* positive. Further, some somatic cells (e.g. in placenta) expressed tdTomato, confirming the presence of both transgenes. The very low recombination efficiency suggests either a high degree of transgene silencing, leading to low levels of iCre expression or presence of non-functional iCre. Subsequently, these two lines were not analysed further.

In the remaining 5 founder lines, iCre recombination was mostly specific to germ cells within the genital ridge at E11.5 (Figure 5.2 B). Analysis of whole embryo sections revealed iCre recombination at various different locations within the embryo. This is in line with published reports of widely expressed endogenous BLIMP1 protein during embryonic development (Chang and Calame 2002; Vincent et al. 2005; Ohinata et al. 2005; Robertson et al. 2007). Recombination patterns throughout the embryos appeared similar between different founder lines. In addition, all founder lines but #1784, exhibited some recombination in the placenta in line with endogenous Blimp1 protein expression in the placenta (Table 5.3) (Robertson et al. 2007; Mould et al. 2012; Mikedis and Downs 2017).

In summary, given the high recombination efficiency of over 99% at E11.5, founder lines #1784 and #555309 are both very good candidates for future experiments to generate germ cell specific knockout tissues. Subsequently, line #555309 was analysed in more detail as it was the first line out of the two to be characterised.

A

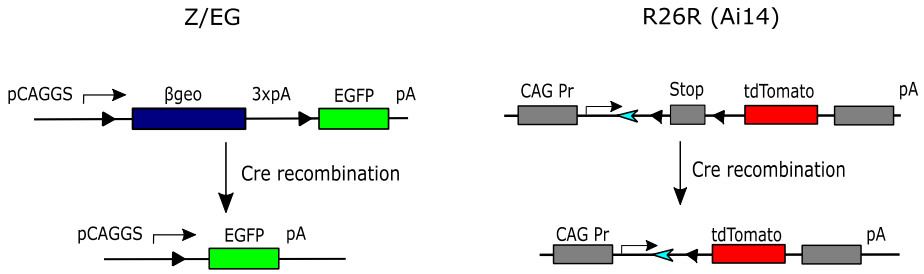
Z/EG
R26R (Ai14)
pCAGGS
βgeo
3xpA
EGFP
pA
Cre recombination
pCAGGS
EGFP
pA
CAG Pr
Stop
tdTomato
pA
Cre recombination
CAG Pr
tdTomato
pA

B

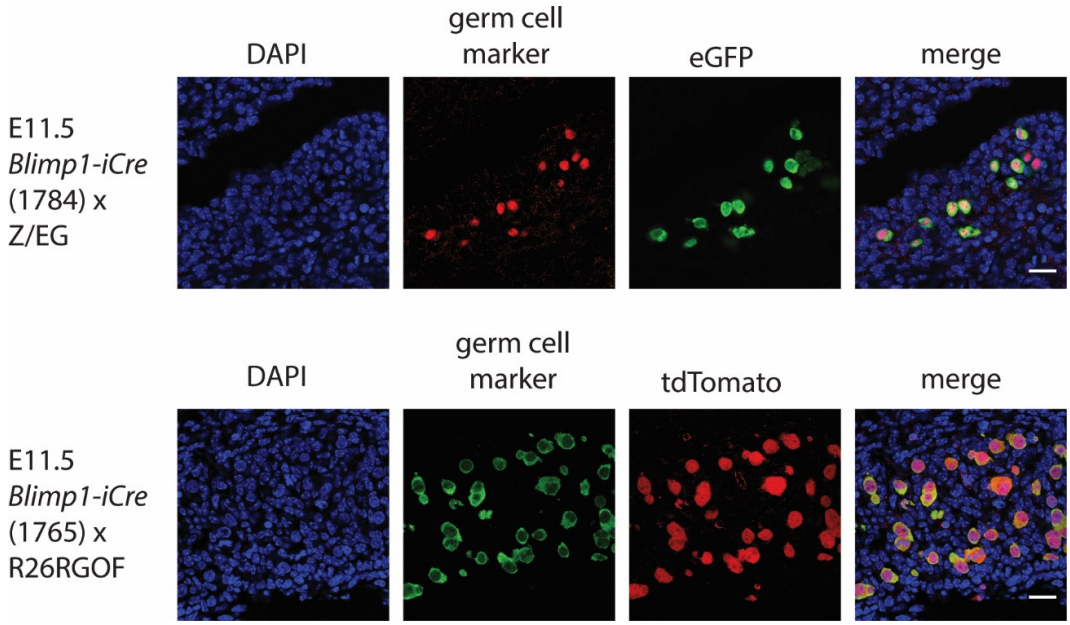
DAPI
germ cell marker
eGFP
merge
E11.5 *Blimp1-iCre* (1784) x Z/EG
DAPI
germ cell marker
tdTomato
merge
E11.5 *Blimp1-iCre* (1765) x R26RGOF

C

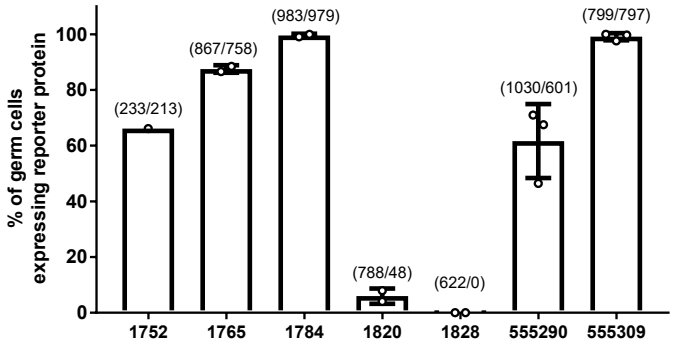
% of germ cells expressing reporter protein
100
80
60
40
20
0
(233/213)
(867/758)
(983/979)
(788/48)
(622/0)
(1030/601)
(799/797)
1752
1765
1784
1820
1828
555290
555309

Figure 5.2: Cre recombination analysis in different founder lines using two different reporter strains.

A Schematic of reporter transgenes from the used reporter mouse strains (Z/EG and R26RGOF). From the Z/EG transgene, the *βgeo* (lacZ/neomycin-resistance) fusion gene is expressed. Upon Cre recombination, the downstream reporter EGFP is expressed instead (Novak et al. 2000). In R26RGOF reporter strain, the R26R (Ai14) transgene containing a tdTomato reporter was inserted into the endogenous Rosa26 locus. A stop codon prevents expression of tdTomato. Upon Cre dependent excision, the tdTomato reporter is expressed (Madisen et al. 2010). **B** Examples of successful iCre recombination of reporter transgenes in E11.5 genital ridges. Embryo sections derived from crosses between *Blimp1-iCre* males and Z/EG females were stained with OCT4 to identify germ cells (germ cell marker). Expression of EGFP indicates recombination of the Z/EG transgene. Embryo sections derived from crosses between *Blimp1-iCre* males and R26RGOF females contain GFP labelled germ cells (expression is under the control of the *Oct4* promoter, germ cell marker). Expression of the tdTomato reporter indicates recombination of the R26R (Ai14) transgene. Number in brackets is the identification number of different *Blimp1-iCre* founder lines. Nuclei are stained with DAPI. Representative images are shown, scale bar = 20μm. **C** Cre recombination efficiencies of 7 different founder lines. Mean percentage of germ cells expressing EGFP (Z/EG reporter) or tdTomato (R26RGOF reporter) is shown. Each dot represents one biological replicate (embryo). Error bars = standard deviation. Numbers in brackets are total number of germ cells counted versus germ cells positive for recombined protein.

Table 5.3: Summary of iCre recombination analysis of 7 founder lines.

	matings for Cre analysis					
Founder line	generation of *Blimp1-iCre* male	reporter line used (female)	nr of litters analysed (E11.5)	nr of embryos analysed	recombination efficiency	recombination in placenta
1752	F1	Z/EG	1	1	66.15%	yes
1765	F2	R26RGOF	1	2	87.52%	yes
1784	F1	Z/EG	1	2	99.55%	no
1820	F2	Z/EG	1	2	5.98%	yes
1828	F2	R26RGOF	1	2	0.00%	yes
555290	2x F1	Z/EG	2	3	61.65%	yes
555309	2x F1, 1 x F3	Z/EG and R26RGOF	3	3	99.11.%	yes

5.2.4.2. Detailed characterisation of founder line #555309

Founder line #555309 exhibited a germ cell recombination efficiency over 99% at E11.5 using both reporter strains. Within the genital ridge, iCre recombination was specific to germ cells (Figure 5.3 A-B). In addition to E11.5, iCre recombination in germ cells was also assessed in E9.5 embryos using the Z/EG reporter strain. In both embryos analysed, iCre recombination of the reporter transgene was observed in 100% of germ cells (Figure 5.3 A- B). Of note, many somatic cells surrounding the germ cells also expressed the reporter gene (Figure 5.3 A).

To further determine the overall Cre recombination pattern in founder line #555309, whole embryo sections were analysed. At E11.5, iCre recombination was observed in the branchial arches and the developing heart (Figure 5.4 A). Further, olfactory epithelium and gut epithelium were positive for the reporter (Figure 5.4 A). In addition, few cells in the placenta also showed recombination of the reporter transgene (Figure 5.4 B). All observed locations of iCre recombination are in line with previously described endogenous BLIMP1 protein expression sites (D. H. Chang and Calame 2002; Vincent et al. 2005; Ohinata et al. 2005; Robertson et al. 2007). Of note, in embryos from matings of *Blimp1-iCre* males with R26RGOF females, iCre recombination and expression of the tdTomato reporter protein seemed stronger in non-germ cell sites compared to signal in germ cells (Figure 5.4 A). Nevertheless, the signal detected in germ cells was still high and clearly visible (40x, Figure 5.4 A).

At E9.5, iCre recombination was also observed in the hindgut, first branchial arch and the aortic sac giving origin to first and second branchial arch arteries (Figure 5.4 B). All observed iCre recombination sites are in line with previously described endogenous BLIMP1 protein expression sites (Chang and Calame 2002; Vincent et al. 2005; Ohinata et al. 2005; Robertson et al. 2007).

Taken together, founder line 555309 exhibits very high recombination efficiency at E9.5 and E11.5 in germ cells. Apart from germ cells, other Cre recombination sites are similar to reported endogenous BLIMP1 protein expression patterns, indicating that the *Blimp1-iCre* BAC transgene reflects endogenous *Blimp1* expression closely. Most importantly, litter size of the new *Blimp1-iCre* line is normal so far, suggesting the successful generation of a healthy new *Blimp1-iCre* line for efficient germ cell specific gene deletion. Subsequently, the founder line #555309 has been backcrossed to C57BL/6 females in order to create a congenic *Blimp1-iCre* line.

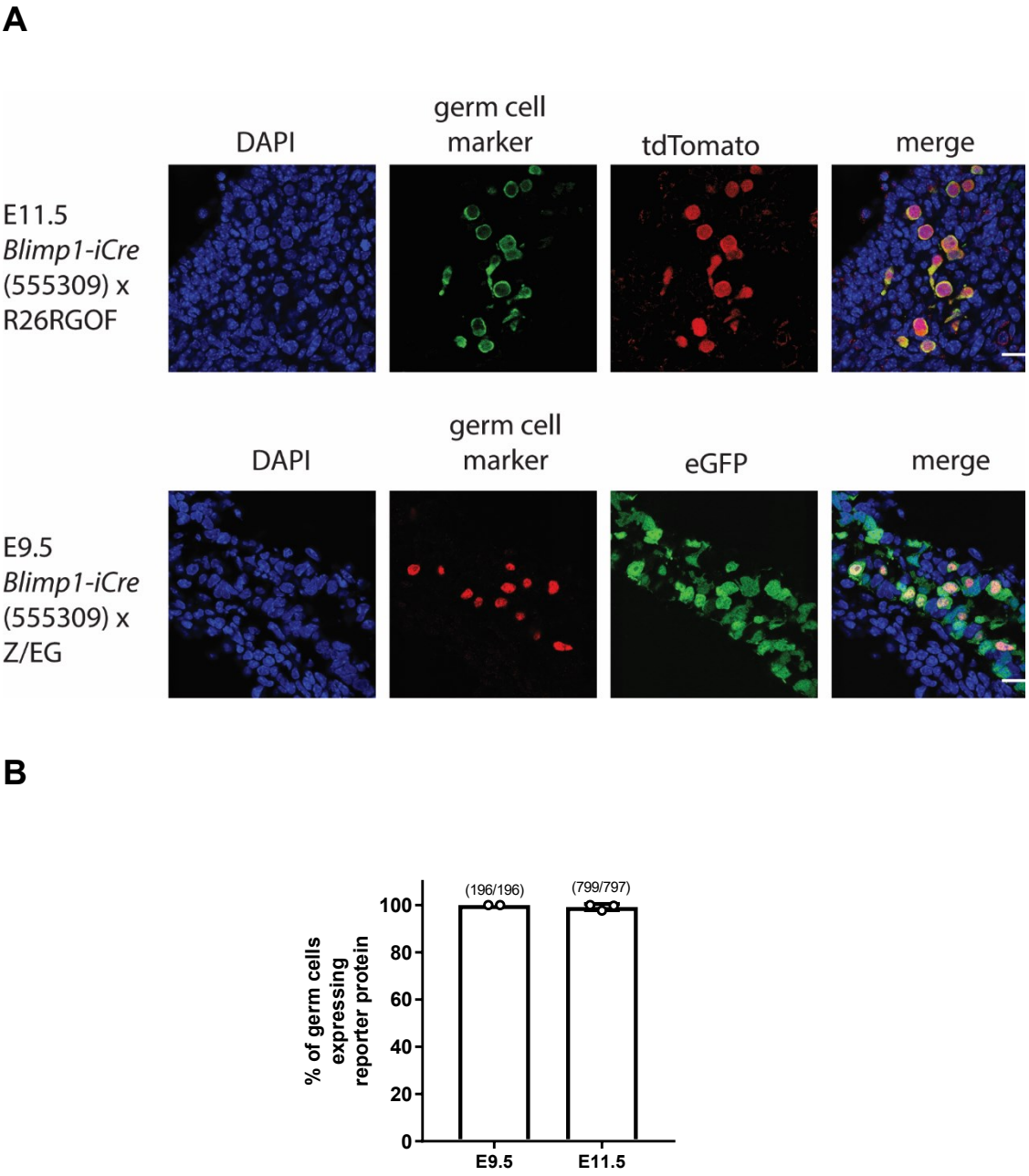

Figure 5.3: Cre recombination efficiency analysis of founder line 555309 at E11.5 and E9.5.

A Immunofluorescent images of E11.5 and E9.5 genital ridges from embryos of *Blimp1-iCre* males and reporter females. Germ cell marker is GFP at E11.5 and OCT4 at E9.5. Nuclei are stained with DAPI. Representative images are shown, scale bar = 20μm, biological replicates = 3 embryos (at E11.5), 2 embryos (at E9.5) **B** Quantification of Cre recombination efficiency observed in (A). Mean percentage of germ cells expressing EGFP (Z/EG reporter) or tdTomato (R26RGOF reporter) is shown. Each dot represents one biological replicate (embryo). Error bars = standard deviation. Numbers in brackets are total number of germ cells counted versus germ cells positive for recombined protein.

A

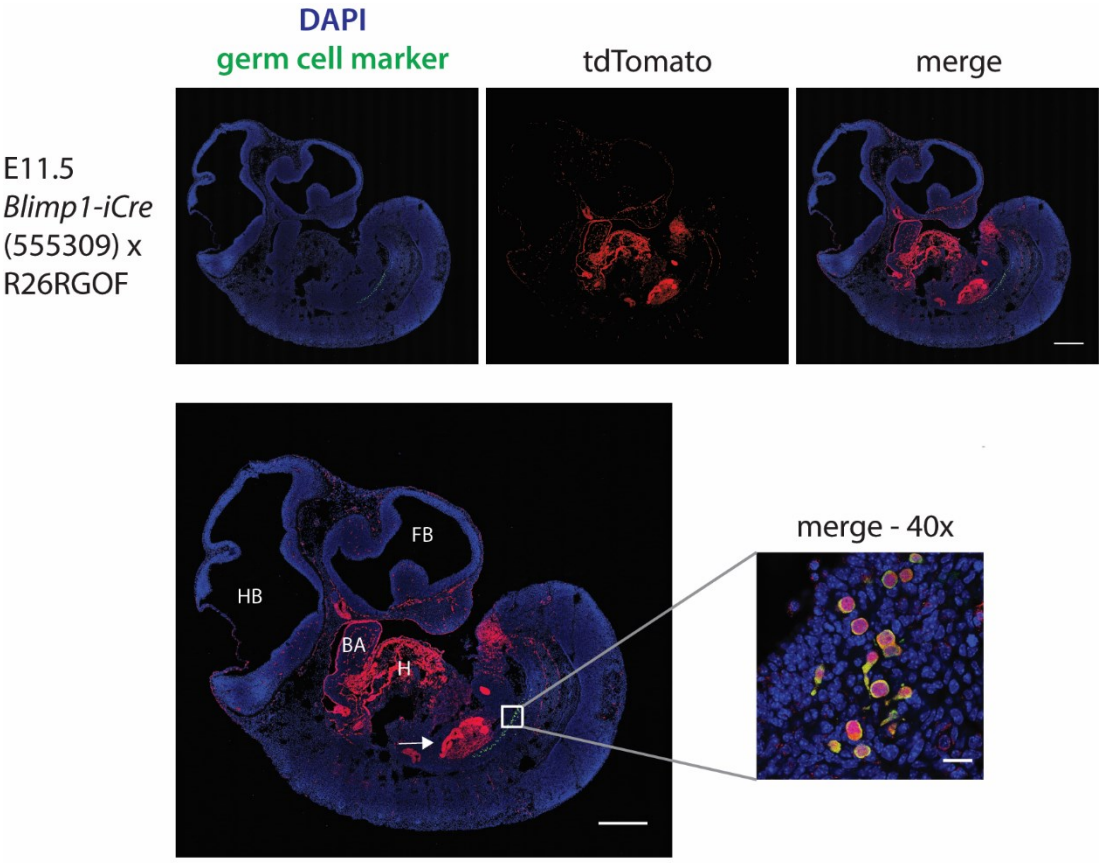
DAPI
germ cell marker
tdTomato
merge
E11.5
Blimp1-iCre
(555309) x
R26RGOF
FB
HB
BA
H
merge - 40x

B

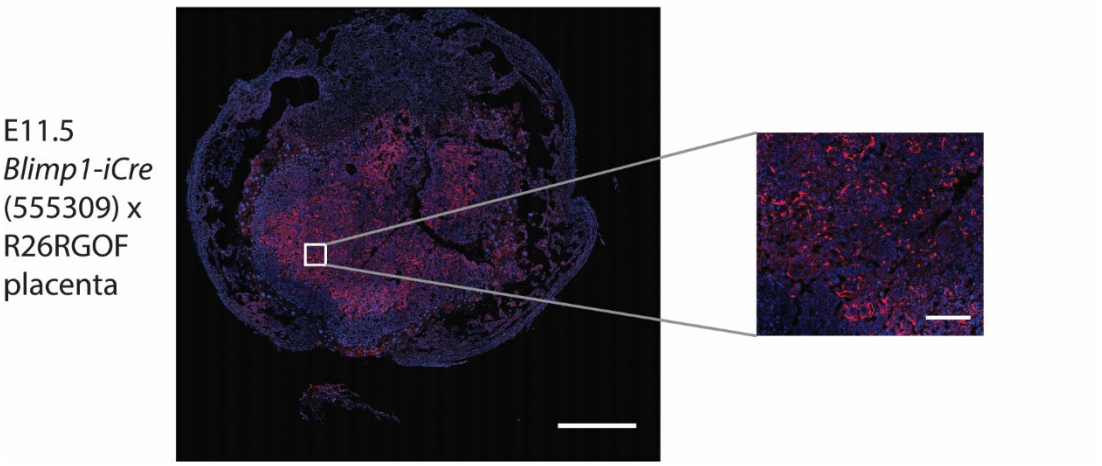
E11.5
Blimp1-iCre
(555309) x
R26RGOF
placenta

C

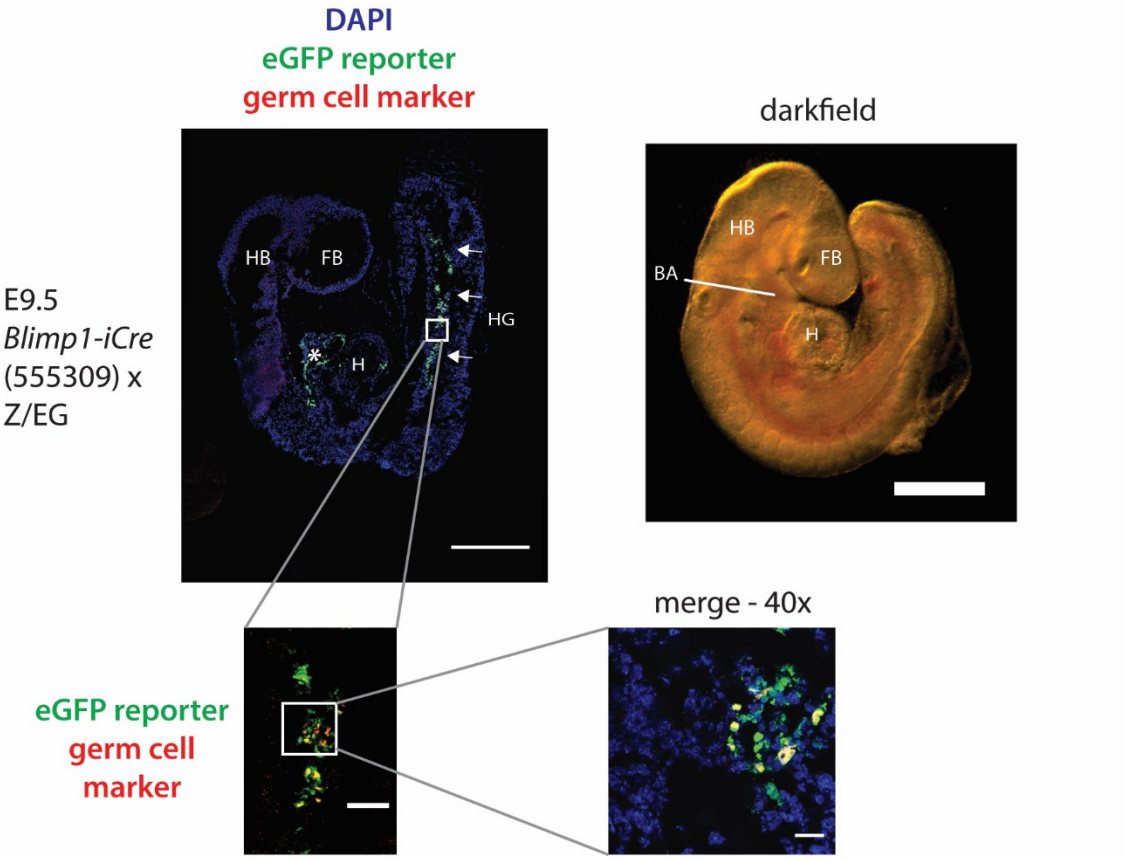

Figure 5.4: iCre recombination pattern of founder line 555309 in whole embryo at E11.5 and E9.5.

A Sagittal section of E11.5 embryo from *Blimp1-iCre* male and R26RGOF reporter female. Germ cells were identified via GFP expression, nuclei were stained with DAPI. tdTomato expression indicates Cre recombination of R26R reporter transgene. Representative images shown. scale bar = 500µm, 40x zoomed in image scale bar = 20µm. Arrow points to gut epithelium. **B** Section of E11.5 placenta from embryo shown in (A). scale bar = 1mm, zoomed in image scale bar = 200µm **C** Cre recombination pattern in E9.5 embryo. Sagittal section of E9.5 embryo from *Blimp1-iCre* male and Z/EG reporter female (left). Germ cells were identified via OCT4 staining, nuclei were stained with DAPI. EGFP expression indicates Cre recombination of Z/EG transgene. Representative images shown. Scale bar = 500µm. Zoomed in images of embryonic hindgut depicting germ cells and EGFP expressing cells. Scale bar = 80µm; enlarged 40x image scale bar = 20µm. Darkfield image of E9.5 embryo for orientation (right), scale bar = 500µm. Representative images shown. Biological replicate = 2 embryos. * depicts aortic sac. FB = forebrain, HB = hindbrain, H = heart, HG = hindgut, BA = branchial arch;

5.3. Discussion & Future Work

In this chapter, the successful generation and characterisation of a new transgenic iCre driver mouse line under the control of the *Blimp1* promoter was described. Out of 9 founder mice, 7 showed germline transmission of the transgene and 2 different lines exhibited recombination efficiency of close to 100%. Most importantly, litter size appeared normal, in contrast to the original existing *Prdm1-Cre* line, which is associated with poor breeding outcomes.

Recombination efficiency was tested using two different reporter strains. It should be mentioned that recombination efficiency of a floxed allele depends on many factors such as the cell type specific epigenetic context of floxed loci, the location of LoxP sites and distances between LoxP sites (J. Liu et al. 2013). Therefore, different reporter strains can have different recombination efficiencies (J. Liu et al. 2013). In fact, a study comparing the sensitivity of several reporter strains showed that the Z/EG reporter was the least sensitive reporter tested. In contrast, reporter strain R26R (Ai9), a reporter highly similar (CAG driven tdTomato expression) to the one used in this study (R26R (Ai14)), was the most sensitive one (J. Liu et al. 2013). Founder line #555309 was the only line analysed using both reporter strains at E11.5. Germ cell recombination efficiencies were similar between replicates at E11.5 regardless of the reporter strain used. Further, recombination efficiency at E9.5 was similar to E11.5, indicating that there are no gross differences between the two reporter strains regarding germ cell recombination using *Blimp1-iCre*. It should be noted though that overall iCre recombination throughout the embryo seemed stronger when using the R26RGOF reporter compared to the Z/EG reporter.

In addition, iCre recombination efficiency and expression pattern can differ depending on whether Cre is transmitted via the female or male. So far, Cre recombination has only been analysed when transmitted from the male.

5.3.1. iCre recombination in the developing embryo

In the developing embryo, iCre recombination was observed in all germ cells at E9.5 (100% efficiency). However, many surrounding somatic cells also expressed the reporter protein. At this stage, PGCs migrate through the embryonic hindgut towards the genital ridges (Anne McLaren 2003). It is likely that the surrounding cells are part of the hindgut endoderm. Endogenous BLIMP1 protein has been detected in endodermal epithelium of midgut and

hindgut from E9.5 onwards until birth (D. H. Chang and Calame 2002). In fact, the original *Prdm1-Cre* line was also observed to induce recombination in the hindgut endoderm when crossed to the R26R- EYFP reporter line (Hirota et al. 2011).

At E11.5, iCre recombination within the genital ridge was specific to germ cells. In contrast, in the original *Prdm1-Cre* line some recombination was also observed in Mullerian ducts and some somatic cells within E12.5 genital ridges (Hirota et al. 2011). It has been suggested by the authors that presumably somatic cells which expressed the reporter were forming BLIMP1 expressing blood vessels (Hirota et al. 2011). Mullerian duct formation only starts at around E11.5 and is fully completed at E12.5 (Orvis and Behringer 2007). Hence, it is possible that E11.5 was too early to detect possible recombination in developing Mullerian ducts. Analysis of E12.5 genital ridges would allow to determine any recombination in Mullerian ducts or other somatic cells within genital ridges.

More importantly though, future work will focus on time points even earlier than E9.5. Gene expression of iCre recombinase can be delayed compared to endogenous driver gene expression (Nagy 2000). In the *Vasa-Cre* line, for instance, *Vasa-Cre* was only detected from E15.5 onwards (Gallardo et al. 2007), while endogenous *Vasa (Mvh)* is expressed from E10.5 onwards in germ cells (Tanaka et al. 2000). In addition, there is a delay between iCre gene expression, functional iCre protein and recombination (Nagy 2000). Hence it is crucial to determine at what time iCre recombination is initiated in order to understand data generated in future experiments. Future analysis of E8.0/E8.5 embryos will be undertaken to determine recombination efficiency at such early time points. In addition, whole mount stainings to preserve tissue structure will allow to determine the recombination pattern.

5.3.2. iCre recombination and BLIMP1 expression in the embryo

iCre recombination was detected in a variety of tissues at E9.5 and E11.5. This was not surprising, given that endogenous BLIMP1 protein expression has been detected in a number of endoderm, ectoderm and mesoderm-derived tissues in the embryo.

BLIMP1 (PRDM1) is a transcriptional repressor and plays distinct roles during cell fate specification of distinct progenitor cells throughout embryonic development. *Blimp1* transcript expression is first detected in the posterior and anterior visceral endoderm (extraembryonic tissue layers) of the early streak stage embryo at around E6.25-E6.5 (de Souza et al. 1999; Vincent et al. 2005; Robertson et al. 2007). Around E7.0-E7.5, other parts of the embryo such as the anterior definitive endoderm and mesoderm (or mesendoderm) and

the prechordal plate, two signalling centers patterning the developing forebrain, are BLIMP1 positive (de Souza et al. 1999; D. H. Chang and Calame 2002; Vincent et al. 2005). At the headfold stage (E7.25-8), BLIMP1 expression is detected in the foregut (in a subset of endodermal epithelial cells) and adjacent midgut (de Souza et al. 1999; D. H. Chang and Calame 2002). From E8.5 onwards, BLIMP1 expression is observed in a variety of tissues such as telencephalon, optic placode, in subsets of endoderm and ectoderm cells of the pharyngeal/branchial arches (pharyngeal epithelia of individual arches), as well as splanchnic mesoderm, endothelial cells and somites (de Souza et al. 1999; Vincent et al. 2005; Robertson et al. 2007). In addition, papillae of teeth, hair and taste buds and papillae of the sensory vibrissae (from E12.5 onwards) are BLIMP1 positive (D. H. Chang and Calame 2002; Robertson et al. 2007). BLIMP1 expression in a sub-region of the splanchnic mesoderm was identified as marking a set of myocardial progenitor cells in the secondary heart field (SHF), which give rise to the inflow and outflow poles of the heart tube and hence are crucial for heart morphogenesis (Vincent et al. 2005; Robertson et al. 2007). The developing posterior forelimb bud also expresses BLIMP1 (Robertson et al. 2007; Vincent et al. 2005).

Taken together, observed iCre recombination sites such as the gut epithelium, branchial arches and the developing heart (amongst others) are in line with endogenous *Blimp1* expression. These non-germ cell specific iCre expression sites are important to keep in mind when using the new *Blimp1-iCre* line to delete candidate genes in the future.

5.3.3. iCre recombination in the placenta

In most founder lines, including founder line #555309, iCre recombination of the reporter gene was detected in a small subset of cells in the placenta. In contrast, the original *Prdm1-Cre* transgene (Ohinata et al. 2005) was not expressed in the placenta (Mould et al. 2012).

Observed iCre recombination is in line with endogenous BLIMP1 protein expression in multiple trophoblast cell types in the developing placenta. (Robertson et al. 2007; Mould et al. 2012). In fact, endogenous BLIMP1 expression defines multipotent progenitors called spongiotrophoblasts (Mould et al. 2012). These cells give rise to three mature BLIMP1 positive subtypes: highly invasive spiral artery - associated TGCs (SpA-TGCs) that invade the maternal decidua to surround and remodel incoming maternal vasculature; glycogen trophoblasts and canal trophoblast giant cells (Mould et al. 2012). *Blimp1* expression is essential for terminal differentiation of SpA-TGCs and *Blimp1* knockout embryos show severe placental defects due to disrupted specification of these endovascular trophoblast

giant cells (Mould et al. 2012). This results in impaired remodelling of the maternal vasculature and subsequent impaired development of the spongiotrophoblast layer, secondarily causing the underlying labyrinth layer to collapse (Mould et al. 2012). Eventually, *Blimp1* knockout embryos die around E10.5, exhibiting widespread blood leakage/haemorrhaging in addition to defects in the formation of caudal branchial arches (Vincent et al. 2005; Mould et al. 2012).

Given the described endogenous BLIMP1 expression in spongiotrophoblast progenitor cells (Mould et al. 2012), one would expect the observed iCre recombination to be in the spongiotrophoblast tissue layer of the placenta. However, the observed reporter signal could not be further narrowed down to specific placental layers or specific cell subtypes due to technical reasons. Rather than sagittal sections allowing visualization and easy identification of all different layers within each section, transverse sections of the placenta were obtained. Further, only every 5th -8thsection was collected (50µm – 80µm apart), making exact identification of tissue layers difficult. Of note, the absence of observed iCre recombination in the placenta of founder line 1784 could also be due to technical reasons. Hence, future work will involve fresh tissue collections for further analysis of founder line 555309 using sagittal sections.

Nevertheless, some iCre recombination occurs in the placenta when using the new *Blimp1-iCre* line (#555309), which is important to keep in mind when deleting candidate genes in the future. Any severe phenotype could be possibly caused by deletion of that gene in the placenta and subsequent placental defects.

Taken together, a new *Blimp1-iCre* driver line has been created which demonstrated high recombination efficiency at E9.5 and E11.5 in germ cells. Further, the observed Cre recombination pattern closely resembles endogenous *Blimp1* gene expression. Most importantly, so far, the litter sizes appear normal. Hence, the new *Blimp1-iCre* mouse strains is a valuable tool to generate germ cell specific gene knockouts at a greater efficiency compared to the old *Prdm1-Cre* line. Further characterisation is still ongoing.

6. Chapter 6 – Conditional deletion of *Mtor* in primordial germ cells.

6.1. Introduction

Observations in wild-type germ cells indicated active mTORC1-4E-BP1 signalling from E10.5 onwards. In contrast, mTOR-S6K1-S6 signalling was not specifically enriched in germ cells or somatic cells. Subsequent analysis of global S6 kinase or 4E-binding protein knockout genital ridges revealed only a minor or no phenotype respectively, suggesting mTORC1 effectors in isolation do not play an essential role during germ cell development. This might be caused by compensatory mechanisms between mTORC1 effectors and other signalling pathways, in addition to genetic background effects of the mouse lines.

Global *Mtor* deletion is embryonic lethal around E5.5-E6.5 due to impaired trophoblast outgrowth following implantation and a proliferation defect of the inner cell mass (Gangloff et al. 2004; Murakami et al. 2004). Hence, analysis of primordial germ cells in global *Mtor* knockout embryos is not possible.

Further, analysis of global knockout tissue does not allow to disentangle cell autonomous from non-cell autonomous effects. The successful generation of the new healthy *Blimp1-iCre* line allows to delete genes specifically in primordial germ cells very early on and with high recombination efficiency. Since all of the analysed S6 kinase or 4E-BP global knockout genital ridges did not reveal a strong phenotype, we decided to move upstream of the mTORC1 signalling pathway and to delete *Mtor*. This will lead to the ablation of mTORC1 and mTORC2 signalling in primordial germ cells and allows to directly study the role of mTOR signalling during primordial germ cell development.

6.2. Results

6.2.1. Strategy to delete *Mtor* in primordial germ cells

To achieve conditional *Mtor* deletion in germ cells, the newly generated *Blimp1-iCre* mouse line was crossed with a floxed *Mtor* ($Mtor^{fl/fl}$) mouse strain (Risson et al. 2009) (Figure 6.1). $Mtor^{fl/fl}$ mice have loxP sites flanking the promoter region and intron preceding exon 6 of the *Mtor* allele. Cre recombination leads to a deletion of the promoter region and exon 1-5 (Figure 6.1 A). *Mtor* $^{fl/fl}$ mice are viable and fertile.

In the first breeding step, homozygous $Mtor^{fl/fl}$ males were mated with females heterozygous for the transgene *Blimp-iCre* (F4). Of note, iCre transmission was tested through the male (*Blimp1-iCre*) only (see 5.2.4, p. 186). Due to limited availability of $Mtor^{fl/fl}$ females and time constraints, $Mtor^{fl/fl}$ males were crossed with *Blimp-iCre* females. Male offspring heterozygous for the floxed *Mtor* allele and *Blimp1-iCre* transgene ($Mtor^{fl/+}$, Tg(*Blimp1-iCre*)/+) were subsequently bred to homozygous $Mtor^{fl/fl}$ females and embryos were collected at E13.5 (Figure 6.1 B). The genotype was determined using DNA from embryonic tails. Presence of the *Blimp1-iCre* transgene and floxed *Mtor* allele was determined using PCR. Embryos homozygous for the floxed *Mtor* allele and heterozygous for the *Blimp1-iCre* transgene ($Mtor^{\Delta/fl}$, Tg(*Blimp1-iCre*)/+) have *Mtor* deleted in their germ line. Experimental samples will be referred to as $Mtor^{-/-}$ conditional knockout (CKO) from now on. Embryos heterozygous for the floxed *Mtor* allele and the *Blimp1-iCre* transgene were used as control samples ($Mtor^{\Delta/+}$, Tg(*Blimp1-iCre*)/+) and will be referred to as $Mtor^{+/-}$ control (ctrl).

Litters from 5 females were collected and the average litter size was 8.6 ± 1.52 (SD) conceptuses per litter. Cre positive conceptuses and Cre negative conceptuses occurred at the expected Mendelian Ratio of 1:1 (5±1 $iCre^{+}$ vs 3.6±1.14 $iCre^{-}$) (Pearson $X^2 = 1.271$, df=4, p=0.86) (Table 6.1). Within each litter, 25% of all the conceptuses are expected to have the conditional knockout genotype ($Mtor^{\Delta/fl}$, Tg(*Blimp1-iCre*)/+). Genotyping revealed that on average 1.4 ±1.14 $Mtor^{-/-}$ CKO conceptuses per litter were present, which is not significantly different from the expected value of 2.15±0.38 $Mtor^{-/-}$ CKO conceptuses per litter (paired Student's t-test, t=1.704, df=4, p=0.16) (Table 6.1). Of note, living conceptuses with the conditional knockout genotype ($Mtor^{\Delta/fl}$, Tg(*Blimp1-iCre*)/+) were obtained despite the widely observed expression pattern of *Blimp1-iCre* within the embryo and the essential role of mTOR during development (Murakami et al. 2004; Gangloff et al. 2004). Overall, $mTOR^{-/-}$ CKO embryos appeared normal and healthy by eye (observation only).

Taken together, the average litter size and Cre inheritance further confirm that the newly generated *Blimp1-iCre* mouse line has normal litter sizes and no breeding phenotype, even after 4 backcrosses to C57BL6/J wild-type mice. The newly generated *Blimp1-iCre* mouse line allows efficient generation of *Mtor* $^{-/-}$conditional knockout embryos for analysis of mTOR signalling during primordial germ cell development.

A

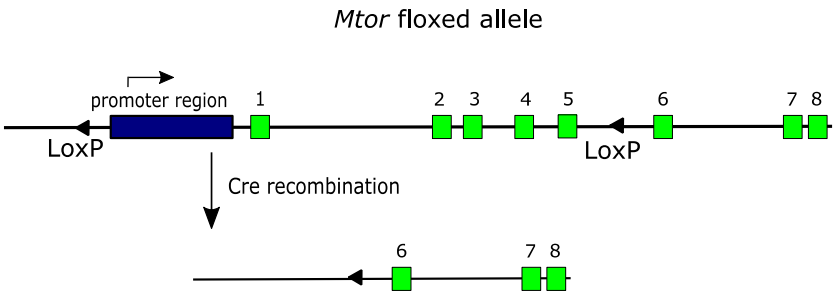

B

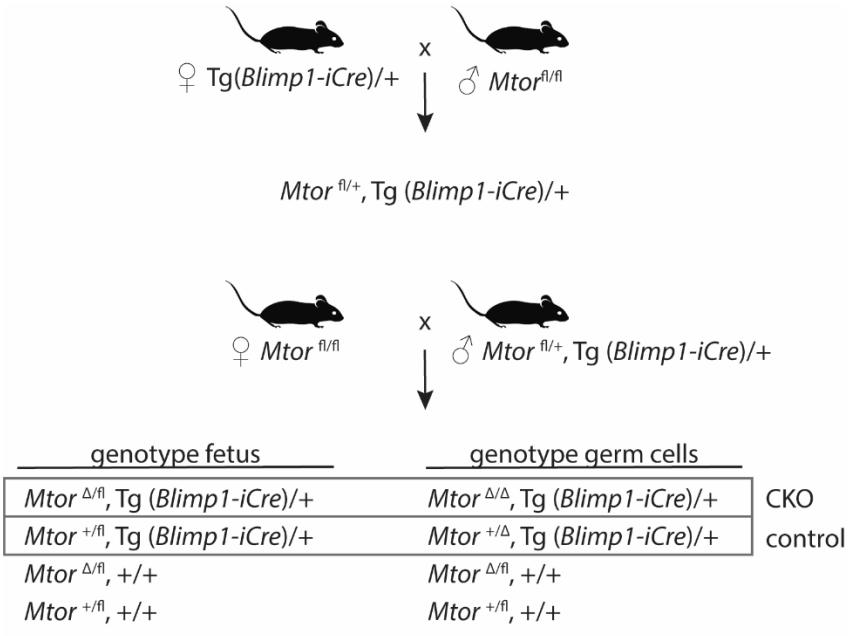

genotype fetus	genotype germ cells	
Mtor Δ/fl, Tg (*Blimp1-iCre*)/+	*Mtor* Δ/Δ, Tg (*Blimp1-iCre*)/+	CKO
Mtor +/fl, Tg (*Blimp1-iCre*)/+	*Mtor* +/Δ, Tg (*Blimp1-iCre*)/+	control
Mtor Δ/fl, +/+	*Mtor* Δ/fl, +/+	
Mtor +/fl, +/+	*Mtor* +/fl, +/+	

Figure 6.1: Strategy of conditional *Mtor* deletion in germ cells.

A Structure of *Mtor* floxed allele. LoxP sites are located upstream of the promoter region and in the intron preceding exon 6. Cre recombination leads to deletion of exon 1-5 in addition to the upstream promoter region. (Risson et al. 2009). **B** Breeding scheme for the generation of germ cell specific *Mtor* knockout mice. fl = floxed allele, + = wild-type, Δ = deleted floxed allele due to iCre recombination, Tg(*Blimp1-iCre*) = newly generated transgenic mice expressing iCre under the control of the *Blimp1* promoter (described in chapter 5); CKO = conditional knockout, control = genotype used as control;

Table 6.1: Recovery of conceptuses from (*Mtor*$^{fl/fl}$ x *Mtor*$^{fl/+}$ tg(*Blimp1-iCre*)/+) litters at E13.5.

total nr litters	average litter size (SD)	male (SD)	female (SD)	Cre positive (SD)	Cre negative (SD)	expected CKO (SD)	observed CKO (SD)
5	8.6 (±1.52)	3.8 (±1.92)	4.8±1.48	5 (±1) [a]	3.6 (±1.14) [a]	2.15 (±0.38)[b]	1.4 (±1.14)[b]

[a] Expected percentage of Cre^{+} inheritance from wild-type and heterozygous crosses is 50%. Chi-square test (X^2=1.271, df=4, p=0.86).

[b] Expected percentage of CKO genotype is 25%. Comparison between expected and observed value using paired Student's t-test (t=1.704, df=4, p=0.16).

6.2.2. Characterisation of *Mtor* $^{-/-}$ conditional knockout PGCs at E13.5

Control and *Mtor*$^{-/-}$ CKO genital ridges were analysed using the previously described immunofluorescence-based staining approach (Figure 4.1, p. 129). Briefly, germ cells were stained for germ cell proteins DAZL and MVH, in addition to pluripotency markers OCT4 and SSEA1.

In females, the overall appearance and gross tissue morphology of control and *Mtor*$^{-/-}$ CKO genital ridges was similar (Figure 6.2). *Mtor*$^{-/-}$ CKO genital ridges appeared slightly smaller compared to control genital ridges, possibly due to the observed slight growth retardation of *Mtor*$^{-/-}$ CKO embryos. Most strikingly, germ cell number (identified via MVH expression) was greatly reduced in *Mtor*$^{-/-}$ CKO genital ridges (arrows, Figure 6.2). While control samples contained many germ cells spread throughout the genital ridge, *Mtor*$^{-/-}$ CKO samples contained very few germ cells located towards the edges of the genital ridge (dashed line, Figure 6.2). The same observations were made when sections from the same sample were stained with OCT4 or DAZL to identify germ cells (Figure 6.4).

In male genital ridges, a similar drastic reduction in germ cell numbers was observed in *Mtor*$^{-/-}$ CKO genital ridges, as identified via DAZL expression (arrows, Figure 6.2). While control genital ridges contained many germ cells organized into seminiferous cords, *Mtor*$^{-/-}$ CKO samples contained only very few germ cells within the genital ridge (dashed line, Figure 6.2). Like in female *Mtor*$^{-/-}$ CKO tissues, the few observed germ cells were located towards the edges of the genital ridge, with no germ cells detected towards the middle of the tissue. The same observations were made when germ cells of the same tissue were identified via MVH or OCT4 expression (Figure 6.4). Of note, these observations are based on one male *Mtor*$^{-/-}$

CKO embryo analysed. Analysis of a second male *Mtor*$^{-/-}$ CKO genital ridge revealed complete lack of germ cells as identified via the lack of DAZL, OCT4 or MVH staining, possibly indicating eventual loss of germ cells in *Mtor*$^{-/-}$ CKO embryos.

Following these observations, *Mtor* deletion efficiency was analysed in the few detected germ cells at the protein level. In E13.5 control genital ridges, total mTOR protein was expressed evenly throughout the tissue with no clear enrichment in germ cells or somatic cells (Figure 6.3). In *Mtor*$^{-/-}$ CKO tissues, all identified germ cells (positive for germ cell protein MVH) stained negative for the mTOR protein (Figure 6.3). Surrounding somatic cells stained positive for mTOR. These results indicate successful recombination and deletion of the floxed *Mtor* allele in the few germ cells identified at E13.5.

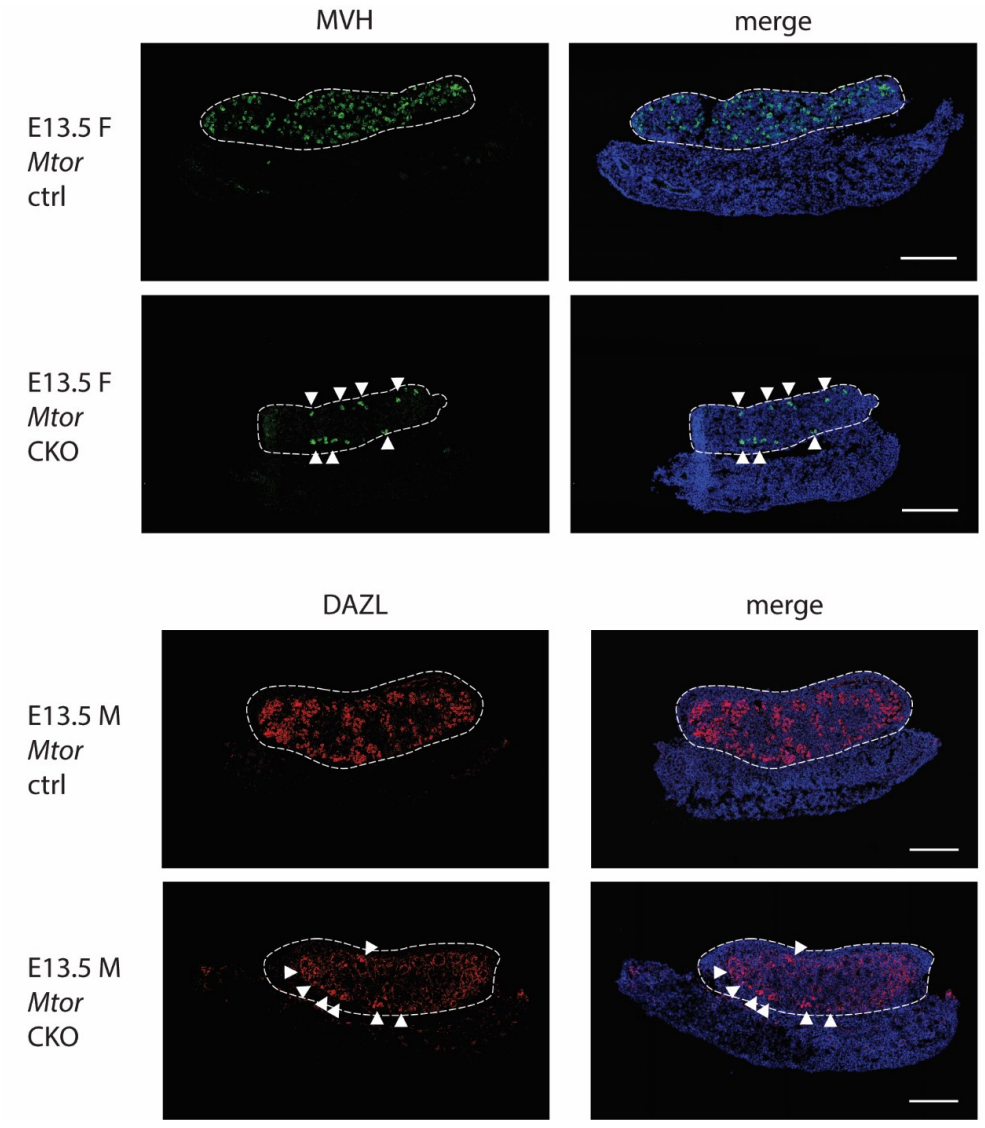

Figure 6.2: Morphology of control and *Mtor*$^{-/-}$ conditional knockout genital ridges at E13.5.

Immunofluorescence stainings of female and male genital ridges at E13.5. Germ cells were identified via mouse Vasa homologue (MVH) expression in female genital ridges and DAZL expression in male genital ridges. Nuclei were stained with DAPI (blue). White dashed line depicts gonad. Arrow heads point to germ cells. Representative images shown, n=1 (males), n=2 (females) (embryos per genotype), scale bar = 200µm; Control and CKO tissues were littermates. Genotype was analysed via PCR. Ctrl: *Mtor*$^{\Delta/+}$, Tg(*Blimp1-iCre*)/+; CKO: *Mtor*$^{\Delta/fl}$, Tg(*Blimp1-iCre*)/+;

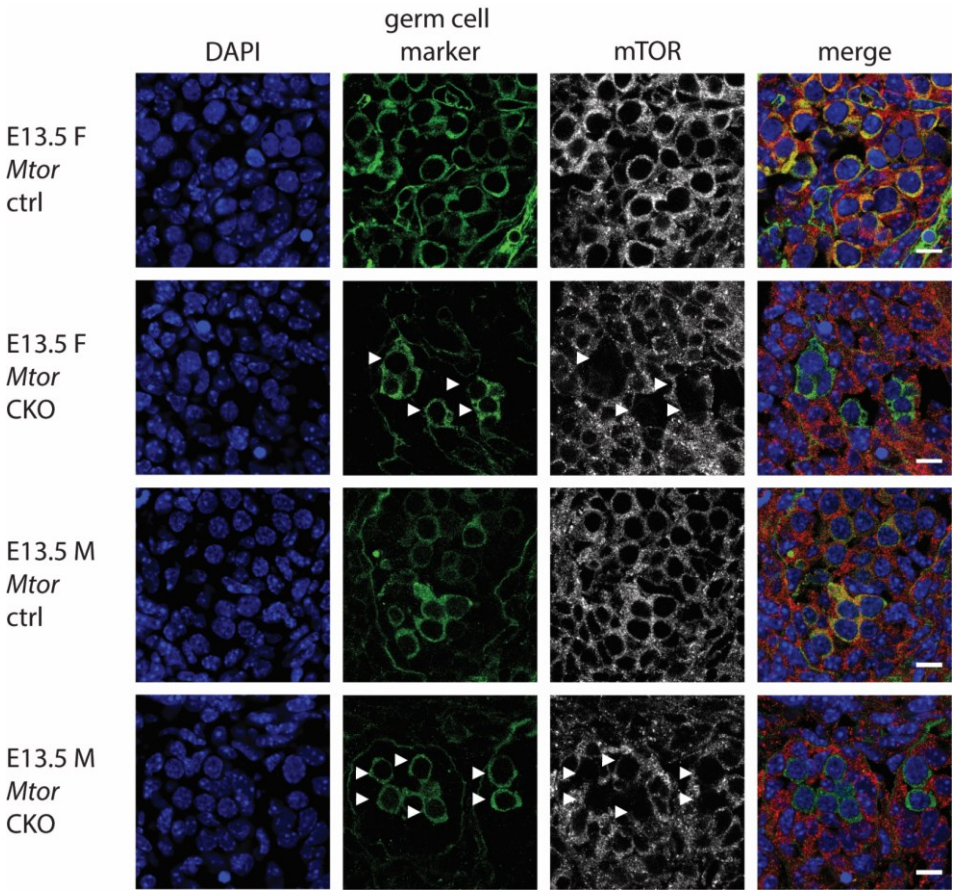

Figure 6.3: Loss of mTOR expression in *Mtor*$^{-/-}$ conditional knockout germ cells at E13.5.

Immunofluorescence stainings of female and male genital ridges at E13.5. Expression of total mTOR protein is shown. Germ cells were identified via mouse Vasa homologue (MVH) expression (germ cell marker), nuclei were stained with DAPI (blue). Arrow heads point to germ cells. Representative images shown, n=1 (males), n=2 (females) (embryos per genotype), scale bar = 10µm; Control and CKO tissues were littermates. Genotype was analysed via PCR. Ctrl: *Mtor*$^{\Delta/+}$, Tg(*Blimp1-iCre*)/+ CKO: *Mtor*$^{\Delta/fl}$, Tg(*Blimp1-iCre*)/+;

Next, the few remaining *Mtor*$^{-/-}$ CKO germ cells were analysed in more detail. In female genital ridges, all of the *Mtor*$^{-/-}$ CKO germ cells co-stained for MVH and DAZL, just like germ cells from control genital ridges (Figure 6.4 A). In addition, all identified *Mtor*$^{-/-}$ CKO germ cells co-stained for MVH and OCT4, while in control genital ridges, OCT4 expression was more heterogeneous among germ cells (Figure 6.4 A). SSEA1 expression was detected at varying levels in MVH positive control germ cells and *Mtor*$^{-/-}$ CKO germ cells (Figure 6.4 A). Of note, in *Mtor*$^{-/-}$ CKO genital ridges, DAPI staining revealed a higher number of pyknotic nuclei compared to control genital ridges, as identified by their small size, round shape and densely stained chromosomes, possibly indicating increased rates of cell death (observation only). Future work is needed to confirm this observation.

In male genital ridges, *Mtor*$^{-/-}$ CKO germ cells stained positive for MVH and DAZL or MVH and OCT4 (Figure 6.4 B). Further, most of the MVH positive *Mtor*$^{-/-}$ CKO germ cells also expressed SSEA1 at varying levels, similar to control germ cells (Figure 6.4 B). Of note, control as well as *Mtor*$^{-/-}$ CKO genital ridges formed seminiferous cords containing germ cells. In control genital ridges, seminiferous cords contained mainly germ cells as identified with germ cell markers. However, although in *Mtor*$^{-/-}$ CKO genital ridges seminiferous cords contained similar cell numbers, only very few of those cells were identified as germ cells (MVH, DAZL, OCT4 positive) (Figure 6.4 B). These observations are in line with previous reports of unperturbed genital ridge formation in the absence of primordial germ cells (Svingen and Koopman 2013).

Taken together, preliminary analysis of *Mtor*$^{-/-}$ CKO germ cells revealed that germ cell proteins DAZL, MVH, OCT4 and SSEA1 are expressed even in the absence of mTOR protein and mTOR signalling. Most strikingly, however, *Mtor*$^{-/-}$ CKO genital ridges contained greatly reduced germ cell numbers compared to control genital ridges at E13.5. These observations suggest that although mTOR signalling is dispensable for the correct expression of some key germ cell genes at E13.5, it is essential for the establishment or maintenance of correct germ cell numbers during normal germ cell development.

A

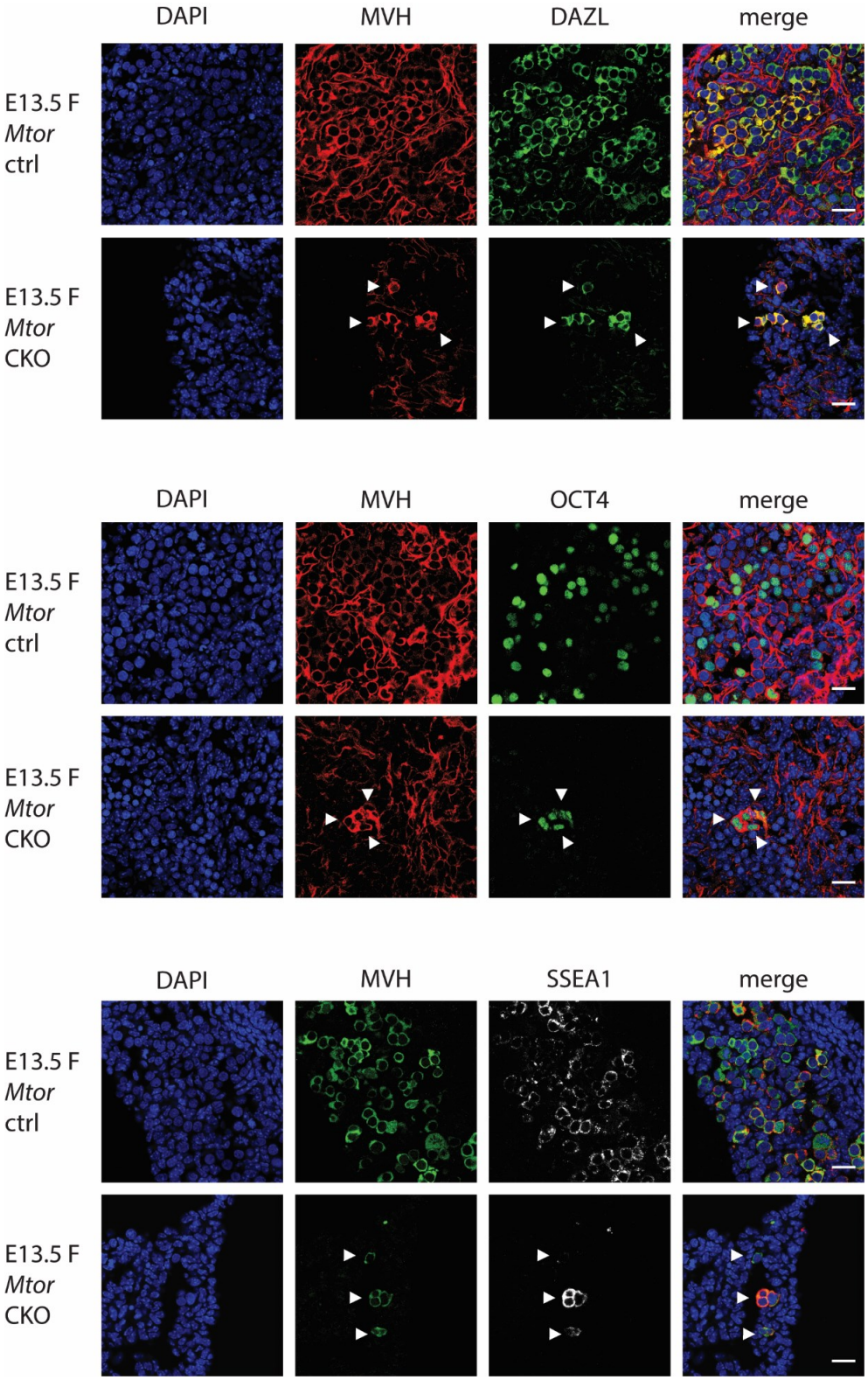
DAPI
MVH
DAZL
merge
E13.5 F
Mtor
ctrl
E13.5 F
Mtor
CKO
DAPI
MVH
OCT4
merge
E13.5 F
Mtor
ctrl
E13.5 F
Mtor
CKO
DAPI
MVH
SSEA1
merge
E13.5 F
Mtor
ctrl
E13.5 F
Mtor
CKO

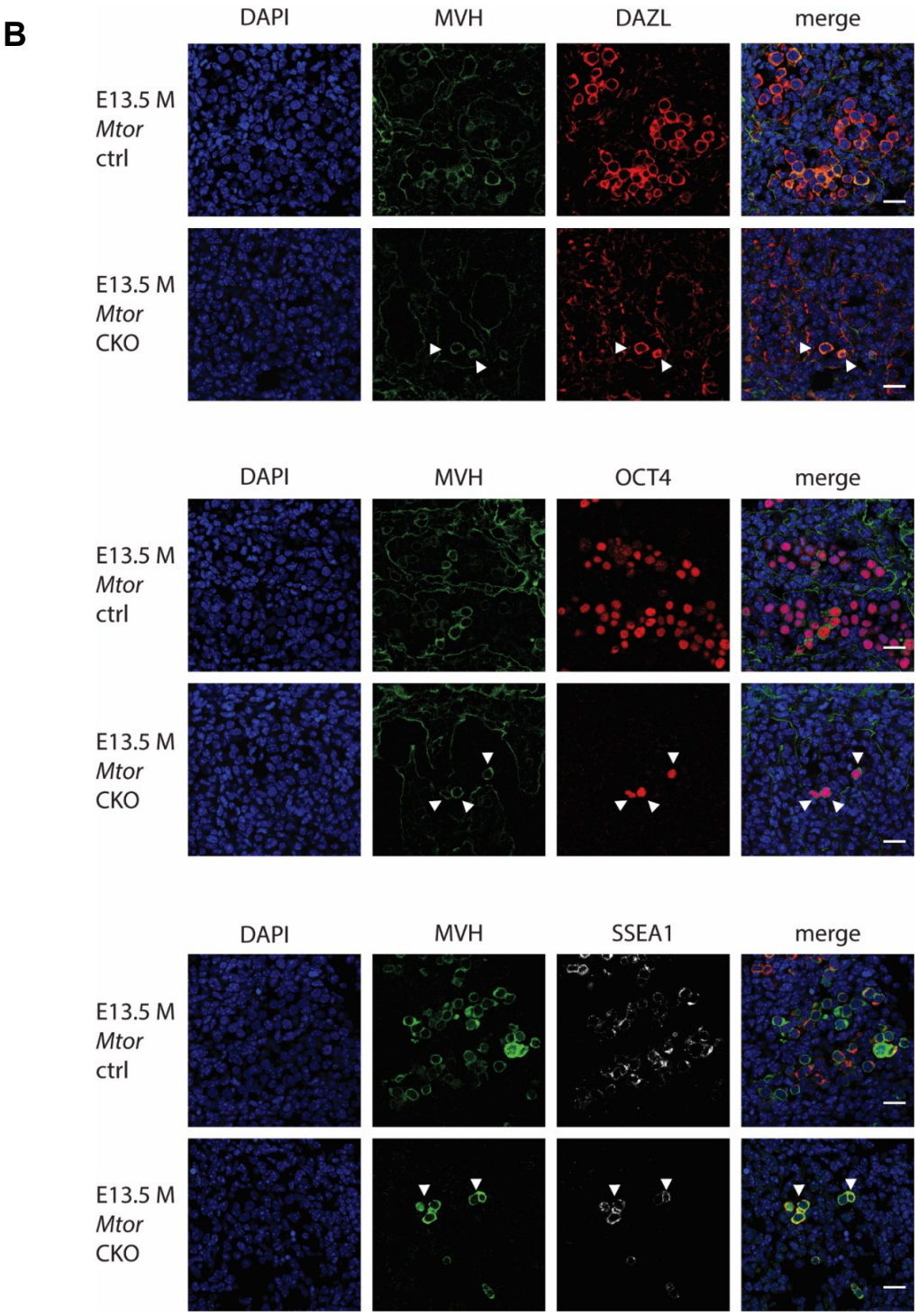

Figure 6.4: Expression of key germ cell proteins in control and *Mtor*$^{-/-}$ conditional knockout germ cells at E13.5.

Immunofluorescence stainings of female (**A**) and male (**B**) genital ridges at E13.5. Expression of MVH in combination with either DAZL, OCT4 or SSEA1 in germ cells is shown. Nuclei were stained with DAPI (blue). Arrow heads point to germ cells. Representative images shown. n=1 (males), n=2 (females) (embryos per genotype), scale bar = 20µm; Control and CKO tissues were littermates. Genotype was analysed via PCR. Ctrl: *Mtor*$^{\Delta/+}$, Tg(*Blimp1-iCre*)/+; CKO: *Mtor*$^{\Delta/fl}$, Tg(*Blimp1-iCre*)/+;

6.3. Discussion

Conditional deletion of *Mtor* using the new *Blimp1-iCre* driver line resulted in greatly reduced germ cell numbers compared to control tissues detected at E13.5. These exciting preliminary observations suggest a critical role of mTOR signalling during primordial germ cell development. The few surviving *Mtor*$^{-/-}$ CKO germ cells identified in genital ridges expressed key germ cell markers VASA, DAZL, OCT4 and SSEA1, suggesting gene or mRNA expression of these specific proteins is mTOR independent. A shift in timing of expression upon loss of mTOR signalling could occur though. Further work is needed to characterise the phenotype in more detail in order to start elucidating the underlying mechanism.

Low germ cell numbers in E13.5 genital ridges can be due to impaired germ cell proliferation, increased germ cell death and/or impaired germ cell migration towards the genital ridge. The observation that some *Mtor*$^{-/-}$ CKO germ cells were still identified in genital ridges indicates that mTOR signalling is not essential for migration. Of course, deletion of *Mtor* could still result in a migration defect and subsequently, an increased number of ectopic PGCs which are usually eliminated via apoptosis. However, I will focus on impaired cell proliferation and/or increased cell death as potential underlying causes of low germ cells numbers in *Mtor*$^{-/-}$ CKO genital ridges.

6.3.1. Increased germ cell death

Reduced germ cell numbers can be due to increased rates of cell death. In fact, in *Mtor* CKO female genital ridges, more pyknotic nuclei were observed compared to control genital ridges, indicating increased rates of cell death.

Increased cell death upon *Mtor* deletion can be the consequence of defective germ cell development. Active mTORC1 signalling, for instance, stimulates biological functions such as protein synthesis and cell metabolism (lipid and nucleotide biosynthesis, glycolysis), while inhibiting protein turnover processes such as autophagy and lysosome biogenesis (Saxton and Sabatini 2017). De-regulation of such processes could result in impaired developmental progression of germ cells, subsequently leading to cell death. This will be discussed in more detail in the next chapter (see 7.2.1, p. 222).

Alternatively, increased cell death upon *Mtor* deletion can be due to an impaired response to survival factors. PGCs are dependent on extrinsic and intrinsic signals for cell survival

during migration and when they reside in the genital ridge (Massimo De Felici and Klinger 2015). Several growth factors and cytokines have been identified as survival factors, including KIT ligand, LIF, FGF-7, SDF1 and IL-4, amongst others (Leitch, Tang, and Surani 2013).

Although the exact signal transducing pathways are not well studied, some evidence suggests that one elicited response is AKT activation (Massimo De Felici and Klinger 2015; De Miguel et al. 2002). Generally speaking, AKT signalling can promote cell survival via inhibition of apoptosis through several downstream effectors including GSK3b, FoxO1/3a transcription factors and pro-apoptotic factor BAD (Saxton and Sabatini 2017; Massimo De Felici and Klinger 2015). Whether AKT activates any of these downstream pathways in PGCs has not been studied.

mTOR signalling and AKT signalling are tightly linked. Active AKT can inhibit the negative mTORC1 regulator TSC1/2 (Saxton and Sabatini 2017). Further, mTORC2 can phosphorylate and fully activate AKT at the Ser473 site (Sarbassov et al. 2005). Of note, lack of pAKT (Ser473) upon mTORC2 ablation only impairs phosphorylation of some downstream targets, including FoxO1/3a transcription factors, while other AKT targets such as TSC2 and GSK3-β are not affected (Guertin et al. 2006; Jacinto et al. 2006).

Hence, it is possible that loss of intrinsic mTORC1 and mTORC2 signalling renders primordial germ cells unresponsive or less responsive to extrinsic survival factors, resulting in increased rates of cell death. In fact, short term *in vitro* culture experiments of E13.5 and E15.5 female germ cells indicate that basal levels of mTOR are required for cell survival (Lobascio et al. 2007), as addition of rapamycin (MTORC1 inhibitor) to the medium increases cell apoptosis (Lobascio et al. 2007). Future work is needed to first identify and quantify apoptotic cells in CKO genital ridges, followed by analysis of the underlying mechanism.

6.3.2. Impaired germ cell proliferation

Alternatively, reduced germ cell numbers can also be caused by reduced cell proliferation rates. PGCs proliferate from a starting founder population of about 40 PGCs at E7.25 to approximately 25.000 cells at E13.5 (P. P. L. Tam and Snow 1981). Many of the above mentioned survival factors also stimulate proliferation. KIT ligand, for instance, is required for PGC proliferation between E9.5 and E10.5 *in vivo* (Runyan et al. 2006) and *in vitro* during PGC culture (Godin et al. 1991; Yasuhisa Matsui et al. 1991; Dolci et al. 1991; M. Pesce et al. 1993).

Downstream of the C-KIT receptor, *in vitro* culture experiments of PGCs revealed that AKT signalling is activated likely via a PI3K independent pathway, promoting cell proliferation (De Miguel et al. 2002). Interestingly, an inhibitor against mTOR (rapamycin) also decreased PGC cell proliferation. Based on these observations, the authors suggested a model in which KIT ligand – C-KIT signalling likely drives germ cell proliferation via activation of mTOR through AKT or RAS/MEK/ERK signalling (De Miguel et al. 2002). Of note, *in vivo* migratory PGCs have been shown to have repressed ERK signalling, based on lack of phospho ERK and upstream FGFR2 (receptor) immunofluorescence staining at E8.75 and E8.5. (Grabole et al. 2013).

Although direct evidence of mTOR signalling mediating primordial germ cell proliferation is still missing, the concept of mTORC1 as a key mediator of cellular growth and proliferation is well accepted (Laplante and Sabatini 2009, 2012; Saxton and Sabatini 2017). In favourable conditions, mTORC1 signalling promotes several anabolic processes and inhibits catabolic processes. Protein translation, for instance, is promoted via inactivation of downstream mTORC1 effector 4E-BP1, which selectively regulate translation of specific mRNA subclasses. These subclasses encode proteins involved in general protein synthesis (ribosomal proteins, elongation factors and translation initiation factors) and proteins involved in cell proliferation, cell cycle and survival (Meyuhas and Kahan 2015; Musa et al. 2016; Dowling et al. 2010). Further, mTORC2 signalling is tightly linked with AKT signalling, which has many downstream effectors involved in cell cycle progression and proliferation (Xu et al. 2012).

At later stages in germ cell development, condition *Mtor* deletion (using *Vasa-Cre*, deletion form E15.5 onwards) leads to impaired proliferation of spermatogonial stem cells (Serra et al. 2017). Further, in ESC cells, conditional deletion of *Mtor* or chemical inhibition of mTOR results in greatly reduced proliferation rates and cell size (Gangloff et al. 2004; Murakami et al. 2004)

Hence, it is likely that germ cell proliferation is affected to some extent upon *Mtor* deletion. Future experiments are needed to further characterise possible cell proliferation defects and identify downstream signalling mechanisms.

6.3.2.1. Conclusion & Future Work

To conclude, given the strong phenotype and based on the described literature, a combination of impaired cell survival/increased cell death and impaired cell proliferation are most likely the main causes of reduced germ cell numbers.

To characterise the phenotype in more detail and experimentally determine the underlying cause of reduced germ cell numbers, future work is needed. Detailed analysis of germ cell numbers over different time points preceding E13.5 will reveal kinetics of germ cell number changes. In addition, analysis of cell apoptosis rates in combination with analysis of cell proliferation rates will allow to determine why and how germ cell numbers change**.** For this**,** TUNEL assay or immunofluorescence staining of caspases and BrdU incorporation can be used. Once the underlying cause for reduced germ cells numbers is identified, the underlying mechanism can be elucidated. Further, analysis of later time points will reveal whether the few remaining germ cells survive or eventually undergo cell death. In males, a second biological *Mtor*$^{-/-}$ CKO genital ridge did not contain any germ cells, suggesting that germ cells eventually undergo cell death during embryonic development (in males at least).

Of note, it should be mentioned that Blimp1-iCre is also expressed in the hindgut epithelium. Therefore it is likely that surrounding somatic cells which produce molecules involved in migration, survival and proliferation also lack mTOR signalling.

7. Final Discussion

7.1. On the role of mTORC1 signalling in gonadal PGCs

Upon their entry into the genital ridge, germ cells undergo epigenetic reprogramming, induce expression of genes involved in progression of gametogenesis and initiate sexual differentiation including entry into meiosis or mitotic arrest (Saitou and Yamaji 2012).

To what extent inductive signalling from the gonadal environment plays a role in the initiation of these processes, in addition to intrinsic signalling, is still not well understood. Especially extrinsic signalling events and their role in inducing sexual differentiation and initiation of meiosis have been extensively studied (see 1.1.5, p. 33).

Preceding entry into meiosis, primordial germ cells change their gene expression profiles and transition to gametogenesis-competent cells (Gill et al. 2011). This licensing step is driven by DAZL and allows cells to progress through male or female differentiation (Gill et al. 2011). Early observational studies *in vivo* and *in vitro* support the hypothesis that germ cell licensing occurs in the absence of the genital ridge environment. Ectopic germ cells in the adrenal glands, as well as isolated germ cells cultured with embryonic lung cells or on feeder cells can enter meiosis in a cell-autonomous manner (Zamboni and Upadhyay 1983; A. McLaren and Southee 1997; Chuma and Nakatsuji 2001). However, a more recent study suggests that germ cell licensing is dependent on extrinsic signals from the genital ridge (Y.-C. Hu et al. 2015). In *Gata4* conditional knockout embryos, which lack genital ridges, primordial germ cells were not able to undergo licensing – while expression of pluripotency genes was maintained, DAZL and MVH expression was not induced and meiosis could not be initiated (Y.-C. Hu et al. 2015).

Preliminary data suggested that the AKT-mTORC1-4E-BP1 signalling axis might be activated in PGCs upon entry into the genital ridge (Peter Hill, personal communication). During my PhD, a detailed analysis of mTORC1 signalling in primordial germ cells was carried out to take an extensive look at the role of mTORC1 signalling during germ cell development.

Upstream of mTORC1, I have shown that total AKT protein expression is kept low and fairly constant in wild-type primordial germ cells, while activated pAKT (Ser473) was detected in up to 40% of PGCs between E11.5 and E12.5. Although AKT activation was only detected in a subset of PGCs, this observed activation might be transient and possibly all PGCs have to activate AKT at some point for a short period. Transient activation could allow for tight control of AKT signalling and avoid aberrant effects. Mice with AKT overactivation via

conditional PTEN deletion have increased germ cell proliferation and testicular teratomas (in male mice only) (Kimura et al. 2003). On the other hand, global AKT1$^{-/-}$ deletion leads to increased cell apoptosis and combined global deletion of two AKT isoforms is either embryonic lethal or post-natally lethal (W. S. Chen et al. 2001; Yu and Cui 2016). Future work is needed to determine the role of AKT signalling in germ cells *in vivo* and to identify possible upstream activators of mTORC1 signalling.

Further, analysis of downstream effectors of mTORC1 signalling revealed that mTORC1 signals mainly via the effector 4E-BP1, rather than the S6K1-S6 signalling axis, in wild-type germ cells. In fact, S6K1-S6 signalling was neither particularly enriched in germ cells nor somatic cells and deletion of S6 kinases revealed only a minor phenotype. These observations suggest that S6 kinases are not essential for germ cell development in the mouse.

In contrast, active mTORC1-4E-BP1 signalling (as judged by p4E-BP1) was detected specifically in germ cells from E10.5 onwards, indicating a possible role of mTORC1-4E-BP1 signalling during primordial germ cell development. Interestingly, the highest levels of active mTORC1-4E-BP1 signalling in wild-type germ cells coincide with two key germ cell processes, epigenetic reprogramming (E11.5) and initiation of meiosis (E13.5 F).

Epigenetic reprogramming and mTORC1 signalling. Gonadal epigenetic reprogramming entails global loss of DNA methylation (including genomic imprints) as well as the loss of repressive histone marks (see 1.2.2) (Hajkova 2011). Subsequently, the epigenome of PGCs reaches the most 'naïve' state during development. Reprogramming events enable the expression of "germline reprogramming-responsive" genes which include genes involved in gametogenesis and meiosis (Hill et al. 2018). Further, PGCs exhibit global hypertranscription at E11.5 (compared to somatic cells), including increased expression of ribosomal proteins (Percharde, Wong, and Ramalho-Santos 2017)

Interestingly, coinciding with these reprogramming events, I have shown that total 4E-BP1 protein levels increase significantly from E10.5 onwards and that mTORC1-4E-BP1 signalling is first detected at E11.5. 4E-binding proteins selectively regulate translation of specific mRNA subclasses with certain structural features (Meyuhas and Kahan 2015; Musa et al. 2016). Given the low levels of repressive epigenetic marks following epigenetic reprograming in combination with the observed hypertranscription, mTORC1-4E-BP1 mediated translational regulation could represent an additional mechanism of tightly controlling gene/protein expression. However, further work is needed to elucidate the role

of mTORC1-4E-BP1 signalling during or shortly after reprogramming events in primordial germ cells.

Meiosis and mTORC1 signalling. Surprisingly, only male 4E-BP1 knockout germ cells were affected upon loss of 4E-BP1 (increased SSEA1 and SCP3 levels), while in female germ cells no phenotype was detected. These observations likely reflect the observed differences of mTORC1-4E-BP1 signalling in wild-type germ cells and possibly indicate a sexually dimorphic role of 4E-BPs. Male germ cells had lower p4E-BP1 signal compared to female germ cells at E12.5 and E13.5, indicating lower levels of mTORC1-4E-BP1 signalling. As females already have high mTORC1-4E-BP1 signalling to start with, the loss of 4E-BP1 (mimicking active mTORC1-4E-BP1 signalling) might therefore affect male knockout germ cells more strongly.

At E13.5, female germ cells initiate meiosis. High mTORC1-4E-BP1 signalling at E13.5 presumably leads to increased rates of translation. In contrast, in male germ cells, lower levels of mTORC1-4E-BP1 signalling presumably leads to more active 4E-BP1 protein and the translational repression of specific mRNAs. Consistently with this, male 4E-BP1 knockout germ cells did show a delayed downregulation of SSEA1 and SCP3, as detected at E13.5 and E15.5 respectively.

It can be therefore hypothesized that mTORC1-4E-BP1 signalling is involved in the translational regulation of specific mRNAs involved in gametogenesis and meiosis, ensuring female germ cells enter meiosis while male germ cells inhibit meiosis. However, future work is needed to determine whether and to what extent translational regulation mediated by mTORC1-4E-BP1 signalling plays a role during sexual differentiation.

7.1.1. mTORC1 – 4E-BP1 signalling and possible delayed male germ cell differentiation

A possible developmental delay specifically in male germ cells (based on delayed SSEA1 and SCP3 downregulation) upon 4E-BP1 deletion was observed. This is particularly interesting with respect to risk of testicular germ cell tumours as part of the human testicular dysgenesis syndrome (TDS).

Human testicular dysgenesis syndrome is comprised of several disorders affecting male reproduction, including (but not limited to) poor semen quality and testicular cancer in young adults (type II) (Skakkebæk, Rajpert-De Meyts, and Main 2001; Virtanen et al. 2005). Although these disorders are only visible postnatally, it has been hypothesized that they have a common origin during foetal development, based on clinical observations and epidemiological studies (Skakkebæk, Rajpert-De Meyts, and Main 2001; Virtanen et al. 2005). Rare genetic abnormalities can result in the syndrome (such as androgen insensitivity and 45X0/46XY), however, in most cases the underlying causes are unclear. *In utero* exposure to endogenous or environmental factors (in particular endocrine disruptors), which negatively affect male gonadal development, are hypothesized to play a role (Virtanen et al. 2005; Skakkebæk, Rajpert-De Meyts, and Main 2001).

Testicular cancers (type II) arise from premalignant carcinoma in-situ cells (CIS), which can be detected in human testes postnatally. It is thought that CIS cells develop from primordial germ cells or gonocytes which fail to differentiate properly due to impaired gonadal development and defects in male sexual differentiation (MEYTS et al. 1998).

Given our observations of a possible delay in male germ cell differentiation upon genetic ablation of 4E-BP1, mimicking aberrant mTORC1-4E-BP1 activation, one could speculate that the mTORC1-4E-BP1 signalling axis plays a role in the formation of CIS cells, potentially increasing the risk of germ cell tumours. In fact, mTORC1 signalling is hyperactivated in many human cancers (Saxton and Sabatini 2017), with the downstream 4E-BP1/eIF4E signalling axis and translational control being complex and intensively studied (Ruggero 2013). In several mouse cancer models, for instance, downstream phosphorylation and inactivation of 4E-BP1 and subsequent promotion of translational initiation is a critical step in cancer development (Hsieh et al. 2012, 2010).

Surprisingly, analysis of global 4E-BP single and double knockout mouse lines (mimicking active mTORC1-4E-BP1 signalling), including adult testis, did not reveal a strong phenotype. However, the lack of testicular cancer in adult mice is not surprising, given that the mouse as a model system does not develop testicular cancers of this sub-type (type II) (Oosterhuis and Looijenga 2005). Specific inbred mouse strains (such as 129, 129-Ter) spontaneously develop testicular teratomas (Stevens and Hummel 1957), which are similar to the type I germ cell tumours occurring in human infants (Oosterhuis and Looijenga 2005). In contrast, the more common type I testicular cancer typically found in young human males and part of the testicular dysgenesis syndrome does not occur in these or any other mouse strains (R. Zhu, Bhattacharya, and Matin 2007; Oosterhuis and Looijenga 2005). Differing developmental time frames between mouse (months) and human (years) germ cell development have been speculated to play a role (R. Zhu, Bhattacharya, and Matin 2007). It is hypothesized that although carcinoma in situ cells are formed during embryogenesis (Skakkebæk et al. 1987), the prolonged time until puberty in humans (about 10 years) allows these cells to acquire additional genetic/epigenetic changes, driving formation of more aggressive germ cell tumours (Dolci, Campolo, and De Felici 2015).

Based on these observations and using our model system, it is impossible to experimentally validate whether the observed delayed differentiation in male germ cells upon 4E-BP1 deletion promotes formation of CIS cells and subsequently increases the risk of testicular cancer. Interestingly, *in utero* dibutyl phthalate exposed rats develop similar symptoms to human TDS, however, they did not develop germ cell tumours likely due to death of abnormal gonocytes (Fisher et al. 2003). So far, no animal model for testicular germ cell tumours (type II) has been reported (Oosterhuis and Looijenga 2005).

In addition, the mixed genetic background used in this study is not ideal to study testicular teratomas either, which are similar to type I germ cell tumours (Oosterhuis and Looijenga 2005). Spontaneous formation of testicular teratomas is in fact highly dependent on the genetic background. For instance, the 129-Ter mouse strain carries a spontaneous mutation in the Dnd1 gene (Youngren et al. 2005), leading to loss of expression and an extremely high incidence (94%) of germ cell teratomas (Stevens 1973; Noguchi and Noguchi 1985). Interestingly, the TER defect only causes tumours on the inbred 129 genetic background (Noguchi and Noguchi 1985; Cook et al. 2011). Further studies on different genetic backgrounds identified that the primary defect is germ cell loss after E8.5 in all strains at least partially caused by BAX-mediated cell death (Sakurai et al. 1995; Cook et al. 2009).

Hence, given the used model system and genetic background, it is possibly that upon 4E-BP1 deletion any potentially aberrant germ cells are likely eliminated before they can transform and contribute to testis cancer or teratomas. Further, the only minor phenotype detected in male 4E-BP1 knockout germ cells can be due to compensatory mechanisms at play. It would be interesting to see if on a pure 129 background, deletion of 4E-BP1 does lead to an increased incidence of teratomas due to delayed germ cell differentiation. In addition, it would be interesting to test the effect of complete loss of mTORC1-4E-BP1 signalling in germ cells via overexpression of a constitutively active, phospho-mutant 4E-BP1 protein.

7.2. *Mtor* deletion in PGCs

Conditional deletion of *Mtor* resulted in greatly reduced germ cell numbers compared to control genital ridges, demonstrating for the first time a critical role of mTOR signalling during primordial germ cell development. Some possible causes underlying this phenotype, such as impaired germ cell survival and/or impaired germ cell proliferation, have been discussed in the previous chapter. Here, I want to focus on a possible impaired developmental progression of primordial germ cells upon the loss of mTOR signalling.

7.2.1. On the role of mTOR during the developmental progression of germ cells

Between E11.5 and E13.5, similar to mESCs, gonadal PGCs express the pluripotency network (Seisenberger et al. 2012). From E13.5 onwards, transcription of pluripotency genes is downregulated (more rapid in females), while genes involved in meiosis are induced specifically in female germ cells (Seisenberger et al. 2012). As sexual differentiation progresses, PGCs either commit to oogenesis or spermatogenesis (Bowles and Koopman 2010). Subsequently, PGCs lose the ability to reprogram to pluripotent EGCs *in vitro* – the efficiency of EGC derivation sharply decreases from E13.5 onwards, and at E15.5, no EGCs can be derived (Yasuhisa Matsui, Zsebo, and Hogan 1992; Kimura et al. 2008).

How the loss of mTOR signalling affects developmental progression and sexual differentiation of gonadal germ cells is currently not known. Several studies in mouse ESCs indicate that low levels of mTOR signalling are necessary to maintain pluripotency *in vitro* and upregulation of mTOR signalling promotes differentiation (see 1.4.2, p.60) (Agrawal et al. 2014; Cherepkova, Sineva, and Pospelov 2016; Gómez-Salinero et al. 2016; Y. Zhu et al.

2018). Furthermore, differentiation in wild-type mESCs is accompanied via a global increase in protein synthesis and mTORC1-4E-BP1 signalling (Sampath et al. 2008).

However, a recently published genome-wide CRISPR-Cas9 knockout screen in mESCs reveals a more complex picture of mTOR signalling and its role during differentiation (Li et al. 2018). Deletion of different components of the mTOR signalling cascade results in opposing phenotypes of either accelerated or delayed differentiation upon exit of naïve pluripotency (as determined by loss of expression of REX1 GFP reporter). In two mutant cell lines lacking the negative mTORC1 regulator Gator1 or TSC2, it has further been shown that context-dependent rewiring of the signalling cascade has opposing effects on the activation status of GSK3b, which underlies the observed difference in phenotypes (Li et al. 2018). Deletion of either protein results in the overactivation of mTORC1-S6K1-S6 signalling axis. However, loss of Gator1 leads to loss of pAKT (Ser473), subsequent increased active GSK3b and accelerated differentiation. In contrast, loss of TSC2 leads to increased pAKT (Ser473) levels, AKT-independent increased phosphorylation of GSK3b (likely via S6K1 directly) and delayed differentiation (Li et al. 2018). In summary, in mESCs, the role of mTORC1 signalling is complex and context-dependent, able to promote either maintenance of pluripotency or differentiation.

Based on these observations, it is likely that developmental progression in Mtor$^{-/-}$ CKO germ cells is affected in some way. *Mtor*$^{-/-}$ CKO germ cells do express DAZL upon entry into the genital ridge, which is a prerequisite for germ cells to be able to transition to "gametogenesis competent cells", able to respond to extrinsic cues and initiate meiosis or spermatogenesis (Gill et al. 2011). At later stages in germ cell development, mTOR deletion (using Vasa-Cre, deletion from E15.5 onwards) leads to impaired differentiation of spermatogonial stem cells (Serra et al. 2017). In line with that, but in sharp contrast to mESCs, mTORC1 overactivation (via conditional deletion of TSC1 and TSC2) in adult spermatogonial stem cells results in increased differentiation (Hobbs et al. 2015; Wang et al. 2016).

Future studies analysing later time points are required to see whether mTOR$^{-/-}$ CKO germ cells are able to progress further in development and undergo sexual differentiation, including entry into and successful progression of meiosis.

7.2.2. On the role of mTOR and the link to translation

Regulation of protein translation is mediated via mTORC1 signalling and downstream effectors S6 kinases and 4E-binding proteins (Musa et al. 2016; Magnuson, Ekim, and Fingar

2012). Upon *Mtor* deletion, loss of mTORC1 signalling presumably results in reduced or absent S6K1 activation. Global deletion of S6 kinases (mimicking loss of mTORC1-S6K1 signalling) did not reveal a big phenotype, suggesting that S6 kinases are not likely to underlie the observed phenotype in *Mtor*$^{-/-}$ CKO germ cells.

On the other hand, loss of mTORC1 signalling upon *Mtor* deletion presumably leads to increased levels of the active 4E-BP1 protein, negatively regulating translation. This is the opposite situation of global 4E-BP1 deletion (mimicking mTORC1-4E-BP1 activation), when only a minor phenotype in male germ cells was observed.

In combination with the observed active mTORC1-4E-BP1 signalling in wild-type germ cells, the strong phenotype upon *Mtor* deletion further strengthens the hypothesis of a role for mTORC1-4E-BP1 mediated translational regulation during germ cell development. To what extent protein translation is affected upon deletion of *Mtor* in primordial germ cells is not known at this point. Given the complexity of mTOR signalling, it is likely that the observed phenotype in *Mtor*$^{-/-}$ CKO germ cells is due to the combined loss of mTORC1 and mTORC2 signalling, possibly involving several downstream effectors. Nevertheless, future work will involve detailed analysis of how protein translation mediated via 4E-BPs is affected upon loss of *Mtor* in primordial germ cells.

7.3. The generation of a new *Blimp1-iCre* line

Last but not least, I describe a successful generation of a new *Blimp1-iCre* mouse line. The new *Blimp1-iCre* mouse line exhibits very high recombination efficiency at E9.5 (100%) and E11.5 (99.11%). Most importantly, litter sizes are normal which will allow a more efficient generation of germ cell specific knockout models. Characterisation of the iCre expression pattern showed expression in the hindgut epithelium, developing heart, branchial arches, which is in line with endogenous Blimp1 expression. Taken together, this *Blimp1-iCre* driver line represents a new tool which, beyond being an invaluable tool for our team, will benefit the whole germline community.

7.4. Future Work

mTOR is a multifaceted kinase nucleating two distinct signalling complexes (mTORC1 and mTORC2) through which a number of effectors are stimulated or inhibited in order to exert varied biological functions (Saxton and Sabatini 2017).

Based on the observations in this study, many new questions arise and several important questions remain to be addressed. First and foremost, what leads to the reduced germ cell number observed at E13.5 upon *Mtor* deletion? In order to answer this question, a detailed analysis of germ cell numbers from E8.0 to E13.5 in control and mTOR CKO genital ridges is required. This can be achieved through IF analysis of consecutive sections of the whole embryonic trunk (E8.0-E10.5) or genital ridge (from E11.5 onwards) and subsequent counting of germ cells. To determine defects in proliferation or increased apoptosis rates, markers such as KI-67 or cleaved caspase 3 can be used in combination with an IF approach to determine the percentage of proliferating and apoptotic cells. In addition, combination of *Mtor* deficiency with $Bax^{-/-}$ deficiency (Knudson et al. 1995), to repress apoptosis, would be a genetic approach to test if germ cell numbers can be rescued and whether BAX mediated cell death plays a role.

Second, what are the downstream signalling pathways through which mTOR signals? What role does mTORC1-4E-BP1 mediated translation play during PGC development? In order to investigate how global translation or translation of selective mRNA transcripts changes upon *Mtor* deletion, RNA sequencing of ribosome associated RNA and total RNA is the method of choice. Separation can be achieved either through sucrose gradient centrifugation (Potireddy et al. 2006) or genetically, using the Ribotag mouse line which expresses an HA tagged ribosomal protein (Rpl22) (Sanz et al. 2009). The tagged protein is incorporated into active polyribosomes, allowing isolation of actively translated mRNA transcripts. Combination of the $mTOR^{fl/fl}$ line with the Oct4-GFP line (Yeom et al. 1996) and the Ribotag line will allow isolation of PGCs and somatic control cells based on GFP expression. Further, using an antibody against HA, polyribosomes containing actively translating mRNAs can be isolated through immunoprecipitation of HA-tagged RPL22. RNA sequencing of total mRNAs and ribosome associated mRNAs will give some insights into which mRNAs are actively translated in PGCs and how these mRNAs change upon *Mtor* deletion. Low cell numbers might be a potential bottleneck to perform the IP though and current optimization is ongoing. Alternatively, changes in global translational rates can be assessed using labelling

of newly translated proteins with OPP, a puromycin analogue, followed by visualization using a Click-it assay (Percharde, Wong, and Ramalho-Santos 2017).

In addition, a different transgenic mouse line overexpressing a phospho-mutant 4E-BP1 protein (mimicking loss of mTOR-4E-BP1 signalling), can be analysed (Dominic Withers, personal communication). If the mTORC1-4E-BP1 mediated translational regulation is crucial in PGCs, a more severe phenotype, possibly similar to the observed phenotype in mTOR CKO germ cells, is expected upon loss of signalling in contrast to the mild phenotype upon 4E-BP1 deletion.

Apart from translation, additional roles of mTOR signalling in PGCs can be investigated probing common downstream signalling targets using an IF approach. For instance, putative activation of autophagy upon mTOR deletion can assessed using an antibody against ULK1 or LC3-II.

Alternatively, in case the low germ cell numbers in the conditional mTOR knockout embryos are a limiting factor, an inverse genetic approach can be pursued. Deletion of the negative mTORC1 regulators TSC1 (Kwiatkowski et al. 2002) and/or TSC2 (Onda et al. 1999) will lead to hyperactive mTORC1 signalling (H. Zhang et al. 2003), which presumably will not affect germ cell numbers as severely. This will allow further analysis to depict the role of mTOR signalling during germ cell development.

In summary, the presented findings in this thesis mark only the beginning of elucidating the essential role of mTOR signalling during primordial germ cell development. Future studies will lead to a better understanding of the underlying signal transducing pathways and possibly identify extrinsic signals which lead to mTOR activation at specific times.

8. Bibliography

Abaza, Irina, and Fátima Gebauer. 2008. "Trading Translation with RNA-Binding Proteins." *RNA (New York, N.Y.)* 14 (3): 404–9.

Adams, Ian R., and Anne McLaren. 2002. "Sexually Dimorphic Development of Mouse Primordial Germ Cells: Switching from Oogenesis to Spermatogenesis." *Development* 129 (5).

Adhikari, D., G. Flohr, N. Gorre, Y. Shen, H. Yang, E. Lundin, Z. Lan, M. J. Gambello, and K. Liu. 2009. "Disruption of Tsc2 in Oocytes Leads to Overactivation of the Entire Pool of Primordial Follicles." *Molecular Human Reproduction* 15 (12): 765–70.

Adhikari, D., W. Zheng, Y. Shen, N. Gorre, T. Hamalainen, A. J. Cooney, I. Huhtaniemi, Z.-J. Lan, and K. Liu. 2010. "Tsc/MTORC1 Signaling in Oocytes Governs the Quiescence and Activation of Primordial Follicles." *Human Molecular Genetics* 19 (3): 397–410.

Agrawal, Pooja, Joseph Reynolds, Shereen Chew, Deepak A Lamba, and Robert E Hughes. 2014. "DEPTOR Is a Stemness Factor That Regulates Pluripotency of Embryonic Stem Cells." *The Journal of Biological Chemistry* 289 (46): 31818–26.

Ahmed, Emad A., and Dirk G. de Rooij. 2009. "Staging of Mouse Seminiferous Tubule Cross-Sections." In , 263–77. Humana Press, Totowa, NJ.

Aitken, Colin Echeverría, and Jon R Lorsch. 2012. "A Mechanistic Overview of Translation Initiation in Eukaryotes." *Nature Structural & Molecular Biology* 19 (6): 568–76.

Alessi, Dario R., Mark T. Kozlowski, Qing-Ping Weng, Nick Morrice, and Joseph Avruch. 1998. "3-Phosphoinositide-Dependent Protein Kinase 1 (PDK1) Phosphorylates and Activates the P70 S6 Kinase in Vivo and in Vitro." *Current Biology* 8 (2): 69–81.

Alessi, S R James, C P Downes, A B Holmes, P R Gaffney, C B Reese, and P Cohen. 1997. "Characterization of a 3-Phosphoinositide-Dependent Protein Kinase Which Phosphorylates and Activates Protein Kinase Balpha." *Current Biology : CB* 7 (4): 261–69.

Ancelin, Katia, Ulrike C. Lange, Petra Hajkova, Robert Schneider, Andrew J. Bannister, Tony Kouzarides, and M. Azim Surani. 2006. "Blimp1 Associates with Prmt5 and Directs Histone Arginine Methylation in Mouse Germ Cells." *Nature Cell Biology* 8 (6): 623–30.

Anderson, Ericka L, Andrew E Baltus, Hermien L Roepers-Gajadien, Terry J Hassold, Dirk G de Rooij, Ans M M van Pelt, and David C Page. 2008. "Stra8 and Its Inducer, Retinoic Acid, Regulate Meiotic Initiation in Both Spermatogenesis and Oogenesis in Mice." *Proceedings of the National Academy of Sciences of the United States of America* 105 (39): 14976–80.

Anderson, Robert, Trevor K. Copeland, Hans Schöler, Janet Heasman, and Christopher Wylie. 2000. "The Onset of Germ Cell Migration in the Mouse Embryo." *Mechanisms of Development* 91 (1–2): 61–68.

Ara, Toshiaki, Yuri Nakamura, Takeshi Egawa, Tatsuki Sugiyama, Kuniya Abe, Tadamitsu Kishimoto, Yasuhisa Matsui, and Takashi Nagasawa. 2003. "Impaired Colonization of the Gonads by Primordial Germ Cells in Mice Lacking a Chemokine, Stromal Cell-Derived Factor-1 (SDF-1)." *Proceedings of the National Academy of Sciences of the United States of America* 100 (9): 5319–23.

Aramaki, Shinya, Katsuhiko Hayashi, Kazuki Kurimoto, Hiroshi Ohta, Yukihiro Yabuta, Hiroko Iwanari,

Yasuhiro Mochizuki, et al. 2013. "A Mesodermal Factor, T, Specifies Mouse Germ Cell Fate by Directly Activating Germline Determinants." *Developmental Cell* 27 (5): 516–29.

Bacquer, Olivier Le, Emmanuel Petroulakis, Sabina Paglialunga, Francis Poulin, Denis Richard, Katherine Cianflone, and Nahum Sonenberg. 2007. "Elevated Sensitivity to Diet-Induced Obesity and Insulin Resistance in Mice Lacking 4E-BP1 and 4E-BP2." *The Journal of Clinical Investigation* 117 (2): 387–96.

Baltus, Andrew E, Douglas B Menke, Yueh-Chiang Hu, Mary L Goodheart, Anne E Carpenter, Dirk G de Rooij, and David C Page. 2006. "In Germ Cells of Mouse Embryonic Ovaries, the Decision to Enter Meiosis Precedes Premeiotic DNA Replication." *Nature Genetics* 38 (12): 1430–34.

Banko, Jessica L, Francis Poulin, Lingfei Hou, Christine T DeMaria, Nahum Sonenberg, and Eric Klann. 2005. "The Translation Repressor 4E-BP2 Is Critical for EIF4F Complex Formation, Synaptic Plasticity, and Memory in the Hippocampus." *The Journal of Neuroscience : The Official Journal of the Society for Neuroscience* 25 (42): 9581–90.

Bao, Jianqiang, Jingwen Wu, Andrew S. Schuster, Grant W. Hennig, and Wei Yan. 2013. "Expression Profiling Reveals Developmentally Regulated LncRNA Repertoire in the Mouse Male Germline1." *Biology of Reproduction* 89 (5).

Barrios, Florencia, Doria Filipponi, Manuela Pellegrini, Maria Paola Paronetto, Sara Di Siena, Raffaele Geremia, Pellegrino Rossi, Massimo De Felici, Emmanuele A Jannini, and Susanna Dolci. 2010. "Opposing Effects of Retinoic Acid and FGF9 on Nanos2 Expression and Meiotic Entry of Mouse Germ Cells." *Journal of Cell Science* 123 (Pt 6): 871–80.

Bartolomei, Marisa S, and Anne C Ferguson-Smith. 2011. "Mammalian Genomic Imprinting." *Cold Spring Harbor Perspectives in Biology* 3 (7): a002592.

Batool, Asiya, Sabreena Aashaq, and Khurshid Iqbal Andrabi. 2017. "Reappraisal to the Study of 4E-BP1 as an MTOR Substrate – A Normative Critique." *European Journal of Cell Biology* 96 (4): 325–36.

Ben-Sahra, Issam, Jessica J. Howell, John M. Asara, and Brendan D. Manning. 2013. "Stimulation of de Novo Pyrimidine Synthesis by Growth Signaling Through MTOR and S6K1." *Science* 339 (6125): 1323–28.

Ben-Sahra, Issam, Gerta Hoxhaj, Stéphane J H Ricoult, John M Asara, and Brendan D Manning. 2016. "MTORC1 Induces Purine Synthesis through Control of the Mitochondrial Tetrahydrofolate Cycle." *Science (New York, N.Y.)* 351 (6274): 728–33.

Best, Diana, Daniela A Sahlender, Norbert Walther, Andrew A Peden, and Ian R Adams. 2008. "Sdmg1 Is a Conserved Transmembrane Protein Associated with Germ Cell Sex Determination and Germline-Soma Interactions in Mice." *Development (Cambridge, England)* 135 (8): 1415–25.

Bianchi, Enrica, and Claudio Sette. 2011. "Post-Transcriptional Control of Gene Expression in Mouse Early Embryo Development: A View from the Tip of the Iceberg." *Genes* 2 (2): 345–59.

Bierer, B E, P S Mattila, R F Standaert, L A Herzenberg, S J Burakoff, G Crabtree, and S L Schreiber. 1990. "Two Distinct Signal Transmission Pathways in T Lymphocytes Are Inhibited by Complexes Formed between an Immunophilin and Either FK506 or Rapamycin." *Proceedings of the National Academy of Sciences of the United States of America* 87 (23): 9231–35.

Blackshear, P J, D J Stumpo, E Carballo, and J C Lawrence. 1997. "Disruption of the Gene Encoding the Mitogen-Regulated Translational Modulator PHAS-I in Mice." *The Journal of Biological Chemistry* 272 (50): 31510–14.

Borgel, Julie, Sylvain Guibert, Yufeng Li, Hatsune Chiba, Dirk Schübeler, Hiroyuki Sasaki, Thierry Forné,

and Michael Weber. 2010. “Targets and Dynamics of Promoter DNA Methylation during Early Mouse Development.” *Nature Genetics* 42 (12): 1093–1100.

Borum, Kirstine. 1961. “Oogenesis in the Mouse: A Study of the Meiotic Prophase.” *Experimental Cell Research* 24 (3): 495–507.

Bostick, Magnolia, Jong Kyong Kim, Pierre-Olivier Estève, Amander Clark, Sriharsa Pradhan, and Steven E Jacobsen. 2007. “UHRF1 Plays a Role in Maintaining DNA Methylation in Mammalian Cells.” *Science (New York, N.Y.)* 317 (5845): 1760–64.

Bowles, Josephine, Chun-Wei Feng, Cassy Spiller, Tara-Lynne Davidson, Andrew Jackson, and Peter Koopman. 2010. “FGF9 Suppresses Meiosis and Promotes Male Germ Cell Fate in Mice.” *Developmental Cell* 19 (3): 440–49.

Bowles, Josephine, Deon Knight, Christopher Smith, Dagmar Wilhelm, Joy Richman, Satoru Mamiya, Kenta Yashiro, et al. 2006. “Retinoid Signaling Determines Germ Cell Fate in Mice.” *Science (New York, N.Y.)* 312 (5773): 596–600.

Bowles, Josephine, and Peter Koopman. 2010. “Sex Determination in Mammalian Germ Cells: Extrinsic versus Intrinsic Factors.” *Reproduction (Cambridge, England)* 139 (6): 943–58.

Bozulic, Lana, and Brian A Hemmings. 2009. “PIKKing on PKB: Regulation of PKB Activity by Phosphorylation.” *Current Opinion in Cell Biology* 21 (2): 256–61.

Bozulic, Lana, Banu Surucu, Debby Hynx, and Brian A. Hemmings. 2008. “PKBα/Akt1 Acts Downstream of DNA-PK in the DNA Double-Strand Break Response and Promotes Survival.” *Molecular Cell* 30 (2): 203–13.

Braude, Peter, Hugh Pelham, Gin Flach, and Rita Lobatto. 1979. “Post-Transcriptional Control in the Early Mouse Embryo.” *Nature* 282 (5734): 102–5.

Braun, Robert E. 1998. “Post–transcriptional Control of Gene Expression during Spermatogenesis.” *Seminars in Cell & Developmental Biology* 9 (4): 483–89.

Brower, Peter T., Elena Gizang, Stuart M. Boreen, and Richard M. Schultz. 1981. “Biochemical Studies of Mammalian Oogenesis: Synthesis and Stability of Various Classes of RNA during Growth of the Mouse Oocyte in Vitro.” *Developmental Biology* 86 (2): 373–83.

Brown, Eric J., Mark W. Albers, Tae Bum Shin, Kazuo ichikawa, Curtis T. Keith, William S. Lane, and Stuart L. Schreiber. 1994. “A Mammalian Protein Targeted by G1-Arresting Rapamycin–receptor Complex.” *Nature* 369 (6483): 756–58.

Brunn, G J, C C Hudson, A Sekulić, J M Williams, H Hosoi, P J Houghton, J C Lawrence, and R T Abraham. 1997. “Phosphorylation of the Translational Repressor PHAS-I by the Mammalian Target of Rapamycin.” *Science (New York, N.Y.)* 277 (5322): 99–101.

Buaas, F William, Andrew L Kirsh, Manju Sharma, Derek J McLean, Jamie L Morris, Michael D Griswold, Dirk G de Rooij, and Robert E Braun. 2004. “Plzf Is Required in Adult Male Germ Cells for Stem Cell Self-Renewal.” *Nature Genetics* 36 (6): 647–52.

Bullejos, Monica, and Peter Koopman. 2001. “Spatially Dynamic Expression OfSry in Mouse Genital Ridges.” *Developmental Dynamics* 221 (2): 201–5.

———. 2004. “Germ Cells Enter Meiosis in a Rostro-Caudal Wave during Development of the Mouse Ovary.” *Molecular Reproduction and Development* 68 (4): 422–28.

Bulut-Karslioglu, Aydan, Steffen Biechele, Hu Jin, Trisha A. Macrae, Miroslav Hejna, Marina Gertsenstein, Jun S. Song, and Miguel Ramalho-Santos. 2016. "Inhibition of MTOR Induces a Paused Pluripotent State." *Nature* 540 (7631): 119–23.

Burnett, P E, R K Barrow, N A Cohen, S H Snyder, and D M Sabatini. 1998. "RAFT1 Phosphorylation of the Translational Regulators P70 S6 Kinase and 4E-BP1." *Proceedings of the National Academy of Sciences of the United States of America* 95 (4): 1432–37.

Busada, Jonathan T., Vesna A. Chappell, Bryan A. Niedenberger, Evelyn P. Kaye, Brett D. Keiper, Cathryn A. Hogarth, and Christopher B. Geyer. 2015. "Retinoic Acid Regulates Kit Translation during Spermatogonial Differentiation in the Mouse." *Developmental Biology* 397 (1): 140–49.

Busada, Jonathan T., Bryan A. Niedenberger, Ellen K. Velte, Brett D. Keiper, and Christopher B. Geyer. 2015. "Mammalian Target of Rapamycin Complex 1 (MTORC1) Is Required for Mouse Spermatogonial Differentiation in Vivo." *Developmental Biology* 407 (1): 90–102.

Campolo, Federica, Manuele Gori, Rebecca Favaro, Silvia Nicolis, Manuela Pellegrini, Flavia Botti, Pellegrino Rossi, Emmanuele A. Jannini, and Susanna Dolci. 2013. "Essential Role of Sox2 for the Establishment and Maintenance of the Germ Cell Line." *STEM CELLS* 31 (7): 1408–21.

Carlo, A D Di, G Travia, and M De Felici. 2000. "The Meiotic Specific Synaptonemal Complex Protein SCP3 Is Expressed by Female and Male Primordial Germ Cells of the Mouse Embryo." *The International Journal of Developmental Biology* 44 (2): 241–44.

Chambers, Ian, Jose Silva, Douglas Colby, Jennifer Nichols, Bianca Nijmeijer, Morag Robertson, Jan Vrana, Ken Jones, Lars Grotewold, and Austin Smith. 2007. "Nanog Safeguards Pluripotency and Mediates Germline Development." *Nature* 450 (7173): 1230–34.

Chandler, Kelly J, Ronald L Chandler, Eva M Broeckelmann, Yue Hou, E Michelle Southard-Smith, and Douglas P Mortlock. 2007. "Relevance of BAC Transgene Copy Number in Mice: Transgene Copy Number Variation across Multiple Transgenic Lines and Correlations with Transgene Integrity and Expression." *Mammalian Genome : Official Journal of the International Mammalian Genome Society* 18 (10): 693–708.

Chang, David H, and Kathryn L Calame. 2002. "The Dynamic Expression Pattern of B Lymphocyte Induced Maturation Protein-1 (Blimp-1) during Mouse Embryonic Development." *Mechanisms of Development* 117 (1–2): 305–9.

Chang, H, and M M Matzuk. 2001. "Smad5 Is Required for Mouse Primordial Germ Cell Development." *Mechanisms of Development* 104 (1–2): 61–67.

Chassot, A.-A., F. Ranc, E. P. Gregoire, H. L. Roepers-Gajadien, M. M. Taketo, G. Camerino, D. G. de Rooij, A. Schedl, and M.-C. Chaboissier. 2008. "Activation of -Catenin Signaling by Rspo1 Controls Differentiation of the Mammalian Ovary." *Human Molecular Genetics* 17 (9): 1264–77.

Chauvin, C, V Koka, A Nouschi, V Mieulet, C Hoareau-Aveilla, A Dreazen, N Cagnard, et al. 2014. "Ribosomal Protein S6 Kinase Activity Controls the Ribosome Biogenesis Transcriptional Program." *Oncogene* 33 (4): 474–83.

Chen, Jing, Collin Melton, NaYoung Suh, Robert Blelloch, and Marco Conti. 2010. "Global Analysis of Maternal MRNA Translation during Mouse Oocyte Meiotic Maturation." *Biology of Reproduction* 83 (Suppl_1): 327–327.

Chen, W S, P Z Xu, K Gottlob, M L Chen, K Sokol, T Shiyanova, I Roninson, et al. 2001. "Growth Retardation and Increased Apoptosis in Mice with Homozygous Disruption of the Akt1 Gene." *Genes &*

Development 15 (17): 2203–8.

Cherepkova, M Y, G S Sineva, and V A Pospelov. 2016. "Leukemia Inhibitory Factor (LIF) Withdrawal Activates MTOR Signaling Pathway in Mouse Embryonic Stem Cells through the MEK/ERK/TSC2 Pathway." *Cell Death & Disease* 7 (1): e2050.

Chiquoine, A D. 1954. "The Identification, Origin, and Migration of the Primordial Germ Cells in the Mouse Embryo." *The Anatomical Record* 118 (2): 135–46.

Choo, Andrew Y., and John Blenis. 2009. "Not All Substrates Are Treated Equally: Implications for MTOR, Rapamycin-Resistance, and Cancer Therapy." *Cell Cycle* 8 (4): 567–72.

Chu, Gerald C, N Ray Dunn, Dorian C Anderson, Leif Oxburgh, and Elizabeth J Robertson. 2004. "Differential Requirements for Smad4 in TGFbeta-Dependent Patterning of the Early Mouse Embryo." *Development (Cambridge, England)* 131 (15): 3501–12.

Chuang, L S, H I Ian, T W Koh, H H Ng, G Xu, and B F Li. 1997. "Human DNA-(Cytosine-5) Methyltransferase-PCNA Complex as a Target for P21WAF1." *Science (New York, N.Y.)* 277 (5334): 1996–2000.

Chuma, Shinichiro, and Norio Nakatsuji. 2001. "Autonomous Transition into Meiosis of Mouse Fetal Germ Cells in Vitro and Its Inhibition by Gp130-Mediated Signaling." *Developmental Biology* 229 (2): 468–79.

Chuva de Sousa Lopes, Susana M., Katsuhiko Hayashi, Tanya C. Shovlin, Will Mifsud, M. Azim Surani, and Anne McLaren††. 2008. "X Chromosome Activity in Mouse XX Primordial Germ Cells." *PLoS Genetics* 4 (2): e30.

Clarke, Hugh J. 2012. "Post-Transcriptional Control of Gene Expression During Mouse Oogenesis." In , 1–21. Springer, Berlin, Heidelberg.

Cook, Matthew S, Douglas Coveney, Iordan Batchvarov, Joseph H Nadeau, and Blanche Capel. 2009. "BAX-Mediated Cell Death Affects Early Germ Cell Loss and Incidence of Testicular Teratomas in Dnd1(Ter/Ter) Mice." *Developmental Biology* 328 (2): 377–83.

Cook, Matthew S, Steven C Munger, Joseph H Nadeau, and Blanche Capel. 2011. "Regulation of Male Germ Cell Cycle Arrest and Differentiation by DND1 Is Modulated by Genetic Background." *Development (Cambridge, England)* 138 (1): 23–32.

Cooke, Howard J, Muriel Lee, Shona Kerr, and Matteo Ruggiu. 1996. "A Murine Homologue of the Human DAZ Gene Is Autosomal and Expressed Only in Male and Female Gonads." *Human Molecular Genetics* 5 (4): 513–16.

Cortellino, Salvatore, Jinfei Xu, Mara Sannai, Robert Moore, Elena Caretti, Antonio Cigliano, Madeleine Le Coz, et al. 2011. "Thymine DNA Glycosylase Is Essential for Active DNA Demethylation by Linked Deamination-Base Excision Repair." *Cell* 146 (1): 67–79.

Costoya, José A, Robin M Hobbs, Maria Barna, Giorgio Cattoretti, Katia Manova, Meena Sukhwani, Kyle E Orwig, Debra J Wolgemuth, and Pier Paolo Pandolfi. 2004. "Essential Role of Plzf in Maintenance of Spermatogonial Stem Cells." *Nature Genetics* 36 (6): 653–59.

Cruz, Irene da, Rosana Rodríguez-Casuriaga, Federico F. Santiñaque, Joaquina Farías, Gianni Curti, Carlos A. Capoano, Gustavo A. Folle, Ricardo Benavente, José Roberto Sotelo-Silveira, and Adriana Geisinger. 2016. "Transcriptome Analysis of Highly Purified Mouse Spermatogenic Cell Populations: Gene Expression Signatures Switch from Meiotic-to Postmeiotic-Related Processes at Pachytene Stage." *BMC Genomics* 17 (1): 294.

Cui, Li, Kohei Johkura, Fengming Yue, Naoko Ogiwara, Yasumitsu Okouchi, Kazuhiko Asanuma, and Katsunori Sasaki. 2004. "Spatial Distribution and Initial Changes of SSEA-1 and Other Cell Adhesion-Related Molecules on Mouse Embryonic Stem Cells before and during Differentiation." *The Journal of Histochemistry and Cytochemistry : Official Journal of the Histochemistry Society* 52 (11): 1447–57.

Cullinane, Danielle L, Tamjid A Chowdhury, and Kenneth C Kleene. 2015. "Mechanisms of Translational Repression of the Smcp MRNA in Round Spermatids." *REPRODUCTION* 149 (1): 43–54.

Dawlaty, Meelad M., Kibibi Ganz, Benjamin E. Powell, Yueh-Chiang Hu, Styliani Markoulaki, Albert W. Cheng, Qing Gao, et al. 2011. "Tet1 Is Dispensable for Maintaining Pluripotency and Its Loss Is Compatible with Embryonic and Postnatal Development." *Cell Stem Cell* 9 (2): 166–75.

Dennis, Michael D., Leonard S. Jefferson, and Scot R. Kimball. 2012. "Role of P70S6K1-Mediated Phosphorylation of EIF4B and PDCD4 Proteins in the Regulation of Protein Synthesis." *Journal of Biological Chemistry* 287 (51): 42890–99.

Doetschman, Thomas. 2009. "Influence of Genetic Background on Genetically Engineered Mouse Phenotypes." *Methods in Molecular Biology (Clifton, N.J.)* 530: 423–33.

Dokshin, Gregoriy A, Andrew E Baltus, John J Eppig, and David C Page. 2013. "Oocyte Differentiation Is Genetically Dissociable from Meiosis in Mice." *Nature Publishing Group* 45 (8).

Dolci, Susanna, Federica Campolo, and Massimo De Felici. 2015. "Gonadal Development and Germ Cell Tumors in Mouse and Humans." *Seminars in Cell & Developmental Biology* 45 (September): 114–23.

Dolci, Susanna, Douglas E. Williams, Mary K. Ernst, James L. Resnick, Camilynn I. Brannan, Leslie F. Lock, Stewart D. Lyman, H. Scott Boswell, and Peter J. Donovan. 1991. "Requirement for Mast Cell Growth Factor for Primordial Germ Cell Survival in Culture." *Nature* 352 (6338): 809–11.

Donovan. 1994. "6 Growth Factor Regulation of Mouse Primordial Germ Cell Development." *Current Topics in Developmental Biology* 29 (January): 189–225.

Donovan, Peter J, and Maria P de Miguel. 2003. "Turning Germ Cells into Stem Cells." *Current Opinion in Genetics & Development* 13 (5): 463–71.

Dorrello, N Valerio, Angelo Peschiaroli, Daniele Guardavaccaro, Nancy H Colburn, Nicholas E Sherman, and Michele Pagano. 2006. "S6K1- and BetaTRCP-Mediated Degradation of PDCD4 Promotes Protein Translation and Cell Growth." *Science (New York, N.Y.)* 314 (5798): 467–71.

Dowling, Ryan J O, Ivan Topisirovic, Tommy Alain, Michael Bidinosti, Bruno D Fonseca, Emmanuel Petroulakis, Xiaoshan Wang, et al. 2010. "MTORC1-Mediated Cell Proliferation, but Not Cell Growth, Controlled by the 4E-BPs." *Science (New York, N.Y.)* 328 (5982): 1172–76.

Düvel, Katrin, Jessica L. Yecies, Suchithra Menon, Pichai Raman, Alex I. Lipovsky, Amanda L. Souza, Ellen Triantafellow, et al. 2010. "Activation of a Metabolic Gene Regulatory Network Downstream of MTOR Complex 1." *Molecular Cell* 39 (2): 171–83.

Eggens, Ivan, Bruce Fenderson, Tatsushi Toyokuni, Barbara Dean, Mark Stroud, Sen-Itiroh Hakomoris, I Eggens, et al. 1989. *Specific Interaction between Lex and Lex Determinants*. *The Journal of Biological Chemistry*. Vol. 264.

Espenshade, Peter J., and Adam L. Hughes. 2007. "Regulation of Sterol Synthesis in Eukaryotes." *Annual Review of Genetics* 41 (1): 401–27.

Extavour, Cassandra G, and Michael Akam. 2003. "Mechanisms of Germ Cell Specification across the

Metazoans: Epigenesis and Preformation." *Development (Cambridge, England)* 130 (24): 5869–84.

Felici, M De, and A McLaren. 1983. "In Vitro Culture of Mouse Primordial Germ Cells." *Experimental Cell Research* 144 (2): 417–27.

Felici, Massimo De, and Francesca G Klinger. 2015. "Programmed Cell Death in Mouse Primordial Germ Cells." *The International Journal of Developmental Biology* 59 (1–3): 41–49.

Feng, Chun-Wei, Josephine Bowles, and Peter Koopman. 2014. "Control of Mammalian Germ Cell Entry into Meiosis." *Molecular and Cellular Endocrinology* 382 (1): 488–97.

Fisher, J. S., S. Macpherson, N. Marchetti, and Richard M. Sharpe. 2003. "Human 'Testicular Dysgenesis Syndrome': A Possible Model Using in-Utero Exposure of the Rat to Dibutyl Phthalate." *Human Reproduction* 18 (7): 1383–94.

Fonseca, Bruno D., Ewan M. Smith, Nicolas Yelle, Tommy Alain, Martin Bushell, and Arnim Pause. 2014. "The Ever-Evolving Role of MTOR in Translation." *Seminars in Cell & Developmental Biology* 36 (December): 102–12.

Fox, Niles, Ivan Damjanov, Antonio Martinez-Hernandez, Barbara B. Knowles, and Davor Solter. 1981. "Immunohistochemical Localization of the Early Embryonic Antigen (SSEA-1) in Postimplantation Mouse Embryos and Fetal and Adult Tissues." *Developmental Biology* 83 (2): 391–98.

Frauer, Carina, Thomas Hoffmann, Sebastian Bultmann, Valentina Casa, M. Cristina Cardoso, Iris Antes, and Heinrich Leonhardt. 2011. "Recognition of 5-Hydroxymethylcytosine by the Uhrf1 SRA Domain." Edited by Shuang-yong Xu. *PLoS ONE* 6 (6): e21306.

Fraune, Johanna, Sabine Schramm, Manfred Alsheimer, and Ricardo Benavente. 2012. "The Mammalian Synaptonemal Complex: Protein Components, Assembly and Role in Meiotic Recombination." *Experimental Cell Research* 318 (12): 1340–46.

Fujiwara, Y, T Komiya, H Kawabata, M Sato, H Fujimoto, M Furusawa, and T Noce. 1994. "Isolation of a DEAD-Family Protein Gene That Encodes a Murine Homolog of Drosophila Vasa and Its Specific Expression in Germ Cell Lineage." *Proceedings of the National Academy of Sciences of the United States of America* 91 (25): 12258–62.

Fulka, J, J Motlík, J Fulka, and F Jílek. 1986. "Effect of Cycloheximide on Nuclear Maturation of Pig and Mouse Oocytes." *Journal of Reproduction and Fertility* 77 (1): 281–85.

Gallardo, Teresa, Lane Shirley, George B. John, and Diego H. Castrillon. 2007. "Generation of a Germ Cell-Specific Mouse Transgenic Cre Line,Vasa-Cre." *Genesis* 45 (6): 413–17.

Gan, Haiyun, Tanxi Cai, Xiwen Lin, Yujian Wu, Xiuxia Wang, Fuquan Yang, and Chunsheng Han. 2013. "Integrative Proteomic and Transcriptomic Analyses Reveal Multiple Post-Transcriptional Regulatory Mechanisms of Mouse Spermatogenesis." *Molecular & Cellular Proteomics : MCP* 12 (5): 1144–57.

Gandin, Valentina, Laia Masvidal, Laura Hulea, Simon-Pierre Gravel, Marie Cargnello, Shannon McLaughlan, Yutian Cai, et al. 2016. "NanoCAGE Reveals 5′ UTR Features That Define Specific Modes of Translation of Functionally Related MTOR-Sensitive MRNAs." *Genome Research* 26 (5): 636–48.

Gangloff, Yann-Gaël, Matthias Mueller, Stephen G Dann, Petr Svoboda, Melanie Sticker, Jean-Francois Spetz, Sung Hee Um, et al. 2004. "Disruption of the Mouse MTOR Gene Leads to Early Postimplantation Lethality and Prohibits Embryonic Stem Cell Development." *Molecular and Cellular Biology* 24 (21): 9508–16.

Gebauer, Fátima, and Matthias W. Hentze. 2004. "Molecular Mechanisms of Translational Control." *Nature Reviews Molecular Cell Biology* 5 (10): 827–35.

Gill, Mark E, Yueh-Chiang Hu, Yanfeng Lin, and David C Page. 2011. "Licensing of Gametogenesis, Dependent on RNA Binding Protein DAZL, as a Gateway to Sexual Differentiation of Fetal Germ Cells." *Proceedings of the National Academy of Sciences of the United States of America* 108 (18): 7443–48.

Gingras, A C, S P Gygi, B Raught, R D Polakiewicz, R T Abraham, M F Hoekstra, R Aebersold, and N Sonenberg. 1999. "Regulation of 4E-BP1 Phosphorylation: A Novel Two-Step Mechanism." *Genes & Development* 13 (11): 1422–37.

Gingras, A C, B Raught, S P Gygi, A Niedzwiecka, M Miron, S K Burley, R D Polakiewicz, A Wyslouch-Cieszynska, R Aebersold, and N Sonenberg. 2001. "Hierarchical Phosphorylation of the Translation Inhibitor 4E-BP1." *Genes & Development* 15 (21): 2852–64.

Ginsburg, M., M.H. Snow, and A. McLaren. 1990. "Primordial Germ Cells in the Mouse Embryo during Gastrulation." *Development* 110 (2).

Glickman, Michael H., and Aaron Ciechanover. 2002. "The Ubiquitin-Proteasome Proteolytic Pathway: Destruction for the Sake of Construction." *Physiological Reviews* 82 (2): 373–428.

Godin, I., R. Deed, J. Cooke, K. Zsebo, M. Dexter, and C. C. Wylie. 1991. "Effects of the Steel Gene Product on Mouse Primordial Germ Cells in Culture." *Nature* 352 (6338): 807–9.

Gómez-Salinero, Jesús M., Marina M. López-Olañeta, Paula Ortiz-Sánchez, Javier Larrasa-Alonso, Alberto Gatto, Leanne E. Felkin, Paul J.R. Barton, et al. 2016. "The Calcineurin Variant CnAβ1 Controls Mouse Embryonic Stem Cell Differentiation by Directing MTORC2 Membrane Localization and Activation." *Cell Chemical Biology* 23 (11): 1372–82.

Gooi, H C, T Feizi, A Kapadia, B B Knowles, D Solter, and M J Evans. 1981. "Stage-Specific Embryonic Antigen Involves A1-3 Fucosylated Type 2 Blood Group Chains." *Nature* 292 (5819): 156–58.

Grabole, Nils, Julia Tischler, Jamie A Hackett, Shinseog Kim, Fuchou Tang, Harry G Leitch, Erna Magnúsdóttir, and M Azim Surani. 2013. "Prdm14 Promotes Germline Fate and Naive Pluripotency by Repressing FGF Signalling and DNA Methylation." *EMBO Reports* 14 (7): 629–37.

Griswold, Michael D. 2016. "Spermatogenesis: The Commitment to Meiosis." *Physiological Reviews* 96 (1): 1–17.

Gu, H, J D Marth, P C Orban, H Mossmann, and K Rajewsky. 1994. "Deletion of a DNA Polymerase Beta Gene Segment in T Cells Using Cell Type-Specific Gene Targeting." *Science (New York, N.Y.)* 265 (5168): 103–6.

Gu, Ying, Chris Runyan, Amanda Shoemaker, Azim Surani, and Chris Wylie. 2009. "Steel Factor Controls Primordial Germ Cell Survival and Motility from the Time of Their Specification in the Allantois, and Provides a Continuous Niche throughout Their Migration." *Development (Cambridge, England)* 136 (8): 1295–1303.

Gubbay, John, Jérôme Collignon, Peter Koopman, Blanche Capel, Androulla Economou, Andrea Münsterberg, Nigel Vivian, Peter Goodfellow, and Robin Lovell-Badge. 1990. "A Gene Mapping to the Sex-Determining Region of the Mouse Y Chromosome Is a Member of a Novel Family of Embryonically Expressed Genes." *Nature* 346 (6281): 245–50.

Guertin, David A, Deanna M Stevens, Carson C Thoreen, Aurora A Burds, Nada Y Kalaany, Jason Moffat, Michael Brown, Kevin J Fitzgerald, and David M Sabatini. 2006. "Ablation in Mice of the MTORC

Components Raptor, Rictor, or MLST8 Reveals That MTORC2 Is Required for Signaling to Akt-FOXO and PKCalpha, but Not S6K1." *Developmental Cell* 11 (6): 859–71.

Guibert, Sylvain, Thierry Forné, and Michael Weber. 2012. "Global Profiling of DNA Methylation Erasure in Mouse Primordial Germ Cells." *Genome Research* 22 (4): 633–41.

Gunter, Kara M., and Eileen A. McLaughlin. 2011. "Translational Control in Germ Cell Development: A Role for the RNA-Binding Proteins Musashi-1 and Musashi-2." *IUBMB Life* 63 (9): n/a-n/a.

Guzeloglu-Kayisli, Ozlem, Maria D Lalioti, Fulya Aydiner, Isaac Sasson, Orkan Ilbay, Denny Sakkas, Katie M Lowther, Lisa M Mehlmann, and Emre Seli. 2012. "Embryonic Poly(A)-Binding Protein (EPAB) Is Required for Oocyte Maturation and Female Fertility in Mice." *The Biochemical Journal* 446 (1): 47–58.

Hackett, Jamie A., Roopsha Sengupta, Jan J. Zylicz, Kazuhiro Murakami, Caroline Lee, Thomas A. Down, and M. Azim Surani. 2013. "Germline DNA Demethylation Dynamics and Imprint Erasure Through 5-Hydroxymethylcytosine." *Science* 339 (6118): 448–52.

Hackett, Jamie A., Jan J. Zylicz, and M. Azim Surani. 2012. "Parallel Mechanisms of Epigenetic Reprogramming in the Germline." *Trends in Genetics* 28 (4): 164–74.

Hajkova, Petra. 2011. "Epigenetic Reprogramming in the Germline: Towards the Ground State of the Epigenome." *Philosophical Transactions of the Royal Society of London. Series B, Biological Sciences* 366 (1575): 2266–73.

Hajkova, Petra, Katia Ancelin, Tanja Waldmann, Nicolas Lacoste, Ulrike C. Lange, Francesca Cesari, Caroline Lee, Genevieve Almouzni, Robert Schneider, and M. Azim Surani. 2008. "Chromatin Dynamics during Epigenetic Reprogramming in the Mouse Germ Line." *Nature* 452 (7189): 877–81.

Hajkova, Petra, Sylvia Erhardt, Natasha Lane, Thomas Haaf, Osman El-Maarri, Wolf Reik, Jörn Walter, and M.Azim Surani. 2002. "Epigenetic Reprogramming in Mouse Primordial Germ Cells." *Mechanisms of Development* 117 (1–2): 15–23.

Hajkova, Petra, Sean J Jeffries, Caroline Lee, Nigel Miller, Stephen P Jackson, and M Azim Surani. 2010. "Genome-Wide Reprogramming in the Mouse Germ Line Entails the Base Excision Repair Pathway." *Science (New York, N.Y.)* 329 (5987): 78–82.

Hamatani, Toshio, Mark G. Carter, Alexei A. Sharov, and Minoru S.H. Ko. 2004. "Dynamics of Global Gene Expression Changes during Mouse Preimplantation Development." *Developmental Cell* 6 (1): 117–31.

Hampl, Ale?, and John J. Eppig. 1995. "Translational Regulation of the Gradual Increase in Histone H1 Kinase Activity in Maturing Mouse Oocytes." *Molecular Reproduction and Development* 40 (1): 9–15.

Han, Dong, Xin-Yong Liu, Guang-Zhong Jiao, Bo Liang, Nan He, W.-Q. Gao, and Jing-He Tan. 2012. "Cyclin B1 Turnover and the Mechanism Causing Insensitivity of Fully Grown Mouse Oocytes to Cycloheximide Inhibition of Meiotic Resumption." *Theriogenology* 77 (9): 1900–1910.

Handel, Mary Ann, and John C. Schimenti. 2010. "Genetics of Mammalian Meiosis: Regulation, Dynamics and Impact on Fertility." *Nature Reviews Genetics* 11 (2): 124–36.

Harrington, Laura S, Greg M Findlay, Alex Gray, Tatiana Tolkacheva, Simon Wigfield, Heike Rebholz, Jill Barnett, et al. 2004. "The TSC1-2 Tumor Suppressor Controls Insulin-PI3K Signaling via Regulation of IRS Proteins." *The Journal of Cell Biology* 166 (2): 213–23.

Haruyama, Naoto, Andrew Cho, and Ashok B Kulkarni. 2009. "Overview: Engineering Transgenic Constructs and Mice." *Current Protocols in Cell Biology* Chapter 19 (March): Unit 19.10.

Hayashi, Katsuhiko, Sugako Ogushi, Kazuki Kurimoto, So Shimamoto, Hiroshi Ohta, and Mitinori Saitou. 2012. "Offspring from Oocytes Derived from in Vitro Primordial Germ Cell-like Cells in Mice." *Science (New York, N.Y.)* 338 (6109): 971–75.

Hayashi, Katsuhiko, Hiroshi Ohta, Kazuki Kurimoto, Shinya Aramaki, and Mitinori Saitou. 2011. "Reconstitution of the Mouse Germ Cell Specification Pathway in Culture by Pluripotent Stem Cells." *Cell* 146 (4): 519–32.

He, Yu-Fei, Bin-Zhong Li, Zheng Li, Peng Liu, Yang Wang, Qingyu Tang, Jianping Ding, et al. 2011. "Tet-Mediated Formation of 5-Carboxylcytosine and Its Excision by TDG in Mammalian DNA." *Science* 333 (6047): 1303–7.

Hikabe, Orie, Nobuhiko Hamazaki, Go Nagamatsu, Yayoi Obata, Yuji Hirao, Norio Hamada, So Shimamoto, et al. 2016. "Reconstitution in Vitro of the Entire Cycle of the Mouse Female Germ Line." *Nature* 539 (7628): 299–303.

Hill, Peter W. S., Harry G. Leitch, Cristina E. Requena, Zhiyi Sun, Rachel Amouroux, Monica Roman-Trufero, Malgorzata Borkowska, et al. 2018. "Epigenetic Reprogramming Enables the Transition from Primordial Germ Cell to Gonocyte." *Nature* 555 (7696): 392–96.

Hill, Peter W.S., Rachel Amouroux, and Petra Hajkova. 2014. "DNA Demethylation, Tet Proteins and 5-Hydroxymethylcytosine in Epigenetic Reprogramming: An Emerging Complex Story." *Genomics* 104 (5): 324–33.

Hiramatsu, Ryuji, Kyoko Harikae, Naoki Tsunekawa, Masamichi Kurohmaru, Isao Matsuo, Yoshiakira Kanai, Y. Sanai, H. Yonekawa, K. Yazaki, and P. P. Tam. 2010. "FGF Signaling Directs a Center-to-Pole Expansion of Tubulogenesis in Mouse Testis Differentiation." *Development (Cambridge, England)* 137 (2): 303–12.

Hirota, Takayuki, Hiroshi Ohta, Mayo Shigeta, Hitoshi Niwa, and Mitinori Saitou. 2011. "Drug-Inducible Gene Recombination by the Dppa3-MER Cre MER Transgene in the Developmental Cycle of the Germ Cell Lineage in Mice1." *Biology of Reproduction* 85 (2): 367–77.

Hobbs, Robin M., Marco Seandel, Ilaria Falciatori, Shahin Rafii, and Pier Paolo Pandolfi. 2010. "Plzf Regulates Germline Progenitor Self-Renewal by Opposing MTORC1." *Cell* 142 (3): 468–79.

Hobbs, Robin M, Hue M La, Juho-Antti Mäkelä, Toshiyuki Kobayashi, Tetsuo Noda, and Pier Paolo Pandolfi. 2015. "Distinct Germline Progenitor Subsets Defined through Tsc2-MTORC1 Signaling." *EMBO Reports* 16 (4): 467–80.

Holz, Marina K, and John Blenis. 2005. "Identification of S6 Kinase 1 as a Novel Mammalian Target of Rapamycin (MTOR)-Phosphorylating Kinase." *The Journal of Biological Chemistry* 280 (28): 26089–93.

Hresko, Richard C, and Mike Mueckler. 2005. "MTOR.RICTOR Is the Ser473 Kinase for Akt/Protein Kinase B in 3T3-L1 Adipocytes." *The Journal of Biological Chemistry* 280 (49): 40406–16.

Hsieh, Andrew C., Maria Costa, Ornella Zollo, Cole Davis, Morris E. Feldman, Joseph R. Testa, Oded Meyuhas, Kevan M. Shokat, and Davide Ruggero. 2010. "Genetic Dissection of the Oncogenic MTOR Pathway Reveals Druggable Addiction to Translational Control via 4EBP-EIF4E." *Cancer Cell* 17 (3): 249–61.

Hsieh, Andrew C., Yi Liu, Merritt P. Edlind, Nicholas T. Ingolia, Matthew R. Janes, Annie Sher, Evan Y. Shi, et al. 2012. "The Translational Landscape of MTOR Signalling Steers Cancer Initiation and Metastasis." *Nature* 485 (7396): 55–61.

Hu, C, S Pang, X Kong, M Velleca, J C Lawrence, and Jr. 1994. "Molecular Cloning and Tissue Distribution of PHAS-I, an Intracellular Target for Insulin and Growth Factors." *Proceedings of the National Academy of Sciences of the United States of America* 91 (9): 3730–34.

Hu, Yueh-Chiang, Peter K Nicholls, Y Q Shirleen Soh, Joseph R Daniele, Jan Philipp Junker, Alexander Van Oudenaarden, and David C Page. 2015. "Licensing of Primordial Germ Cells for Gametogenesis Depends on Genital Ridge Signaling." *PLoS Genet* 11 (3).

Huang, Jingxiang, and Brendan D Manning. 2009. "A Complex Interplay between Akt, TSC2 and the Two MTOR Complexes." *Biochemical Society Transactions* 37 (Pt 1): 217–22.

Huang, Yun, William A. Pastor, Yinghua Shen, Mamta Tahiliani, David R. Liu, and Anjana Rao. 2010. "The Behaviour of 5-Hydroxymethylcytosine in Bisulfite Sequencing." Edited by Jun Liu. *PLoS ONE* 5 (1): e8888.

Huyghe, Eric, Anas Zairi, Joe Nohra, Nassim Kamar, Pierre Plante, and Lionel Rostaing. 2007. "Gonadal Impact of Target of Rapamycin Inhibitors (Sirolimus and Everolimus) in Male Patients: An Overview." *Transplant International* 20 (4): 305–11.

Idler, R Keegan, and Wei Yan. 2012. "Control of Messenger RNA Fate by RNA-Binding Proteins: An Emphasis on Mammalian Spermatogenesis." *Journal of Andrology* 33 (3): 309–37.

Iguchi, Naoko, John W Tobias, and Norman B Hecht. 2006. "Expression Profiling Reveals Meiotic Male Germ Cell MRNAs That Are Translationally Up- and down-Regulated." *Proceedings of the National Academy of Sciences of the United States of America* 103 (20): 7712–17.

Illmensee, K, and A P Mahowald. 1974. "Transplantation of Posterior Polar Plasm in Drosophila. Induction of Germ Cells at the Anterior Pole of the Egg." *Proceedings of the National Academy of Sciences of the United States of America* 71 (4): 1016–20.

Inoki, Ken, Hongjiao Ouyang, Tianqing Zhu, Charlotta Lindvall, Yian Wang, Xiaojie Zhang, Qian Yang, et al. 2006. "TSC2 Integrates Wnt and Energy Signals via a Coordinated Phosphorylation by AMPK and GSK3 to Regulate Cell Growth." *Cell* 126 (5): 955–68.

Ishikura, Yukiko, Yukihiro Yabuta, Hiroshi Ohta, Katsuhiko Hayashi, Tomonori Nakamura, Ikuhiro Okamoto, Takuya Yamamoto, et al. 2016. "In Vitro Derivation and Propagation of Spermatogonial Stem Cell Activity from Mouse Pluripotent Stem Cells." *Cell Reports* 17 (10): 2789–2804.

Isotani, S, K Hara, C Tokunaga, H Inoue, J Avruch, and K Yonezawa. 1999. "Immunopurified Mammalian Target of Rapamycin Phosphorylates and Activates P70 S6 Kinase Alpha in Vitro." *The Journal of Biological Chemistry* 274 (48): 34493–98.

Ito, Shinsuke, Li Shen, Qing Dai, Susan C. Wu, Leonard B. Collins, James A. Swenberg, Chuan He, and Yi Zhang. 2011. "Tet Proteins Can Convert 5-Methylcytosine to 5-Formylcytosine and 5-Carboxylcytosine." *Science* 333 (6047): 1300–1303.

Jacinto, Estela, Valeria Facchinetti, Dou Liu, Nelyn Soto, Shiniu Wei, Sung Yun Jung, Qiaojia Huang, Jun Qin, and Bing Su. 2006. "SIN1/MIP1 Maintains Rictor-MTOR Complex Integrity and Regulates Akt Phosphorylation and Substrate Specificity." *Cell* 127 (1): 125–37.

Jacinto, Estela, Robbie Loewith, Anja Schmidt, Shuo Lin, Markus A. Rüegg, Alan Hall, and Michael N. Hall. 2004. "Mammalian TOR Complex 2 Controls the Actin Cytoskeleton and Is Rapamycin Insensitive." *Nature Cell Biology* 6 (11): 1122–28.

Jesus, Tito T, Pedro F Oliveira, Mário Sousa, C Yan Cheng, and Marco G Alves. 2017. "Mammalian Target

of Rapamycin (MTOR): A Central Regulator of Male Fertility?" *Critical Reviews in Biochemistry and Molecular Biology* 52 (3): 235–53.

Kagiwada, Saya, Kazuki Kurimoto, Takayuki Hirota, Masashi Yamaji, and Mitinori Saitou. 2013. "Replication-Coupled Passive DNA Demethylation for the Erasure of Genome Imprints in Mice." *The EMBO Journal* 32 (3): 340–53.

Kanatsu-Shinohara, Mito, and Takashi Shinohara. 2013. "Spermatogonial Stem Cell Self-Renewal and Development." *Annual Review of Cell and Developmental Biology* 29 (1): 163–87.

Kehler, James, Elena Tolkunova, Birgit Koschorz, Maurizio Pesce, Luca Gentile, Michele Boiani, Hilda Lomelí, et al. 2004. "Oct4 Is Required for Primordial Germ Cell Survival." *EMBO Reports* 5 (11): 1078–83.

Keuren, Margaret L Van, Galina B Gavrilina, Wanda E Filipiak, Michael G Zeidler, and Thomas L Saunders. 2009. "Generating Transgenic Mice from Bacterial Artificial Chromosomes: Transgenesis Efficiency, Integration and Expression Outcomes." *Transgenic Research* 18 (5): 769–85.

Kim, Joungmok, Mondira Kundu, Benoit Viollet, and Kun-Liang Guan. 2011. "AMPK and MTOR Regulate Autophagy through Direct Phosphorylation of Ulk1." *Nature Cell Biology* 13 (2): 132–41.

Kim, Yuna, Akio Kobayashi, Ryohei Sekido, Leo DiNapoli, Jennifer Brennan, Marie-Christine Chaboissier, Francis Poulat, Richard R Behringer, Robin Lovell-Badge, and Blanche Capel. 2006. "Fgf9 and Wnt4 Act as Antagonistic Signals to Regulate Mammalian Sex Determination." *PLoS Biology* 4 (6): e187.

Kimura, Tohru, Akira Suzuki, Yukiko Fujita, Kentaro Yomogida, Hilda Lomeli, Noriko Asada, Megumi Ikeuchi, Andras Nagy, Tak W Mak, and Toru Nakano. 2003. "Conditional Loss of PTEN Leads to Testicular Teratoma and Enhances Embryonic Germ Cell Production." *Development (Cambridge, England)* 130 (8): 1691–1700.

Kimura, Tohru, Maya Tomooka, Noriko Yamano, Kazushige Murayama, Shogo Matoba, Hiroki Umehara, Yoshiakira Kanai, and Toru Nakano. 2008. "AKT Signaling Promotes Derivation of Embryonic Germ Cells from Primordial Germ Cells." *Development* 135 (5).

Kleene, Kenneth C. 2001. "A Possible Meiotic Function of the Peculiar Patterns of Gene Expression in Mammalian Spermatogenic Cells." *Mechanisms of Development* 106 (1–2): 3–23.

Knudson, C M, K S Tung, W G Tourtellotte, G A Brown, and S J Korsmeyer. 1995. "Bax-Deficient Mice with Lymphoid Hyperplasia and Male Germ Cell Death." *Science (New York, N.Y.)* 270 (5233): 96–99.

Kocer, A., J. Reichmann, D. Best, and I. R. Adams. 2009. "Germ Cell Sex Determination in Mammals." *Molecular Human Reproduction* 15 (4): 205–13.

Koopman, Peter, John Gubbay, Nigel Vivian, Peter Goodfellow, and Robin Lovell-Badge. 1991. "Male Development of Chromosomally Female Mice Transgenic for Sry." *Nature* 351 (6322): 117–21.

Koubova, Jana, Douglas B Menke, Qing Zhou, Blanche Capel, Michael D Griswold, and David C Page. 2006. "Retinoic Acid Regulates Sex-Specific Timing of Meiotic Initiation in Mice." *Proceedings of the National Academy of Sciences of the United States of America* 103 (8): 2474–79.

Kudo, Takashi, Mika Kaneko, Hiroko Iwasaki, Akira Togayachi, Shoko Nishihara, Kuniya Abe, and Hisashi Narimatsu. 2004. "Normal Embryonic and Germ Cell Development in Mice Lacking Alpha 1,3-Fucosyltransferase IX (Fut9) Which Show Disappearance of Stage-Specific Embryonic Antigen 1." *Molecular and Cellular Biology* 24 (10): 4221–28.

Kumar, Sandeep, Christina Chatzi, Thomas Brade, Thomas J. Cunningham, Xianling Zhao, and Gregg Duester. 2011. "Sex-Specific Timing of Meiotic Initiation Is Regulated by Cyp26b1 Independent of Retinoic Acid Signalling." *Nature Communications* 2 (1): 151.

Kurimoto, Kazuki, Yukihiro Yabuta, Yasuhide Ohinata, Mayo Shigeta, Kaori Yamanaka, and Mitinori Saitou. 2008. "Complex Genome-Wide Transcription Dynamics Orchestrated by Blimp1 for the Specification of the Germ Cell Lineage in Mice." *Genes & Development* 22 (12): 1617–35.

Kwiatkowski, David J, Hongbing Zhang, Jennifer L Bandura, Kristina M Heiberger, Michael Glogauer, Nisreen el-Hashemite, and Hiroaki Onda. 2002. "A Mouse Model of TSC1 Reveals Sex-Dependent Lethality from Liver Hemangiomas, and up-Regulation of P70S6 Kinase Activity in Tsc1 Null Cells." *Human Molecular Genetics* 11 (5): 525–34.

Lackner, Daniel H., and Jürg Bähler. 2008. "Chapter 5 Translational Control of Gene Expression: From Transcripts to Transcriptomes." *International Review of Cell and Molecular Biology* 271 (January): 199–251.

Laird, Diana J., Svetlana Altshuler-Keylin, Michael D. Kissner, Xin Zhou, and Kathryn V. Anderson. 2011. "Ror2 Enhances Polarity and Directional Migration of Primordial Germ Cells." Edited by Patrick P. L. Tam. *PLoS Genetics* 7 (12): e1002428.

Laplante, Mathieu, and David M Sabatini. 2009. "MTOR Signaling at a Glance." *Journal of Cell Science* 122 (Pt 20): 3589–94.

———. 2012. "MTOR Signaling in Growth Control and Disease." *Cell* 149 (2): 274–93.

Lawson, K A, N R Dunn, B A Roelen, L M Zeinstra, A M Davis, C V Wright, J P Korving, and B L Hogan. 1999. "Bmp4 Is Required for the Generation of Primordial Germ Cells in the Mouse Embryo." *Genes & Development* 13 (4): 424–36.

Lawson, K A, and W J Hage. 1994. "Clonal Analysis of the Origin of Primordial Germ Cells in the Mouse." *Ciba Foundation Symposium* 182: 68-84; discussion 84-91.

Lee-Fruman, Kay K, Calvin J Kuo, John Lippincott, Naohiro Terada, and John Blenis. 1999. "Characterization of S6K2, a Novel Kinase Homologous to S6K1." *Oncogene* 18 (36): 5108–14.

Lee, Jibak, Toshiharu Iwai, Takehiro Yokota, and Masakane Yamashita. 2003. "Temporally and Spatially Selective Loss of Rec8 Protein from Meiotic Chromosomes during Mammalian Meiosis." *Journal of Cell Science* 116 (Pt 13): 2781–90.

Lee, K, H S Haugen, C H Clegg, and R E Braun. 1995. "Premature Translation of Protamine 1 MRNA Causes Precocious Nuclear Condensation and Arrests Spermatid Differentiation in Mice." *Proceedings of the National Academy of Sciences of the United States of America* 92 (26): 12451–55.

Lei, L., and A. C. Spradling. 2013. "Mouse Primordial Germ Cells Produce Cysts That Partially Fragment Prior to Meiosis." *Development* 140 (10): 2075–81.

Leitch, Harry G., Walfred W.C. Tang, and M. Azim Surani. 2013. "Primordial Germ-Cell Development and Epigenetic Reprogramming in Mammals." *Current Topics in Developmental Biology* 104 (January): 149–87.

Leitch, Harry G, Kirsten R McEwen, Aleksandra Turp, Vesela Encheva, Tom Carroll, Nils Grabole, William Mansfield, et al. 2013. "Naive Pluripotency Is Associated with Global DNA Hypomethylation." *Nature Structural & Molecular Biology* 20 (3): 311–16.

Levey, Irwin L., G.B. Stull, and R.L. Brinster. 1978. "Poly(A) and Synthesis of Polyadenylated RNA in the Preimplantation Mouse Embryo." *Developmental Biology* 64 (1): 140–48.

Li, Meng, Jason S L Yu, Katarzyna Tilgner, Swee Hoe Ong, Hiroko Koike-Yusa, and Kosuke Yusa. 2018. "Genome-Wide CRISPR-KO Screen Uncovers MTORC1-Mediated Gsk3 Regulation in Naive Pluripotency Maintenance and Dissolution." *Cell Reports* 24 (2): 489–502.

Licatalosi, Donny D. 2016. "Roles of RNA-Binding Proteins and Post-Transcriptional Regulation in Driving Male Germ Cell Development in the Mouse." *Advances in Experimental Medicine and Biology* 907: 123–51.

Lin, T A, X Kong, T A Haystead, A Pause, G Belsham, N Sonenberg, and J C Lawrence. 1994. "PHAS-I as a Link between Mitogen-Activated Protein Kinase and Translation Initiation." *Science (New York, N.Y.)* 266 (5185): 653–56.

Lin, T A, and J C Lawrence. 1996. "Control of the Translational Regulators PHAS-I and PHAS-II by Insulin and CAMP in 3T3-L1 Adipocytes." *The Journal of Biological Chemistry* 271 (47): 30199–204.

Lin, Yanfeng, Mark E Gill, Jana Koubova, and David C Page. 2008. "Germ Cell-Intrinsic and -Extrinsic Factors Govern Meiotic Initiation in Mouse Embryos." *Science (New York, N.Y.)* 322 (5908): 1685–87.

Lin, Yanfeng, and David C. Page. 2005. "Dazl Deficiency Leads to Embryonic Arrest of Germ Cell Development in XY C57BL/6 Mice." *Developmental Biology* 288 (2): 309–16.

Liu, Jing, Spencer G Willet, Eric D Bankaitis, Yanwen Xu, Chris V E Wright, and Guoqiang Gu. 2013. "Non-Parallel Recombination Limits Cre-LoxP-Based Reporters as Precise Indicators of Conditional Genetic Manipulation." *Genesis (New York, N.Y. : 2000)* 51 (6): 436–42.

Liu, Pengda, Wenjian Gan, Y Rebecca Chin, Kohei Ogura, Jianping Guo, Jinfang Zhang, Bin Wang, et al. 2015. "PtdIns(3,4,5)P3-Dependent Activation of the MTORC2 Kinase Complex." *Cancer Discovery* 5 (11): 1194–1209.

Liu, Yansheng, Andreas Beyer, and Ruedi Aebersold. 2016. "On the Dependency of Cellular Protein Levels on MRNA Abundance." *Cell* 165 (3): 535–50.

Lobascio, A M, F G Klinger, M L Scaldaferri, D Farini, and M De Felici. 2007. "Analysis of Programmed Cell Death in Mouse Fetal Oocytes." *Reproduction* 134 (2): 241–52.

Lomelí, Hilda, Verónica Ramos-Mejía, Marina Gertsenstein, Corrinne G. Lobe, and Andras Nagy. 2000. "Targeted Insertion of Cre Recombinase into the TNAP Gene: Excision in Primordial Germ Cells." *Genesis* 26 (2): 116–17.

Ma, Xiaoju Max, and John Blenis. 2009. "Molecular Mechanisms of MTOR-Mediated Translational Control." *Nature Reviews Molecular Cell Biology* 10 (5): 307–18.

Ma, Xiaoju Max, Sang-Oh Yoon, Celeste J Richardson, Kristina Jülich, and John Blenis. 2008. "SKAR Links Pre-MRNA Splicing to MTOR/S6K1-Mediated Enhanced Translation Efficiency of Spliced MRNAs." *Cell* 133 (2): 303–13.

Maatouk, Danielle M, Lori D Kellam, Mellissa R W Mann, Hong Lei, En Li, Marisa S Bartolomei, and James L Resnick. 2006. "DNA Methylation Is a Primary Mechanism for Silencing Postmigratory Primordial Germ Cell Genes in Both Germ Cell and Somatic Cell Lineages." *Development (Cambridge, England)* 133 (17): 3411–18.

MacGregor, G.R., B.P. Zambrowicz, and P. Soriano. 1995. "Tissue Non-Specific Alkaline Phosphatase Is

Expressed in Both Embryonic and Extraembryonic Lineages during Mouse Embryogenesis but Is Not Required for Migration of Primordial Germ Cells." *Development* 121 (5).

MacLean, Glenn, Hui Li, Daniel Metzger, Pierre Chambon, and Martin Petkovich. 2007. "Apoptotic Extinction of Germ Cells in Testes of *Cyp26b1* Knockout Mice." *Endocrinology* 148 (10): 4560–67.

Mader, Sylvie, Han Lee, Arnim Pause, and Nahum Sonenberg. 1995. "The Translation Initiation Factor EIF-4E Binds to a Common Motif Shared by the Translation Factor EIF-4⊙ and the Translational Repressors 4E-Binding Proteins." *Molecular and Cellular Biology* 15 (9): 4990–97.

Madisen, Linda, Theresa A Zwingman, Susan M Sunkin, Seung Wook Oh, Hatim A Zariwala, Hong Gu, Lydia L Ng, et al. 2010. "A Robust and High-Throughput Cre Reporting and Characterization System for the Whole Mouse Brain." *Nature Neuroscience* 13 (1): 133–40.

Magnúsdóttir, Erna, Sabine Dietmann, Kazuhiro Murakami, Ufuk Günesdogan, Fuchou Tang, Siqin Bao, Evangelia Diamanti, Kaiqin Lao, Berthold Gottgens, and M. Azim Surani. 2013. "A Tripartite Transcription Factor Network Regulates Primordial Germ Cell Specification in Mice." *Nature Cell Biology* 15 (8): 905–15.

Magnuson, Brian, Bilgen Ekim, and Diane C Fingar. 2012. "Regulation and Function of Ribosomal Protein S6 Kinase (S6K) within MTOR Signalling Networks." *The Biochemical Journal* 441 (1): 1–21.

Makker, Annu, Madhu Mati Goel, and Abbas Ali Mahdi. 2014. "PI3K/PTEN/Akt and TSC/MTOR Signaling Pathways, Ovarian Dysfunction, and Infertility: An Update." *Journal of Molecular Endocrinology* 53 (3): R103-18.

Manning, Brendan D, and Alex Toker. 2017. "AKT/PKB Signaling: Navigating the Network." *Cell* 169 (3): 381–405.

Marcotrigiano, Joseph, Anne-Claude Gingras, Nahum Sonenberg, and Stephen K Burley. 1999. "Cap-Dependent Translation Initiation in Eukaryotes Is Regulated by a Molecular Mimic of EIF4G." *Molecular Cell* 3 (6): 707–16.

Martelli, Alberto M., Giovanna Tabellini, Daniela Bressanin, Andrea Ognibene, Kaoru Goto, Lucio Cocco, and Camilla Evangelisti. 2012. "The Emerging Multiple Roles of Nuclear Akt." *Biochimica et Biophysica Acta (BBA) - Molecular Cell Research* 1823 (12): 2168–78.

Martina, Jose A, Yong Chen, Marjan Gucek, and Rosa Puertollano. 2012. "MTORC1 Functions as a Transcriptional Regulator of Autophagy by Preventing Nuclear Transport of TFEB." *Autophagy* 8 (6): 903–14.

Masvidal, Laia, Laura Hulea, Luc Furic, Ivan Topisirovic, and Ola Larsson. 2017. "MTOR-Sensitive Translation: Cleared Fog Reveals More Trees." *RNA Biology* 14 (10): 1299–1305.

Matsui, Y., A. Takehara, Y. Tokitake, M. Ikeda, Y. Obara, Y. Morita-Fujimura, T. Kimura, and T. Nakano. 2014. "The Majority of Early Primordial Germ Cells Acquire Pluripotency by AKT Activation." *Development* 141 (23): 4457–67.

Matsui, Yasuhisa, Deniz Toksoz, Satomi Nishikawa, Shin-Ichi Nishikawa, David Williams, Krisztina Zsebo, and Brigid L. M. Hogan. 1991. "Effect of Steel Factor and Leukaemia Inhibitory Factor on Murine Primordial Germ Cells in Culture." *Nature* 353 (6346): 750–52.

Matsui, Yasuhisa, Krisztina Zsebo, and Brigid L.M. Hogan. 1992. "Derivation of Pluripotential Embryonic Stem Cells from Murine Primordial Germ Cells in Culture." *Cell* 70 (5): 841–47.

McLaren, A., and D. Southee. 1997. “Entry of Mouse Embryonic Germ Cells into Meiosis.” *Developmental Biology* 187 (1): 107–13.

McLaren, Anne. 2003. “Primordial Germ Cells in the Mouse.” *Developmental Biology* 262 (1): 1–15.

Meng, Delong, Anderson R Frank, and Jenna L Jewell. 2018. “MTOR Signaling in Stem and Progenitor Cells.” *Development (Cambridge, England)* 145 (1): dev152595.

Meng, X, M Lindahl, M E Hyvönen, M Parvinen, D G de Rooij, M W Hess, A Raatikainen-Ahokas, et al. 2000. “Regulation of Cell Fate Decision of Undifferentiated Spermatogonia by GDNF.” *Science (New York, N.Y.)* 287 (5457): 1489–93.

Menke, Douglas B, Jana Koubova, and David C Page. 2003. “Sexual Differentiation of Germ Cells in XX Mouse Gonads Occurs in an Anterior-to-Posterior Wave.” *Developmental Biology* 262 (2): 303–12.

Messerschmidt, Daniel M, Barbara B Knowles, and Davor Solter. 2014. “DNA Methylation Dynamics during Epigenetic Reprogramming in the Germline and Preimplantation Embryos.” *Genes & Development* 28 (8): 812–28.

MEYTS, EWA RAJPERT-DE, NIELS JØRGENSEN, KAREN BRØNDUM-NIELSEN, JØRN MÜLLER, and NIELS E. SKAKKEBAEK. 1998. “Developmental Arrest of Germ Cells in the Pathogenesis of Germ Cell Neoplasia.” *APMIS* 106 (1–6): 198–206.

Meyuhas, Oded. 2015. “Ribosomal Protein S6 Phosphorylation: Four Decades of Research.” *International Review of Cell and Molecular Biology* 320 (January): 41–73.

Meyuhas, Oded, and Tamar Kahan. 2015. “The Race to Decipher the Top Secrets of TOP MRNAs.” *Biochimica et Biophysica Acta (BBA) - Gene Regulatory Mechanisms* 1849 (7): 801–11.

Miguel, Maria P De, Linzhao Cheng, Eric C Holland, Mark J Federspiel, and Peter J Donovan. 2002. “Dissection of the C-Kit Signaling Pathway in Mouse Primordial Germ Cells by Retroviral-Mediated Gene Transfer.” *Proceedings of the National Academy of Sciences of the United States of America* 99 (16): 10458–63.

Mikedis, Maria M, and Karen M Downs. 2017. “PRDM1/BLIMP1 Is Widely Distributed to the Nascent Fetal-Placental Interface in the Mouse Gastrula.” *Developmental Dynamics : An Official Publication of the American Association of Anatomists* 246 (1): 50–71.

Miloslavski, Rachel, Elad Cohen, Adam Avraham, Yifat Iluz, Zvi Hayouka, Judith Kasir, Rajini Mudhasani, et al. 2014. “Oxygen Sufficiency Controls TOP MRNA Translation via the TSC-Rheb-MTOR Pathway in a 4E-BP-Independent Manner.” *Journal of Molecular Cell Biology* 6 (3): 255–66.

Molyneaux, Kathleen A., Jim Stallock, Kyle Schaible, and Christopher Wylie. 2001. “Time-Lapse Analysis of Living Mouse Germ Cell Migration.” *Developmental Biology* 240 (2): 488–98.

Molyneaux, Kathleen A, Hélène Zinszner, Prabhat S Kunwar, Kyle Schaible, Jürg Stebler, Mary Jean Sunshine, William O’Brien, et al. 2003. “The Chemokine SDF1/CXCL12 and Its Receptor CXCR4 Regulate Mouse Germ Cell Migration and Survival.” *Development (Cambridge, England)* 130 (18): 4279–86.

Montagutelli, X. 2000. “Effect of the Genetic Background on the Phenotype of Mouse Mutations.” *Journal of the American Society of Nephrology : JASN* 11 Suppl 16 (November): S101-5.

Moore, G. P. M. 1975. “The RNA Polymerase Activity of the Preimplantation Mouse Embryo.” *Development* 34 (2).

Moore, G P, S Lintern-Moore, H Peters, and M Faber. 1974. "RNA Synthesis in the Mouse Oocyte." *The Journal of Cell Biology* 60 (2): 416–22.

Morgan, Hugh D, Wendy Dean, Heather A Coker, Wolf Reik, and Svend K Petersen-Mahrt. 2004. "Activation-Induced Cytidine Deaminase Deaminates 5-Methylcytosine in DNA and Is Expressed in Pluripotent Tissues: Implications for Epigenetic Reprogramming." *The Journal of Biological Chemistry* 279 (50): 52353–60.

Morohaku, Kanako, Ren Tanimoto, Keisuke Sasaki, Ryouka Kawahara-Miki, Tomohiro Kono, Katsuhiko Hayashi, Yuji Hirao, and Yayoi Obata. 2016. "Complete in Vitro Generation of Fertile Oocytes from Mouse Primordial Germ Cells." *Proceedings of the National Academy of Sciences of the United States of America* 113 (32): 9021–26.

Mould, Arne, Marc A J Morgan, Li Li, Elizabeth K Bikoff, and Elizabeth J Robertson. 2012. "Blimp1/Prdm1 Governs Terminal Differentiation of Endovascular Trophoblast Giant Cells and Defines Multipotent Progenitors in the Developing Placenta." *Genes & Development* 26 (18): 2063–74.

Murakami, Mirei, Tomoko Ichisaka, Mitsuyo Maeda, Noriko Oshiro, Kenta Hara, Frank Edenhofer, Hiroshi Kiyama, Kazuyoshi Yonezawa, and Shinya Yamanaka. 2004. "MTOR Is Essential for Growth and Proliferation in Early Mouse Embryos and Embryonic Stem Cells." *Molecular and Cellular Biology* 24 (15): 6710–18.

Musa, J, M F Orth, M Dallmayer, M Baldauf, C Pardo, B Rotblat, T Kirchner, G Leprivier, and T G P Grünewald. 2016. "Eukaryotic Initiation Factor 4E-Binding Protein 1 (4E-BP1): A Master Regulator of MRNA Translation Involved in Tumorigenesis." *Oncogene* 35 (36): 4675–88.

Nagamori, Ippei, V Adam Cruickshank, and Paolo Sassone-Corsi. 2011. "Regulation of an RNA Granule during Spermatogenesis: Acetylation of MVH in the Chromatoid Body of Germ Cells." *Journal of Cell Science* 124 (Pt 24): 4346–55.

Nagy, Andras. 2000. "Cre Recombinase: The Universal Reagent for Genome Tailoring." *Genesis* 26 (2): 99–109.

Napoles, Mariana de, Tatyana Nesterova, and Neil Brockdorff. 2007. "Early Loss of Xist RNA Expression and Inactive X Chromosome Associated Chromatin Modification in Developing Primordial Germ Cells." Edited by Edith Heard. *PLoS ONE* 2 (9): e860.

Nef, Serge, Sunita Verma-Kurvari, Jussi Merenmies, Jean-Dominique Vassalli, Argiris Efstratiadis, Domenico Accili, and Luis F. Parada. 2003. "Testis Determination Requires Insulin Receptor Family Function in Mice." *Nature* 426 (6964): 291–95.

Nichols, Jennifer, and Austin Smith. 2009. "Naive and Primed Pluripotent States." *Cell Stem Cell* 4 (6): 487–92.

Noguchi, T, and M Noguchi. 1985. "A Recessive Mutation (Ter) Causing Germ Cell Deficiency and a High Incidence of Congenital Testicular Teratomas in 129/Sv-Ter Mice." *Journal of the National Cancer Institute* 75 (2): 385–92.

Novak, A, C Guo, W Yang, A Nagy, and CG Lobe. 2000. "Z/EG, a Double Reporter Mouse Line That Expresses Enhanced Green Fluorescent Protein upon Cre-Mediated Excision." *Genesis* 28 (3–4): 147–55.

Oh, Won Jun, Chang-chih Wu, Sung Jin Kim, Valeria Facchinetti, Louis-André Julien, Monica Finlan, Philippe P Roux, Bing Su, and Estela Jacinto. 2010. "MTORC2 Can Associate with Ribosomes to Promote Cotranslational Phosphorylation and Stability of Nascent Akt Polypeptide." *The EMBO*

Journal 29 (23): 3939–51.

Ohinata, Yasuhide, Hiroshi Ohta, Mayo Shigeta, Kaori Yamanaka, Teruhiko Wakayama, and Mitinori Saitou. 2009. "A Signaling Principle for the Specification of the Germ Cell Lineage in Mice." *Cell* 137 (3): 571–84.

Ohinata, Yasuhide, Bernhard Payer, Dónal O'Carroll, Katia Ancelin, Yukiko Ono, Mitsue Sano, Sheila C. Barton, et al. 2005. "Blimp1 Is a Critical Determinant of the Germ Cell Lineage in Mice." *Nature* 436 (7048): 207–13.

Okamura, Daiji, Yuko Tokitake, Hitoshi Niwa, and Yasuhisa Matsui. 2008. "Requirement of Oct3/4 Function for Germ Cell Specification." *Developmental Biology* 317 (2): 576–84.

Oliveira, Pedro F, C Y Cheng, and Marco G Alves. 2017. "Emerging Role for Mammalian Target of Rapamycin in Male Fertility." *Trends in Endocrinology and Metabolism: TEM* 28 (3): 165–67.

Onda, Hiroaki, Andreas Lueck, Peter W. Marks, Henry B. Warren, and David J. Kwiatkowski. 1999. "Tsc2+/– Mice Develop Tumors in Multiple Sites That Express Gelsolin and Are Influenced by Genetic Background." *Journal of Clinical Investigation* 104 (6): 687–95.

Oosterhuis, J. Wolter, and Leendert H. J. Looijenga. 2005. "Testicular Germ-Cell Tumours in a Broader Perspective." *Nature Reviews Cancer* 5 (3): 210–22.

Pardo, Olivier E, and Michael J Seckl. 2013. "S6K2: The Neglected S6 Kinase Family Member." *Frontiers in Oncology* 3: 191.

Parma, Pietro, Orietta Radi, Valerie Vidal, Marie Christine Chaboissier, Elena Dellambra, Stella Valentini, Liliana Guerra, Andreas Schedl, and Giovanna Camerino. 2006. "R-Spondin1 Is Essential in Sex Determination, Skin Differentiation and Malignancy." *Nature Genetics* 38 (11): 1304–9.

Pause, Arnim, Graham J. Belsham, Anne-Claude Gingras, Olivier Donzé, Tai-An Lin, John C. Lawrence, and Nahum Sonenberg. 1994. "Insulin-Dependent Stimulation of Protein Synthesis by Phosphorylation of a Regulator of 5′-Cap Function." *Nature* 371 (6500): 762–67.

Pende, Mario, Sara C. Kozma, Muriel Jaquet, Viola Oorschot, Rémy Burcelin, Yannick Le Marchand-Brustel, Judith Klumperman, Bernard Thorens, and George Thomas. 2000. "Hypoinsulinaemia, Glucose Intolerance and Diminished β-Cell Size in S6K1-Deficient Mice." *Nature* 408 (6815): 994–97.

Pende, Mario, Sung Hee Um, Virginie Mieulet, Melanie Sticker, Valerie L Goss, Jurgen Mestan, Matthias Mueller, Stefano Fumagalli, Sara C Kozma, and George Thomas. 2004. "S6K1(-/-)/S6K2(-/-) Mice Exhibit Perinatal Lethality and Rapamycin-Sensitive 5′-Terminal Oligopyrimidine MRNA Translation and Reveal a Mitogen-Activated Protein Kinase-Dependent S6 Kinase Pathway." *Molecular and Cellular Biology* 24 (8): 3112–24.

Pepling, Melissa E. 2006. "From Primordial Germ Cell to Primordial Follicle: Mammalian Female Germ Cell Development." *Genesis* 44 (12): 622–32.

Pepling, Melissa E., and Allan C. Spradling. 2001. "Mouse Ovarian Germ Cell Cysts Undergo Programmed Breakdown to Form Primordial Follicles." *Developmental Biology* 234 (2): 339–51.

Percharde, Michelle, Priscilla Wong, and Miguel Ramalho-Santos. 2017. "Global Hypertranscription in the Mouse Embryonic Germline." *Cell Reports* 19 (10): 1987–96.

Pesce, M., M.G. Farrace, M. Piacentini, S. Dolci, and M. De Felici. 1993. "Stem Cell Factor and Leukemia Inhibitory Factor Promote Primordial Germ Cell Survival by Suppressing Programmed Cell Death

(Apoptosis)." *Development* 118 (4).

Pesce, Maurizio, Xiangyuan Wang, Debra J Wolgemuth, and Hans R Schöler. 1998. "Differential Expression of the Oct-4 Transcription Factor during Mouse Germ Cell Differentiation." *Mechanisms of Development* 71 (1–2): 89–98.

Peterson, Timothy R., Shomit S. Sengupta, Thurl E. Harris, Anne E. Carmack, Seong A. Kang, Eric Balderas, David A. Guertin, et al. 2011. "MTOR Complex 1 Regulates Lipin 1 Localization to Control the SREBP Pathway." *Cell* 146 (3): 408–20.

Pitetti, Jean-Luc, Pierre Calvel, Yannick Romero, Béatrice Conne, Vy Truong, Marilena D. Papaioannou, Olivier Schaad, et al. 2013. "Insulin and IGF1 Receptors Are Essential for XX and XY Gonadal Differentiation and Adrenal Development in Mice." Edited by Humphrey Yao. *PLoS Genetics* 9 (1): e1003160.

Popp, Christian, Wendy Dean, Suhua Feng, Shawn J. Cokus, Simon Andrews, Matteo Pellegrini, Steven E. Jacobsen, and Wolf Reik. 2010. "Genome-Wide Erasure of DNA Methylation in Mouse Primordial Germ Cells Is Affected by AID Deficiency." *Nature* 463 (7284): 1101–5.

Porstmann, Thomas, Claudio R. Santos, Beatrice Griffiths, Megan Cully, Mary Wu, Sally Leevers, John R. Griffiths, Yuen-Li Chung, and Almut Schulze. 2008. "SREBP Activity Is Regulated by MTORC1 and Contributes to Akt-Dependent Cell Growth." *Cell Metabolism* 8 (3): 224–36.

Potireddy, Santhi, Rita Vassena, Bela G. Patel, and Keith E. Latham. 2006. "Analysis of Polysomal MRNA Populations of Mouse Oocytes and Zygotes: Dynamic Changes in Maternal MRNA Utilization and Function." *Developmental Biology* 298 (1): 155–66.

Poulin, F, A C Gingras, H Olsen, S Chevalier, and N Sonenberg. 1998. "4E-BP3, a New Member of the Eukaryotic Initiation Factor 4E-Binding Protein Family." *The Journal of Biological Chemistry* 273 (22): 14002–7.

Pullen, N, P B Dennis, M Andjelkovic, A Dufner, S C Kozma, B A Hemmings, and G Thomas. 1998. "Phosphorylation and Activation of P70s6k by PDK1." *Science (New York, N.Y.)* 279 (5351): 707–10.

Raught, Brian, Franck Peiretti, Anne-Claude Gingras, Mark Livingstone, David Shahbazian, Greg L Mayeur, Roberto D Polakiewicz, Nahum Sonenberg, and John W B Hershey. 2004. "Phosphorylation of Eucaryotic Translation Initiation Factor 4B Ser422 Is Modulated by S6 Kinases." *The EMBO Journal* 23 (8): 1761–69.

Rawson, Robert B. 2003. "The SREBP Pathway — Insights from Insigs and Insects." *Nature Reviews Molecular Cell Biology* 4 (8): 631–40.

Razquin Navas, Patricia, and Kathrin Thedieck. 2017. "Differential Control of Ageing and Lifespan by Isoforms and Splice Variants across the MTOR Network." *Essays in Biochemistry* 61 (3): 349–68.

Reddy, Pradeep, Deepak Adhikari, Wenjing Zheng, Shawn Liang, Tuula Hämäläinen, Virpi Tohonen, Wataru Ogawa, et al. 2009. "PDK1 Signaling in Oocytes Controls Reproductive Aging and Lifespan by Manipulating the Survival of Primordial Follicles." *Human Molecular Genetics* 18 (15): 2813–24.

Reddy, Pradeep, Lian Liu, Deepak Adhikari, Krishna Jagarlamudi, Singareddy Rajareddy, Yan Shen, Chun Du, et al. 2008. "Oocyte-Specific Deletion of Pten Causes Premature Activation of the Primordial Follicle Pool." *Science (New York, N.Y.)* 319 (5863): 611–13.

Renfree, Marilyn B, and Jane C Fenelon. 2017. "The Enigma of Embryonic Diapause." *Development (Cambridge, England)* 144 (18): 3199–3210.

Resnick, James L., Lynn S. Bixler, Linzhao Cheng, and Peter J. Donovan. 1992. "Long-Term Proliferation of Mouse Primordial Germ Cells in Culture." *Nature* 359 (6395): 550–51.

Reynolds, Nicola, Brian Collier, Victoria Bingham, Nicola K Gray, and Howard J Cooke. 2007. "Translation of the Synaptonemal Complex Component Sycp3 Is Enhanced in Vivo by the Germ Cell Specific Regulator Dazl." *RNA (New York, N.Y.)* 13 (7): 974–81.

Reynolds, Nicola, Brian Collier, Klio Maratou, Victoria Bingham, Robert M. Speed, Mary Taggart, Colin A. Semple, Nicola K. Gray, and Howard J. Cooke. 2005. "Dazl Binds in Vivo to Specific Transcripts and Can Regulate the Pre-Meiotic Translation of Mvh in Germ Cells." *Human Molecular Genetics* 14 (24): 3899–3909.

Richardson, Brian E., and Ruth Lehmann. 2010. "Mechanisms Guiding Primordial Germ Cell Migration: Strategies from Different Organisms." *Nature Reviews Molecular Cell Biology* 11 (1): 37–49.

Richardson, Mark Bröenstrup, Diane C. Fingar, Kristina Jülich, Bryan A. Ballif, Steven Gygi, and John Blenis. 2004. "SKAR Is a Specific Target of S6 Kinase 1 in Cell Growth Control." *Current Biology* 14 (17): 1540–49.

Risson, Valérie, Laetitia Mazelin, Mila Roceri, Hervé Sanchez, Vincent Moncollin, Claudine Corneloup, Hélène Richard-Bulteau, et al. 2009. "Muscle Inactivation of MTOR Causes Metabolic and Dystrophin Defects Leading to Severe Myopathy." *The Journal of Cell Biology* 187 (6): 859–74.

Robertson, Elizabeth J, Iphigenie Charatsi, Clive J Joyner, Chad H Koonce, Marc Morgan, Ayesha Islam, Carol Paterson, et al. 2007. "Blimp1 Regulates Development of the Posterior Forelimb, Caudal Pharyngeal Arches, Heart and Sensory Vibrissae in Mice." *Development (Cambridge, England)* 134 (24): 4335–45.

Robitaille, Aaron M, Stefan Christen, Mitsugu Shimobayashi, Marion Cornu, Luca L Fava, Suzette Moes, Cristina Prescianotto-Baschong, Uwe Sauer, Paul Jenoe, and Michael N Hall. 2013. "Quantitative Phosphoproteomics Reveal MTORC1 Activates de Novo Pyrimidine Synthesis." *Science (New York, N.Y.)* 339 (6125): 1320–23.

Roczniak-Ferguson, Agnes, Constance S. Petit, Florian Froehlich, Sharon Qian, Jennifer Ky, Brittany Angarola, Tobias C. Walther, and Shawn M. Ferguson. 2012. "The Transcription Factor TFEB Links MTORC1 Signaling to Transcriptional Control of Lysosome Homeostasis." *Sci. Signal.* 5 (228): ra42-ra42.

Rosner, M., and M. Hengstschlager. 2008. "Cytoplasmic and Nuclear Distribution of the Protein Complexes MTORC1 and MTORC2: Rapamycin Triggers Dephosphorylation and Delocalization of the MTORC2 Components Rictor and Sin1." *Human Molecular Genetics* 17 (19): 2934–48.

Rossant, Janet, and James C. Cross. 2001. "PLACENTAL DEVELOPMENT: LESSONS FROM MOUSE MUTANTS." *Nature Reviews Genetics* 2 (7): 538–48.

Rousseau, Adrien, and Anne Bertolotti. 2016. "An Evolutionarily Conserved Pathway Controls Proteasome Homeostasis." *Nature* 536 (7615): 184–89.

Roux, Philippe P., David Shahbazian, Hieu Vu, Marina K. Holz, Michael S. Cohen, Jack Taunton, Nahum Sonenberg, and John Blenis. 2007. "RAS/ERK Signaling Promotes Site-Specific Ribosomal Protein S6 Phosphorylation via RSK and Stimulates Cap-Dependent Translation." *Journal of Biological Chemistry* 282 (19): 14056–64.

Roux, Philippe P, and Ivan Topisirovic. 2018. "Signaling Pathways Involved in the Regulation of MRNA Translation." *Molecular and Cellular Biology* 38 (12).

Ruggero, Davide. 2013. "Translational Control in Cancer Etiology." *Cold Spring Harbor Perspectives in Biology* 5 (2).

Ruggiu, Matteo, Robert Speed, Mary Taggart, Stewart J. McKay, Fiona Kilanowski, Philippa Saunders, Julia Dorin, and Howard J. Cooke. 1997. "The Mouse Dazla Gene Encodes a Cytoplasmic Protein Essential for Gametogenesis." *Nature* 389 (6646): 73–77.

Runyan, Christopher, Kyle Schaible, Kathleen Molyneaux, Zhuoqiao Wang, Linda Levin, and Christopher Wylie. 2006. "Steel Factor Controls Midline Cell Death of Primordial Germ Cells and Is Essential for Their Normal Proliferation and Migration." *Development (Cambridge, England)* 133 (24): 4861–69.

Ruvinsky, Igor, Nitzan Sharon, Tal Lerer, Hannah Cohen, Miri Stolovich-Rain, Tomer Nir, Yuval Dor, Philip Zisman, and Oded Meyuhas. 2005. "Ribosomal Protein S6 Phosphorylation Is a Determinant of Cell Size and Glucose Homeostasis." *Genes & Development* 19 (18): 2199–2211.

Sabatini, David M., Hediye Erdjument-Bromage, Mary Lui, Paul Tempst, and Solomon H. Snyder. 1994. "RAFT1: A Mammalian Protein That Binds to FKBP12 in a Rapamycin-Dependent Fashion and Is Homologous to Yeast TORs." *Cell* 78 (1): 35–43.

Sabers, C J, M M Martin, G J Brunn, J M Williams, F J Dumont, G Wiederrecht, and R T Abraham. 1995. "Isolation of a Protein Target of the FKBP12-Rapamycin Complex in Mammalian Cells." *The Journal of Biological Chemistry* 270 (2): 815–22.

Saitou, Mitinori, Sheila C. Barton, and M. Azim Surani. 2002. "A Molecular Programme for the Specification of Germ Cell Fate in Mice." *Nature* 418 (6895): 293–300.

Saitou, Mitinori, and Masashi Yamaji. 2012. "Primordial Germ Cells in Mice." *Cold Spring Harbor Perspectives in Biology* 4 (11).

Sakurai, Takayuki, Taisen Iguchi, Kazuo Moriwaki, and Motoko Noguchi. 1995. "The Ter Mutation First Causes Primordial Germ Cell Deficiency in Ter/Ter Mouse Embryos at 8 Days of Gestation." *Development, Growth and Differentiation* 37 (3): 293–302.

Sampath, Prabha, David K Pritchard, Lil Pabon, Hans Reinecke, Stephen M Schwartz, David R Morris, and Charles E Murry. 2008. "A Hierarchical Network Controls Protein Translation during Murine Embryonic Stem Cell Self-Renewal and Differentiation." *Cell Stem Cell* 2 (5): 448–60.

Sancak, Yasemin, Timothy R Peterson, Yoav D Shaul, Robert A Lindquist, Carson C Thoreen, Liron Bar-Peled, and David M Sabatini. 2008. "The Rag GTPases Bind Raptor and Mediate Amino Acid Signaling to MTORC1." *Science (New York, N.Y.)* 320 (5882): 1496–1501.

Sanford, L. Philip, Suhas Kallapur, Ilona Ormsby, and Thomas Doetschman. 2001. "Influence of Genetic Background on Knockout Mouse Phenotypes." In *Gene Knockout Protocols*, 217–25. New Jersey: Humana Press.

Sanz, Elisenda, Linghai Yang, Thomas Su, David R. Morris, G. Stanley McKnight, and Paul S. Amieux. 2009. "Cell-Type-Specific Isolation of Ribosome-Associated MRNA from Complex Tissues." *Proceedings of the National Academy of Sciences* 106 (33): 13939–44.

Saper, Clifford B. 2009. "A Guide to the Perplexed on the Specificity of Antibodies." *The Journal of Histochemistry and Cytochemistry : Official Journal of the Histochemistry Society* 57 (1): 1–5.

Sarbassov, Dos D., Siraj M. Ali, Shomit Sengupta, Joon-Ho Sheen, Peggy P. Hsu, Alex F. Bagley, Andrew L. Markhard, and David M. Sabatini. 2006. "Prolonged Rapamycin Treatment Inhibits MTORC2 Assembly and Akt/PKB." *Molecular Cell* 22 (2): 159–68.

Sarbassov, Dos D., Siraj M Ali, Do-Hyung Kim, David A Guertin, Robert R Latek, Hediye Erdjument-Bromage, Paul Tempst, and David M Sabatini. 2004. "Rictor, a Novel Binding Partner of MTOR, Defines a Rapamycin-Insensitive and Raptor-Independent Pathway That Regulates the Cytoskeleton." *Current Biology* 14 (14): 1296–1302.

Sarbassov, David A Guertin, Siraj M Ali, and David M Sabatini. 2005. "Phosphorylation and Regulation of Akt/PKB by the Rictor-MTOR Complex." *Science (New York, N.Y.)* 307 (5712): 1098–1101.

Sato, Masatake, Tohru Kimura, Ken Kurokawa, Yukiko Fujita, Koichiro Abe, Masaaki Masuhara, Teruo Yasunaga, Akihide Ryo, Mikio Yamamoto, and Toru Nakano. 2002. "Identification of PGC7, a New Gene Expressed Specifically in Preimplantation Embryos and Germ Cells." *Mechanisms of Development* 113 (1): 91–94.

Sauer, B, and N Henderson. 1988. "Site-Specific DNA Recombination in Mammalian Cells by the Cre Recombinase of Bacteriophage P1." *Proceedings of the National Academy of Sciences of the United States of America* 85 (14): 5166–70.

Saunders, P T K, J M A Turner, M Ruggiu, M Taggart, P S Burgoyne, D Elliott, and H J Cooke. 2003. "Absence of MDazl Produces a Final Block on Germ Cell Development at Meiosis." *Reproduction (Cambridge, England)* 126 (5): 589–97.

Saxton, Robert A., and David M. Sabatini. 2017. "MTOR Signaling in Growth, Metabolism, and Disease." *Cell* 168 (6): 960–76.

Scheid, Michael P, Paola A Marignani, and James R Woodgett. 2002. "Multiple Phosphoinositide 3-Kinase-Dependent Steps in Activation of Protein Kinase B." *Molecular and Cellular Biology* 22 (17): 6247–60.

Seisenberger, Stefanie, Simon Andrews, Felix Krueger, Julia Arand, Jörn Walter, Fátima Santos, Christian Popp, Bernard Thienpont, Wendy Dean, and Wolf Reik. 2012. "The Dynamics of Genome-Wide DNA Methylation Reprogramming in Mouse Primordial Germ Cells." *Molecular Cell* 48 (6): 849–62.

Seki, Yoshiyuki, Katsuhiko Hayashi, Kunihiko Itoh, Michinao Mizugaki, Mitinori Saitou, and Yasuhisa Matsui. 2005. "Extensive and Orderly Reprogramming of Genome-Wide Chromatin Modifications Associated with Specification and Early Development of Germ Cells in Mice." *Developmental Biology* 278 (2): 440–58.

Seki, Yoshiyuki, Masashi Yamaji, Yukihiro Yabuta, Mitsue Sano, Mayo Shigeta, Yasuhisa Matsui, Yumiko Saga, Makoto Tachibana, Yoichi Shinkai, and Mitinori Saitou. 2007. "Cellular Dynamics Associated with the Genome-Wide Epigenetic Reprogramming in Migrating Primordial Germ Cells in Mice." *Development (Cambridge, England)* 134 (14): 2627–38.

Sekido, Ryohei, Isabelle Bar, Véronica Narváez, Graeme Penny, and Robin Lovell-Badge. 2004. "SOX9 Is Up-Regulated by the Transient Expression of SRY Specifically in Sertoli Cell Precursors." *Developmental Biology* 274 (2): 271–79.

Sekido, Ryohei, and Robin Lovell-Badge. 2008. "Sex Determination Involves Synergistic Action of SRY and SF1 on a Specific Sox9 Enhancer." *Nature* 453 (7197): 930–34.

Seligman, Judith, and David C Page. 1998. "The Dazh Gene Is Expressed in Male and Female Embryonic Gonads before Germ Cell Sex Differentiation." *Biochemical and Biophysical Research Communications* 245: 878–82.

Selman, Colin, Jennifer M A Tullet, Daniela Wieser, Elaine Irvine, Steven J Lingard, Agharul I Choudhury, Marc Claret, et al. 2009. "Ribosomal Protein S6 Kinase 1 Signaling Regulates Mammalian Life Span." *Science (New York, N.Y.)* 326 (5949): 140–44.

Serra, Nicholas D., Ellen K. Velte, Bryan A. Niedenberger, Oleksander Kirsanov, and Christopher B. Geyer. 2017. "Cell-Autonomous Requirement for Mammalian Target of Rapamycin (Mtor) in Spermatogonial Proliferation and Differentiation in the Mouse†." *Biology of Reproduction* 96 (4): 816–28.

Settembre, Carmine, Roberto Zoncu, Diego L Medina, Francesco Vetrini, Serkan Erdin, SerpilUckac Erdin, Tuong Huynh, et al. 2012. "A Lysosome-to-nucleus Signalling Mechanism Senses and Regulates the Lysosome via MTOR and TFEB." *The EMBO Journal* 31 (5): 1095–1108.

Shade, Kai-Ting C., Barbara Platzer, Nathaniel Washburn, Vinidhra Mani, Yannic C. Bartsch, Michelle Conroy, Jose D. Pagan, et al. 2015. "A Single Glycan on IgE Is Indispensable for Initiation of Anaphylaxis." *The Journal of Experimental Medicine* 212 (4): 457–67.

Shama, S, D Avni, R M Frederickson, N Sonenberg, and O Meyuhas. 1995. "Overexpression of Initiation Factor EIF-4E Does Not Relieve the Translational Repression of Ribosomal Protein MRNAs in Quiescent Cells." *Gene Expression* 4 (4–5): 241–52.

Sharif, Jafar, Masahiro Muto, Shin-ichiro Takebayashi, Isao Suetake, Akihiro Iwamatsu, Takaho A. Endo, Jun Shinga, et al. 2007. "The SRA Protein Np95 Mediates Epigenetic Inheritance by Recruiting Dnmt1 to Methylated DNA." *Nature* 450 (7171): 908–12.

Shen, Li, Hao Wu, Dinh Diep, Shinpei Yamaguchi, Ana C. D'Alessio, Ho-Lim Fung, Kun Zhang, and Yi Zhang. 2013. "Genome-Wide Analysis Reveals TET- and TDG-Dependent 5-Methylcytosine Oxidation Dynamics." *Cell* 153 (3): 692–706.

Shima, H, M Pende, Y Chen, S Fumagalli, G Thomas, and S C Kozma. 1998. "Disruption of the P70(S6k)/P85(S6k) Gene Reveals a Small Mouse Phenotype and a New Functional S6 Kinase." *The EMBO Journal* 17 (22): 6649–59.

Shimobayashi, Mitsugu, and Michael N. Hall. 2014. "Making New Contacts: The MTOR Network in Metabolism and Signalling Crosstalk." *Nature Reviews Molecular Cell Biology* 15 (3): 155–62.

Shinoda, Gen, T Yvanka De Soysa, Marc T Seligson, Akiko Yabuuchi, Yuko Fujiwara, Pei Yi Huang, John P Hagan, Richard I Gregory, Eric G Moss, and George Q Daley. 2013. "Lin28a Regulates Germ Cell Pool Size and Fertility." *Stem Cells (Dayton, Ohio)* 31 (5): 1001–9.

Shiota, Chiyo, Jeong-Taek Woo, Jill Lindner, Kathy D Shelton, and Mark A Magnuson. 2006. "Multiallelic Disruption of the Rictor Gene in Mice Reveals That MTOR Complex 2 Is Essential for Fetal Growth and Viability." *Developmental Cell* 11 (4): 583–89.

Shyh-Chang, Ng, and George Q. Daley. 2013. "Lin28: Primal Regulator of Growth and Metabolism in Stem Cells." *Cell Stem Cell* 12 (4): 395–406.

Siddiqui, Nadeem, Wolfram Tempel, Lucy Nedyalkova, Laurent Volpon, Amy K Wernimont, Michael J Osborne, Hee-Won Park, and Katherine L B Borden. 2012. "Structural Insights into the Allosteric Effects of 4EBP1 on the Eukaryotic Translation Initiation Factor EIF4E." *Journal of Molecular Biology* 415 (5): 781–92.

Skakkebæk, N. E., J. G. Berthelsen, A. Giwercman, and J. Müller. 1987. "Carcinoma-in-Situ of the Testis: Possible Origin from Gonocytes and Precursor of All Types of Germ Cell Tumours except Spermatocytoma." *International Journal of Andrology* 10 (1): 19–28.

Skakkebæk, N.E., E. Rajpert-De Meyts, and K.M. Main. 2001. "Testicular Dysgenesis Syndrome: An Increasingly Common Developmental Disorder with Environmental Aspects: Opinion." *Human Reproduction* 16 (5): 972–78.

Smith, Mark A., Loukia Katsouri, Elaine E. Irvine, Mohammed K. Hankir, Silvia M.A. Pedroni, Peter J. Voshol, Matthew W. Gordon, et al. 2015. "Ribosomal S6K1 in POMC and AgRP Neurons Regulates Glucose Homeostasis but Not Feeding Behavior in Mice." *Cell Reports* 11 (3): 335.

Solter, Davor, and Barbara B Knowles. 1978. "Monoclonal Antibody Defining a Stage-Specific Mouse Embryonic Antigen (SSEA-1)." *Developmental Biology*. Vol. 75.

Sousa Lopes, Susana M Chuva de, Bernard A J Roelen, Rui M Monteiro, Roul Emmens, Herbert Y Lin, En Li, Kirstie A Lawson, and Christine L Mummery. 2004. "BMP Signaling Mediated by ALK2 in the Visceral Endoderm Is Necessary for the Generation of Primordial Germ Cells in the Mouse Embryo." *Genes & Development* 18 (15): 1838–49.

Souza, F S de, V Gawantka, A P Gómez, H Delius, S L Ang, and C Niehrs. 1999. "The Zinc Finger Gene Xblimp1 Controls Anterior Endomesodermal Cell Fate in Spemann's Organizer." *The EMBO Journal* 18 (21): 6062–72.

Spiller, Cassy M, and Josephine Bowles. 2015. "Sex Determination in Mammalian Germ Cells." *Asian Journal of Andrology* 17 (3): 427–32.

Stephens, L, K Anderson, D Stokoe, H Erdjument-Bromage, G F Painter, A B Holmes, P R Gaffney, et al. 1998. "Protein Kinase B Kinases That Mediate Phosphatidylinositol 3,4,5-Trisphosphate-Dependent Activation of Protein Kinase B." *Science (New York, N.Y.)* 279 (5351): 710–14.

Stevens, L C. 1967. "Origin of Testicular Teratomas from Primordial Germ Cells in Mice." *Journal of the National Cancer Institute* 38 (4): 549–52.

———. 1973. "A New Inbred Subline of Mice (129-TerSv) with a High Incidence of Spontaneous Congenital Testicular Teratomas." *Journal of the National Cancer Institute* 50 (1): 235–42.

———. 1984. "Spontaneous and Experimentally Induced Testicular Teratomas in Mice." *Cell Differentiation* 15 (2–4): 69–74.

Stevens, L C, and K P Hummel. 1957. "A Description of Spontaneous Congenital Testicular Teratomas in Strain 129 Mice." *Journal of the National Cancer Institute* 18 (5): 719–47.

Strome, Susan, and Dustin Updike. 2015. "Specifying and Protecting Germ Cell Fate." *Nature Reviews. Molecular Cell Biology* 16 (7): 406–16.

Sugimoto, Michihiko, and Kuniya Abe. 2007. "X Chromosome Reactivation Initiates in Nascent Primordial Germ Cells in Mice." *PLoS Genetics* 3 (7): e116.

Sun, H, R Lesche, D M Li, J Liliental, H Zhang, J Gao, N Gavrilova, B Mueller, X Liu, and H Wu. 1999. "PTEN Modulates Cell Cycle Progression and Cell Survival by Regulating Phosphatidylinositol 3,4,5,-Trisphosphate and Akt/Protein Kinase B Signaling Pathway." *Proceedings of the National Academy of Sciences of the United States of America* 96 (11): 6199–6204.

Suzuki, Atsushi, Katsuhide Igarashi, Ken-Ichi Aisaki, Jun Kanno, and Yumiko Saga. 2010. "NANOS2 Interacts with the CCR4-NOT Deadenylation Complex and Leads to Suppression of Specific RNAs." *Proceedings of the National Academy of Sciences of the United States of America* 107 (8): 3594–99.

Suzuki, Atsushi, Rie Saba, Kei Miyoshi, Yoshinori Morita, and Yumiko Saga. 2012. "Interaction between NANOS2 and the CCR4-NOT Deadenylation Complex Is Essential for Male Germ Cell Development in Mouse." Edited by Austin John Cooney. *PLoS ONE* 7 (3): e33558.

Suzuki, Atsushi, and Yumiko Saga. 2008. "Nanos2 Suppresses Meiosis and Promotes Male Germ Cell

Differentiation." *Genes & Development* 22 (4): 430–35.

Suzuki, Hitomi, Masayuki Tsuda, Makoto Kiso, and Yumiko Saga. 2008. "Nanos3 Maintains the Germ Cell Lineage in the Mouse by Suppressing Both Bax-Dependent and -Independent Apoptotic Pathways." *Developmental Biology* 318 (1): 133–42.

Svingen, Terje, and Peter Koopman. 2013. "Building the Mammalian Testis: Origins, Differentiation, and Assembly of the Component Cell Populations." *Genes & Development* 27 (22): 2409–26.

Tada, Haru, Makoto Mochii, Hidefumi Orii, and Kenji Watanabe. 2012. "Ectopic Formation of Primordial Germ Cells by Transplantation of the Germ Plasm: Direct Evidence for Germ Cell Determinant in Xenopus." *Developmental Biology* 371 (1): 86–93.

Tahiliani, Mamta, Kian Peng Koh, Yinghua Shen, William A Pastor, Hozefa Bandukwala, Yevgeny Brudno, Suneet Agarwal, et al. 2009. "Conversion of 5-Methylcytosine to 5-Hydroxymethylcytosine in Mammalian DNA by MLL Partner TET1." *Science (New York, N.Y.)* 324 (5929): 930–35.

Tam, P. P. L., and M. H. L. Snow. 1981. "Proliferation and Migration of Primordial Germ Cells during Compensatory Growth in Mouse Embryos." *Development* 64 (1).

Tam, Patrick P.L., and Sheila X. Zhou. 1996. "The Allocation of Epiblast Cells to Ectodermal and Germ-Line Lineages Is Influenced by the Position of the Cells in the Gastrulating Mouse Embryo." *Developmental Biology* 178 (1): 124–32.

Tanaka, S S, Y Toyooka, R Akasu, Y Katoh-Fukui, Y Nakahara, R Suzuki, M Yokoyama, and T Noce. 2000. "The Mouse Homolog of Drosophila Vasa Is Required for the Development of Male Germ Cells." *Genes & Development* 14 (7): 841–53.

Teletin, Marius, Nadège Vernet, Norbert B. Ghyselinck, and Manuel Mark. 2017. "Roles of Retinoic Acid in Germ Cell Differentiation." *Current Topics in Developmental Biology* 125 (January): 191–225.

Thoreen, Carson C., Lynne Chantranupong, Heather R. Keys, Tim Wang, Nathanael S. Gray, and David M. Sabatini. 2012. "A Unifying Model for MTORC1-Mediated Regulation of MRNA Translation." *Nature* 485 (7396): 109–13.

Toyooka, Yayoi, Naoki Tsunekawa, Yoshihiko Takahashi, Yasuhisa Matsui, Michio Satoh, and Toshiaki Noce. 2000. "Expression and Intracellular Localization of Mouse Vasa-Homologue Protein during Germ Cell Development." *Mechanisms of Development* 93 (1–2): 139–49.

Tremblay, K D, N R Dunn, and E J Robertson. 2001. "Mouse Embryos Lacking Smad1 Signals Display Defects in Extra-Embryonic Tissues and Germ Cell Formation." *Development (Cambridge, England)* 128 (18): 3609–21.

Tseden, Khailun, Özlem Topaloglu, Andreas Meinhardt, Arvind Dev, Ibrahim Adham, Christian Müller, Stephan Wolf, et al. 2007. "Premature Translation of Transition Protein 2 MRNA Causes Sperm Abnormalities and Male Infertility." *Molecular Reproduction and Development* 74 (3): 273–79.

Tsuda, Masayuki, Yumiko Sasaoka, Makoto Kiso, Kuniya Abe, Seiki Haraguchi, Satoru Kobayashi, and Yumiko Saga. 2003. "Conserved Role of Nanos Proteins in Germ Cell Development." *Science (New York, N.Y.)* 301 (5637): 1239–41.

Tsukiyama-Kohara, Kyoko, Francis Poulin, Michinori Kohara, Christine T. DeMaria, Alan Cheng, Zhidan Wu, Anne-Claude Gingras, et al. 2001. "Adipose Tissue Reduction in Mice Lacking the Translational Inhibitor 4E-BP1." *Nature Medicine* 7 (10): 1128–32.

Um, Sung Hee, Francesca Frigerio, Mitsuhiro Watanabe, Frédéric Picard, Manel Joaquin, Melanie Sticker, Stefano Fumagalli, et al. 2004. "Erratum: Absence of S6K1 Protects against Age- and Diet-Induced Obesity While Enhancing Insulin Sensitivity." *Nature* 431 (7005): 200–205.

Vainio, Seppo, Minna Heikkilä, Andreas Kispert, Norman Chin, and Andrew P. McMahon. 1999. "Female Development in Mammals Is Regulated by Wnt-4 Signalling." *Nature* 397 (6718): 405–9.

Valinluck, Victoria, and Lawrence C Sowers. 2007. "Endogenous Cytosine Damage Products Alter the Site Selectivity of Human DNA Maintenance Methyltransferase DNMT1." *Cancer Research* 67 (3): 946–50.

Vézina, C, A Kudelski, and S N Sehgal. 1975. "Rapamycin (AY-22,989), a New Antifungal Antibiotic. I. Taxonomy of the Producing Streptomycete and Isolation of the Active Principle." *The Journal of Antibiotics* 28 (10): 721–26.

Vincent, Stéphane D, N Ray Dunn, Roger Sciammas, Miriam Shapiro-Shalef, Mark M Davis, Kathryn Calame, Elizabeth K Bikoff, and Elizabeth J Robertson. 2005. "The Zinc Finger Transcriptional Repressor Blimp1/Prdm1 Is Dispensable for Early Axis Formation but Is Required for Specification of Primordial Germ Cells in the Mouse." *Development (Cambridge, England)* 132 (6): 1315–25.

Virtanen, H.E., E. Rajpert-De Meyts, K.M. Main, N.E. Skakkebaek, and J. Toppari. 2005. "Testicular Dysgenesis Syndrome and the Development and Occurrence of Male Reproductive Disorders." *Toxicology and Applied Pharmacology* 207 (2): 501–5.

Wang, C., Z. Wang, Z. Xiong, H. Dai, Z. Zou, C. Jia, X. Bai, and Z. Chen. 2016. "MTORC1 Activation Promotes Spermatogonial Differentiation and Causes Subfertility in Mice." *Biology of Reproduction* 95 (5): 97–97.

Wang, X, W Li, M Williams, N Terada, D R Alessi, and C G Proud. 2001. "Regulation of Elongation Factor 2 Kinase by P90(RSK1) and P70 S6 Kinase." *The EMBO Journal* 20 (16): 4370–79.

Weber, Susanne, Dawid Eckert, Daniel Nettersheim, Ad J.M. Gillis, Sabine Schäfer, Peter Kuckenberg, Julia Ehlermann, et al. 2010. "Critical Function of AP-2gamma/TCFAP2C in Mouse Embryonic Germ Cell Maintenance1." *Biology of Reproduction* 82 (1): 214–23.

Weng, Q P, M Kozlowski, C Belham, A Zhang, M J Comb, and J Avruch. 1998. "Regulation of the P70 S6 Kinase by Phosphorylation in Vivo. Analysis Using Site-Specific Anti-Phosphopeptide Antibodies." *The Journal of Biological Chemistry* 273 (26): 16621–29.

West, Jason A., Srinivas R. Viswanathan, Akiko Yabuuchi, Kerianne Cunniff, Ayumu Takeuchi, In-Hyun Park, Julia E. Sero, et al. 2009. "A Role for Lin28 in Primordial Germ-Cell Development and Germ-Cell Malignancy." *Nature* 460 (7257): 909–13.

Western, Patrick S., Denise C. Miles, Jocelyn A. van den Bergen, Matt Burton, and Andrew H. Sinclair. 2008. "Dynamic Regulation of Mitotic Arrest in Fetal Male Germ Cells." *Stem Cells* 26 (2): 339–47.

Wilson, K F, W J Wu, and R A Cerione. 2000. "Cdc42 Stimulates RNA Splicing via the S6 Kinase and a Novel S6 Kinase Target, the Nuclear Cap-Binding Complex." *The Journal of Biological Chemistry* 275 (48): 37307–10.

Windley, Simon P, and Dagmar Wilhelm. 2015. "Signaling Pathways Involved in Mammalian Sex Determination and Gonad Development." *Sexual Development : Genetics, Molecular Biology, Evolution, Endocrinology, Embryology, and Pathology of Sex Determination and Differentiation* 9 (6): 297–315.

Xu, Naihan, Yuanzhi Lao, Yaou Zhang, and David A Gillespie. 2012. "Akt: A Double-Edged Sword in Cell Proliferation and Genome Stability." *Journal of Oncology* 2012: 951724.

Yabuta, Yukihiro, Kazuki Kurimoto, Yasuhide Ohinata, Yoshiyuki Seki, and Mitinori Saitou. 2006. "Gene Expression Dynamics During Germline Specification in Mice Identified by Quantitative Single-Cell Gene Expression Profiling1." *Biology of Reproduction* 75 (5): 705–16.

Yadav, Ram Prakash, and Noora Kotaja. 2014. "Small RNAs in Spermatogenesis." *Molecular and Cellular Endocrinology* 382 (1): 498–508.

Yamaguchi, Shinpei, Kwonho Hong, Rui Liu, Azusa Inoue, Li Shen, Kun Zhang, and Yi Zhang. 2013. "Dynamics of 5-Methylcytosine and 5-Hydroxymethylcytosine during Germ Cell Reprogramming." *Cell Research* 23 (3): 329–39.

Yamaguchi, Shinpei, Kwonho Hong, Rui Liu, Li Shen, Azusa Inoue, Dinh Diep, Kun Zhang, and Yi Zhang. 2012. "Tet1 Controls Meiosis by Regulating Meiotic Gene Expression." *Nature* 492 (7429): 443–47.

Yamaguchi, Shinpei, Kazuki Kurimoto, Yukihiro Yabuta, Hiroyuki Sasaki, Norio Nakatsuji, Mitinori Saitou, and Takashi Tada. 2009. "Conditional Knockdown of Nanog Induces Apoptotic Cell Death in Mouse Migrating Primordial Germ Cells." *Development (Cambridge, England)* 136 (23): 4011–20.

Yamaguchi, Shinpei, Li Shen, Yuting Liu, Damian Sendler, and Yi Zhang. 2013. "Role of Tet1 in Erasure of Genomic Imprinting." *Nature* 504 (7480): 460–64.

Yamaji, Masashi, Yoshiyuki Seki, Kazuki Kurimoto, Yukihiro Yabuta, Mihoko Yuasa, Mayo Shigeta, Kaori Yamanaka, Yasuhide Ohinata, and Mitinori Saitou. 2008. "Critical Function of Prdm14 for the Establishment of the Germ Cell Lineage in Mice." *Nature Genetics* 40 (8): 1016–22.

Yanagisawa, Makoto. 2011. "Stem Cell Glycolipids." *Neurochemical Research* 36 (9): 1623–35.

Yang, Haijuan, Derek G. Rudge, Joseph D. Koos, Bhamini Vaidialingam, Hyo J. Yang, and Nikola P. Pavletich. 2013. "MTOR Kinase Structure, Mechanism and Regulation." *Nature* 497 (7448): 217–23.

Yang, Jing, Peter Cron, Vivienne Thompson, Valerie M Good, Daniel Hess, Brian A Hemmings, and David Barford. 2002. "Molecular Mechanism for the Regulation of Protein Kinase B/Akt by Hydrophobic Motif Phosphorylation." *Molecular Cell* 9 (6): 1227–40.

Yeom, Y.I., G. Fuhrmann, C.E. Ovitt, A. Brehm, K. Ohbo, M. Gross, K. Hubner, and H.R. Scholer. 1996. "Germline Regulatory Element of Oct-4 Specific for the Totipotent Cycle of Embryonal Cells." *Development* 122 (3).

Ying, Ying, Xiao-Ming Liu, Amy Marble, Kirstie A. Lawson, and Guang-Quan Zhao. 2000. "Requirement of *Bmp8b* for the Generation of Primordial Germ Cells in the Mouse." *Molecular Endocrinology* 14 (7): 1053–63.

Ying, Ying, and Guang-Quan Zhao. 2001. "Cooperation of Endoderm-Derived BMP2 and Extraembryonic Ectoderm-Derived BMP4 in Primordial Germ Cell Generation in the Mouse." *Developmental Biology* 232 (2): 484–92.

Yoshimizu, Tomomi, Noriyuki Sugiyama, Mario De Felice, Young Ii Yeom, Kazuyuki Ohbo, Kazue Masuko, Masuo Obinata, Kuniya Abe, Hans R. Scholer, and Yasuhisa Matsui. 1999. "Germline-Specific Expression of the Oct-4/Green Fluorescent Protein (GFP) Transgene in Mice." *Development, Growth and Differentiation* 41 (6): 675–84.

Youngren, Kirsten K., Douglas Coveney, Xiaoning Peng, Chitralekha Bhattacharya, Laura S. Schmidt, Michael L. Nickerson, Bruce T. Lamb, et al. 2005. "The Ter Mutation in the Dead End Gene Causes Germ Cell Loss and Testicular Germ Cell Tumours." *Nature* 435 (7040): 360–64.

Yu, Jason S L, and Wei Cui. 2016. "Proliferation, Survival and Metabolism: The Role of PI3K/AKT/MTOR Signalling in Pluripotency and Cell Fate Determination." *Development (Cambridge, England)* 143 (17): 3050–60.

Zamboni, Luciano, and Shakti Upadhyay. 1983. "Germ Cell Differentiation in Mouse Adrenal Glands." *Journal of Experimental Zoology* 228 (2): 173–93.

Zhang, Hongbing, Gregor Cicchetti, Hiroaki Onda, Henry B Koon, Kirsten Asrican, Natalia Bajraszewski, Francisca Vazquez, Christopher L Carpenter, and David J Kwiatkowski. 2003. "Loss of Tsc1/Tsc2 Activates MTOR and Disrupts PI3K-Akt Signaling through Downregulation of PDGFR." *The Journal of Clinical Investigation* 112 (8): 1223–33.

Zhang, Yanjie, and X F Steven Zheng. 2012. "MTOR-Independent 4E-BP1 Phosphorylation Is Associated with Cancer Resistance to MTOR Kinase Inhibitors." *Cell Cycle (Georgetown, Tex.)* 11 (3): 594–603.

Zhao, Jinghui, Bo Zhai, Steven P Gygi, and Alfred Lewis Goldberg. 2015. "MTOR Inhibition Activates Overall Protein Degradation by the Ubiquitin Proteasome System as Well as by Autophagy." *Proceedings of the National Academy of Sciences of the United States of America* 112 (52): 15790–97.

Zhou, Quan, Mei Wang, Yan Yuan, Xuepeng Wang, Rui Fu, Haifeng Wan, Mingming Xie, et al. 2016. "Complete Meiosis from Embryonic Stem Cell-Derived Germ Cells In Vitro." *Cell Stem Cell* 18 (3): 330–40.

Zhou, Zhi, Takayuki Shirakawa, Kazuyuki Ohbo, Aiko Sada, Quan Wu, Kazuteru Hasegawa, Rie Saba, and Yumiko Saga. 2015. "RNA Binding Protein Nanos2 Organizes Post-Transcriptional Buffering System to Retain Primitive State of Mouse Spermatogonial Stem Cells." *Developmental Cell* 34 (1): 96–107.

Zhu, Rui, Chitralekha Bhattacharya, and Angabin Matin. 2007. "The Role of Dead-End in Germ-Cell Tumor Development." *Annals of the New York Academy of Sciences* 1120 (December): 181–86.

Zhu, Youming, Peng Wang, Li Zhang, Guo Bai, Chi Yang, Yuanying Wang, Jiacai He, Zhiyuan Zhang, Guoping Zhu, and Duohong Zou. 2018. "Superhero Rictor Promotes Cellular Differentiation of Mouse Embryonic Stem Cells." *Cell Death & Differentiation*, August.